EXPLORANDO EL PAPEL DE LOS MICROORGANISMOS Y PARÁMETROS FISICOQUÍMICOS EN LOS PROCESOS BIOGEOQUÍMICOS EN LA INTERFAZ CONTENEDOR DE COBRE/BENTONITA/SELENIO: CON VISTAS A UN ALMACENAMIENTO GEOLÓGICO PROFUNDO DE RESIDUOS RADIACTIVOS

UNIVERSIDAD DE GRANADA

Universidad de Granada

Facultad de Ciencias

Departamento de Microbiología

Exploring the role of microorganisms and physicochemical parameters on the biogeochemical processes at the metal container/bentonite/selenium interface: in view of a Deep Geological Repository of nuclear waste

TESIS DOCTORAL

Marcos Felipe Martínez Moreno

Granada, 2024

Programa de Doctorado en Biología Fundamental y de Sistemas

EXPLORANDO EL PAPEL DE LOS MICROORGANISMOS Y PARÁMETROS FISICOQUÍMICOS EN LOS PROCESOS BIOGEOQUÍMICOS EN LA INTERFAZ CONTENEDOR DE COBRE/BENTONITA/SELENIO: CON VISTAS A UN ALMACENAMIENTO GEOLÓGICO PROFUNDO DE RESIDUOS RADIACTIVOS

TESIS DOCTORAL

Programa de Doctorado en Biología Fundamental y de Sistemas

Departamento de Microbiología, Facultad de Ciencias

Universidad de Granada

Granada, 2024

Memoria presentada por D. Marcos Felipe Martínez Moreno para aspirar al Grado de Doctor por la Universidad de Granada con Mención Internacional. Esta Tesis Doctoral ha sido dirigida por D. Mohamed Larbi Merroun, Catedrático de la Universidad de Granada, y D. Jesús Javier Ojeda Ledo, Profesor Titular en la Universidad de Swansea (Reino Unido)

Vº Bº del Director

Vº Bº del Director

Mohamed Larbi Merroun
Catedrático de Universidad
Universidad de Granada

El Doctorando

Jesús Javier Ojeda Ledo
Associate Professor
Swansea University

UNIVERSIDAD DE GRANADA

Marcos Felipe Martínez Moreno

Swansea University
Prifysgol Abertawe

Editor: Universidad de Granada. Tesis Doctorales
Autor: Marcos Felipe Martínez Moreno
ISBN: 978-84-1195-288-0
URI: https://hdl.handle.net/10481/91116

El doctorando Marcos Felipe Martínez Moreno y los directores de la tesis Mohamed Larbi Merroun y Jesús Javier Ojeda Ledo, garantizamos, al firmar esta tesis doctoral, que el trabajo ha sido realizado por el doctorando bajo la dirección de los directores de la tesis y hasta donde nuestro conocimiento alcanza, en la realización del trabajo, se han respetado los derechos de otros autores a ser citados, cuando se han utilizado sus resultados o publicaciones.

/

The doctoral candidate Marcos Felipe Martínez Moreno and the thesis supervisors Mohamed Larbi Merroun and Jesús Javier Ojeda Ledo, guarantee, by signing this doctoral thesis, that the work has been done by the doctoral candidate under the direction of the thesis supervisors and, as far as our knowledge reaches, in the performance of the work, the rights of other authors to be cited (when their results or publications have been used) have been respected.

Director Director

Mohamed Larbi Merroun **Jesús Javier Ojeda Ledo**

El Doctorando

Marcos Felipe Martínez Moreno

Esta Tesis Doctoral ha sido realizada en el Departamento de Microbiología (Facultad de Ciencias) de la Universidad de Granada durante los años 2020-2024 dentro del Grupo de Investigación Mixobacterias (BIO103).

Para la realización de este trabajo, el doctorando disfrutó de varios contratos: i) Promoción de Empleo Joven e Implantación de la Garantía Juvenil en I+D+i del Ministerio de Ciencia e Innovación (ref. PEJ2018-003299-A), ii) contrato con cargo al Proyecto del Plan Nacional "*Impacto de los procesos microbianos en la interface contenedor de cobre-bentonita compactada y sus efectos sobre la movilización del selenio*" (ref. RTI2018-101548-B-I00) financiado por el Ministerio de Ciencia, Innovación y Universidades, y iii) un contrato con cargo al Proyecto Europeo "*EURAD - European Joint Programme on Radioactive Waste Management*" (ref. 847593, EURATOM - NFRP-2018) financiado por la Comisión Europea.

Además, el doctorando disfrutó de la beca de movilidad del programa Erasmus Prácticas (Erasmus+) del Vicerrectorado de Estudiantes de la Universidad de Granada y una *FEMS Research and Training Grant* (FEMS-GO-2021-077) para la realización de una estancia de tres meses en el centro de investigación extranjero *Belgian Nuclear Research Centre* (Bélgica) bajo la supervisión de la Dra. Kristel Mijnendonckx.

Durante el desarrollo de esta Tesis Doctoral, parte de los resultados han sido publicados en revistas científicas de alto impacto, así como en congresos a nivel e internacional:

1) Publicaciones científicas relacionadas con esta tesis doctoral:

Martinez-Moreno, M. F*., Povedano-Priego, C., Morales-Hidalgo, M., Mumford, A. D., Ojeda, J. J., Jroundi, F., & Merroun, M. L. (2023). Impact of compacted bentonite microbial community on the clay mineralogy and copper canister corrosion: a multidisciplinary approach in view of a safe Deep Geological Repository of nuclear wastes. Journal of Hazardous Materials, 131940. https://doi.org/10.1016/j.jhazmat.2023.131940 **IF: 13.6 - Q1 (D1)**.

Martinez-Moreno, M. F*., Povedano-Priego, C., Mumford, A. D., Morales-Hidalgo, M., Mijnendonckx, K., Jroundi, F., Ojeda, J. J., & Merroun, M. L. (2024). Microbial responses to elevated temperature: Evaluating bentonite mineralogy and copper canister corrosion within the long-term stability of deep geological repositories of nuclear waste. Science of The Total Environment, 170149. https://doi.org/10.1016/j.scitotenv.2024.170149 **IF: 9.8 - Q1 (D1)**

Ruiz-Fresneda, M. A*., **Martinez-Moreno, M. F.**, Povedano-Priego, C., Morales-Hidalgo, M., Jroundi, F., & Merroun, M. L. (2023). Impact of microbial processes on the safety of deep geological repositories for radioactive waste. Frontiers in Microbiology, 14, 1134078. https://doi.org/10.3389/fmicb.2023.1134078 **IF: 5.2 – Q2**

2) Artículo científico afín publicado durante el periodo doctoral:

Ruiz-Fresneda, M. A.*, Lopez-Fernandez, M., **Martinez-Moreno, M. F.**, Cherkouk, A., Ju-Nam, Y., Ojeda, J. J., Mol, H., & Merroun, M. L. (2020). Molecular Binding of EuIII/CmIII by *Stenotrophomonas bentonitica* and Its Impact on the Safety of Future Geodisposal of Radioactive Waste. Environmental Science & Technology, 54(23), 15180-15190. https://doi.org/10.1021/acs.est.0c02418

3) Congresos nacionales e internacionales dónde se han presentado resultados de esta Tesis Doctoral:

Martinez-Moreno, Marcos F.*; Povedano-Priego, Cristina; Morales-Hidalgo, Mar; Mumford, Adam; Ojeda, Jesus J., Jroundi, Fadwa; Merroun, Mohamed L. (July 9th – 13th, 2023) *Copper corrosion and microbial communities shifts in compacted bentonite: in view of a safe Deep Geological Repository of radioactive waste.* [**Poster**]. FEMS2023. Hamburgo (Alemania).

Martinez-Moreno, M.F.*, Povedano-Priego, C., Jimenez-Garcia, I., Huertas, F.J., Villar, M.V., Jroundi, F., Merroun M.L. (June 28th – July 1st, 2022) *Impacto de los procesos microbianos en la corrosión de cobre y en bentonita compactada: en vista a un Almacenamiento Geológico Profundo seguro de los residuos radiactivos* [**Oral communication**]. XXXIX Reunión Científica de la Sociedad Española de Mineralogía y XXVI Reunión Científica de la Sociedad Española de Arcillas. Baeza (Spain).

Lazúen-López, G.*, **Martinez-Moreno, M.F**., Povedano-Priego, C., Morales-Hidalgo, M., Jroundi, F., Merroun M.L. (June 22th – 24th, 2022). *Caracterización microscópica y espectroscópica de nanopartículas de selenio (SeNPs) de microcosmos de bentonita saturada en el marco del Almacenamiento Geológico Profundo (AGP)* [**Oral communication**]. III Congreso / V Jornadas: Investigadores en Formación (JIFFI). Fomentando la Interdisciplinaridad. Granada (Spain).

Martinez-Moreno, M.F.*, Povedano-Priego, C., Jimenez-Garcia, I., Huertas, F.J., Jroundi, F., Merroun M.L. (June 22th – 24th, 2022). *Impacto de los procesos microbianos en la estabilidad de los Almacenamientos Geológicos Profundos de residuos radiactivos: corrosión de cobre y mineralogía de la bentonita compactada* [**Oral communication**]. III Congreso / V Jornadas: Investigadores en Formación (JIFFI). Fomentando la Interdisciplinaridad. Granada (Spain).

Martinez-Moreno, M.F.*, Povedano-Priego, C., Jimenez-Garcia, I., Huertas, F.J., Jroundi, F., Merroun, M.L. (June 13th-16th, 2022). *Looking for the microbial processes related to the compacted bentonite and copper canisters to gain insights into a safe Deep Geological Repository of radioactive waste* [**Poster**]. Clay Conference 2022: 8th International Conference on clays in Natural and Engineered Barriers for Radioactive Waste Confinement. Nancy (France).

Lazúen-López, G.*, **Martinez-Moreno, M.F**., Povedano-Priego, C., Torres-Cánovas, A., Morales-Hidalgo, M., Jroundi, F., Merroun, M.L. (June 1st-3rd, 2022). *Aislamiento de cepas bacterianas procedentes de microcosmos de bentonita saturada y caracterización de nanopartículas de selenio en el marco del biorremedio de ambientes contaminados con metales pesados* [**Poster**]. VIII Congreso Nacional de Microbiología Industrial y Biotecnología Microbiana. Valencia (Spain).

Martinez-Moreno, M.F.*, Povedano-Priego, C., Lazuen-Lopez, G., Gonzalez-Morales, E., Ojeda, J.J., Jroundi, F., Merroun, M.L. (December 2nd – 3rd, 2021). *Microbially influenced changes in saturated bentonite microcosms: selenium biotransformation and copper disc corrosion* [**Poster**]. New Topics in Mineralogy 2: The mineral-microbe interface through time and space. On line.

Martínez-Moreno, M.F.*, Povedano-Priego, C., Lazúen-López, G., González-Morales, E., Jroundi, F., Merroun, M.L. (June 28th – July 2nd, 2021). *Efecto de la actividad microbiana en microcosmos de bentonita saturada: corrosión de cobre y*

producción de nanopartículas de selenio [**Poster**]. XXVIII Congreso de la Sociedad Española de Microbiología. On line.

4) Otras comunicaciones y divulgación científica relacionadas con la Tesis Doctoral:

Martínez-Moreno, M.F.* (June 16th, 2023). Audience Award at the 1st Doctoral Monologue Contest [**Monologue**]. Doctoral school and scientific culture unit at the University of Granada.

Martinez-Moreno, M.F.*, Ruiz-Fresneda, M.A., Lopez-Fernandez, M., Cherkouk, A., Ju-Nam, Y., Ojeda, J.J., Moll, H., and Merroun, M.L. (July 4th - 9th, 2021). *Deciphering the Molecular Interaction of Stenotrophomnas bentonitica with Eu(III)/Cm(III) Related to the Safety of Future Deep Geological Repositories of Nuclear Wastes* [**Oral communication – Invited speaker**]. Goldschmidt2021 Virtual Conference. On line.

Martínez-Moreno, M.F.* (May 28th, 2021). *Bacterias y residuos radiactivos* [**Interview**]. Science Dissemination Podcast (https://lnkd.in/dAVXHPp).

Martínez-Moreno, M.F.*, Ruiz-Fresneda, M.A., Ojeda, J.J., Ju-Nam, Y., Merroun, M.L. (March 19th, 2021). *Interaction mechanisms of Stenotrophomonas bentonitica with Eu(III) and its impact on the safety of future deep geological repositories of nuclear wastes* [**Oral communication**]. Annual conference 2021 of the VAAM. On line.

AGRADECIMIENTOS

En primer lugar, me gustaría agradecer a mis directores de tesis Mohamed L. Merroun y Jesús J. Ojeda Ledo. Gracias a los dos por haber depositado vuestra confianza en mí para llevar a cabo esta Tesis Doctoral. Gracias también por haberme ayudado a crecer tanto a nivel profesional como personal. Gracias Mohamed por haber encendido en mí la chispa del interés por la Microbiología desde que, hace casi 9 años, apostaste por mí durante mi Trabajo de Fin de Grado y entré a formar parte de esta gran familia científica. Jesús, recuerdo mi primera vez en Swansea, allá por el 2016. Gracias por haberme acogido durante mis primeras experiencias internacionales. Junto con Yon, transformasteis mi "miedo a lo desconocido" en una aventura gratificante y acogedora, haciendo que me sintiera como en casa a pesar de los kilómetros de distancia. En definitiva, gracias Mohamed y Jesús, vuestra confianza en mi potencial ha sido fundamental para llegar donde estoy hoy, ya que ese Marcos de hace casi 9 años jamás hubiera imaginado llegar hasta aquí. Seguiré aplicando vuestras valiosas enseñanzas y la pasión por la ciencia en cada nuevo camino que emprenda allá donde vaya.

I would like to thank my external supervisor, Dr. Kristel Mijnendonckx, during my three-months research stay at SCK CEN (Mol, Belgium). It was such a great experience. I would also like to thank the 'Boeretang forever' family. Without them, my time in Belgium would not have been nearly so unforgettable.

Gracias también a la sección bentonitica, Fadwa y Cristina, por enseñarme a apreciar la gratificante sensación que surge cuando, a pesar de los retos que presenta la bentonita, se consiguen resultados. A Javier

Huertas, por convertir los muestreos de bentonita en una aventura no solo divertida, sino también profundamente enriquecedora.

A todos los compañeros y estudiantes de TFG y TFM. En especial a Alfredo, Nacho, Chacho y Guillermo; quienes, de una forma u otra, me han enseñado a enseñar, al mismo tiempo que he aprendido yo de ellos.

Agradecer a todos los compañeros que han pasado por el departamento estos años. Espero que hayáis disfrutado mi *Caudillato* de los Cinco Reinos durante mi mandato. Mi agradecimiento es para vosotros, ya que las tardes en el Soho (el templo) y el espíritu de "¡y lo que surja!" es de las mejores terapias grupales que puedan existir. Como siempre digo, lo que tenemos es difícil de encontrar, ¡que no se pierda! Me llevo unos recuerdos que durarán para siempre. Al Reino Antagónico, con Sonia la buena, y Manolo liderando, nunca imaginé que podríamos compartir este gusto por la buena música y el humor más absurdo. Al Reino Ecológico, Claudia, gracias por el subidón de adrenalina que me daba cuando venías a preguntarme algo levitando; y al Reino Quintuplantiano. Al Reino Submundo: Ylenia, Tamara y mi italiana favorita, Francesca, ¡qué gran descubrimiento! *Grazie per ogni "riposo visuale", concerti, qualche dramma e per non aver mai detto di no.*

A nuestra gran familia, el Reino Radiactivo. Migue, gracias por haber sido parte de mi primer contacto con la ciencia y por tener el humor tan roto como yo, por ello te llevaste el merecido título de Dr. Seleneda. Jaime, gracias por tus clases magistrales de galénica y bioquímica, y tu increíble mente para elegir entre dos opciones. Newman, siempre seremos Don Quijote y Sancho Panza, dándonos apoyo mutuo en esta montaña rusa emocional. Esther, ¡ojo, Esther!, juntos hacemos una “persona completa”, siempre nos quedarán los bares. Chacho, *the best*

assistant to the regional manager, que maravilla que todo siempre te venga bien. Adam, *the least English Englishman I know, you're a member of our family now.* Alex, ¡mi mejor coincidencia!, gracias por aparecer en mi camino durante esta etapa. Mar, gracias por ser uno de mis pilares esenciales tanto en lo personal como en lo profesional. Imposible imaginar una mejor compañera de viaje a lo largo de esta aventura. A Marga, Pablo, Guille, Lidia y un largo etcétera que seguro me dejo sin nombrar.

A María y Esther que, a pesar de las distancias que nos separan, siempre habéis estado ahí. Gracias por tantos años de amistad y momentos compartidos. Ya queda *un día menos para la jubilación* y poder retirarnos en el pueblo para montar la granja escuela / retiro espiritual que siempre hemos querido.

A pesar de creer que "una tesis se la dan a cualquiera", este viaje no hubiera sido el mismo sin contar con un *comité de expertos* al que recurrir para manejar la *gestión ansiedad predoc* o para fundar un *club de petanca* donde organizar *cenitas* para *canijos* que no superen la altura de un *pepino*. En definitiva, *ChatGPT team* nos ha confirmado que nos hemos convertido en unos verdaderos *Power Rangers*, capaces de enfrentarnos incluso a los *Illuminati*.

A mi familia, a mis tíos y primos, por el interés y el cariño mostrados a lo largo de estos años. Un agradecimiento muy especial va dirigido a mis padres, Ángel y Marcas, y a mi hermana Ángela. Su esfuerzo incondicional, apoyo y confianza sin límites han sido fundamentales para llegar hasta aquí. Sin ellos nunca hubiera podido imaginar alcanzar las metas que he logrado. Las palabras se quedan cortas para agradecer todo lo que habéis hecho por mí. Gracias por estar siempre a mi lado.

LIST OF ABREVIATIONS

AGP: Almacenamiento Geológico Profundo

ANDRA: Agence Nationale pour la gestión des Déchets Radioactifs

***a*-Se**: amorphous selenium

ATCC: American Type Culture Collection

ATR-FTIR: Attenuated total reflectance - Fourier transform infrared spectroscopy

BLAST: Basic Local Alignment Search Tool

BPAS: *Bacillus*, *Pseudomonas*, *Amycolatopsis*, and *Stenotrophomonas*

CMIC: Chemical Microbially Induced Corrosion

DGR: Deep Geological Repository

DMDSe: dimethyl diselenide

DMSe: dimethyl selenide

DMSeS: dimethyl selenenyl sulfide

DNA: Deoxyribonucleic acid

DRX: Difracción de Rayos-X

DSMZ: Deutsche Sammlung Von Mikroorganismen Und Zellkulturen

EDX: Energy Dispersive X-ray

EG: ethylene glycol

EMIC: Electrical Microbially Influenced Corrosion

EPS: Extracellular Polymeric Substance

EW: Equilibrium Water

FEBEX: Full-scale Engineered Barriers Experiment

FFT: Fast Fourier Transform

FTIR: Fourier Transform Infrared spectroscopy

HAADF-STEM: High-Angle Annular Dark Field Scanning Electron Microscopy

HLW: High-Level Wastes

HPIC: High Pressure Ion Chromatography

HRSEM: High Resolution Scanning Electron Microscopy

HRTEM: High Resolution Transmission Electron Microscopy

IAEA: International Atomic Energy Agency

ICP-MS: Inductively Coupled Plasm-Mass Spectrometry

ILW: Intermediate Level Waste

IRB: Iron-Reducing Bacteria

LB: Luria-Bertani

LLW: Low Level Waste

LOI: Loss On Ignition

LPS: lipopolysaccharides

MIC: Microbially Influenced Corrosion

MPN: Most Probable Number

***m*-Se**: monoclinic selenium

NCIMB: National Collection of Industrial Food and Marine Bacteria

NEA: Nuclear Energy Agency

NCBI: National Centre for Biotechnology Information

NGS: Next Generation Sequencing

NUMO: Nuclear Waste Management Organization of Japan

NWMO: Nuclear Waste Management Organization

OA: Oriented Aggregates

OFHC: Oxygen-Free High Conductivity

OTU: Operational Taxonomical Unit

PCoA: Principal Coordinate Analysis

PCR: Polymerase Chain Reaction

qPCR: quantitative Polymerase Chain Reaction

rRNA: ribosomal Ribonucleic Acid

SAED: Selected-Area Electron Diffraction

SE: Secondary Electrons

SEM: Scanning Electron Microscopy

Se(0): elemental selenium

Se(IV): selenite

SeNP: Selenium Nanoparticle

SeRP: Selenium Reduction Product

SRB: Sulfate-Reducing Bacteria

TRLFS: Time Resolved Laser-Induced Fluorescence Spectroscopy

***t*-Se**: trigonal selenium

UNS: Unified Numbering System

VLLW: Very Low-Level Waste

VSLW: Very Short-Lived Waste

VP-FESEM: Variable Pressure Field Emission Scanning Electron Microscopy

WNA: World Nuclear Association

XPS: X-ray Photoelectron Spectroscopy

XRD: X-Ray Diffraction

XRF: X-ray Fluorescence

ÍNDICE DE CONTENIDOS

Sampling site at ‘Cortijo de Archidona’

Personal archive

Resumen

Summary

RESUMEN

Uno de los temas más relevantes en relación a la energía nuclear es la gestión y almacenamiento final de los residuos radiactivos de alta actividad, los cuales presentan una vida media de cientos a millones de años. Por esta razón, han de ser almacenados de forma adecuada y segura durante, al menos, 100.000 años en instalaciones apropiadas hasta que la radiotoxicidad disminuya a niveles comparables a los naturales. La opción más aceptada a nivel internacional para su almacenamiento final es el denominado Almacenamiento Geológico Profundo (AGP), basado en un sistema multibarrera que prevendrá la liberación de los residuos a la biosfera. Los residuos se almacenarán en contenedores metálicos resistentes a la corrosión, que estarán rodeados por un material de relleno y sellado (barreras de ingeniería), y se depositarán a varios cientos de metros de profundidad en una formación geológica estable (barrera natural).

En el caso de España, el material propuesto como relleno y sellado es la bentonita procedente del yacimiento Cortijo de Archidona (Almería), comercializada como FEBEX, debido a sus buenas propiedades fisicoquímicas (ej. conductividad térmica, capacidad de hinchamiento, alta plasticidad y baja permeabilidad, entre otras). Debido a que la bentonita no es ni estará estéril, estudiar la estructura de las comunidades microbianas presentes en ella es crucial para entender los procesos biogeoquímicos que puedan comprometer la estabilidad y la seguridad del AGP a largo plazo. Los microorganismos podrían alterar las propiedades de la bentonita, dañar la integridad de los contenedores metálicos y contribuir a la producción de gases aumentando la presión dentro del AGP. Tras el sellado del AGP, la actividad microbiana y la oxidación de los contenedores crearán un ambiente anaerobio, donde bacterias específicas como las hierrorreductoras y sulfatorreductoras (IRB y SRB, por sus siglas en inglés) podrían mantenerse metabólicamente activas. Como resultado de su actividad metabólica, podrían producir la corrosión de los contenedores de hierro y cobre, o afectar a la composición química de la bentonita.

El ambiente cercano a los contenedores será caliente, seco y oxidante debido al calor emitido por la desintegración de los radionucleidos presente en los residuos, mientras que, más alejado de la superficie de los contenedores, será menos cálido, húmedo y anóxico. Por lo tanto, se espera que la generación de sulfuro (principal agente corrosivo de los contenedores metálicos en condiciones anaerobias) como consecuencia del metabolismo microbiano ocurra lejos del contenedor, dónde las condiciones son más favorables. Este sulfuro podría difundir por la bentonita e influir en la corrosión del contenedor. En el peor de los casos, esto podría llevar a la formación de fisuras en los contenedores y, por tanto, a la posible interacción de los microorganismos con los radionucleidos.

Por todo ello, la presente Tesis Doctoral trata de explorar, en el contexto de los AGP, cómo diversos parámetros fisicoquímicos, entre ellos la alta densidad de compactación de la bentonita, las elevadas temperaturas, la adición de nutrientes (donadores y aceptores de electrones) y la presencia de selenio, afectan a las comunidades microbianas. Además de examinar el impacto de estas comunidades en la mineralogía de la bentonita, la corrosión del cobre (como material constituyente de los contenedores) y la interacción con el selenio [en forma de Se(IV)], mediante un enfoque multidisciplinar que integra técnicas de microbiología convencional, biología molecular, química analítica, microscopía y espectroscopía.

Con la finalidad expuesta, en primer lugar, se investigaron los procesos biogeoquímicos y fisicoquímicos en la interfaz cobre/bentonita compactada y la corrosión en la superficie del cobre. Para ello, se elaboraron bloques de bentonita compactada con discos de cobre de alta pureza en su interior, añadiendo acetato, lactato y sulfato para estimular la actividad de bacterias anaerobias como las SRB. Estos bloques se incubaron en condiciones anaerobias durante un año a 30 ºC y 60 ºC.

Tras el periodo de incubación, independientemente de la temperatura, no se detectó la transformación de esmectita a illita (transformación irreversible que afectaría a la capacidad de hinchamiento de la bentonita), confirmando la estabilidad de la bentonita bajo estas condiciones experimentales. El proceso de tindalización de la bentonita previo a la elaboración de los bloques redujo la diversidad microbiana tras un año de incubación a 30 ºC. Además, en las muestras incubadas a 60 ºC, tras un año de incubación, se produjo una disminución más acusada de la diversidad bacteriana, con *Pseudomonas* volviéndose el género predominante de la comunidad en términos de abundancia relativa. La presencia de donadores de electrones (acetato y lactato) y sulfato (como aceptor de electrones) tuvo un ligero efecto en las comunidades, estimulando ciertos géneros bacteriano y, en menor medida, estimuló la abundancia de géneros pertenecientes al grupo de SRB. Este grupo de bacterias no presentó viabilidad a 60 ºC en condiciones enriquecidas, mientras que, a 30 ºC y bajo condiciones de enriquecimiento, presentaron capacidad de crecimiento. Además, a 60 ºC ciertas bacterias aerobias como *Aeribacillus* y *Staphylococcus* mostraron viabilidad. Esto hace patente la capacidad de algunas bacterias de permanecer en estados latentes (ej. en forma de esporas o células desecadas) para hacer frente a las duras condiciones ambientales de modo que, cuando las condiciones se vuelven favorables serán, de nuevo, metabólicamente activas. En cuanto al grupo de SRB, al presentar baja presencia y baja actividad metabólica, no se detectaron productos de corrosión de gran tamaño en la superficie de los discos de cobre. La mayor diferencia radicó en la detección de pequeños acúmulos aislados de Cu_xS (relacionado con productos de corrosión de cobre) tras la incubación a 30 ºC; mientras que a 60 ºC se detectaron, pero no se visualizaron, precipitados.

Adicionalmente, se profundizó más en cómo los microorganismos afectarían a las condiciones geoquímicas en un estudio a corto plazo. Para ello, se simularon condiciones óptimas para la actividad microbiana mediante la elaboración de microcosmos de bentonita hipersaturados en agua y enriquecidos con acetato,

lactato y sulfato, siendo inoculados con un consorcio de bacterias conocidas y presentes en la bentonita (consorcio BPAS: *Bacillus* sp. BII-C3, *Pseudomonas putida*, *Amycolatopsis ruanii* y *Stenotrophomonas bentonitica*). Además, mini contenedores de cobre (Cu-mCan, por sus siglas en inglés) fueron añadidos a cada microcosmo.

Tras un año de incubación, el pH en los microcosmos se volvió menos alcalino debido, posiblemente, a la generación de gases como consecuencia del metabolismo microbiano o a procesos de intercambio iónico con los minerales de la bentonita. En cuanto a los procesos biogeoquímicos, se observó un rápido consumo de lactato asociado a la generación, y posterior consumo, de acetato y, en menor medida, asociado al consumo de sulfato, justificando las rutas de oxidación incompleta de lactato a acetato.

A los 45 días de incubación (dónde los microcosmos mostraban mayor heterogeneidad entre ellos), se observó que la presencia del consorcio BPAS redujo la diversidad bacteriana, observando predominancia de *Pseudomonas* y *Stenotrophomonas*. Además, la presencia de acetato, lactato y sulfato estimuló ciertas SRB, las cuales podrían participar en la corrosión del material de cobre. Por otra parte, a los 45 días, se detectó la formación de CuO en todas las superficies de los Cu-mCan, posiblemente debido a oxígeno atrapado en la bentonita o a la reducción del H_2O, mientras que compuestos de Cu_2S, como resultado de la generación de sulfuro procedente de la actividad metabólica bacteriana, solo fueron detectados en los microcosmos dónde los procesos biogeoquímicos fueron más pronunciados.

La adición de 2 mM de selenito [Se(IV)], como análogo inactivo del ^{79}Se presente en los residuos radiactivos, afectó a los procesos biogeoquímicos en los microcosmos mencionados anteriormente. La presencia de este metaloide resultó tóxica para algunas bacterias, reduciendo su actividad metabólica, ralentizando la

dinámica de consumo y/o producción de lactato, acetato y sulfato. Además, la presencia de este metaloide tuvo un impacto en la diversidad bacteriana aumentando la presencia de ciertas bacterias selenotolerantes y afectando a la abundancia de algunas SRB. La formación de una fina capa de coloración rojiza en la interfase bentonita:sobrenadante en los microcosmos, además de manchas aisladas en la bentonita, indicó la reducción de Se(IV) a selenio elemental [Se(0)]. Mediante técnicas microscópicas y espectroscópicas se confirmó la reducción e inmovilización de Se(IV) a Se(0) amorfo (*a*-Se). Este hecho ha llevado a proponer un mecanismo en el cual el Se(IV) es reducido intracelularmente a Se(0) en forma de nanoesferas con alotropía amorfa (*a*-Se) que, una vez liberadas al espacio extracelular mediante lisis celular, podían sufrir procesos de transformación a estructuras cristalinas de selenio monoclínico (*m*-Se) y, posteriormente, a la forma más termodinámicamente estable y menos tóxica: selenio trigonal (*t*-Se).

En resumen, los microorganismos presentes en la bentonita juegan un rol clave (ya sea beneficioso, perjudicial o neutro) en la evolución de las condiciones geoquímicas de los AGP, influenciando potencialmente la estabilidad de sus diversas barreras. Los resultados de esta Tesis Doctoral aportan nuevo conocimiento sobre cómo los microorganismos y los procesos biogeoquímicos relacionados pueden impactar en la interacción entre el contenedor de cobre, la bentonita española y el selenio. Estas aportaciones son de gran interés, puesto que ayudan a entender procesos cruciales para garantizar la seguridad y estabilidad de los AGP a largo plazo.

SUMMARY

One of the biggest challenges facing the nuclear power industry is the nuclear waste management, which includes the final disposal of high-level radioactive waste (HLW), with a half-life of hundreds to millions of years. Therefore, this type of waste must be properly and safely stored for at least 100,000 years in appropriate facilities until their radiotoxicity decreases to levels comparable to the natural ones. The most internationally accepted option for their final disposal is the Deep Geological Repository (DGR), which is based on a multi-barrier system that will be used to prevent the release of the radioactive chemicals to the biosphere. This hazardous waste will be stored in corrosion-resistant metal canisters, typically surrounded by a backfill and sealing material (engineered barriers) and placed several hundreds of meters deep in a stable geological formation (natural barrier).

In the case of Spain, the filling and sealing material proposed is the bentonite from the 'Cortijo de Archidona' deposit found in the Almeria region. This bentonite is commercialized as FEBEX, due to its favorable physicochemical properties (e.g., thermal conductivity, swelling capacity, high plasticity and low permeability, among others). Since bentonite is not and will not be sterile, studying the structure of its microbial communities is crucial to understand the biogeochemical processes that may compromise the long-term stability of the DGR. Microorganisms could have an impact on the properties of the bentonite, which can potentially compromise the integrity of the metal canisters, mobilize the stored wastes, and contribute to the build-up of gases and pressure increase within the DGR. Once the DGR is sealed, microbial activity and the canisters corrosion will create an anaerobic environment, where specific microorganisms such as iron-reducing (IRB) and sulfate-reducing bacteria (SRB) may remain metabolically active. Thus, bacteria could cause corrosion of the iron and copper-based canisters, and/or affect the chemical composition of the bentonite. The environment near the canisters will

be hot and dry due to the heat released by the decay of the radionuclides present in the waste, which in turn can also create oxidative conditions. Farther from the surface of the canisters, the environment will be wet, less warm and anoxic. Therefore, it is expected that the production of sulfide (the main corrosive agent of metal canisters under anoxic conditions) resulting from bacterial metabolism will occur far from the canisters, where conditions are more favorable. This sulfide could then diffuse through the bentonite and influence the corrosion of the canisters. In the worst-case scenario, this could lead to the formation of cracks in the canisters and thus to the possible interaction of microorganisms with the radionuclides.

Therefore, this PhD thesis aims to explore how various physicochemical parameters, in the context of DGR, such as the high compaction density of bentonite, high temperatures, the addition of nutrients (electron donors and acceptors) and the presence of selenium, affect the microbial communities. In addition, the impact of these communities on bentonite mineralogy, copper corrosion (as a constituent material of the canisters) and interaction with selenium [in the form of Se(IV)] was examined, using a multidisciplinary approach integrating techniques of conventional microbiology, molecular biology, analytical chemistry, microscopy and spectroscopy.

First, biogeochemical and physicochemical processes at the copper/ compacted bentonite interface and the corrosion at the copper surface were investigated. For this purpose, compacted bentonite blocks were produced with high purity copper disks embedded in the core, adding acetate, lactate and sulfate to stimulate the activity of anaerobic bacteria such as SRB. These blocks were then incubated under anoxic conditions for one year at 30 ºC and 60 ºC.

After the incubation, regardless of the temperature, the smectite-to-illite transformation (irreversible transformation that would affect the swelling capacity

of bentonite) was not detected, indicating the stability of bentonite under these experimental conditions. The tyndallization process (pre-sterilization of the bentonite) reduced the microbial diversity in the blocks. On the other hand, incubation of the blocks at 60ºC for one year led to a more pronounced decrease in diversity, with *Pseudomonas* becoming the predominant genus in the community. The presence of electron donors (acetate and lactate) and sulfate (as electron acceptor) had a slight effect on the communities, stimulating certain bacterial genera and, to a lesser extent, genera belonging to the SRB group. Under enriched conditions using culture media, this group of bacteria showed no metabolic activity at 60 ºC but they grow at 30 ºC. In addition, at 60 ºC certain aerobic bacteria such as *Aeribacillus* and *Staphylococcus* showed viability. This highlights the ability of some bacteria to remain in dormant states (e.g., in the form of spores or desiccated cells) to cope with harsh environmental conditions and, when conditions become favorable, become metabolically active again. Regarding the SRB group, as they showed low abundance and metabolic activity, no large corrosion products were detected on the surface of the copper disks. The main difference was the detection of small and isolated Cu_xS compounds (related to copper corrosion products) after incubation at 30 ºC; whereas, at 60 ºC they were detected, but no precipitates were observed.

In addition, further investigation was conducted on how microorganisms would affect geochemical conditions in a short-term study. For this purpose, optimal conditions for microbial metabolic activity were replicated by developing bentonite microcosms hyper-saturated in water with acetate, lactate and sulfate, in addition to being inoculated with a consortium of bentonite isolates (BPAS consortium: *Bacillus* sp. BII-C3, *Pseudomonas putida*, *Amycolatopsis ruanii* and *Stenotrophomonas bentonitica*). Moreover, three copper mini-canisters (Cu-mCan) were incorporated in each microcosm.

After one year of incubation, the pH in the microcosms became less alkaline, possibly due to the generation of gases as a consequence of microbial metabolism, or to ion exchange processes with the bentonite minerals. In addition, a rapid consumption of lactate associated with the generation, and subsequent consumption of acetate and, to a lesser extent, associated with the consumption of sulfate, was observed, supporting the incomplete lactate-to-acetate oxidation pathways.

At 45 days of incubation (where the microcosms showed greater heterogeneity among them), it was observed that the presence of the BPAS consortium reduced bacterial diversity, with a predominance of *Pseudomonas* and *Stenotrophomonas*. In addition, the presence of acetate, lactate and sulfate stimulated certain SRB, which could play a key role in the corrosion of the copper material. At 45 days, CuO formation was detected on all Cu-mCan surfaces, possibly due to oxygen trapped in the bentonite or H_2O reduction, while Cu_2S compounds (sulfide generation from bacterial metabolic activity) were only detected in microcosms where biogeochemical processes were more dominant.

The addition of 2 mM selenite [Se(IV)], as an inactive analogue of ^{79}Se present in the radioactive waste, affected the biogeochemical processes in the previously mentioned microcosms. The presence of this metalloid exhibit toxicity to some bacteria, reducing their metabolic activity, slowing down the dynamics of lactate, acetate and sulfate consumption and/or production. In addition, the presence of this metalloid affected bacterial diversity by increasing the presence of certain selenium-tolerant bacteria and affecting the abundance of some SRB. The formation of a thin layer of reddish coloration at the bentonite:supernatant interface in the microcosms, in addition to isolated spots in the bentonite, indicated the reduction of Se(IV) to elemental selenium [Se(0)]. Microscopic and spectroscopic techniques confirmed the reduction and immobilization of Se(IV) to amorphous Se(0) (*a*-Se). A mechanism was proposed in which Se(IV) is intracellularly

reduced to Se(0) in the form of nanospheres with amorphous allotropy (*a*-Se) that, once released to the extracellular space through cell lysis, could undergo transformation processes to crystalline structures of monoclinic selenium (*m*-Se), and subsequently, to the more thermodynamically stable and less toxic form: trigonal selenium (*t*-Se).

Overall, one of the main findings from this work is that microorganisms present in bentonite play a key role (whether beneficial, detrimental or neutral) in the evolution of the geochemical conditions of DGR, potentially influencing the stability of their various barriers. The results of this PhD Thesis provide new insights and better understanding of how microorganisms and related biogeochemical processes may impact the interaction between the copper canisters, Spanish bentonite and selenium. This newly generated knowledge is crucial to ensure the long-term safety and stability of DGR.

Sweden nuclear waste repository

Modified from Svensk Kärnbränslehantering AB (SKB) company

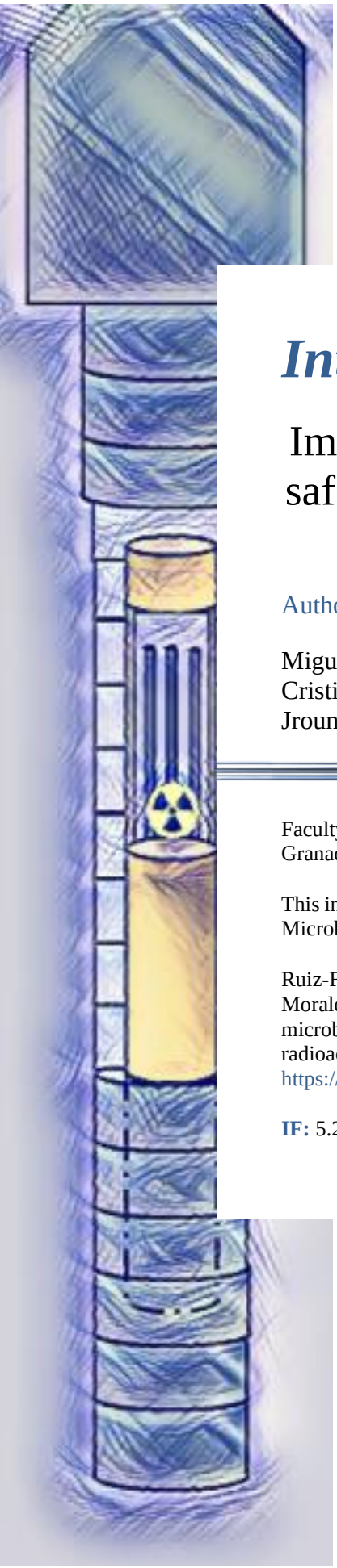

Introduction:

Impact of microbial processes on the safety of deep geological repositories for radioactive waste

Authors

Miguel A. Ruiz-Fresneda*, Marcos F. Martinez-Moreno, Cristina Povedano-Priego, Mar Morales-Hidalgo, Fadwa Jroundi and Mohamed L. Merroun

Faculty of Sciences, Department of Microbiology, University of Granada, Granada, Spain

This introduction section has been published as review article in Frontiers in Microbiology:

Ruiz-Fresneda, M. A., Martinez-Moreno, M. F., Povedano-Priego, C., Morales-Hidalgo, M., Jroundi, F., & Merroun, M. L. (2023). Impact of microbial processes on the safety of deep geological repositories for radioactive waste. Frontiers in Microbiology, 14, 1134078. https://doi.org/10.3389/fmicb.2023.1134078

IF: 5.2 / **Q**2

frontiers | Frontiers in Microbiology

Abstract

To date, the increasing production of radioactive waste due to the extensive use of nuclear power is becoming a global environmental concern for society. For this reason, many countries have been considering the use of deep geological repositories (DGRs) for the safe disposal of this waste in the near future. Several DGR designs have been chemically, physically, and geologically well characterised. However, less is known about the influence of microbial processes for the safety of these disposal systems. The existence of microorganisms in many materials selected for their use as barriers for DGRs, including clay, cementitious materials, or crystalline rocks (e.g., granites), has previously been reported. The role that microbial processes could play in the metal corrosion of canisters containing radioactive waste, the transformation of clay minerals, gas production, and the mobility of the radionuclides characteristic of such residues is well known. Amongst the radionuclides present in radioactive waste, selenium (Se), uranium (U), and curium (Cm) are of great interest. Se and Cm are common components of the spent nuclear fuel residues, mainly as ^{79}Se isotope (half-life 3.27 x 10^5 years), ^{247}Cm (half-life: 1.6 x 10^7 years) and ^{248}Cm (half-life: 3.5 x 10^6 years) isotopes, respectively. This review presents an up-to-date overview about how microbes occurring in the surroundings of a DGR may influence their safety, with a particular focus on the radionuclide-microbial interactions. Consequently, this paper will provide an exhaustive understanding about the influence of microorganisms in the safety of planned radioactive waste repositories, which in turn might improve their implementation and efficiency.

Keywords: *radioactivity, waste, deep geological repository, microorganisms, perspectives*

1_ Introduction

The risk associated to the generation and storage of radioactive waste produced by the activities of nuclear power plants is an environmental problem that must be seriously considered. It is well known that these kinds of residues contain radionuclide contaminated materials, which must be contained and managed for a long period of time until their radio toxicity decreases to natural levels. For this purpose, deep geological repositories (DGRs) have been proposed by many countries as the most immediate and safest option for their disposal. This multi-barrier system is based on the encapsulation of the radioactive waste in containers of steel, copper, titanium and nickel-based materials, which will be placed underground at depths of 500-1000 m (Hall et al., 2021; IAEA, 2018). In addition, the containers will be surrounded by engineered (bentonite clay, cementitious materials, etc.) and natural (host rocks) barriers for their mechanical, hydraulic, and thermal protection. Indeed, clay formations will play a crucial role in many DGR designs as a host rock and engineered barriers will be used in many countries, including France, Spain, Belgium, and Switzerland. Specifically in Spain, bentonite clay from the Cabo de Gata (Almería) has been selected as a reference material for the engineered barriers due to its well-characterized physical and geochemical properties (Villar et al., 2006).

A wide distribution of microorganisms has been previously reported in many materials selected to be used as barriers in the DGRs, including bentonite formations (Burzan et al., 2022; Mijnendonckx et al., 2021). Many studies have evidenced the role that many microbial processes may play in the corrosion of metal containers, on the clay mineral transformation, gas production, and the mobility of radionuclides present in radioactive waste (Beaton et al., 2019; Hall et al., 2021; Lopez-Fernandez et al., 2020). It is clear that microorganisms could threaten the safety of DGR systems. Several microbial mechanisms such as biotransformation, biosorption, biomineralization, and bioaccumulation are

thought to be involved, probably affecting the radionuclide migration behaviour throughout the repository. Among the radionuclides present in radioactive waste, selenium (Se), curium (Cm), and uranium (U) stand out as being of great interest. Selenium is a common component of the spent nuclear fuel present mainly as ^{79}Se isotope (half-life 3.27 x 10^5 years) (Hassan et al., 2021). Although other Se isotopes such as ^{75}Se (half-life 120 days) or ^{80}Se (stable isotope) can be found in radioactive residues, only ^{79}Se present in high-level radioactive waste is radiotoxic enough (betta particle emitter) to compromise long-term security (Abdalla et al., 2020). This element can exist in nature in different oxidation states: +VI, +IV, 0, and –II. Selenite (Se^{IV}) and selenate (Se^{VI}) are the most soluble and toxic forms, whilst elemental Se (Se^0) and selenide (Se^{-II}) are very insoluble. Cm is also a highly radiotoxic element present in nuclear spent fuel, mainly as ^{247}Cm and ^{248}Cm isotopes (Kooyman et al., 2018). The excellent luminescence properties of this element, as a representative of trivalent actinides (An^{III}), are suitable for the study of their chemical speciation at environmentally relevant concentrations. In the same way, europium (Eu), an inactive analogue of An^{III}, also provides excellent luminescence properties. This inactivity makes Eu a suitable element for speciation studies of An^{III}. Uranium is the main component of the spent nuclear fuel from nuclear plants constituting approximately 95% of their composition, (Kumari et al., 2020). Several radioactive isotopes of uranium, such as ^{238}U, ^{235}U, and ^{234}U, are known to have long half-lives (e.g., 4.47 x 10^9 years for ^{238}U) (Mitchell et al., 2013).

This review focuses on a fundamental understanding of the microbial processes including container corrosion, gas production, clay mineral transformation, and direct interaction with radionuclides, in the safety of DGRs. Therefore, it provides useful information in predicting the microbial impact on the performance of the radioactive waste repositories. Furthermore, knowledge about these underlying mechanisms could be essential for the development of effective and accurate bioremediation strategies.

2_ Radioactivity, nuclear energy and radioactive waste

Radioactivity is defined as the process by which certain chemical elements emit radiation because of the spontaneous decay of their atomic nuclei. This phenomenon is characteristic of unstable isotopes, which tend to directly or progressively decay in more stable isotopes, by producing the emission of high energy radiation (Porcelli, 2018). Radioactive isotopes, also known as radionuclides, can emit 3 different types of ionizing radiation: alpha (α), beta (β), and gamma (γ). Electromagnetic waves produced by unstable nuclei are known as gamma radiation. This is the highest penetrating ionizing radiation due to the lack of mass and charge and consequently, the most dangerous to living beings. Only very thick and electron dense materials can retain them. Radioactive contamination of natural habitats may cause detrimental effects on living organisms, depending on several factors, including radiation type, received dose, affected tissue, etc. In human beings, the main radioactivity effect is based on water radiolysis, which triggers the formation of hazardous free radicals due to the ionizing action of the emitted radiation. Free radicals could lead to structural changes in biomolecules, preventing the successful fulfilling of biological functions. For example, irrevocable changes in the chemical structure of DNA would result in different kinds of tumors.

Radioactive isotopes exist naturally in soils, rocks (such as Radon-222 (^{222}Rn)) and in the atmosphere (Porcelli, 2018; Kónya y Nagy, 2018). However, radioactivity is not unique to natural isotopes. Artificially produced radionuclides are much more abundant in the environment. These radioisotopes are mainly due to man-made activities, such as in medical applications in hospitals, research activities, and the nuclear power industry. One of the major global environmental risks associated to the use of these radionuclides derives from nuclear reactor accidents and nuclear waste management (Zhang et al., 2019). The large-scale release of radionuclides to the environment from nuclear activities may cause serious social

and environmental problems to society (Prăvălie y Bandoc, 2018). Since 1950, approximately 20 nuclear accidents have occurred in the world (Burns, 2012; Lelieveld et al., 2012), being that of Chernobyl on April 26, 1986, undoubtedly the biggest nuclear disaster ever known. To date, this catastrophic event has contributed to the highest release of radioactive material to the environment (Burns, 2012; UNSCEAR, 2013). Cesium-137 (^{137}Cs) and Iodine-131 (^{131}I) are examples of some of the most dangerous radionuclides emitted during that episode. Not all radionuclides have a deep impact on our lives, but some of them are especially hazardous due to their half-life, type of radiation emitted, concentration, etc. The study of trivalent actinides (An^{III}) such as curium (^{247}Cm, ^{248}Cm) or americium (^{242}Am), other actinides such as neptunium (^{237}Np) or uranium (^{235}U), and some significant radioisotopes of selenium (Se), is extremely important due to their high radiotoxicity (Hamed et al., 2017; Kooyman et al., 2018). Amongst all the An^{III}, curium (Cm) is one of the most studied. Cm is a very toxic radionuclide due to the α-activity of some isotopes, such as ^{247}Cm and ^{248}Cm, characteristic of spent nuclear fuel (Gorietti et al., 2017; Kooyman et al., 2018). Many of the studies focused on the study of Cm use europium (Eu) as an inactive analogous of An^{III}. This inactivity, together with its excellent luminescent properties, makes Eu an exceptional element for the study of An^{III} (Ansoborlo et al., 2007). Most of the Se radioisotopes have a short half-life ranging from 20 s, in the case of ^{77m}Se, to 120 days, in the case of ^{75}Se. The only one of special interest due to its high radioactivity and hazard to the environment and the long-term safety of future DGR, is ^{79}Se (Atwood, 2010). The radioisotope ^{79}Se presents a half-life of about 3.27×10^5 years and is mainly produced in the nuclear industry through fission reactions of ^{235}U and other radionuclides such as ^{239}Pu. As an artificial radionuclide, the only possible source of ^{79}Se in nature would be nuclear accidents or the release of nuclear waste to the environment.

The high global energy demand is considerably increasing nowadays, mainly due to demographic and industrial growth. Almost the total global energy is still

supplied by non-renewable sources such as fossil fuels and resources. This fact makes the development of renewable energies or new alternatives such as the nuclear power crucial. Despite the danger of nuclear reactors present, this low-carbon technology could be a great opportunity to minimize the consequences of global warming, one of the toughest environmental problems facing human society today (IAEA, 2015). Obviously, simultaneous strategies based on the establishment of renewable energies are crucial for this purpose. Despite the above mentioned comments, there is a continuous controversy about the use of nuclear energy due to the associated risk involved, such as environmental pollution and the generation and management of radioactive waste. The proper and safe storage of the nuclear residues produced implies a real threat to the environment because a completely safe solution is still non-existent. The IAEA, which is officially in charge of radioactive waste management, classify this in six different types (IAEA, 2009a):

- Exempt waste (EW): contains very low concentration of radionuclides, resulting in their exclusion from the regulatory control of radiation protection.

- Very short-lived waste (VSLW): contains very short half-life radionuclides that must be stored until the end of their radioactivity. It is mainly produced in hospitals and research centres.

- Very low-level waste (VLLW): waste containing a radioisotope concentration slightly higher than EW, which can be disposed in near surface landfill type facilities with limited regulatory control. These residues usually include natural radionuclides from soil, rocks, or the mining industry.

- Low level waste (LLW): includes limited amounts of long-lived radioisotopes, which requires isolation for periods of up to a few hundred years in near surface disposal.

- Intermediate level waste (ILW): waste including long-lived radionuclides in significant quantities to be stored in higher security levels than those provided by near surface facilities. Therefore, this type of residue requires to be isolated at greater depths ranging between tens to hundreds of metres.

- High level waste (HLW): contains large amounts of long-lived radionuclides and requires a greater degree of containment and isolation than ILW to guarantee long-term security. This type of residue is mainly composed of nuclear waste, which is the most hazardous one because of its radioactivity, which may persist for up to one hundred thousand years (Horvath and Rachlew, 2016). HLW generates significant quantities of heat as a result of the atomic nuclei decay of radionuclides. For this reason, heat dissipation is an important issue to be considered during the design of a repository for this kind of waste. Nowadays, the production of HLW is extremely alarming, since it is estimated that each nuclear reactor (approximately 440 operational worldwide) produces around 30 tons per year (Alwaeli and Mannheim, 2022; Gerstner, 2009; IAEA, 2009b; Rosa et al., 2010).

The high generation rate of radioactive waste is a major environmental concern that needs to be adequately solved as soon as possible. Reprocessing spent nuclear waste is an example to partially solve this problem. According to the IAEA, more than 5,000 tons are reprocessed every year (Handrlica, 2019; IAEA, 2009). However, it seems evident that this procedure is not enough to reduce the total volume of radioactive waste in the world. In the last few years, the global scientific and political consensus has determined the isolation of radioactive waste in deep

geological repositories (DGRs) as being the safest option for its long-term management (NEA, 2020a).

3_ Deep geological repository systems

The deep geological repository (DGR) concept was introduced in 1995 by the Nuclear Energy Agency (NEA) with the aim to safely isolate radioactive waste for long-term periods (NEA, 2020b). The DGR system is based on the disposal of radioactive waste at a depth of around 1,000 metres underground (**Fig. 1**). Multi-barrier systems composed of natural (soil, host rock, etc.) and artificial barriers such as metal canisters and filling/sealing materials are planned to properly isolate the residues (Ma et al., 2018). Clay, crystalline rock and salt deposits have been studied and selected as the best options for natural barriers due to their excellent physico-chemical properties (Ahonen et al., 2016). France, Belgium, and Switzerland have chosen clay formations as the preferred host rock option for their repositories, whilst crystalline rock (granite) has been selected by other countries such as Finland, Sweden, Canada, and the Czech Republic (Ahonen et al., 2016). However, the EEUU is considering salt deposits for their geological repository emplacements. Regarding the artificially engineered barriers, copper, steel, and concrete are planned to be used as canister materials, whilst cementitious materials and bentonite clay formations seem to have the best sealing capabilities. It is worth noting that all these materials would act as a protective shield against radiation (Abrahamsen et al., 2015). In these systems, an initial period with aerobic conditions is expected mainly for the introduction of oxygen accumulated during the construction of the disposal facility. However, after the closure of the repository, anaerobic and reducing conditions will prevail because of the low oxygen levels underground, the presence of specific electron donors and acceptors, and the dilution of reduced minerals (Duro et al., 2014). For all the above-mentioned reasons, DGR systems provide a stable environment, making them the

best solution for the long-term isolation of long-lived radionuclides characterizing HLW.

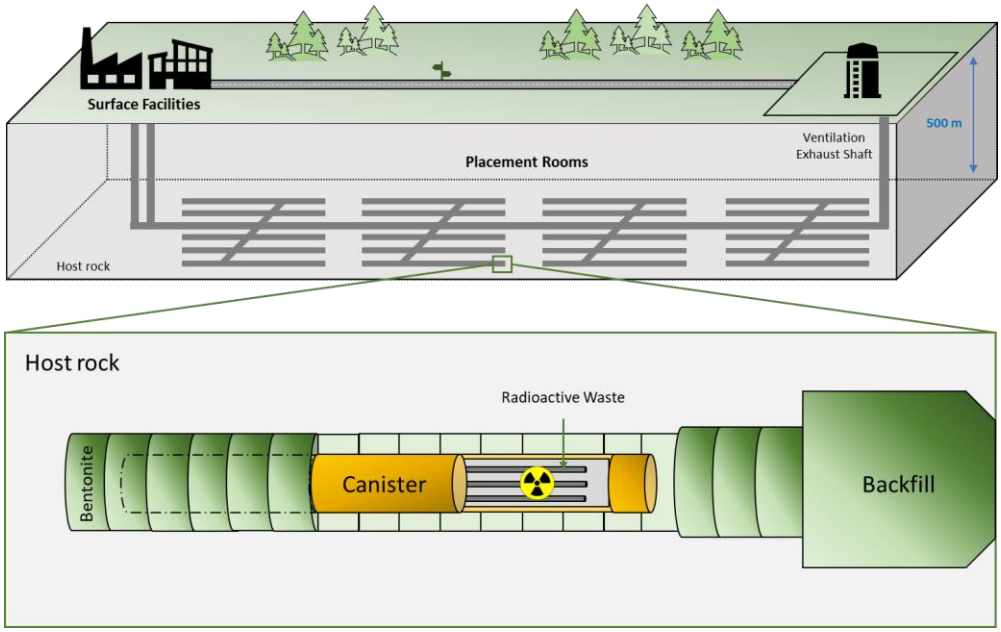

Figure 1. Diagram of the deep geological repository system according to the Nuclear Waste Management Organization (NWMO).

Nowadays, several countries are planning or have already started the construction of their own DGRs (NWMO, 2022). For example, The Netherlands, Ukraine or Spain are currently investigating the type of geology to be used (crystalline rocks, clays or salt deposits). The U.S. and South Korea governments have agreed to build a DGR facility, but they are still in the early planning stages. The *Nuclear Waste Management Organization* (NWMO) of Canada is currently studying about the crystalline and sedimentary site selection both in the province of Ontario. Similarly, the *Nuclear Waste Management Organization of Japan* (NUMO) has an active program for the site selection. Further, China has announced the pre-selection of a national plan for the storage of radioactive waste in granite geological areas in the Gansu province. Switzerland has also already selected the location of its DGR (north of Zürich), but still expects to submit a licence application by 2026. France, one of the biggest nuclear energy producers, is

designing through the *Agence Nationale pour la gestión des Déchets Radioactifs* (ANDRA), a DGR called Cigéo over a clay rock emplacement to the east of the country. Licence applications are still being prepared for Cigéo and its construction is programmed to begin as early as 2023. Similarly, the Swedish government has recently granted permission to the SKB company to build a deep disposal approximately around the mid-2020s with final disposal structure expected to be finished around 2030. The most advanced country in this respect is Finland, where the Onkalo Facility is expected to begin operating in 2025. The Onkalo DGR will be the first in the world to start the final disposal of spent nuclear fuel. The objective is to store HLW and ILW using a system based on cementitious materials for both containers and sealing materials.

4_ Diversity and influence of microorganisms in DGR systems

Microorganisms are widely described for their ability to colonize almost every single habitat on earth, and DGRs are no exception. The high diversity of microorganisms in geological formations selected for their optimal use in the disposal of radioactive waste such as clay, granite, and saline deposits, have been reported (Bachran et al., 2018; Lopez-Fernandez et al., 2018a; Lopez-Fernandez et al., 2021a). Many studies not only about microbial diversity, but also the activity and influence of biochemical processes on the safety of these systems are currently on-going. In those countries where clay has been chosen for their respective DGRs, there have been recent studies. This is the case of Opalinus clay in Switzerland, Boom clay in Belgium, Cavallo-Oxfordian in France, and bentonite clay in Spain (Burzan et al., 2022; Mijnendonckx et al., 2021; Povedano-Priego et al., 2021; Shrestha et al., 2022). Bentonite clay formations have been described as a reference material for their use as artificial barriers in DGRs due to their excellent mineralogic, physic-chemical, mechanistic, geochemical and hydraulic properties (Villar et al., 2006). Specifically, they present low permeability (decrease in groundwater filtrations), mechanical support (provide stability against container

weight), high ion exchange capacity (radionuclide retention), high plasticity, swelling capacity (self-sealing of cracks), thermal conductivity, and optimal compaction properties (García-Romero et al., 2019). The results obtained by Lopez-Fernandez et al. (2018b; 2015; 2014) revealed the high microbial diversity in bentonite formations from the Cabo Gata (Almería, Spain). Most of the species identified correspond to facultative and obligate aerobic microorganisms. Some of them have been previously described for their ability to interact with radionuclides and heavy metals characteristic of radioactive waste. This is the case of bacterial genera such as *Acidovorax, Variovorax, Pseudomonas, Stenotrophomonas*, and *Ralstonia* (Choudhary and Sar, 2009; Gerber et al., 2016; Hedrich et al., 2011; Hupert-Kocurek et al., 2013; Ruiz Fresneda et al., 2018; Ruiz-Fresneda et al., 2020a). Indeed, the bentonite-isolate bacterium *Stenotrophomonas bentonitica*, exhibits a great versatility and capacity to interact with different elements such as Se^{IV}, Cm^{III}, or U^{VI} through different microbial mechanisms (Lopez-Fernandez et al., 2014; Ruiz Fresneda et al., 2018; Ruiz-Fresneda et al., 2020b; Ruiz-Fresneda et al., 2019). Opalinus clay from the Mont Terri rock laboratory (Canton Jura, Switzerland) also shows the presence of relevant microbial activity. Although there are limited conditions for microbial survival in Opalinus clay, a rich and diverse group of microorganisms seem to be ubiquitous. This suggests that many microorganisms could have been introduced mainly as a result of anthropogenic activities including construction, operational activities and experimental installations and also due to natural geological processes such as water infiltration, landslides, fissures, etc. Specifically, sulphate-reducing bacteria (*Desulfosporosinus, Desulfotomaculum, Desulfocapsa*), nitrate- and nitrite-reducing bacteria (*Pseudomonas, Thiobacillus, Acidovorax)* and other bacterial genera *(Pleomorphomonas, Peptococcaceae*, *Sphingomonas*) have been found (Leupin et al. 2017). Another clay type that has been investigated in depth is Boom clay, considered as a potential host formation in Belgium. Mijnendonckx et al. (2019, 2022) detected the presence of methanogenic Archaea, such as

Methanobacterium alcaliphilum and *Methanomassiliicoccus luminyensis*, nitrate-reducing bacteria (*Acidovorax*, *Simplicispira*, *Hydrogenophaga*), or sulphate reducing bacteria (*Pseudomonas*), amongst others.

To summarize, most certainly the DGR systems will not be sterile environments. Not only will indigenous microorganisms from soils, barriers and different materials be present, but also allochthonous microbes introduced accidentally during the construction of the repositories. Although the conditions will not be the best for microbial growth, it should be emphasized that the presence of nutrients, electron donors and acceptors, carbon and nitrogen sources will help the development and metabolic activity of the microorganisms. Even in the presence of ionizing radiation, some microorganisms from sediments have been described to be able to tolerate dose rates representative of gamma radiation emitted from radioactive waste (Brown et al. 2015). Not only microorganisms, but also components of these sediments such as Fe^{III}, NO_3^-, or SO_4^{2-} can remain active. Anyway, some microorganisms can immobilize radioactive isotopes through passive processes (biosorption, bioaccumulation, etc.), even if they do not survive radiation (see section 4.4)

Sulphate reducing, nitrate-reducing, methanogens, iron-reducing, metal-resistant, and other microorganisms will potentially affect the environment and hence the safety of the DGRs through different processes including gas production, metal corrosion, modification of the redox conditions, mineral clay transformation, and radionuclide interaction. For all the above-mentioned reasons, microorganisms must be considered when evaluating the security level of DGRs.

4.1_ Corrosion of the metal canisters.

Bacteria can adhere to the surface of different inorganic matrices through the production of extracellular polymeric substances (EPSs) promoting bio-corrosion, known as microbially influenced corrosion (MIC) of materials such as steel,

copper, concrete, etc. (Kip and Van Veen, 2015). MIC could be mediated by the direct or indirect action of electrochemical reactions conducted by microorganisms (Videla and Herrera, 2009). Within the concept of the DGRs, the oxygen will be gradually consumed after their closure, so an anoxic environment will be predominant (Rashwan et al., 2022). Under these DGR conditions, sulphate-reducing bacteria (SRB) could obtain energy through the reduction of sulphates or other oxidised inorganic sulphur compounds, resulting in sulphide production (H_2S). This is one of the most important biogenic corrosive compounds in the DGR environment and it accelerates the corrosion rate of metal canisters (Bagnoud et al., 2016a).

The nature of the metal canister to be used depends on the DGR concept of each country. Copper (e.g., Canada, Finland, and Sweden) and steel-based materials (e.g., Belgium and the Czech Republic) are the predominant options for the canisters. Regarding steel-based material, Enning and Garrelfs (2014) reported the SRB contribution to the corrosion of this material through two main mechanisms: electrical microbially influenced corrosion (EMIC), and chemical microbially induced corrosion (CMIC) (**Fig. 2**). EMIC is a direct mechanism where SRB are involved in the speed up of abiotic corrosion. In this process, specially adapted SRB pull out electrons from elemental iron leading to the disposition by means of electro-conductive iron sulphides and releasing excess electron acceptors such as H_2 (**Fig. 2A**). On the other hand, CMIC is the indirect mechanism that results from the sulphidogenic degradation of organic matter under oxygen-free environments resulting in the production of biogenic and corrosive sulphide which reacts with the metallic iron (**Fig. 2B-C**). Furthermore, the biogenic formed hydrogen sulphide can cause sulphide stress cracking of the iron (**Fig. 2D**). FeS may, temporarily, act as a protective action against iron corrosion as it is strongly adhered to the metal surface through the direct reaction of the dissolved sulphide with metallic iron (Newman et al., 1992; Sun and Nešic, 2007). Several studies have reported MIC on steel-based materials by the activity of SRB. Xu et al. (2008) detected the

presence of kansite (Fe_9S_8) and pitting corrosion in stainless steel in the presence of *Desulfovibrio* sp. and *Leptothrix* sp. Hajj et al. (2010) found mackinawite (FeS_x) on P235H steel mediated by the activity of extremophiles and spore-forming SRB such as *Desulfosporosinus* sp., *Desulfotomaculum* sp., and *Thermosubterraneum* sp. The generation of biogenic mackinawite was also reported by Černoušek et al. (2019) when carbon steel MIC with *Desulfomicrobium* sp. and *Desulvibrio* spp. was studied. It should be noted that, although this review focuses on the SRB group, other bacterial communities can promote the steel-based material corrosion processes. Shrestha et al. (2021) highlighted the key role of nitrate-reducing bacteria (NRB), such as *Methyloversatilis*, *Pseudomonas* and *Brevundimonas*, related to carbon steel corrosion since they could be involved in the formation of corrosion compounds such as magenetite, mackinawite ($FeS_{(1-x)}$), akageneite ($Fe^{3+}O(OH, Cl)$) and rozenite ($Fe^{2+}SO_4 \cdot 4(H_2O)$). All these authors concluded that the biofilm formation promotes and accelerates the corrosion.

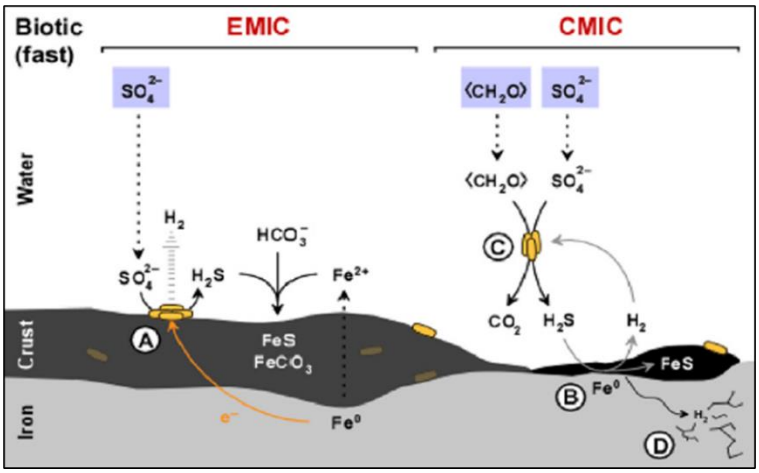

Figure 2. Diagram of the influence of sulphate-reducing bacteria (SRB) activity in the corrosion of iron. (A) Electrical microbially influenced corrosion (EMIC) mechanism. (B) Chemical microbially influenced corrosion (CMIC) mechanism. (C) Overall representation of CMIC. (D) sulphide stress cracking. Modified from Enning and Garrelfs (2014).

As in the case of steel-based materials, sulphide is the main corrosive agent of copper materials. According to Dou et al. (2020), H_2S produced by SRB cause uniform corrosion accompanied by pitting corrosion of Cu (high concentration of

H_2S) or intergranular corrosion of this metal (low levels of H_2S). In this study, the dissimilatory reduction of sulphate mediated by SRB produced HS^- from the secreted H_2S. This metabolite can be decomposed to H^+ and S^{2-} or when combined with H^+ forms H_2S. The HS^- diffuse to Cu surface and reacts with it resulting in Cu_2S (**Fig. 3**). Chen et al. (2011) described the different phases of the anaerobic corrosion of Cu starting with the formation of a chemisorbed Cu^I surface state acting as a precursor to forming a film. In the presence of SH^- in the medium, it can bind to Cu producing the chemisorbed species of Cu $(SH)_{ads}$. SH^- can then react with the Cu surface and the adsorbed species leads to the beginning of the formation of a Cu_2S film with partial protective capacity. In presence of Cl^-, it can react with the surface intermediate Cu $(SH)_{ads}$ forming a chloride complex ($CuCl_2^-$). This compound can lead to Cu^+ transport through the pores to the Cu_2S/solution interface and react with SH^- to form Cu_2S. Several studies have shown the presence of chalcocite (Cu_2S) (Kurmakova et al., 2019; Chen et al., 2014; Pedersen, 2010) and surface pits (Chen et al., 2014) on the surface of oxygen-free copper under anaerobic conditions mediated by SRB.

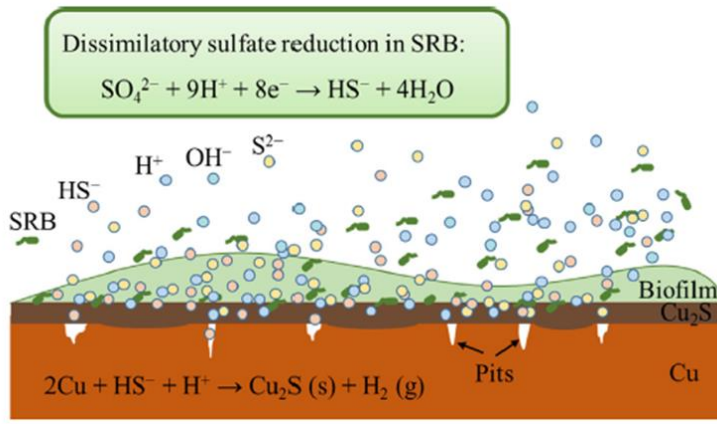

Figure 3. Schematic representation of copper corrosion mediated by sulphate-reducing bacteria (SRB) activity. Obtained from Dou et al. (2020).

As we have seen, the MIC rate of each material mainly depends on the presence of the sulphide produced by the activity of anaerobic microorganisms such as SRB.

In a DGR, the corrosion of metal canisters will probably depend on the sulphide concentration at the boundary between the groundwater and the compacted bentonite (Bengtsson and Pedersen, 2016). Moreover, MIC may not only affect the release of radionuclides from canister, but could also be involved in gas production within the DGR system, which will be discussed in the next section.

4.2_ Gas formation by microorganisms.

As mentioned before, a wide variety of organic and inorganic compounds present in the DGR environment will provide nutrients, electron donors and acceptors, carbon, nitrogen, and sulphur sources which would enhance microbial activity. Not only some physicochemical processes such as corrosion of metal canisters or the radiolysis of water, but also microbial metabolism may contribute to the build-up of a gas phase in DGR environments (Guo and Mamadou, 2021). Gas accumulation derived from microorganisms is mainly produced in form of hydrogen (H_2), methane (CH_4), and carbon dioxide (CO_2), and can lead to an increased pressure within the repositories, compromising the integrity of the clay as barriers (Bagnoud et al. 2016b).

H_2 generation is one of the main gaseous sources within DGRs and may be conducted by the anoxic corrosion of the metal canisters, radiolysis of water, and diverse microbial activities (Hall et al. 2021; Beaton et al. 2019). Although the production of this gaseous form can increase the pressure level, some microorganisms can use it as a source of energy for microbial growth by means of methanogenesis or sulphate reduction (Grigoryan et al., 2021; Hall et al., 2021). CH_4 can be produced through microbial methanogenesis through reactions between H_2 or H_2O and inorganic carbons (CO_2 and CO) or acetate fermentation (CH_3COOH) (**Eq.1 and 2**) (Abramova et al., 2023; Chen et al., 2019). Methanogenesis is assumed to decrease gas pressure in DGR surroundings by consuming both CO_2 and H_2 (**Eq. 1**) (Beaton et al., 2019; Leupin et al., 2017).

However, the production of both CH_4 and CO_2 derived from aceticlastic methanogenesis (**Eq. 2**) could play the opposite role.

(1) $4\ H_2 + CO_2 \rightarrow CH_4 + 2\ H_2O$

(2) $CH_3COOH \rightarrow CH_4 + CO_2$

Recently, metagenomic and metaproteomic analyses on the microbial community present in Opalinus clay under DGR simulated conditions, have been performed to determine the role of microbial metabolic pathways on the safety of DGRs. These analyses indicate the high contribution of the bacterial genus *Pseudomonas*, as an SRB, in the oxidation of H_2 coupled with sulphate (SO_4^{2-}) reduction (**Eqs. 3** and **4**) (Bagnoud et al., 2016a; Smart et al., 2017). SRB from the family *Peptococcaceae* also appear to be involved in the formation of H_2S as a result of the respiration of sulphates and CO_2 from the oxidation of acetates and other organic compounds (**Eq. 5**) (Bagnoud et al., 2016a). Finally, the CO_2 produced as a result of some of the biochemical reactions mentioned above can dissolve in pore water, precipitated through its interaction with cementitious materials or diffused in a gaseous form, depending on the area where it is produced within the storage facilities (Bagnoud et al., 2016a).

(3) $SO_4^{2-} + 4\ H_2 \rightarrow H_2S + 2\ OH^-$

(4) $SO_4^{2-} + 4\ H_2 \rightarrow S^{2-} + 2\ H_2O$

(5) $SO_4^{2-} + CH_3COOH \rightarrow H_2S + 2\ HCO^{3-}$

As commented in previous sections, the presence of methanogenic and sulphate-reducing microbes has been detected in several clay types that will be used in DGR systems. For this reason, it is crucial to investigate in depth the influence of their metabolism on the safety of deep disposal. As different gases are consumed and produced during all these mechanisms, it is important to quantify the in-situ rates of microbial H_2 oxidation and SO_4^{2-} reduction to determine the total net production of gases. The calculations of Bagnoud et al. (2016c) concluded that sulphate-

reducing microorganisms from Opalinus clay could be beneficial for the safety of the geological disposal of nuclear waste as indicated by high hydrogen and sulphate consumption rates, which would reduce the gas pressure build-up. However, it is not easy to estimate the overall role of microbes in terms of security since very different chemical, biological, and physical processes may be involved. For instance, the removal of sulphate gases by SRB may induce steel corrosion of the containers through the production of H_2S or sulphides (S^{2-}) as we discussed in Section 4.1.

To sum up, microorganisms could both positively and negatively influence the safety of DGRs as far as the utilization and production of gases is concerned. However, it is extremely difficult to determine their overall impact due to the complexity of the biogeochemical processes that will be involved. In addition, the final role of microorganisms in terms of gas production will depend partly on the microbial community structure present in the natural and artificial barriers surrounding the canisters. Further research on microbial metabolism and gas formation is crucial to evaluate the safety conditions of DGRs.

4.3_ Bentonite biogeochemical transformations

One of the materials selected as an artificial filling and sealing barrier by current DGR models is bentonite, a volcanic origin phyllosilicate. This type of clay is mainly composed of smectites, highlighting montmorillonite as the principal mineral phase. Montmorillonite is characterized by a layered structure consisting of each one of 3 sheets in a 2:1 ratio, i.e., two tetrahedral silica sheets bordered in between them by an octahedral aluminium sheet (T-O-T structure). These layers have a negative charge balanced by cation exchange, providing the bentonite with most of its physico-chemical properties (Abdullahi and Audu, 2017; García-Romero et al., 2019). Bentonite from multiple locations has been widely studied as a buffer material for DGRs (MX80 from USA, FEBEX from Spain, FoCa from France and GMZ from China, amongst others) (Xu et al., 2019).

Both abiotic (temperature, radiation, etc.) and biotic factors could compromise the stability of the bentonite barrier and therefore jeopardize the safety of the system. During the first phases of the repository, high temperatures are expected to be reached due to the heat generated by the decay of the stored radionuclides (Tripathy et al., 2017). The heat would diffuse throughout the repository reaching up to 100-200ºC in the bentonite buffer with a maximum temperature gradient of up to 24ºC, over a thickness of about 35 cm (Faybishenko et al., 2017; Zhen et al., 2017; Hökmark and Fälth, 2003). Smits et al., (2013) supported that an increase in temperature means an increase in thermal conductivity, probably due to an additional heat transfer as latent heat. However, this temperature effect decreases with high bentonite dry density. High temperatures are also a matter of great concern as they could lead to an abiotic smectite illitization process. Mills et al., (2022) discussed a possible mechanism of illitization at 200°C that would occur through a layer-by-layer transformation. The individual phyllosilicate layers are enriched in charge due to the substitution of Si by Al in the tetrahedral sheet, the substitution of Al by Mg in the octahedral sheet and an interlayer cation exchange of K^+ by Na^+ resulting in the formation of mixed illite/smectite layers. This phenomenon results in chemical alterations which could affect bentonite properties such as swelling and plasticity capacities (Zhen et al., 2017). In addition to temperature, bentonite will inevitably be exposed to certain doses of ionizing radiation, mainly gamma (from Cs-137). Many studies have focused on characterizing the effect of γ-radiation on this clay and reported only negligible effects on the alterations of its physical and chemical properties (Huang and Chen, 2004; Plötze, 2003; Pushkareva et al., 2002). However, Holmboe et al., (2011) tested the effect of this radiation on the ability of MX80 bentonite to retain radionuclides such as Cs^+ and Co^{2+}. Only Co^{2+} sorption was significantly affected by γ-radiation, which decreased in the irradiated samples. This result could indicate that this kind of irradiation would have altered surface characteristics thus decreasing its ability to bind this radionuclide. However, some authors have

reported the stability of bentonite mineralogy when treated with different solutions (e.g., distilled water, sodium nitrate, glycerol-2-phosphate, and uranyl nitrate) after six months of aerobic incubation (Povedano-Priego et al. 2019). XRD semi-quantitative estimation showed the same composition of smectite, quartz, phyllosilicates, and plagioclases. Smectite represented the dominant mineral phase with 91%. Similar results were obtained for bentonite microcosms incubated for six months but under anoxic conditions, which indicates the stability of bentonite and no illitization process under different short-term incubation (Povedano-Priego et al. 2022).

However, the present review focus mainly on biotic factors related to the presence of microorganisms in the different barriers. One of the main concerns related to bentonite buffer is the ability of microorganisms to interact with the minerals causing weathering, dissolution and a second mineral formation (Meleshyn, 2014). In particular, smectite biotransformation into illite through Fe (III) bio-reduction is one of the most alarming processes. Pedersen et al., (2017) reported that both the hydrogen sulphide produced by SRBs (Masurat et al., 2010), and Fe (II) generated by iron-reducing bacteria (IRB) could lead to a possible illitization process that would alter the properties of the smectite. Furthermore, Kim et al. 2019 studied the ability of the strain *Shewanella oneidensis* MR-1 to induce smectite dissolution by Fe (III) bio-reduction processes. Numerous studies reviewed by Dong (2009), demonstrated the bioreduction of Fe (III) by microorganisms in clay minerals. The iron bioreduction rate was related to different factors, including total Fe content in the bentonite, particle size, amount of microorganisms present, pH, etc. (Lopez-Fernandez et al., 2021a).

4.4_ The influence of microorganisms in radionuclide mobilization/immobilization

Radionuclides cannot be entirely removed, but they can be transformed to lower toxicity forms. Microorganisms are known for their capacity to do so, largely due

to their high tolerance to toxic elements and other stressful conditions including radiation, desiccation, and the presence of oxidative agents (Brim et al., 2000). A wide variety of bacteria have been previously described to efficiently resist toxic elements such as uranium, nickel, copper, cadmium, selenium, cesium, strontium, etc., including those belonging to the genera *Bacillus, Pseudomonas,* or *Stenotrophomonas* (Ruiz-Fresneda et al., 2023; Fakhar et al., 2022).

Microbial activity can indirectly influence solubility and hence the mobilization of radionuclides by the alteration of the geochemical conditions within the DGRs (pH, oxidation-reduction potential, etc.). Such modifications can lead to changes in the oxidation state of some radionuclides, affecting their solubility and mobility through the repositories. However, microorganisms can directly influence the mobility of radionuclides and other elements through different processes such as intracellular accumulation, biotransformation (redox reactions) biosorption, or biomineralization (Martinez-Rodríguez et al., 2022; Ruiz-Fresneda et al., 2020a; Lopez-Fernandez et al., 2021b; Shukla et al., 2017) (**Fig. 4**).

Biotransformation occurs when a specific element changes its oxidation state as a result of microbial activity through redox reactions and can lead to changes in its solubility (Francis and Nancharaiah, 2015). The bioreduction of soluble and mobile oxidized forms can trigger their immobilization (Rui et al., 2013). Enzymatic reduction of radionuclides and other toxic elements by bacteria have been widely reported in recent years. Several bacterial species are able to anaerobically reduce the soluble form U^{VI}, to the insoluble U^{IV}, by using U^{VI} as the final electron acceptor (Kolhe et al., 2018). Bacterial genera such as *Geobacter, Desulfovibrio, y Shewanella* are remarkable bacterial genera in uranium reduction (Cologgi et al., 2014; Grouzdev et al., 2018; Stylo et al., 2015). The bioreduction of oxidized forms of other elements have also been described. Se^{VI} and Se^{IV} can be reduced to less mobile forms (Se^{0} and Se^{-II}), amongst others, by the genera *Bacillus* and *Stenotrophomonas* (Kora, 2018; Lampis et al., 2017; Ruiz-Fresneda

et al., 2020a; Tan et al., 2016). Volatilization is another biotransformation process considered as a rising green process because of it generally implies the production of non-toxic compounds through reduction and methylation reactions.

Biosorption can be defined as the binding of positively charged metal ions to negatively charged cell surface components through physico-chemical interactions (Gadd, 2004; Prakash et al., 2013). Specifically, it can occur by electrostatic interactions, ionic exchange, or complexation and chelation processes (Diep et al.,

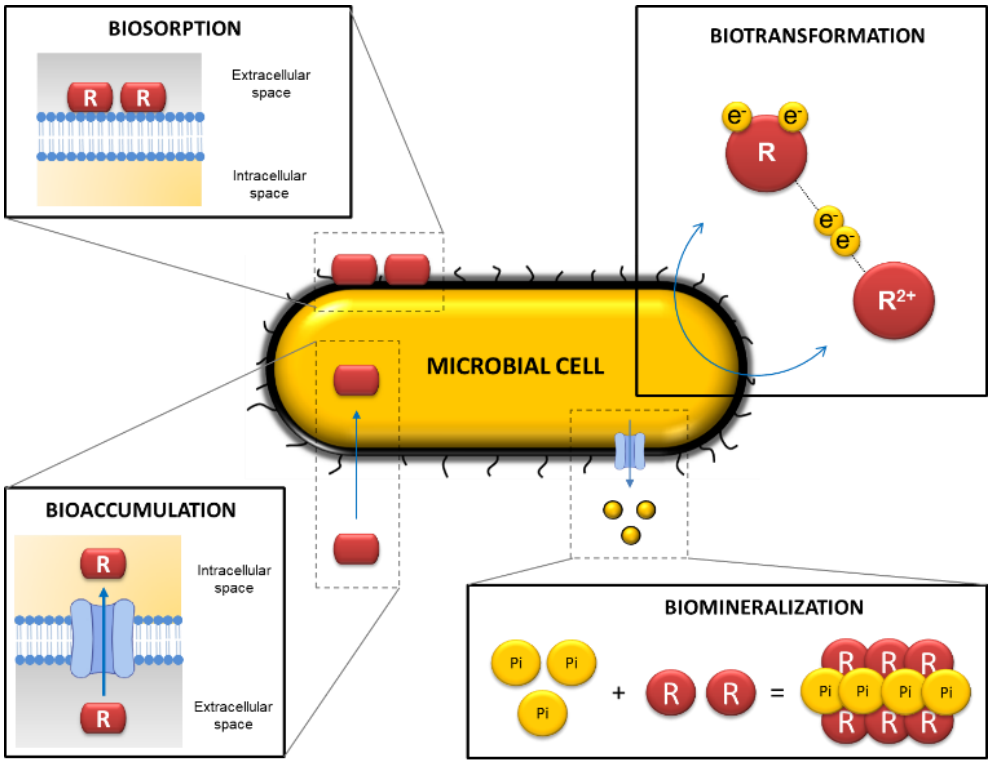

Figure 4. Representative diagram illustrating the main microbial mechanisms involved in radionuclide and heavy metal mobilization. R=radionuclide/ligand

2018; Yang et al., 2015). For this reason, biosorption is considered a passive process and can even take place with cellular fragments (cell membranes, cell walls, etc.) and dead microbial biomass (Ayangbenro and Babalola, 2017; Fomina and Gadd, 2014). Biosorption can act directly between metal cations and anionic

functional groups from cell walls, or indirectly with extracellular polymeric substances (EPS), S-layer proteins, and the bacterial capsule (Dobrowolski et al., 2017; Merroun et al., 2005).

According to Tabak et al. (2005), bioaccumulation consists of accumulating a specific substance or element inside an organism. In contrast to biosorption, intracellular accumulation is usually considered a metabolically active process, in which microorganisms introduce radionuclides or other elements into the intracellular space by using a transport system or altering the permeability of the membrane (Diep et al., 2018). However, some authors indicate that bioaccumulation is closely related to biosorption, since it requires fast interactions with anions from components of the cell surface before being introduced into the intracellular space (Tišáková et al., 2013). For this reason, other authors have considered that intracellular accumulation can occur through both passive sorption (metabolism-independent) and active uptake (metabolism-dependent). Once the radionuclide is inside, it can be sequestered by proteins, packaged in lipid membranes, vacuoles, or different biological storage systems (Mishra y Malik, 2013).

Bioprecipitation is based on the precipitation of elements with ligands (phosphates, sulphides, carbonates, hydroxides, etc.) released by microorganisms resulting in the production of insoluble and immobile complexes (Sreedevi et al., 2022; Shukla et al., 2017). Some bacterial species from the genera *Sphingomonas, Bacillus* and *Stenotrophomonas* have the capacity to release inorganic phosphates (Pi) through phosphatase activity, which precipitates with U^{VI} and produce insoluble uranium phosphates (Zhong et al. 2021; Sánchez-Castro et al. 2020; Chandwadkar et al., 2018; Zhang et al., 2018). When the complex formed is a mineral this bioprecipitation process is called biomineralization (Kolhe et al., 2018). It is important to note that the metals or radionuclides precipitated as a result of this

process do not present any change in their oxidation states, unlike other processes formerly described, such as biotransformation.

Tolerance of microbes to radiation must be considered of particular interest in microorganism-radionuclide interaction. It is well known that radiation can both directly and indirectly affect bacterial biomolecules, including nucleic acids, proteins, lipids, and carbohydrates. For instance, ionizing particles produced as a consequence of radioactivity can damage the DNA structure, disrupting the functionality of the DNA (Close et al., 2013; Jung et al., 2017). Ionizing radiation can also indirectly damage the microbial DNA and other molecules by production of reactive oxygen species through the radiolysis of water, as discussed in Section 2. To neutralize radiotoxicity, microorganisms have developed defence mechanisms, such as the production of regulatory secondary metabolites, DNA repairing machineries, anti-oxidative systems, etc. (Gabani and Singh, 2013). This is the case of ionizing radiation-resistant bacteria such as *Deinococcus radiodurans*, which tolerate high radiation doses (12 kGy), *Kineococcus radiotolerans* (2 kGy), or *Rubrobacter radiotolerans* (1 kGy), amongst others (Jung et al., 2017). However, microorganisms do not implicitly need to tolerate high radiation doses to play a positive role in DGR safety. As mentioned before, radionuclide biosorption is an electro-chemical passive process, in which the cells do not have to be viable to successfully interact with the radionuclides. Even when the viability is almost non-existent in a bacterial population, their metabolism could remain active under stress situations. Indeed, some studies have revealed that less than 2% of the cells of the bentonite isolate *S. bentonitica* are viable under DGR simulated conditions (anaerobiosis, Se^{IV} stress, etc.) after 6 days' incubation, but more than 50% remain metabolically active and interact with Se^{IV} through its biotransformation to Se^{0} (Ruiz-Fresneda et al., 2019). In addition, radiation will be strongly attenuated and absorbed in the proximity of the DGRs overtime and the help of insulating materials and multi-barrier systems. Nevertheless, when we do not specifically know when the interaction may occur (whether the radiation is

active or not), we must study as many conditions as possible in all the interaction cases.

5_ Interaction mechanisms between microorganisms and relevant radionuclides

Despite heavy metal-bacteria interaction having been studied in depth during the last decades, not many studies have been reported in relation to the possible role of these interactions influencing the safety of DGRs in the case of a radionuclide escape. A lot of effort has been put into very interesting studies which have been published in recent years with the aim of elucidating as far as possible how microbial processes can affect the mobility of elements of interest present in radioactive waste. These studies will allow us to evaluate how microorganisms can positively or negatively affect the safety of future DGRs. In this review, we have focussed on Se, as one of the critical radionuclides of radioactive waste, and some representatives of trivalent actinides, such as Cm and their inactive analogues (trivalent lanthanides such as Eu).

5.1_ Microbial interactions with selenium

Microorganisms can interact with Se mainly through biochemical biotransformation processes. There are many which are capable of transforming different species of Se by means of reduction-oxidation (redox) reactions, methylation, and demethylation processes (Eswayah et al., 2016). The microbial reduction of oxidized and soluble forms of Se (Se^{VI} and Se^{IV}) to insoluble Se^{0} has been previously described by bacteria of the genera *Bacillus, Shewanella, Comamonas, Stenotrophomonas, Azospirillum,* and *Pseudomonas,* amongst others (**Fig. 5**) (Baggio et al., 2021; Kora, 2018; Staicu et al., 2022; Vogel et al., 2018; Ruiz-Fresneda et al., 2023). Currently, the number of known Se^{VI} reducing strains is lower than that of Se^{IV} reducing ones. The mechanism of reduction of Se^{VI} varies amongst the microorganisms studied to date. Some bacterial species such as *Thauera selenatis* and *Seleniivibrio woodruffii* are able to respire Se^{VI} when using

it as an electron acceptor (Mohapatra et al. 2022; Rauschenbach et al., 2013). On the other hand, some enzymes such as selenate reductase have shown their ability to reduce Se^{VI} in strains such as *Comamonas testosteroni* S44 (Tan et al., 2018). The reduction of Se^{IV} can also be carried out through different enzymatic mechanisms. Nitrite reductase, sulfite reductase, fumarate reductase and selenite reductase seem to be involved in this process (Wang et al. 2022; Song et al., 2017; Wang et al., 2018). Furthermore, compound-mediated reactions with thiol groups (-SH) have also been studied. The participation of glutathione (GSH) in the reduction of Se^{IV} has been investigated with special interest. Kessi andHanselmann (2004) found that GSH and the enzyme glutathione reductase (GR) are involved in the reduction of Se^{IV} to Se^{0} in *Rhodospirillum rubrum* through a series of reactions. Recently, the studies of Wang et al. (2022) conducted with the strain *Proteus penneri* LAB-1 support this mechanism by suggesting that the gluthathione pathway plays a critical role in the Se^{IV} reduction process carried out by this bacterium.

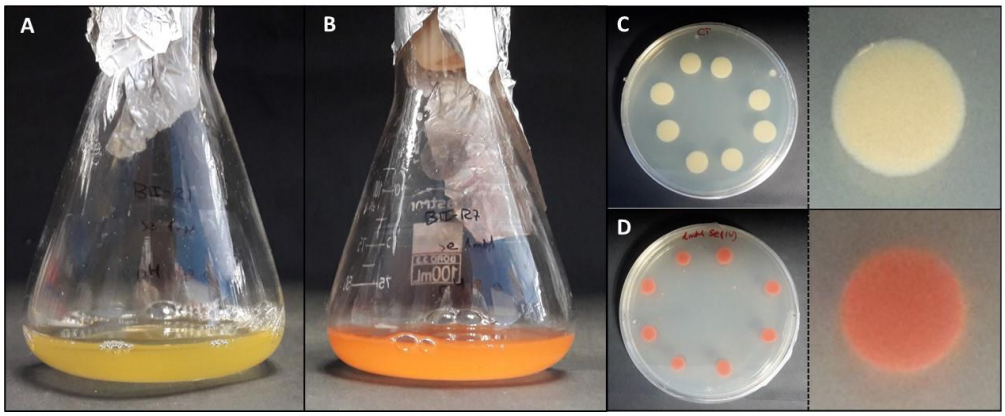

Figure 5. Colourful transition of liquid (A-B) and solid (C-D) cultures of the bacterium *Stenotrophomonas bentonitica* to red Se^{0} when Se^{IV} is added (personal archive of Dr Merroun).

In most cases, the reduced Se^{0} products are accumulated in the form of selenium nanoparticles (SeNPs), known for their use in numerous medical and industrial applications (Zambonino et al. 2021). These nanoparticles are characterized by different physico-chemical properties (morphology, size, structure, etc.), that

could affect their solubility and mobility in the environment (Jain et al., 2017). For example, *Bacillus subtiliis* BSN313, *Bacillus mycoides* SeITE01, and *Stenotrophomonas maltophilia* SeITE02 are able to produce Se spheres with an amorphous nature at the nanoscale (Ullah et al. 2021; Bulgarini et al. 2021). The studies by Benko et al. (2012) demonstrated the lower toxicity of Se nanospheres compared to the oxidized forms (Se^{VI} and Se^{IV}). However, there is some controversy in this respect since different studies have indicated completely the opposite (Li et al., 2008). The formation of Se nanowires by microorganisms present in anaerobic granular sludge has also been proved by Jain et al. (2017). These authors have described the lower colloidal stability and mobility of these nanostructures compared to biologically produced nanospheres. On the other hand, the crystallinity of some Se nanostructures also seems to affect their immobilization by increasing their settleability (Lenz et al., 2009).

Some studies have revealed the presence of organic matter layers, composed mainly of proteins and polysaccharides surrounding the biologically produced Se nanostructures (Bulgarini et al. 2022; Dobias et al., 2011; Kamnev et al., 2017). The physico-chemical properties, and therefore the mobility of Se nanostructures can be largely affected by the presence of these associated organic layers (Jain et al., 2017). In addition, some authors have also suggested the role of proteins in the synthesis and transformation of SeNPs, as well as in controlling their size (Dobias et al., 2011). According to Ruiz-Fresneda et al. (2020a), proteins produced by the bacterium *S. bentonitica* maybe involved in the transformation of amorphous nanospheres to crystalline trigonal Se nanofibers (**Fig. 6**). Although the specific transformation mechanism is still unknown, what seems clear is the direct role of the cells and their proteins during the process.

In the same way as for Se^0, methylated selenide compounds are basically insoluble and poorly bioavailable for living beings (Favorito et al. 2021). For this reason, Se methylation is considered one of the most important transformation processes

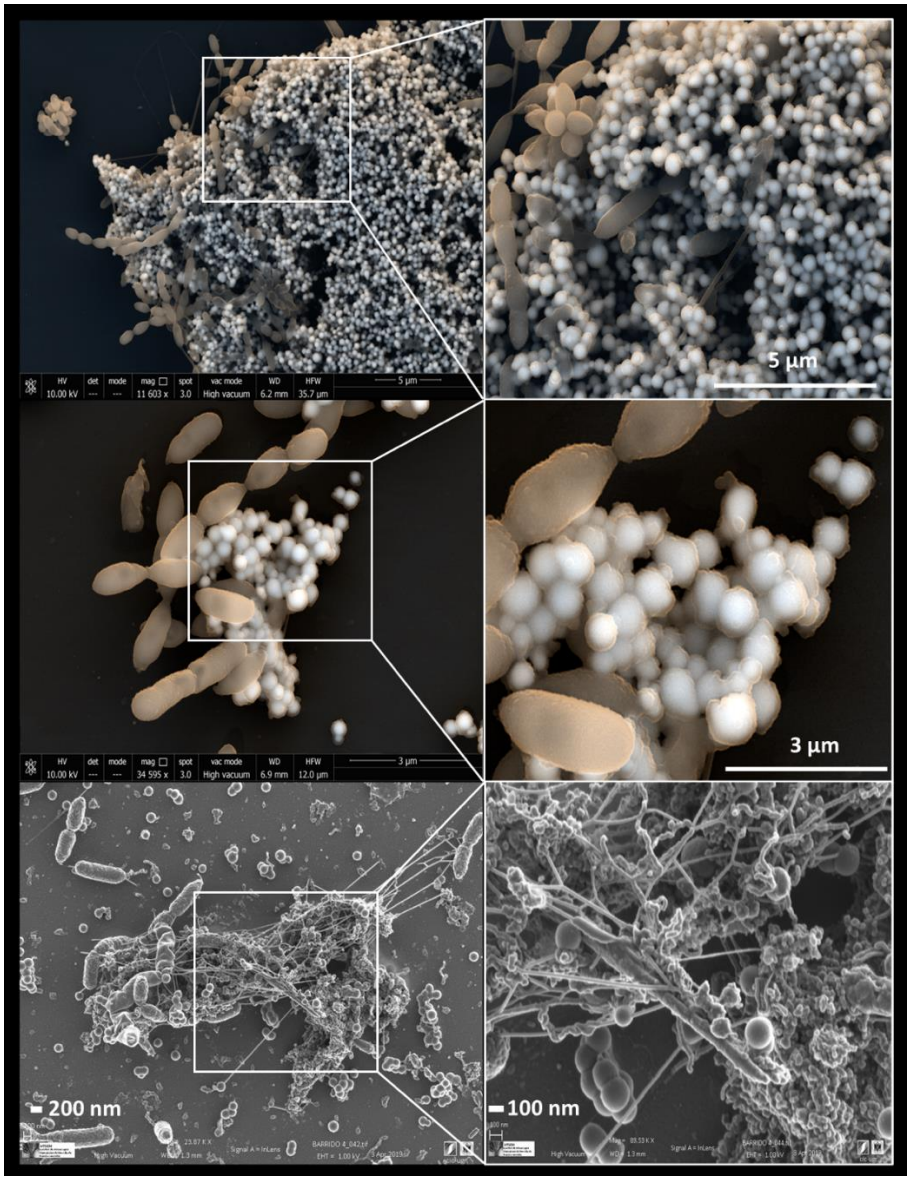

Figure 6. Electron microscopy images showing Se^0 nanostructures produced by the bacterium *Stenotrophomonas bentonitica* when supplemented with Se^{IV} (personal archive of Dr Merroun; growth conditions detailed in Ruiz-Fresneda et al., (2018, 2019, 2020a)).

related to bioremediation. It is a detoxification mechanism for microorganisms since volatile Se methylated compounds are notably less toxic than the oxidized forms (Favorito et al. 2021; Davis et al. 2011). The production of methylated selenides has been proved in different bacterial species such as *Methylococcus capsulatus*, *Methylosinus trichosporium* OB3b, or *Pseudomonas tolaasii*

(Eswayah et al., 2017; Liu et al. 2021). These bacterial strains can produce volatile compounds such as dimethyl selenide (DMSe, CH_3SeCH_3), dimethyl diselenide (DMDSe, $CH_3SeSeCH_3$), and dimethyl selenenyl sulfide (DMSeS, CH_3SeSCH_3). To date, several mechanisms have been proposed for the biomethylation of Se. Chasteen and Bentley (2003) suggested that Se^0 is reduced to the selenide form (H-Se-X), which is subsequently methylated to CH_3SeCH_3 and CH_3SeH. Other mechanisms similarly propose the formation of CH_3SeCH_3 from Se^{IV} through numerous reduction and methylation reactions (Challenger, 1945). Finally, not many studies have reported the oxidation of Se^0 and organic Se by microorganisms present in soils. Very recently, Luo et al. 2022 discovered four bacterial strains (*Dyella* sp. LX-1 and LX-66, and *Rhodanobacter* sp. LX-99 and LX-100) capable of oxidizing Se^{-II} and Se^0 to Se^{IV}. However, unlike reduction processes, the low oxidation rate of Se reduced forms indicates that this process should not be considered as relevant for the environment (Eswayah et al., 2016; Losi y Frankenberger, 1998). Similarly, demethylation processes of Se compounds are not usually considered due to the low rates at which these reactions occur (Eswayah et al., 2016).

On the basis of all the comments mentioned above, it is clear that indigenous microorganisms from natural and engineered barriers in a DGR or are introduced during the disposal construction and could play a direct effect on radionuclide mobilization. For example, the bacterial species *S. bentonitica*, isolated from bentonite clay, has been recently described to efficiently reduce Se^{VI} and Se^{IV} to Se^0 nanostructures and methylated Se (Pinel-Cabello et al., 2021a; Ruiz-Fresneda et al., 2023). The physico-chemical characterization of these Se reduction products suggests that this bacterium plays an important role in Se immobilization in the context of DGRs. Recently, Povedano-Priego et al. (2023) have described the Se^{IV} reduction to Se^0, producing precipitates of different shapes (from nanospheres to complex nanostructures) in bentonite samples treated with Se^{IV}. This is the first time that this process has been shown within a ternary system (bentonite,

indigenous microorganisms, and Se). Several bacteria have been found enriched in Se^{IV}-treated bentonite such as *Pseudomonas*, *Stenotrophomonas*, *Desulfosporosinus*, amongst others, potentially involved in Se reduction (Povedano-Priego et al., 2023).

5.2_ Microbial interactions with Cm/Eu

Different interaction mechanisms such as biosorption, biomineralization/bioprecipitation and intracellular accumulation have been described as affecting the mobility of representatives of trivalent actinides such as Cm, and their inactive analogues including Eu.

Biosorption is one of the main processes involved in the case of Cm and Eu. The cell surfaces of many bacteria have a high density of functional groups that can serve as a binding site of certain components and metal cations (Hufton et al., 2021). Specifically, the carboxyl groups present in the peptidoglycan layer of the cell wall of gram-positive bacteria seem to act as the main binding sites for actinides (Barkleit et al., 2009). Moreover, carboxyl, phosphoryl, and hydroxyl groups present on lipopolysaccharides (LPS) of the outer membrane, characteristic of gram-negative bacteria, can also act as a ligand for actinides such as U, Cm, and Np (Moll et al., 2021). Different bacterial species such as *P. fluorescens* and *Sporomusa* sp. MT-2.99 have been described for the efficient biosorption of Cm^{III} and Eu^{III} to their cell surfaces (Moll et al., 2014, 2013). *P. fluorescence* was isolated from groundwater from the Äspö Hard Rock Laboratory tunnel, a unique research facility testing the safety of final repositories for nuclear fuel, whilst *Sporomusa* sp. MT-2.99 is indigenous from Mont Terri Opalinus clay. In the case of *Sporomusa* sp. MT-2.99, the speciation and structure of the surface complexes formed with Cm^{III} and Eu^{III} was determined by Time Resolved Laser-Induced Fluorescence Spectroscopy (TRLFS). The results show that carboxyl and phosphoryl groups are responsible for Eu^{III} and Cm^{III} binding and the cell surface of this bacterium (Moll et al., 2014). Recent new research has demonstrated the

role of proteins from the plasma membrane fractions of *L. sphaericus* in Cm^{III} complexation (Moll et al. 2021).

Not only have bacterial cells been analysed using this technique, but there have also been recent studies about the yeast *Rhodotorula mucilaginosa* BII-R8, isolated from selected Spanish bentonite, which has shown its ability to retain both Eu^{III} and Cm^{III} at the cell surface Eu^{III} (Lopez-Fernandez et al., 2018c) (**Fig.7**). In the same way, carboxyl and phosphoryl groups present in the cell envelopes of *R. mucilaginosa* BII-R8 seem to be involved in the interaction of these two elements according to the results obtained by TRLFS. This study described for the first time the ability of a yeast to efficiently interact with Cm^{III} and Eu^{III}. Archaea can also interact with Cm^{III} and Eu^{III} as indicated by studies on *Halobacterium noricense* DSM15987T (Bader et al., 2019), where phosphate and carboxylic groups from the cell surface and released by the cells most probably act as binding sites. *H.*

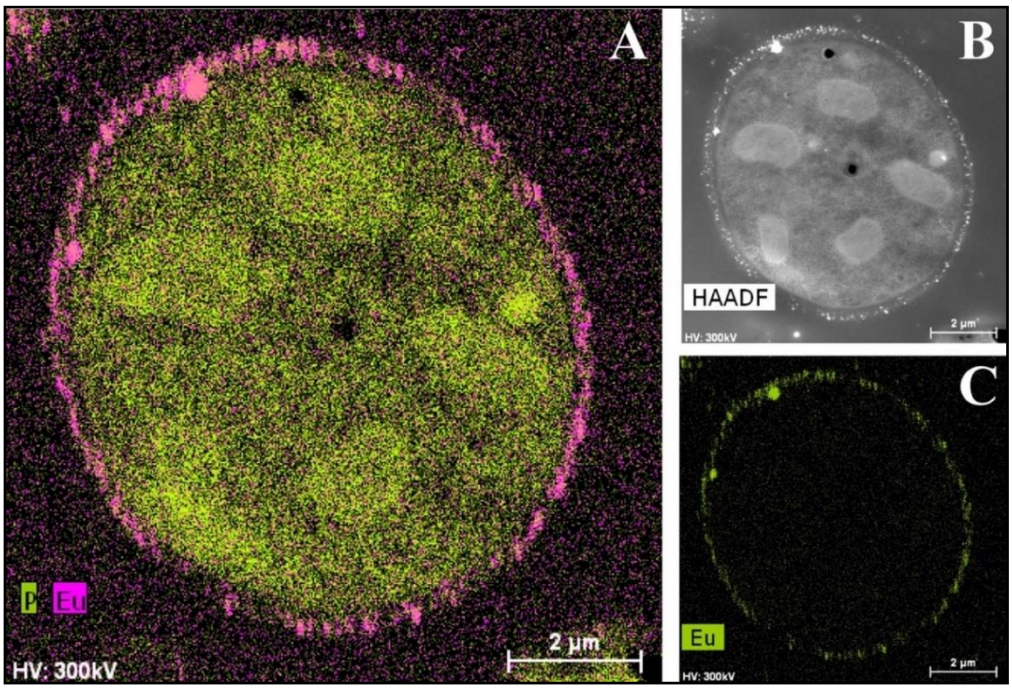

Figure 7. HAADF-STEM micrographs of a thin section and EDX element distribution maps showing the Eu biosorption to the cell surface of *Rhodotorula mucilaginosa* BII-R8 (Lopez-Fernandez et al., 2018c)**.**

noricense DSM15987T was isolated from rock salt, one of the natural barriers being considered for radioactive waste disposal.

Bioaccumulation and biomineralization/bioprecipitation have also played an important role in the microbial interaction with Cm^{III}/Eu^{III}. The bacterial species *Thermus scotoductus* SA-01 accumulates Eu^{III} precipitates both intracellularly and extracellularly and tolerate higher concentrations than those usually found in nature (up to 1 mM) (Maleke et al., 2019). Analysis of these samples by various spectroscopic techniques suggest the presence of extracellular accumulation may be due to a biomineralization process from carbonates produced by the reaction of CO_2, from respiration, with OH- radicals. They have also demonstrated the possible role of carboxyl, carbonyl, and phosphate groups in the biosorption of Eu^{III} according to the data obtained by ATR-FTIR. Specifically, they suggest the formation of Eu^{III} carbonates at surface level as indicated by XPS analyses. These results show how several mechanisms of interaction can simultaneously take place in a cell when it is exposed to a stressful condition. This is also the case of *S. bentonitica*, a bentonite-isolated bacterium which has recently been reported to interact with Eu^{III} and Cm^{III} through biosorption and bioaccumulation mechanisms, and possibly biomineralization (Ruiz-Fresneda et al., 2020b). The ability of this bacterium to additionally interact with Se, as mentioned before, suggests it as a potential positive candidate for the immobilization of radionuclides in the context of DGRs.

To sum up, microbial biosorption and bioaccumulation processes may play an important role in the immobilization of Cm^{III}, Eu^{III}, and other toxic elements if microbial biomass binds to inert supports through the formation of biofilms (Gadd, 2009). Biomineralization may also lead to the immobilization of these elements due to the formation of insoluble precipitates (Shukla et al., 2017). For all these reasons, the study of microbial interactions with actinides (Cm^{III}) and analogous elements (Eu^{III}) has been acquiring a special interest in recent years, both for the

evaluation of the safety of radioactive waste repositories, and for the bioremediation of contaminated environments.

5.3_ Microbial interaction with U

Uranium will be the dominant and the most critical radionuclide in the DGR system. Interactions between bentonite microbial communities and such radionuclide could be an imperative solution for the retention and/or immobilization, avoiding a release of U^{VI} in the environment and allow a safe and long-term storage of the radioactive waste.

The mobility and solubility of U in natural systems are governed by its oxidation state as well as its chemical speciation, which in turn is influenced by abiotic and biotic processes. U has two major oxidation states, U^{VI} and U^{IV}. The oxidized form possesses an elevated number of positive charges that results in its solubility, mobility, and therefore toxicity to the microbial cells, whilst U^{IV} is insoluble and less toxic under anaerobic conditions. The chemical speciation of U^{VI} is highly pH-dependent, in the sense that under alkaline conditions, such as those of bentonite, soluble uranyl ions it may form complexes with carbonate groups (Waite et al., 1994; Kushwaha et al. 2018), which are potentially mobile in presence of water. Under acidic conditions these oxidized forms would be absorbed on the mineral phases, complexed by organic matter or precipitated as uraninite ($Ca(UO_2)_2(PO_4)_2$), one of the insoluble uranyl phosphate minerals (Kolhe et al., 2018). In addition to chemical toxicity, U also displays a radiological (mainly from ^{235}U and ^{238}U isotopes) hazard, although its radiotoxicity is reported to be low. In contrast to other metals, it does not have any biological functions in living organisms. However, it has long been known to cause lung, renal, and hepatic damage in humans (Priest, 2001), as it may provoke oxidative stress in lung epithelial cells, by the loss of glutathione (an effective antioxidant) and superoxide dismutase enzyme (Periyakaruppan et al., 2007). In microorganisms, many effects of U toxicity are recognized including the loss of cell viability and activity,

distortion of cell surfaces, oxidative damage, as well as the suspension of DNA replication and transcriptional and translational processes (Park and Jiao, 2014; Sepulveda-Medina et al., 2015). However, as mentioned above, in order to resist metal and radionuclide toxicity, microbes have developed a variety of mechanisms that allow potential immobilization and bioremediation. Microorganisms that interact with U are reported to be a good remediation strategy for decreasing the solubility and mobility of this toxic element (Sánchez-Castro et al., 2020). They can affect its speciation and migration in different environments, including DGRs (Povedano-Priego et al., 2022; 2019). Among the mechanisms adopted by many microorganisms to tolerate and survive in uranium contaminated sites, biosorption, bioaccumulation, biomineralization, and biotransformation (through oxidation-reduction reactions) constitute the most relevant in the *in situ* and *ex situ* bioremediation techniques. However, the two microbial processes that have beenmost investigated so far, and therefore gained more attention and confidence, are the enzymatically catalysed reduction of U^{VI} to U^{IV} and the bioprecipitation of the oxidized form of U with inorganic phosphates as ligands.

Uranium (as oxidized form U^{VI}) has shown to be highly susceptible to enzymatic reduction by microorganisms, which can occur in the cytoplasm, periplasm, at the outer membrane or extracellularly (You et al., 2021). They could be involved in a direct enzymatic reduction of soluble U^{VI} to insoluble forms, whilst biologically mediated indirect reduction using electrons obtained in the oxidation-reduction reactions of iron or sulphate has also been reported to be important in the immobilization of U^{VI} (Roh et al., 2015). Uranium reducing microorganisms are ubiquitous in the environment. Several species of prokaryotes have been reported to be involved in uranium reduction. Iron-reducing species like *Geobacter uraniireducens, G. daltonii, and Shewanella oneidensis* and sulphate-reducing bacteria (SRB) mainly *Desulfovibrio, Desulfotomaculum,* and *Desulfobacterium* have been described as using uranium as an electron donor in addition to iron and sulphate (Akob et al., 2012). The first ones can conserve energy for their anaerobic

growth through the reduction of uranium, whilst the SRB are unable to conserve such energy for their growth. *Desulfovibrio* has been found in different uranium-contaminated sites such as sub-surface sediments (Castañeda-Carrion, 2010; Newsome, 2014), and water (Jroundi et al., 2020; Parihar et al., 2013). Povedano-Priego et al. (2022) identified *Desulfovibrio* in the bacterial community of uranium-treated bentonite under anoxic conditions in presence of glycerol-2-phosphate (G2P). Significant presence of *Desulfovibrio* in these conditions indicates that a potential U-tolerance mechanism maybe active with the mediation of G2P. The capacity of members of this genus to use glycerol as electron donor has been reported (Ben Ali et al., 2018). In addition, *Desulfovibrio* has been shown to use cytochrome *c3* (*cysA*) functioning as U^{VI} reductase in combination with a hydrogenase as a physiological electron donor, although additional pathways from organic electron donors (such as glycerol) to U^{VI} that can bypass the cytochrome, have been suggested to occur (Payne et al., 2002). Several iron reducers (e.g., *Clostridium*, *Geobacter*) can reduce uranium by different mechanisms mediated by enzymes and cytochromes. Clones related with *Clostridium* species have been detected in the bacterial community of uranium-contaminated sediment from an inactive uranium mine (Midnite mine, eastern Washington), producing the reduction of U^{VI} (Suzuki et al., 2003). The main mechanism involved is an enzymatic reduction of U^{VI} mediated by hydrogenases (Gao and Francis, 2013). Other cytochromes have been found to be imperative to induce uranium reduction in *Geobacter* as well as in other bacteria such as*S. oneidensis*. In addition to the periplasmic c7-type cytochrome PpcA, an important intermediate electron carrier (in the absence of hydrogen), GscA (*Geobacter* sub-surface c-type cytochrome A), MacA (diheme c-type cytochrome peroxidase), MtrC (also known as OmcB; outer membrane c-type cytochrome) and OmcZ (outer-surface c-type cytochrome) has shown to be essential for the reduction of uranium (Rogiers et al., 2022; Yun et al., 2016). Bacterial pili also seem to play a role as an electron conductor between the cells and the electron acceptors. The reduced U^{IV} appears mainly localized in the

periplasm and outside of the cells, indicating the involvement of outer membrane-bound enzymes in the reduction process (Majumder and Wall, 2017). It has also been suggested that uranium reduction maybe linked to iron metabolism, since siderophores have been shown to form stable complexes with several metals and radionuclides, including uranium (Gallois et al., 2022). Siderophores and a large number of proteins associated to iron uptake systems, such as ABC-transport type proteins in the Chernobyl isolate *Microbacterium oleivorans* A9 or a transcriptional regulator of the Fur family in *Desulfotomaculum reducens* MI-1, are upregulated as an iron starvation response to uranium stress (Gallois et al., 2022; Junier et al., 2011).

Microorganism-mediated biomineralization of uranium is a widely used mechanism, which is applied for the remediation of radionuclide contaminated sites. Large numbers of microorganisms are known for their capacity to biomineralize uranium as metautunite-like precipitates using phytase, phosphatases, or complexed with microbe-associated ligands, such as phosphate, carbonate, or hydroxide functional groups (Lin et al., 2023). Thus, U bioprecipitation results frequently from an enzymatic process. Microbial phosphatases are involved in the U biomineralization, since these enzymes release inorganic phosphates (Pi) by hydrolysing organic phosphate substrates, which interact with the radionuclide and precipitate in the form of an insoluble phosphate mineral (**Fig. 8**). A plethora of bacteria isolated from radionuclide and metal contaminated sites have demonstrated uranium precipitation owing their acid or alkaline phosphatase activities. As examples of these, Gram-positive bacteria *Bacillus sphaericus* JG-7B (Merroun et al., 2011), *Paenibacillus* sp. JG-TB8 (facultative anaerobic bacterium) (Reitz et al., 2014), and *Microbacterium* sp A9 (Theodorakopoulos et al., 2015) and many Gram-negative members of Alphaproteobacteria, Deltaproteobacteria, and Gammaproteobacteria clases (Kolhe et al., 2018; Pinel-Cabello et al., 2021b) should be mentioned. In most of these cases, U bioprecipitation occurs in the form of a stable and insoluble meta-

autunite mineral (uranyl phosphate mineral phase).On the contrary, Beazley et al., (2007) isolated an *Arthrobacter* sp., from sub-surface soils at the US Oak Ridge field Research Centre, as a negative phosphatase bacterium, which was unable to precipitate uranium. Different phosphatase enzymes were identified as responsible for the uranium biomineralization that includes PhoY, the alkaline phosphatase PhoK, and the acid phosphatase PhoN in *Caulobacter crescentus*, in *Sphingomonas*, and *Serratia* sp, respectively (Nilgiriwala et al., 2008; Paterson-Beedle et al., 2012; Yung and Jiao, 2014). Biomineralization by polyphosphates has also been proven to occur in many uranium contaminated sites. Polyphosphates (phosphate polymers) can also be degraded as an alternative to obtain phosphates that precipitate with the metal intracellularly (Acharya et al., 2017). For example, in *Pseudomonas aeruginosa*, an over-expression of the polyphosphate kinase (ppk) gene has been reported to result in the release of phosphates, which precipitate in the form of uranyl phosphate minerals in the cell membranes (Renninger et al., 2004). *Pseudomonas* has been identified in several bentonite samples (Lopez-Fernandez et al., 2015; Povedano-Priego et al., 2021), including uranium-treated

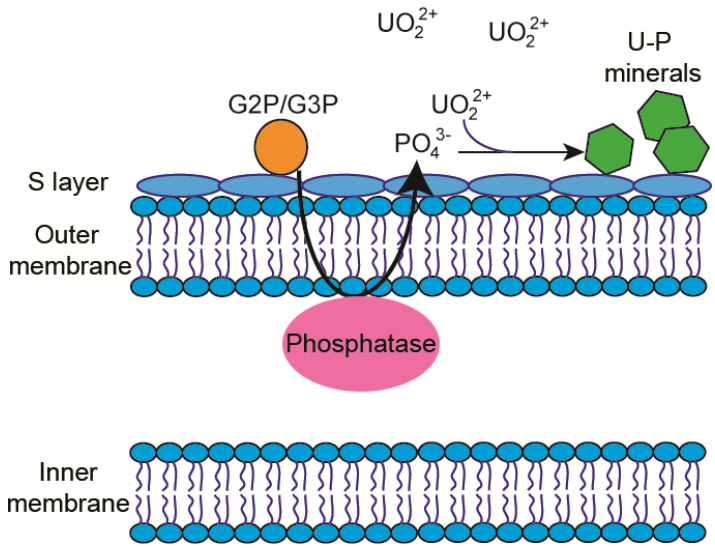

Figure 8. Diagram of the periplasmic phosphatase-mediated biomineralization process. Phosphatase releases inorganic phosphate from an organic phosphate source (e.g., G2P/G3P) to interact with U^{VI} and produce the precipitation of uranium phosphates.

microcosms in the presence of G2P (Povedano-Priego et al., 2022). G2P as an organic phosphate source enrich *Pseudomonas* since these bacteria have been described to possess gene encoding phosphatases that may have the G2P as a substrate to release inorganic phosphate (Sarikhani et al., 2019; Liu et al., 2016). Other environmental microorganisms such as *Bacillus*, *Rhanella*, *Arthrobacter* and *Cellulomonas* have shown their capacity to immobilize U as biogenic uranyl phosphate minerals owing to their polyphosphate metabolism or organophosphate hydrolase activity (Martinez et al., 2007; Sivaswamy et al., 2011). Povedano-Priego et al. (2019) reported the phosphatase activity in *Amycolatopsis ruanii*, a

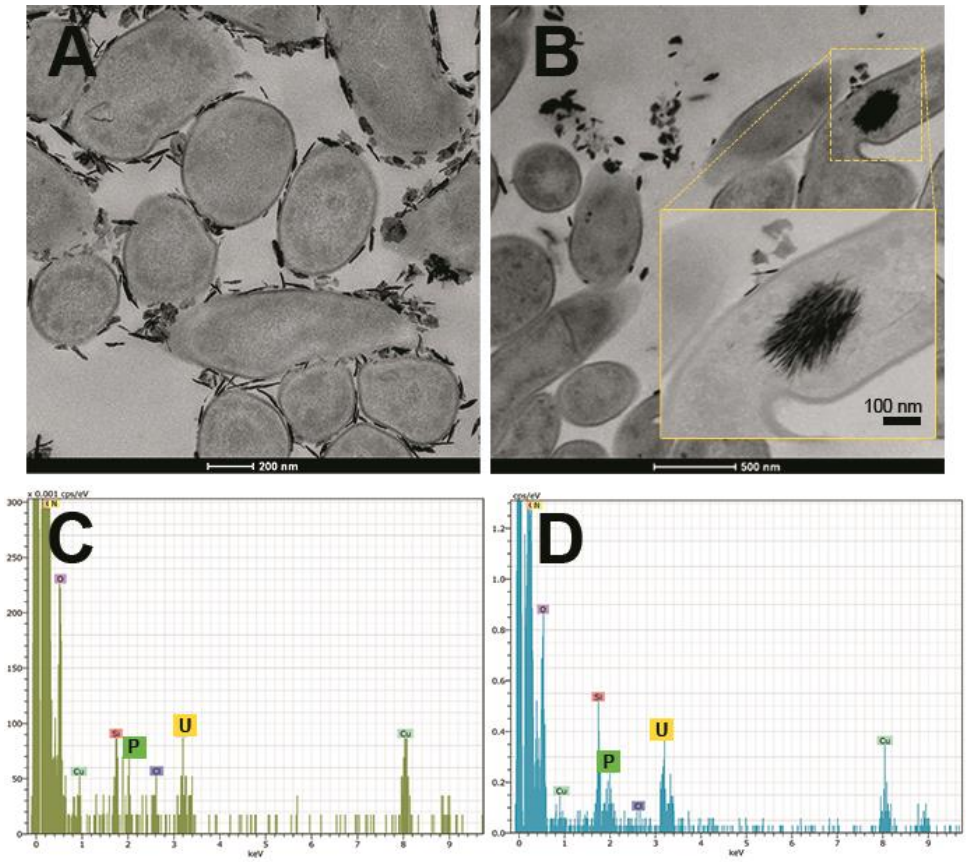

Figure 9. Scanning transmission electron microscopy (STEM) micrographs of thin sections of *Amycolatopsis ruanii*/bacterial consortium (*Bradyrhizobium-Rhizobium* and *Pseudomonas*) cells treated with uranium (A), and uranium+glycerol-2-phosphate (B). Extracellular and intracellular precipitates of uranium phosphates and their corresponding EDX spectra with peaks of U and P (C, and D, respectively). Personal archive of Dr Merroun; growth conditions detailed in Povedano-Priego et al., 2019).

significantly abundant genus in G2P-uranium treated bentonites. The highest concentrations of P_i in solution were observed when *Amycolatopsis* was treated with G2P. However, electron-dense precipitates were found with, and without the G2P amendment (**Fig. 9A-B**). These precipitates were composed of phosphorus and uranium (**Fig. 9C-D**). Thus, the biomineralization of uranium has also been observed without the G2P amendment (**Fig. 9A**). Uranium phosphates have been identified extracellularly and at the cell-wall level with and without G2P (**Fig.9A-B**), whilst intracellular needle-like fibril precipitates were only detected in presence of G2P (**Fig.9B**). These results confirm the capacity of these bacteria to biomineralize uranium, which had been enhanced by the G2P amendment through phosphatase activity. In the study of Martinez-Rodríguez et al. (2022) *Microbacterium* sp. Be9 strain was used, previously isolated from U- mill tailings and determined that the U-biomineralization process was dependent on the type of phosphate source. This is relevant for the bioremediation of uranium since the solubilisation of orthophosphates derived from waste products containing P-compounds could occur (Martinez-Rodríguez et al, 2022). However, high concentrations of uranium could produce a harmful effect on bacterial activity. To avoid this negative effect, Sánchez-Castro et al. (2021) embedded bacterial cells of *Stenotrophomonas* sp. Br8 in an alginate matrix to protect the cells from hazardous agents and enhanced the immobilization rate. This methodology could be applied to bioremediate U-contaminated mining water.

Nonetheless, U-phosphate biomineralization is affected by many environmental factors including temperature, carbonate, pH, and ammonium. In alkaline conditions, for example, carbonate impacts U-phosphate biomineralization due to the higher affinity of CO_3^{2-} with UO_2^{2+} than PO_4^{3-}. Additionally, NH_4^+ can interact with UO_2^{2+} as well as with PO_4^{3-} promoting the precipitation of uranium. A handful of studies have profiled the influence of uranium on the microbial communities of several ecosystems, which is known to induce changes in functional processes as well as in the taxonomic composition (Sánchez-Castro et al., 2020; Suriya et al.,

2017; Sutcliffe et al., 2017). The microbial communities in different U-treated bentonites have been largely studied by using multiple state-of-the-art techniques (Lopez-Fernandez et al., 2018; Povedano-Priego et al., 2019). Anoxic conditions will prevail in such systems and the presence of strict and facultative anaerobes is well established (Povedano-Priego et al., 2022).

6_ Discussion and future perspectives

This review highlights the potential role of microorganisms related to the safety of DGRs. As previously mentioned, this type of disposal is based on a multi-barrier system in which the waste will be encapsulated in corrosion-resistant metal canisters, surrounded by filling and sealing materials, which will be placed at depths of between 500 – 1000 m in a stable geological formation. Microorganisms are able to colonize almost every single habitat on Earth, and the barriers of the DGRs are no exception. Even though microorganisms could be passively introduced through human manipulation of the different materials during the construction of the DGR, natural microbial communities in the different barriers may be the most important source of microbial activity within the repository. It is worth noting the importance of microorganisms naturally occurring in the filling and sealing materials (e.g., bentonite clay) that will be in direct contact with the metal canisters and, therefore, close to the radioactive waste. For this reason, the different bentonites (e.g., Opalinus, Boom and Spanish clay) have been extensively studied at microbiological level in order to understand the different processes in which microorganisms may be involved.

As we have tried to show in this review, microorganisms could influence the stability and security of the DGRs at different levels. Certain types of microbial communities (e.g., SRB) can cause the alteration of metal canisters (e.g., steel-based materials and copper) through direct or indirect processes, also known as microbially influenced corrosion (MIC). The canister corrosion, in the worst-case scenario, could suffer small pits or fissures, leaving the residue exposed to the next

engineered barrier (the filling and sealing material). Moreover, MIC could be involved in the gas production in the DGR environment. MIC, radiolysis of water and microbial metabolism could promote a rise in the gas phase in the DGRs and produce an increase in pressure which would affect the integrity of the clay barrier. However, the metabolism of microorganisms could have a double effect related to gases in the repositories. The production of certain gases due to the metabolism of some bacterial groups may be used by other groups for their own metabolism, thus minimizing the possible pressure produced, positively affecting the safety of the DGR.

Additionally, microbial activity can indirectly influence solubility and hence the mobilization of radionuclides by the alteration of the geochemical conditions within the DGRs. These changes may result in changes in their oxidation state, affecting their solubility and mobility through the different barriers. Nonetheless, microorganisms could be involved in the mobility of these radionuclides. As mentioned before, several mechanisms such as biotransformation, biosorption, bioaccumulation, and biomineralization, may be involved in the interaction microbe-radionuclides. The result of these interactions produces a positive effect since certain microorganisms are able to immobilize elements such as Se, Eu, Cm, and U, making them unavailable to other organisms or, preventing their diffusion through the subsequent engineered barriers and then through to the environment.

Notwithstanding, the purpose of this review is to give an overview of the effect that microorganisms could have on the stability and safety of future DGRs. It will be necessary to consider different factors that could affect the bacterial communities present in the bentonite after the definitive closure of a DGR. One of these parameters is the temperature evolution throughout the confinement period. This temperature will initially increase due to the heat resulting from the decay of the HLW, and then slowly decrease until reaching environmental geosphere conditions over a period of 100,000 years (McMurry et al., 2004). Most models

suggest a maximum temperature of 80 – 100 ºC reached within the first 100 years (McMurry et al., 2004; Butov et al., 2017; Leong et al., 2021). Moreover, another aspect to consider is the compaction density of the bentonite. The compaction has been shown to affect SRB viability demonstrating that the higher the density is, the lower the viability of this bacterial group (Bengsston and Pedersen, 2017). In addition to these determinant factors, others must be considered such as the evolution to an anaerobic environment due to the gradual consumption of oxygen by the organisms, the slow diffusion of pore water through the bentonite and the low concentration of organic matter, amongst others. All these factors make the DGR system a harsh environment for certain groups of microorganisms preventing their growth and even their survival. Otherwise, many bacteria could remain in a dormant state until growth conditions became favourable again, such as size decrease, spore formation or cell desiccation (O'Sullivan et al., 2015). For this reason, it is crucial to investigate the microbial influence and the conditions that affect the bacterial communities within the DGR environment, in order to ensure the safety of the repository facilities throughout their service life.

Conflict of Interest

The authors declare that the research was conducted in the absence of any commercial or financial relationships that could be construed as a potential conflict of interest.

Author Contributions

MARF and MLM planned the work. MARF wrote the first draft of the manuscript, which was revised by MLM. MFMM, CPP, MMH, and FJ assisted writing some sections of the manuscript. The final version was edited and revised by all the authors.

All the authors contributed to the article and approved the final submitted version.

Funding

This work was supported by grant RTI2018-101548-B-I00 of MCIN/AEI/10.13039/501100011033/ FEDER "Una manera de hacer Europa".

Acknowledgments

The authors acknowledge the assistance of Maria del Mar Abad Ortega, Isabel Sánchez Almazo, and Concepción Hernández Castillo (Centro de Instrumentación Científica, University of Granada, Spain) for their help with microscopy measurements and sample preparation.

References

Abdalla, Z. A. Y., Ismail, M. Y. A., Njoroge, E. G., Hlatshwayo, T. T., Wendler, E., and Malherbe, J. B. (2020). Migration behaviour of selenium implanted into polycrystalline 3C–SiC. *Vacuum*, *175*, 109235. https://doi.org/https://doi.org/10.1016/j.vacuum.2020.109235

Abdullahi, S. L., and Audu, A. A. (2017). Comparative analysis on chemical composition of bentonite clays obtained from Ashaka and tango deposits in Gombe State, Nigeria. *ChemSearch Journal*, *8*(2), 35-40.

Abrahamsen, L., Arnold, T., Brinkmann, H., Leys, N., Merroun, M., Mijnendonckx, K., *et al.* (2015). A review of anthropogenic organic wastes and their degradation behaviour, *Microbiology In Nuclear waste Disposal (MIND Project).* Available from: https://igdtp.eu/wpcontent/uploads/2017/10/MIND-2015-12-D1.1-ReviewOfAnthropogenicOrganicWastes.pdf

Abramova, E., Popova, N., Artemiev, G., Boldyrev, K., Kazakov, K., Kryuchkov, D., *et al.* (2023). Biological factors affecting the evolution of safety barrier materials in the Yeniseisky deep geological repository. *Engineering Geology*, 312, 106931. https://doi.org/10.1016/j.enggeo.2022.106931.

Acharya, C., Chandwadkar, P., and Nayak, C. (2017). Unusual Versatility of the Filamentous, Diazotrophic Cyanobacterium *Anabaena torulosa* Revealed for Its Survival during Prolonged Uranium Exposure. *Applied and Environmental Microbiology*, 83, e03356-16. https://doi.org/10.1128/AEM.03356-16

Ahmed, A. S., Salahudeen, N., Ajinomoh, C. S., Hamza, H., and Ohikere, A. (2012). Studies on the mineral and chemical characteristics of Pindiga bentonitic clay. *Petroleum Technology Development Journal*, *1*(1), 56-63.

Ahonen, L., Pedersen, K., Small, J., Mijnendonckx, K., Weetjens, E. and Wouters, K. (2016). Year One Evaluation Report, *Microbiology In Nuclear waste Disposal (MIND Project)*. Available from: https://mind15.eu/wp-content/uploads/2015/11/MIND-Deliverable-3.1-Y1-Evaluation.pdf

Akob, D., Lee, S., Sheth, M., Küsel, K., Watson, D., Palumbo, *et al.* (2012). Gene Expression Correlates with Process Rates Quantified for Sulfate- and Fe(III)-Reducing Bacteria in U^{VI}-

Contaminated Sediments. *Frontiers in Microbiology*. 3, 280. https://doi.org/10.3389/fmicb.2012.00280

Alwaeli, M., and Mannheim, V. (2022). Investigation into the Current State of Nuclear Energy and Nuclear Waste Management—A State-of-the-Art Review. *Energies*, *15*(12), 4275. https://doi.org/10.3390/en15124275

Ansoborlo, E., Bion, L., Doizi, D., Moulin, C., Lourenco, V., Madic, C., *et al.* (2007). Current and future radionuclide speciation studies in biological media. *Radiation Protection Dosimetry*, *127*(1–4), 97–102. https://doi.org/10.1093/rpd/ncm258

Atwood, D.A. (2010). Radionuclides in the Environment (EIC Books). Weinheim: WILEY. Available from: https://www.wiley.com/en-us/Radionuclides+in+the+Environment-p-9780470714348

Ayangbenro, A. S., and Babalola, O. O. (2017). A new strategy for heavy metal polluted environments: A review of microbial biosorbents. In *International Journal of Environmental Research and Public Health*. *14*(1), 94. https://doi.org/10.3390/ijerph14010094

Bachran, M., Kluge, S., Lopez-Fernandez, M., and Cherkouk, A. (2018). Microbial Diversity in an Arid , Naturally Saline Environment. *Microbial Ecology*. *78*, 494-505. https://doi.org/10.1007/s00248-018-1301-2

Bader, M., Moll, H., Steudtner, R., Lösch, H., Drobot, B., Stumpf, T., and Cherkouk, A. (2019). Association of Eu(III) and Cm(III) onto an extremely halophilic archaeon. *Environmental Science and Pollution Research*. *26*, 9352–9364. https://doi.org/10.1007/s11356-019-04165-7

Baggio, G., Groves, R. A., Chignola, R., Piacenza, E., Presentato, A., Lewis, I. A., *et al.* (2021). Untargeted Metabolomics Investigation on Selenite Reduction to Elemental Selenium by Bacillus mycoides SeITE01. *Frontiers in Microbiology*, *12*. https://doi.org/10.3389/fmicb.2021.711000

Bagnoud, A., Chourey, K., Hettich, R. L., de Bruijn, I., Andersson, A. F., Leupin, O. X., *et al.* (2016a). Reconstructing a hydrogen-driven microbial metabolic network in Opalinus Clay rock. *Nature Communications*, *7*, 12770. https://doi.org/10.1038/ncomms12770

Bagnoud, A., de Bruijn, I., Andersson, A. F., Diomidis, N., Leupin, O. X., Schwyn, B. *et al.* (2016b). A minimalistic microbial food web in an excavated deep subsurface clay rock. *FEMS Microbiology Ecology*. *92*(1), fiv138. https://doi.org/10.1093/femsec/fiv138

Bagnoud, A., Leupin, O., Schwyn, B., and Bernier-Latmani, R. (2016c). Rates of microbial hydrogen oxidation and sulfate reduction in Opalinus Clay rock. *Applied Geochemistry*, *72*, 42–50. https://doi.org/10.1016/J.APGEOCHEM.2016.06.011

Barkleit, A., Moll, H., and Bernhard, G. (2009). Complexation of uranium(VI) with peptidoglycan. *Dalton Transactions*. *27*, 5379-5385. https://doi.org/10.1039/b818702a

Beaton, D., Pelletier, P., and Goulet, R. R. (2019). Microbial degradation of cellulosic material and gas generation: Implications for the management of low-and intermediate-level radioactive waste. *Frontiers in Microbiology*, *10*, 1–13. https://doi.org/10.3389/fmicb.2019.00204

Beazley, M.J., Martinez, R.J., Sobecky, P.A., Webb, S.M., and Taillefert, M. (2007). Uranium biomineralization as a result of bacterial phosphatase activity: Insights from bacterial isolates from a contaminated subsurface. *Environ. Sci. Technol*. *41*, 5701–5707. https://doi.org/10.1021/es070567g

Ben Ali Gam, Z., Thioye, A., Cayol, J.-L., Joseph, M., Fauque, G., Labat, M. (2018). Characterization of *Desulfovibrio salinus* sp. nov., a slightly halophilic sulfate-reducing bacterium isolated from a saline lake in Tunisia. *International Journal of Systematic Evolutionary Microbioly*. *68*, 715–720. https://doi.org/10.1099/ijsem.0.002567

Bengtsson, A., and Pedersen, K. (2016). Microbial sulfate-reducing activity overload pressure and density in water saturated Boom Clay. *Applied Clay Science*. *132-133*, 542-551. https://doi.org/10.1016/j.clay.2016.08.002

Bengtsson, A., and Pedersen, K. (2017). Microbial sulphide-producing activity in water saturated Wyoming MX-80, Asha and Calcigel bentonites at wet densities from 1500 to 2000 kg m−3. *Applied Clay Science*, *137*, 203-212. https://doi.org/10.1016/j.clay.2016.12.024

Benko, I., Nagy, G., Tanczos, B., Ungvari, E., Sztrik, A., Eszenyi, P., *et al.* (2012). Subacute toxicity of nano-selenium compared to other selenium species in mice. *Environmental Toxicology and Chemistry*, *31*(12), 2812–2820. https://doi.org/10.1002/etc.1995

Breynaert, E., Scheinost, A. C., Dom, D., Rossberg, A., Vancluysen, J., Gobechiya, E., *et al.* (2010). Reduction of Se(IV) in boom clay: XAS solid phase speciation. *Environmental Science and Technology*, *44*(17), 6649–6655. https://doi.org/10.1021/es100569e

Brim, H., McFarlan, S. C., Fredrickson, J. K., Minton, K. W., Zhai, M., Wackett, L. P., *et al.* (2000). Engineering *Deinococcus radiodurans* for metal remediation in radioactive mixed waste environments. *Nature Biotechnology*. *18*, 85–90. https://doi.org/10.1038/71986.

Brown, A. R., Boothman, C., Pimblott, S. M., and Lloyd, J. R. (2015). The Impact of Gamma Radiation on Sediment Microbial Processes. *Applied and Environmental Microbiology*, *81*(12), 4014–4025. https://doi.org/10.1128/AEM.00590-15

Bulgarini, A., Lampis, S., Turner, R. J., and Vallini, G. (2021). Biomolecular composition of capping layer and stability of biogenic selenium nanoparticles synthesized by five bacterial species. *Microbial Biotechnology*, *14*(1), 198–212. https://doi.org/https://doi.org/10.1111/1751-7915.13666

Burns, P. C. (2012). Nuclear Fuel in a Reactor Accident. *335*(6073), 1184–1189. https://doi.org/10.1126/science.1211285

Burzan, N., Murad Lima, R., Frutschi, M., Janowczyk, A., Reddy, B., Rance, A., *et al.* (2022). Growth and Persistence of an Aerobic Microbial Community in Wyoming Bentonite MX-80 Despite Anoxic in situ Conditions. *Frontiers in Microbiology*, *13*. https://doi.org/10.3389/fmicb.2022.858324

Butov, R. A., Drobyshevsky, N. I., Moiseenko, E. V., and Tokarev, Y. N. (2017, September). 3D numerical modelling of the thermal state of deep geological nuclear waste repositories. *Journal of Physics: Conference Series (IOP Publishing)*, 899 (5), 052002. https://doi.org/10.1088/1742-6596/899/5/052002

Castañeda-Carrión, I.N., Sheik, C.S., Krumholz, L.R. (2010). *Desulfovibrio africanus* subsp. uniflagellum subsp. nov., a sulfate-reducing bacterium from a uranium-contaminated subsurface aquifer. *International Journal of Systematic Evolutionary Microbioly. 60*, 880–886. https://doi.org/10.1099/ijs.0.006668-0

Černoušek, T., Shrestha, R., Kovářová, H., Špánek, R., Ševců, A., Sihelská, K., *et al.* (2019). Microbially influenced corrosion of carbon steel in the presence of anaerobic sulfate-reducing bacteria. *Corrosion Engineering Science and Technology*. *55*, 127–137. https://doi.org/10.1080/1478422X.2019.170064

Chabert, C., Warin, D., Leudet, A., Milot, J.F., Saturnin, A., Lagrange, M.H., *et al.* (2012). Impact of minor actinide transmutation options on interim storage and geological disposal: The French Case. In: Proceedings of the Twelfth Information Exchange Meeting on Actinide and Fission Product Partitioning and Transmutation. Issy-les-Moulineaux (France): Nuclear Energy Agency of the OECD (NEA), 131-140. Available from http://inis.iaea.org/search/search.aspx?orig_q=RN:44100547

Challenger, F. (1945). Biological Methylation. *Chemical Reviews*. 36 (3), 315–361. https://doi.org/10.1021/cr60115a003

Chandwadkar, P., Misra, H. S., and Acharya, C. (2018). Uranium biomineralization induced by a metal tolerant: *Serratia* strain under acid, alkaline and irradiated conditions. *Metallomics*. 10(8), 1078-1088. https://doi.org/10.1039/c8mt00061a

Chasteen, T. G., and Bentley, R. (2003). Biomethylation of Selenium and Tellurium: Microorganisms and Plants. *Chemical reviews. 103*(1), 1-26.

Chen, J., Qin, Z., and Shoesmith, D. W. (2011). Long-term corrosion of copper in a dilute anaerobic sulfide solution. *Electrochimica Acta*, *56*, 7854–7861. https://doi.org/10.1016/j.electacta.2011.04.086

Chen, S., Wang, P., and Zhang, D. (2014). Corrosion behaviour of copper under biofilm of sulfate-reducing bacteria. *Corrosion Science*. *87*, 407–415. https://doi.org/10.1016/j.corsci.2014.07.001

Chen, X., Ottosen, L. D. M., and Kofoed, M. V. W. (2019). How Low Can You Go: Methane Production of *Methanobacterium congolense* at Low CO2 Concentrations. *Frontiers in Bioengineering and Biotechnology*, 7, 34. https://doi.org/10.3389/fbioe.2019.00034

Choudhary, S., and Sar, P. (2009). Characterization of a metal resistant *Pseudomonas* sp. isolated from uranium mine for its potential in heavy metal (Ni2+, Co2+, Cu2+, and Cd2+) sequestration. *Bioresource Technology*. *100*(9), 2482-2492. https://doi.org/10.1016/j.biortech.2008.12.015

Close, D. M., Nelson, W. H., and Bernhard, W. A. (2013). DNA damage by the direct effect of ionizing radiation: Products produced by two sequential one-electron oxidations. *Journal of Physical Chemistry A*, *117*(47), 12608–12615. https://doi.org/10.1021/jp4084844

Cologgi, D. L., Speers, A. M., Bullard, B. A., Kelly, S. D., and Reguera, G. (2014). Enhanced uranium immobilization and reduction by *Geobacter sulfurreducens* biofilms. *Applied and Environmental Microbiology*, *80*(21), 6638–6646. https://doi.org/10.1128/AEM.02289-14

Davis, T. Z., Stegelmeier, B. L., Welch, K. D., Pfister, J. A., Panter, K. E., and Hall, J. O. (2013). Comparative oral dose toxicokinetics of selenium compounds commonly found in selenium accumulator plants. *Journal of Animal Science*, *91*(9), 4501–4509. https://doi.org/10.2527/jas.2012-6101

Di Gregorio, S., Lampis, S., and Vallini, G. (2005). Selenite precipitation by a rhizospheric strain of *Stenotrophomonas* sp. isolated from the root system of *Astragalus bisulcatus*: a biotechnological perspective. *Environment International*, *31*(2), 233–241. https://doi.org/10.1016/j.envint.2004.09.021

Diep, P., Mahadevan, R., and Yakunin, A. F. (2018). Heavy Metal Removal by Bioaccumulation Using Genetically Engineered Microorganisms. *Frontiers in Bioengineering and Biotechnology*. *6*, 157. https://doi.org/10.3389/fbioe.2018.00157

Dobias, J., Suvorova, E. I., and Bernier-Latmani, R. (2011). Role of proteins in controlling selenium nanoparticle size. *Nanotechnology*, *22*(19). https://doi.org/10.1088/0957-4484/22/19/195605

Dobrowolski, R., Szcześ, A., Czemierska, M., and Jarosz-Wikołazka, A. (2017). Studies of cadmium(II), lead(II), nickel(II), cobalt(II) and chromium(VI) sorption on extracellular polymeric substances produced by *Rhodococcus opacus* and *Rhodococcus rhodochrous*. *Bioresource Technology*. 225, 113-120. https://doi.org/10.1016/j.biortech.2016.11.040

Dong, H., Jaisi, D. P., Kim, J., and Zhang, G. (2009). Microbe-clay mineral interactions. *American Mineralogist*, *94*(11-12), 1505-1519. https://doi.org/10.2138/am.2009.3246

Dou, W., Pu, Y., Han, X., Song, Y., Chen, S., and Gu, T. (2020). Corrosion of Cu by a sulfate reducing bacterium in anaerobic vials with different headspace volumes. *Bioelectrochemistry*, *133*, 107478. https://doi.org/10.1016/j.bioelechem.2020.107478

Dungan, R. S., Yates, S. R., and Frankenberger, W. T. (2003). Transformations of selenate and selenite by *Stenotrophomonas maltophilia* isolated from a seleniferous agricultural drainage pond sediment. *Environmental Microbiology*, *5*(4), 287–295. https://doi.org/10.1046/j.1462-2920.2003.00410.x

Duro, L., Domènech, C., Grivé, M., Roman-Ross, G., Bruno, J., and Källström, K. (2014). Assessment of the evolution of the redox conditions in a low and intermediate level nuclear waste repository (SFR1, Sweden). *Applied Geochemistry*. https://doi.org/10.1016/j.apgeochem.2014.04.015

Enning, D., and Garrelfs, J. (2014). Corrosion of iron by sulfate-reducing bacteria: New views of an old problem. *Applied and Environmental Microbiology*. *80*(4), 1226–1236. https://doi.org/10.1128/AEM.02848-13

Eswayah, A. S., Smith, T. J., and Gardiner, P. H. E. (2016). Microbial Transformations of Selenium Species of Relevance to Bioremediation. *82*(16), 4848–4859. https://doi.org/10.1128/AEM.00877-16

Eswayah, A. S., Smith, T. J., Scheinost, A. C., Hondow, N., and Gardiner, P. H. E. (2017). Microbial transformations of selenite by methane-oxidizing bacteria. Applied Microbiology and Biotechnology. *101*(17), 6713–6724. https://doi.org/10.1007/s00253-017-8380-8

Fakhar, A., Gul, B., Gurmani, A. R., Khan, S. M., Ali, S., Sultan, T., *et al.* (2022). Heavy metal remediation and resistance mechanism of *Aeromonas*, *Bacillus*, and *Pseudomonas*: A review. *Critical Reviews in Environmental Science and Technology*, *52*(11), 1868–1914. https://doi.org/10.1080/10643389.2020.1863112

Favorito, J. E., Grossl, P. R., Davis, T. Z., Eick, M. J., and Hankes, N. (2021). Soil-plant-animal relationships and geochemistry of selenium in the Western Phosphate Resource Area (United States): A review. *Chemosphere*, *266*, 128959. https://doi.org/10.1016/J.CHEMOSPHERE.2020.128959

Faybishenko, B., Birkholzer, J., Sassani, D., and Swift, P. (2017). International Approaches for Deep Geological Disposal of Nuclear Waste: Geological Challenges in Radioactive Waste Isolation- 5th Worldwide Review. LBNL-1006984-2016. https://doi.org/10.2172/1353043

Fomina, M., and Gadd, G. M. (2014). Biosorption: Current perspectives on concept, definition and application. *Bioresource Technology*. *160*, 3-14. https://doi.org/10.1016/j.biortech.2013.12.102

Francis, A. J., and Nancharaiah, Y. V. (2015). 9-In situ and ex situ bioremediation of radionuclide-contaminated soils at nuclear and norm sites. In Woodhead Publishing Series in Energy: Environmental Remediation and Restoration of Contaminated Nuclear and Norm Sites. 185-236. Editor: Leo van Velzen. https://doi.org/10.1016/B978-1-78242-231-0.00009-0

Gabani, P., and Singh, O. V. (2013). Radiation-resistant extremophiles and their potential in biotechnology and therapeutics. *Applied Microbiology and Biotechnology*. *97*(3), 993–1004. https://doi.org/10.1007/s00253-012-4642-7

Gadd, G. M. (2004). Microbial influence on metal mobility and application for bioremediation. *Geoderma*. 122(2-4), 109-119. https://doi.org/10.1016/j.geoderma.2004.01.002

Gadd, G. M. (2009). Biosorption: Critical review of scientific rationale, environmental importance and significance for pollution treatment. In *Journal of Chemical Technology and Biotechnology*. *84*(11), 13-28. https://doi.org/10.1002/jctb.1999

Gallois, N., Alpha-Bazin, B., Bremond, N., Ortet, P., Barakat, M., Piette, L., *et al.* (2022). Discovery and characterization of UipA, a uranium- and iron-binding PepSY protein involved in uranium tolerance by soil bacteria. *ISME Journal*, *September*. 16, 705-716. https://doi.org/10.1038/s41396-021-01113-7.

Gao, W., and Francis, A.J. (2013). Fermentation and Hydrogen Metabolism Affect Uranium Reduction by Clostridia. *ISRN Biotechnology*. ID 657160, 11. https://doi.org/10.5402/2013/657160.

García-Romero, E., María Manchado, E., Suárez, M., and García-Rivas, J. (2019). Spanish Bentonites: A review and new data on their geology, mineralogy, and crystal chemistry. *Minerals*, *9*(11), 696. https://doi.org/10.3390/min9110696

Gerber, U., Zirnstein, I., Krawczyk-Bärsch, E., Lünsdorf, H., Arnold, T., and Merroun, M. L. (2016). Combined use of flow cytometry and microscopy to study the interactions between the gram-negative betaproteobacterium *Acidovorax facilis* and uranium(VI). *Journal of Hazardous Materials*. 317, 127-134. https://doi.org/10.1016/j.jhazmat.2016.05.062

Gerstner, E. (2009). Nuclear energy: The hybrid returns. *Nature*, 460, 25–28. https://doi.org/10.1038/460025a

Gorietti, D., Giardina, I., Arginelli, D., and Battisti, P. (2017). Determination of plutonium, americium and curium isotopes in radioactive metal wastes deriving from nuclear decommissioning. *Journal of Radioanalytical and Nuclear Chemistry*, 314(3), 1785–1792. https://doi.org/10.1007/s10967-017-5553-y

Grigoryan, A. A., Jalique, D. R., Stroes-Gascoyne, S., Wolfaardt, G. M., Keech, P. G., and Korber, D. R. (2021). Prediction of bacterial functional diversity in clay microcosms. *Heliyon*, 7(10), e08131. https://doi.org/10.1016/J.HELIYON.2021.E08131

Grouzdev, D. S., Safonov, A. v, Babich, T. L., Tourova, T. P., Krutkina, M. S., and Nazina, T. N. (2018). Draft Genome Sequence of a Dissimilatory U(VI)-Reducing Bacterium, *Shewanella xiamenensis* Strain DCB2-1, Isolated from Nitrate- and Radionuclide-Contaminated Groundwater in Russia. *Genome Announcements*, 6(25), e00555-18. https://doi.org/10.1128/genomeA.00555-18

Guo, G., and Fall, M. (2021). Advances in modelling of hydro-mechanical processes in gas migration within saturated bentonite: A state-of-art review. *Engineering Geology*, 287, 106123. https://doi.org/10.1016/j.enggeo.2021.106123

Hufton, J., Harding, J., Smith, T., and Romero-González, M. E. (2021). The importance of the bacterial cell wall in uranium(VI) biosorption. *Physical Chemistry Chemical Physics*, 23, 1566. https://doi.org/10.1039/d0cp04067c

Hajj, H. El, Abdelouas, A., Grambow, B., Martin, C., and Dion, M. (2010). Microbial corrosion of P235GH steel under geological conditions. *Physics and Chemistry of the Earth*, 35, 248–253. https://doi.org/10.1016/j.pce.2010.04.007

Hall, D. S., Behazin, M., Jeffrey Binns, W., and Keech, P. G. (2021). An evaluation of corrosion processes affecting copper-coated nuclear waste containers in a deep geological repository. *Progress in Materials Science*, 118, 100766. https://doi.org/10.1016/j.pmatsci.2020.100766

Hamed, M. M., Holiel, M., and El-Aryan, Y. F. (2017). Removal of selenium and iodine radionuclides from waste solutions using synthetic inorganic ion exchanger. *Journal of Molecular Liquids*, 242, 722–731. https://doi.org/10.1016/j.molliq.2017.07.035

Handrlica, J. (2019). Reprocessing of nuclear fuel: certain legal issues arising from this unique technology. *International Journal of Legal* Research, 9(2), 150-161. Available from: https://tlq.ilaw.cas.cz/index.php/tlq/article/view/334/339

Hassan, R. S., Abass, M. R., Eid, M. A., and Abdel-Galil, E. A. (2021). Sorption of some radionuclides from liquid waste solutions using anionic clay hydrotalcite sorbent. *Applied Radiation and Isotopes*, *178*, 109985. https://doi.org/10.1016/J.APRADISO.2021.109985

Hedrich, S., Schlömann, M., and Barrie Johnson, D. (2011). The iron-oxidizing proteobacteria. *Microbiology*, 157(6), 1551-1564. https://doi.org/10.1099/mic.0.045344-0

Hökmark, H., and Fälth, B. (2003). Thermal dimensioning of the deep repository. Influence of canister spacing, canister power, rock thermal properties and nearfield design on the maximum

canister surface temperature. SKB Technical Report TR-03-09, Sweden. Available from: http://inis.iaea.org/search/search.aspx?orig_q=RN:35044492

Holmboe, M., Norrfors, K. K., Jonsson, M., and Wold, S. (2011). Effect of γ-radiation on radionuclide retention in compacted bentonite. *Radiation Physics and Chemistry*, *80*(12), 1371-1377. https://doi.org/10.1016/j.radphyschem.2011.08.004

Horvath, A., and Rachlew, E. (2016). Nuclear power in the 21st century: Challenges and possibilities. *Ambio*, 45, 38-49. https://doi.org/10.1007/s13280-015-0732-y

Huang, W.H.,and Chen, W.C. (2004). Swelling behavior of a potential buffer material under simulated near field environment. *Journal of Nuclear Science and Technology*, *41*,1271–1279. https://doi.org/10.1080/18811248.2004.9726356

Hupert-Kocurek, K., Saczyńska, A., and Piotrowska-Seget, Z. (2013). Cadmium increases catechol 2,3-dioxygenase activity in *Variovorax* sp. 12S, a metal-tolerant and phenol-degrading strain. *Antonie van Leeuwenhoek*, 104, 845-853. https://doi.org/10.1007/s10482-013-9997-y

IAEA (2009a). Classification of radioactive waste. General safety guide [Internet]. Vienna, International Atomic Energy Agency. IAEA safety standards series, no. GSG-1 STI/PUB/1419. Available from: https://www-pub.iaea.org/mtcd/publications/pdf/pub1419_web.pdf

IAEA (2009b). Status and trends of nuclear technologies: Report of the International Project on Innovative Nuclear Reactors and Fuel Cycles (INPRO). Vienna, International Atomic Energy Agency. Available from: https://www-pub.iaea.org/MTCD/Publications/PDF/TE_1622_Web.pdf

IAEA (2015). Climate change and nuclear power 2015. Vienna, International Atomic Energy Agency. Available from: https://www-pub.iaea.org/MTCD/Publications/PDF/CCANP2015Web-78834554.pdf

IAEA (2018). Status and trends in spent fuel and radioactive waste management. Vienna, International Atomic Energy Agency. Nuclear Energy Series No. NW-T-1.14, 74. Available from: https://www-pub.iaea.org/MTCD/Publications/PDF/PUB1963_web.pdf

Ikonen, J., Voutilainen, M., Söderlund, M., Jokelainen, L., Siitari-Kauppi, M., and Martin, A. (2016). Sorption and diffusion of selenium oxyanions in granitic rock. *Journal of Contaminant Hydrology*, 192, 203–211. https://doi.org/10.1016/j.jconhyd.2016.08.003

Jain, R., Jordan, N., Tsushima, S., Hübner, R., Weiss, S., and Lens, P. N. L. (2017). Shape change of biogenic elemental selenium nanomaterials from nanospheres to nanorods decreases their colloidal stability. *Environmental Science: Nano*, 4(5), 1054–1063. https://doi.org/10.1039/c7en00145b

Jroundi, F., Descostes, M., Povedano-Priego, C., Sánchez-Castro, I., Suvannagan, V., Grizard, P., *et al.* (2020). Profiling native aquifer bacteria in a uranium roll-front deposit and their role in biogeochemical cycle dynamics: Insights regarding in situ recovery mining. *Science of The Total Environment*, 721, 137758. https://doi.org/10.1016/j.scitotenv.2020.137758

Jung, K. W., Lim, S., and Bahn, Y. S. (2017). Microbial radiation-resistance mechanisms. *Journal of Microbiology*, *55*(7), 499–507. https://doi.org/10.1007/s12275-017-7242-5

Junier, P., Vecchia, E.D., and Bernier-Latmani, R. (2011). The Response of *Desulfotomaculum reducens* MI-1 to U^{VI} Exposure: A Transcriptomic Study. *Geomicrobiology Journal*, 28, 483–496. https://doi.org/10.1080/01490451.2010.512031

Kagami, T., Narita, T., Kuroda, M., Notaguchi, E., Yamashita, M., Sei, K., *et al.* (2013). Effective selenium volatilization under aerobic conditions and recovery from the aqueous phase by *Pseudomonas stutzeri* NT-I. *Water Research*, *47*(3), 1361–1368. https://doi.org/10.1016/j.watres.2012.12.001

Kamnev, A. A., Mamchenkova, P. v., Dyatlova, Y. A., and Tugarova, A. V. (2017). FTIR spectroscopic studies of selenite reduction by cells of the rhizobacterium *Azospirillum brasilense* Sp7 and the formation of selenium nanoparticles. *Journal of Molecular Structure*, *1140*, 106–112. https://doi.org/10.1016/j.molstruc.2016.12.003

Kessi, J., and Hanselmann, K. W. (2004). Similarities between the abiotic reduction of selenite with glutathione and the dissimilatory reaction mediated by *Rhodospirillum rubrum* and *Escherichia coli*. *Journal of Biological Chemistry*, *279*(49), 50662–50669. https://doi.org/10.1074/jbc.M405887200

Kim, J., Dong, H., Yang, K. et al., (2019). Naturally occurring, microbially induced smectite-to-illite reaction. *Geology*, *47*(6), 535–539. https://doi.org/10.1130/G46122.1

Kip, N., and Van Veen, J. A. (2015). The dual role of microbes in corrosion. *International Society for Microbial Ecology Journal*, 9, 542–551. https://doi.org/10.1038/ismej.2014.169

Kolhe, N., Zinjarde, S., and Acharya, C. (2018). Responses exhibited by various microbial groups relevant to uranium exposure. *Biotechnology Advances*, 36(7), 1828-1846. https://doi.org/10.1016/j.biotechadv.2018.07.002

Kónya, J., and Nagy, N. M. (2018). Environmental Radioactivity. In: Kónya J., Nagy, N.M. (Eds.). Nuclear and Radiochemistry. 2nd ed. Netherlands: Elsevier. pp. 399-419. Available from: https://www.sciencedirect.com/book/9780123914309/nuclear-and-radiochemistry

Kooyman, T., Buiron, L., and Rimpault, G. (2018). A comparison of curium, neptunium and americium transmutation feasibility. *Annals of Nuclear Energy*, 112, 748–758. https://doi.org/10.1016/j.anucene.2017.09.041

Kora, A. J. (2018). *Bacillus cereus*, selenite-reducing bacterium from contaminated lake of an industrial area: a renewable nanofactory for the synthesis of selenium nanoparticles. *Bioresources and Bioprocessing*, *5*(1), 30. https://doi.org/10.1186/s40643-018-0217-5

Kumari, I., Kumar, B.V.R., and Khanna, A. (2020). A review on UREX processes for nuclear spent fuel reprocessing. *Nuclear Engineering and Design*, 358, 110410. https://doi.org/10.1016/j.nucengdes.2019.110410

Kurmakova, I., Kupchyk, O., Bondar, O., Demchenko, N., and Vorobyova, V. (2019). Corrosion of copper in a medium of bacteria sulfate reduction proceeding. *Journal of Chemical Technology and Metallurgy*, 54(2), 416–422

Kushwaha, S., Marcus, A.K., and Rittmann, B.E. (2018). pH-dependent speciation and hydrogen (H_2) control U(VI) respiration by *Desulfovibrio vulgaris*. *Biotechnology and Bioengineering*. 115, 1465–1474. https://doi.org/10.1002/bit.26579

Lampis, S., Zonaro, E., Bertolini, C., Cecconi, D., Monti, F., Micaroni, M., Turner, R. J., Butler, C. S., and Vallini, G. (2017). Selenite biotransformation and detoxification by *Stenotrophomonas maltophilia* SeITE02: Novel clues on the route to bacterial biogenesis of selenium nanoparticles. *Journal of Hazardous Materials*, *324*, 3–14. https://doi.org/10.1016/j.jhazmat.2016.02.035

Lelieveld, J., Kunkel, D., and Lawrence, M. G. (2012). Global risk of radioactive fallout after major nuclear reactor accidents. *Atmospheric Chemistry and Physics*, *12*(9), 4245–4258. https://doi.org/10.5194/acp-12-4245-2012

Lenz, M., Van Aelst, A. C., Smit, M., Corvini, P. F. X., and Lens, P. N. L. (2009). Biological production of selenium nanoparticles from waste waters. *Advanced Materials Research*, *71–73*, 721–724. https://doi.org/10.4028/www.scientific.net/AMR.71-73.721

Leong, J., Ponnambalam, K., Binns, J., and Elkamel, A. (2021). Thermally Constrained Conceptual Deep Geological Repository Design under Spacing and Placing Uncertainties. *Applied Sciences*, *11*(24), 11874. https://doi.org/10.3390/app112411874

Leupin, O. X., Bernier-Latmani, R., Bagnoud, A., Moors, H., Leys, N., Wouters, K., and Stroes-Gascoyne, S. (2017). Fifteen years of microbiological investigation in Opalinus Clay at the Mont Terri rock laboratory (Switzerland). *Swiss Journal of Geosciences*, 110, 343–354. https://doi.org/10.1007/s00015-016-0255-y

Li, H., Zhang, J., Wang, T., Luo, W., Zhou, Q. and Jiang, G. (2008). Elemental selenium particles at nano-size (Nano-Se) are more toxic to Medaka (*Oryzias latipes*) as a consequence of hyper-accumulation of selenium: A comparison with sodium selenite. *Aquatic Toxicology*, 89(4), 251–256.

Libert, M., Bildstein, O., Esnault, L., Jullien, M., and Sellier, R. (2011). Molecular hydrogen: An abundant energy source for bacterial activity in nuclear waste repositories. *Physics and Chemistry of the Earth*, 36(17-18), 1616-1623. https://doi.org/10.1016/j.pce.2011.10.010

Lin, H., Zhou, M., Li, B., and Dong, Y., (2023). Mechanisms, application advances and future perspectives of microbial-induced heavy metal precipitation: A review. International Biodeterioration & Biodegradation, 178, 105544. https://doi.org/10.1016/j.ibiod.2022.105544

Liu, Y., Hedwig, S., Schäffer, A., Lenz, M., and Martinez, M. (2021). Sulfur Amino Acid Status Controls Selenium Methylation in *Pseudomonas tolaasii*: Identification of a Novel Metabolite from Promiscuous Enzyme Reactions. *Applied and Environmental Microbiology*, 87(12), e00104-21. https://doi.org/10.1128/AEM.00104-21

Liu, X., Long, D., You, H., Yang, D., Zhou, S., Zhang, S., *et al.* (2016). Phosphatidylcholine affects the secretion of the alkaline phosphatase PhoA in *Pseudomonas* strains. *Microbiological Research*, 192, 21–29. https://doi.org/10.1016/j.micres.2016.02.001

Lopez-Fernandez, M., Fernández-Sanfrancisco, O., Moreno-García, A., Martín-Sánchez, I., Sánchez-Castro, I., and Merroun, M. L. (2014). Microbial communities in bentonite formations and their interactions with uranium. *Applied Geochemistry*, *49*, 77–86. https://doi.org/10.1016/j.apgeochem.2014.06.022

Lopez-Fernandez, M., Cherkouk, A., Vilchez-Vargas, R., Jauregui, R., Pieper, D., Boon, N., *et al.* (2015). Bacterial Diversity in Bentonites, Engineered Barrier for Deep Geological Disposal of

Radioactive Wastes. *Microbial Ecology*, 70, 922–935. https://doi.org/10.1007/s00248-015-0630-7

Lopez-Fernandez, M., Simone, D., Wu, X., Soler, L., Nilsson, E., Holmfeldt, K., *et al.* (2018a). Metatranscriptomes Reveal That All Three Domains of Life Are Active but Are Dominated by Bacteria in the Fennoscandian Crystalline Granitic Continental Deep Biosphere. *MBio*, *9*(6), e01792-18. https://doi.org/10.1128/mBio.01792-18

López-Fernández, M., Vilchez-Vargas, R., Jroundi, F., Boon, N., Pieper, D., and Merroun, M. L. (2018b). Microbial community changes induced by uranyl nitrate in bentonite clay microcosms. *Applied Clay Science*, 160, 206-216 https://doi.org/10.1016/j.clay.2017.12.034

Lopez-Fernandez, M., Moll, H., and Merroun, M. L. (2018c). Reversible pH-dependent curium(III) biosorption by the bentonite yeast isolate *Rhodotorula mucilaginosa* BII-R8. *Journal of Hazardous Materials*, 370, 156-163. https://doi.org/10.1016/j.jhazmat.2018.06.054

Lopez-Fernandez, M., Jroundi, F., Ruiz-Fresneda, M. A., and Merroun, M. L. (2020). Microbial interaction with and tolerance of radionuclides: underlying mechanisms and biotechnological applications. *Microbial Biotechnology*, *14*(3), 810-828. https://doi.org/10.1111/1751-7915.13718

Lopez-Fernandez, M., Matschiavelli, N., and Merroun, M. L. (2021a). Bentonite geomicrobiology. *The Microbiology of Nuclear Waste Disposal*, 137–155. https://doi.org/10.1016/B978-0-12-818695-4.00007-1

Lopez-Fernandez, M., Jroundi, F., Ruiz-Fresneda, M. A., and Merroun, M. L. (2021b). Microbial interaction with and tolerance of radionuclides: underlying mechanisms and biotechnological applications. *Microbial Biotechnology*, *14*(3), 810–828. https://doi.org/https://doi.org/10.1111/1751-7915.13718

Losi, M. E., and Frankenberger, W. T. Jr. (1998). Microbial oxidation and solubilization of precipitated elemental selenium in soil. *Journal of Environmental Quality*, 27(4), 836-843. https://doi.org/10.2134/jeq1998.00472425002700040018x

Luo, X., Wang, Y., Lan, Y., An, L., Wang, G., Li, M., and Zheng, S. (2022). Microbial oxidation of organic and elemental selenium to selenite. *Science of The Total Environment*, 833, 155203. https://doi.org/10.1016/J.SCITOTENV.2022.155203

Ma, B., Charlet, L., Fernandez-Martinez, A., Kang, M. and Madé, B. (2018). Review of the retention mechanisms of redox-sensitive radionuclides in multi-barrier systems. *Applied Geochemistry*, 100, 414–431. https://doi.org/10.1016/j.apgeochem.2018.12.001

Majumder, E.L.-W., and Wall, J.D. (2017). Uranium Bio-Transformations: Chemical or Biological Processes? *Open Journal of Inorganic Chemistry*, 7(2), 28-60. https://doi.org/10.4236/ojic.2017.72003

Maleke, M., Valverde, A., Vermeulen, J.G., Cason, E., Gomez-Arias, A., Moloantoa, K., *et al.* (2019). Biomineralization and Bioaccumulation of Europium by a Thermophilic Metal Resistant Bacterium. *Frontiers in Microbiology*, *10*, 1–10. https://doi.org/10.3389/fmicb.2019.00081

Martinez, R.J., Beazley, M.J., Taillefert, M., Arakaki, A.K., Skolnick, J., and Sobecky, P.A. (2007). Aerobic uranium ^{VI} bioprecipitation by metal-resistant bacteria isolated from radionuclide- and metal-contaminated subsurface soils. *Environmental Microbiology*, 9, 3122–3133. https://doi.org/10.1111/j.1462-2920.2007.01422.x

Martinez-Rodriguez, P., Sanchez-Castro, I., Ojeda, J.J., Abad, M.M., Descostes, M., and Merroun, M.L. (2022). Effect of different phosphate sources on uranium biomineralization by the *Microbacterium* sp. Be9 strain: a multidisciplinary approach study. *Frontiers in Microbiology* (In press). https://doi:10.3389/fmicb.2022.1092184

Masurat, P., Eriksson, S., and Pedersen, K. (2010). Evidence of Indigenous Sulphate-Reducing Bacteria in Commercial Wyoming Bentonite MX- 80. *Applied Clay Science*, *47*(1−2), 51−57. https://doi.org/10.1016/j.clay.2008.07.002

McMurry, J., Dixon, D. A., Garroni, J. D., Ikeda, B. M., Stroes-Gascoyne, S., Baumgartner, P., and Melnyk, T. W. (2003). *Evolution of a Canadian deep geologic repository: Base scenario*, Report 06819, 01200-100092. Ontario Power Generation, Nuclear Waste Management Division. Toronto Canada.

Merroun, M.L., Nedelkova, M., Ojeda, J.J., Reitz, T., Fernández, M.L., Arias, J.M., *et al.* (2011). Bio-precipitation of uranium by two bacterial isolates recovered from extreme environments as estimated by potentiometric titration, TEM and X-ray absorption spectroscopic analyses. Journal of Hazardous Materials, 197, 1–10. https://doi.org/10.1016/j.jhazmat.2011.09.049

Merroun, M. L., Raff, J., Rossberg, A., Hennig, C., Reich, T., and Selenska-Pobell, S. (2005). Complexation of uranium by cells and S-layer sheets of *Bacillus sphaericus* JG-A12. *Applied and Environmental Microbiology*, *71*(9), 5532–5543. https://doi.org/10.1128/AEM.71.9.5532-5543.2005

Mijnendonckx, K., Bleyen, N., van Gompel, A., Coninx, I., and Leys, N. (2022). pH and microbial community determine the denitrifying activity in the presence of nitrate-containing radioactive waste. *Frontiers in Microbiology*, 13, 968220. https://doi.org/10.3389/fmicb.2022.968220

Mijnendonckx, K., Monsieurs, P., Černá, K., Hlaváčková, V., Steinová, J., Burzan, N., *et al.* (2021). Chapter 4: Molecular techniques for understanding microbial abundance and activity in clay barriers used for geodisposal. In: Lloyd, J. L. and Cherkouk, A. (Eds.) *The Microbiology of Nuclear Waste Disposal*, 71–96. https://doi.org/10.1016/B978-0-12-818695-4.00004-6

Mijnendonckx, K., Miroslav, H., Wang, L., Jacops, E., Provoost, A., Mysara, M., *et al.* (2019). An active microbial community in Boom Clay pore water collected from piezometers impedes validating predictive modelling of ongoing geochemical processes. *Applied Geochemistry*, *106*, 149–160. https://doi.org/10.1016/J.APGEOCHEM.2019.05.009

Mills, M. M., Sanchez, A. C., Boisvert, L., Payne, C. B., Ho, T. A., and Wang, Y. (2022). Understanding smectite to illite transformation at elevated (> 100° C) temperature: Effects of liquid/solid ratio, interlayer cation, solution chemistry and reaction time. *Chemical Geology*, 121214. https://doi.org/10.1016/j.chemgeo.2022.121214

Mishra, A., and Malik, A. (2013). Recent advances in microbial metal bioaccumulation. *Critical Reviews in Environmental Science and Technology*, 43(11), 1162-1222. https://doi.org/10.1080/10934529.2011.627044

Mitchell, N., Pérez-Sánchez, D., and Thorne, M.C. (2013). A review of the behaviour of U-238 series radionuclides in soils and plants. *Journal of Radiological Protection*, 33 (2), R17. https://doi.org/10.1088/0952-4746/33/2/R17

Mohapatra, D. P., Robinson, K. A., Huang, F., Kirpalani, D., and Loewen, M. C. (2022). Insights into Increasing Selenate Reductase Enzyme Activity in the Presence of Nitrogen-Doped Graphite Electrodes for Selenium Effluent Treatment. *Water*, *14*(6). https://doi.org/10.3390/w14060931

Moll, H., Lütke, L., Barkleit, A., and Bernhard, G. (2013). Curium(III) Speciation Studies with Cells of a Groundwater Strain of *Pseudomonas fluorescens*. *Geomicrobiology Journal*, *30*(4), 337-346. https://doi.org/10.1080/01490451.2012.688927

Moll, H., Lütke, L., Bachvarova, V., Cherkouk, A., Selenska-Pobell, S., and Bernhard, G. (2014). Interactions of the Mont Terri Opalinus Clay Isolate *Sporomusa* sp. MT-2.99 with Curium(III) and Europium(III). *Geomicrobiology Journal*, *31*(8), 682–696. https://doi.org/10.1080/01490451.2014.889975

Moll, H., Barkleit, A., Frost, L., and Raff, J. (2021). Curium(III) speciation in the presence of microbial cell wall components. *Ecotoxicology and Environmental Safety*, 227, 112887. https://doi.org/10.1016/J.ECOENV.2021.112887

NEA, 2010. Radioactive Waste in Perspective. Paris, Nuclear Energy Agency. Available from: https://www.oecdnea.org/ndd/pubs/2010/6350-waste-perspective.pdf

NEA (2020a). Management and Disposal of High-Level Radioactive Waste: Global Progress and Solutions, OECD Publishing, Paris Available from: https://www.oecd-nea.org/jcms/pl_32567/management-and-disposal-of-high-level-radioactive-waste-global-progress-and-solutions

NEA (2020b). The Environmental and Ethical Basis of Geological Disposal of Long-Lived Radioactive Wastes, OECD Publishing, Paris. Available from: https://oecd-nea.org/jcms/pl_34631/the-environmental-and-ethical-basis-of-geological-disposal-of-long-lived-radioactive-wastes

Newman, R. C., Rumash, K., and Webster, B. J. (1992). The effect of pre-corrosion on the corrosion rate of steel in neutral solutions containing sulphide: relevance to microbially influenced corrosion. *Corrosion Science*, *33*(12), 1877–1884. https://doi.org/10.1016/0010-938X(92)90190-E

Newsome, L., Morris, K., Trivedi, D., Atherton, N., and Lloyd, J.R. (2014). Microbial reduction of uranium^{VI} in sediments of different lithologies collected from Sellafield. *Applied Geochemistry* 51, 55–64. https://doi.org/10.1016/j.apgeochem.2014.09.008

Nilgiriwala, K.S., Alahari, A., Rao, A.S., and Apte, S.K. (2008). Cloning and Overexpression of Alkaline Phosphatase PhoK from *Sphingomonas* sp. Strain BSAR-1 for Bioprecipitation of Uranium from Alkaline Solutions. *Applied and Environmental Microbiology*, 74, 5516–5523. https://doi.org/10.1128/AEM.00107-08

Nuclear Waste Management Organization (2022). Programs around the world for managing used nuclear fuel. Toronto: nwmo; [updated April 2022].Available from:

https://www.nwmo.ca/~/media/Site/Files/PDFs/2022/05/31/12/28/Programs-around-the-world-backgrounder-2022.ashx?la=en

O'sullivan, L. A., Roussel, E. G., Weightman, A. J., Webster, G., Hubert, C. R., Bell, E., *et al.* (2015). Survival of *Desulfotomaculum* spores from estuarine sediments after serial autoclaving and high-temperature exposure. *The ISME journal*, *9*(4), 922-933. https://doi.org/10.1038/ismej.2014.190

Parihar, L., Johal, J.K., and Singh, V. (2013). Bioremediation of Uranium in contaminated water samples of Bathinda, Punjab by *Desulfovibrio* genus. *Journal of Soil Science and Environmental Management* 4, 1–5. https://doi.org/10.5897/JSSEM12.058

Park, D.M., and Jiao, Y. (2014). Modulation of medium pH by *Caulobacter crescentus* facilitates recovery from uranium-induced growth arrest. *Applied and Environmental Microbiology*, 80, 5680–5688. https://doi.org/10.1128/AEM.01294-14

Paterson-Beedle, M., Jeong, B. C., Lee, C. H., Jee, K. Y., Kim, W. H., Renshaw, J. C., *et al.* (2012). Radiotolerance of phosphatases of a *Serratia* sp.: Potential for the use of this organism in the biomineralization of wastes containing radionuclides. *Biotechnology and Bioengineering*. 109, 1937–1946. https://doi.org/10.1002/bit.24467

Payne, R.B., Gentry, D.M., Rapp-Giles, B.J., Casalot, L., and Wall, J.D. (2002). Uranium Reduction by *Desulfovibrio desulfuricans* Strain G20 and a Cytochrome c3 Mutant. *Applied and Environmental Microbioly*, 68, 3129–3132. https://doi.org/10.1128/AEM.68.6.3129-3132.2002

Pedersen, K. (2010). Analysis of copper corrosion in compacted bentonite clay as a function of clay density and growth conditions for sulfate-reducing bacteria. *Journal of Applied Microbiology*, 108, 1094–1104. https://doi.org/10.1111/j.1365-2672.2009.04629.x

Pedersen, K. (2013). Metabolic activity of subterranean microbial communities in deep granitic groundwater supplemented with methane and H_2. *ISME Journal*, 7, 839-849. https://doi.org/10.1038/ismej.2012.144

Pedersen, K., Motamedi, M., Karnland, O., and Sandén, T. (2000). Mixing and sulfate-reducing activity of bacteria in swelling, compacted bentonite clay under high-level radioactive waste repository conditions. *Journal of Applied Microbiology*, 89, 1038–1047. https://doi.org/10.1046/j.1365-2672.2000.01212.x

Periyakaruppan, A., Kumar, F., Sarkar, S., Sharma, C.S., and Ramesh, G.T. (2007). Uranium induces oxidative stress in lung epithelial cells. *Archives of Toxicology*. 81, 389–395. https://doi.org/10.1007/s00204-006-0167-0

Pinel-Cabello, M., Chapon, V., Ruiz-Fresneda, M. A., Alpha-Bazin, B., Berthomieu, C., Armengaud, J., and Merroun, M. L. (2021a). Delineation of cellular stages and identification of key proteins for reduction and biotransformation of Se(IV) by *Stenotrophomonas bentonitica* BII-R7. *Journal of Hazardous Materials*, *418*, 126150. https://doi.org/10.1016/j.jhazmat.2021.126150

Pinel-Cabello, M., Jroundi, F., López-Fernández, M., Geffers, R., Jarek, M., Jauregui, R., *et al.* (2021). Multisystem combined uranium resistance mechanisms and bioremediation potential of *Stenotrophomonas bentonitica* BII-R7: Transcriptomics and microscopic study. *Journal of*

Hazardous Materials, *403*, 123858. https://doi.org/https://doi.org/10.1016/j.jhazmat.2020.123858

Plötze, M., Kahr, G., and Stengele, R. H. (2003). Alteration of clay minerals — gamma-irradiation effects on physico chemical properties. *Applied Clay Science*, 23,195–202. https://doi.org/10.1016/S0169-1317(03)00103-0

Porcelli, D. (2018). Radioactivity. In: White W.M. (Ed.) Encyclopedia of Geochemistry: A Comprehensive Reference Source on the Chemistry of the Earth. Cham: Springer International Publishing. pp. 1295-1298. Available from: https://doi.org/10.1007/978-3-319-39312-4_269

Povedano-Priego, C., Jroundi, F., Lopez-Fernandez, M., Sánchez-Castro, I., Martin-Sánchez, I., Huertas, F.J., *et al.* (2019). Shifts in bentonite bacterial community and mineralogy in response to uranium and glycerol-2-phosphate exposure. *Science of The Total Environment*, 692, 219–232. https://doi.org/10.1016/j.scitotenv.2019.07.228

Povedano-Priego, C., Jroundi, F., Lopez-Fernandez, M., Shrestha, R., Spanek, R., Martín-Sánchez, I., *et al.* (2021). Deciphering indigenous bacteria in compacted bentonite through a novel and efficient DNA extraction method: Insights into biogeochemical processes within the Deep Geological Disposal of nuclear waste concept. *Journal of Hazardous Materials*, 408, 124600. https://doi.org/10.1016/j.jhazmat.2020.124600

Povedano-Priego, C., Jroundi, F., Lopez-Fernandez, M., Morales-Hidalgo, M., Martin-Sánchez, I., Huertas, F.J., *et al.* (2022). Impact of anoxic conditions, uranium^{VI} and organic phosphate substrate on the biogeochemical potential of the indigenous bacterial community of bentonite. *Applied Clay Science*, 216, 106331. https://doi.org/10.1016/j.clay.2021.106331

Povedano-Priego, C., Jroundi, F., Solari, P.L., Guerra-Tschuschke, I., Abad-Ortega, M. del M., Link, A., Vilchez-Vargas, R., Merroun, M.L., (2023). Unlocking the bentonite microbial diversity and its implications in selenium bioreduction and biotransformation: Advances in deep geological repositories. Journal of Hazardous Materials 445, 130557. https://doi.org/10.1016/j.jhazmat.2022.130557

Prakash, D., Gabani, P., Chandel, A. K., Ronen, Z., and Singh, O. v. (2013). Bioremediation: A genuine technology to remediate radionuclides from the environment. *Microbial Biotechnology*, 6(4), 349-360. https://doi.org/10.1111/1751-7915.12059

Prăvălie, R., and Bandoc, G. (2018). Nuclear energy: Between global electricity demand, worldwide decarbonisation imperativeness, and planetary environmental implications. *Journal of Environmental Management*, *209*, 81–92. https://doi.org/10.1016/j.jenvman.2017.12.043

Priest, N.D. (2001). Toxicity of depleted uranium. *The Lancet*, 357, 244–246. https://doi.org/10.1016/S0140-6736(00)03605-9

Pushkareva, R., Kalinichenko, E., Lytovchenko, A., Pushkarev, A., Kadochnikov, V., and Plastynina, M. (2002). Irradiation effect on physico-chemical properties of clay minerals. *Applied Clay Science*, 21,117–123. https://doi.org/10.1016/S0169-1317(01)00097-7

Rashwan, T. L., Asad, M. A., Molnar, I. L., Behazin, M., Keech, P. G., and Krol, M. M. (2022). Exploring the governing transport mechanisms of corrosive agents in a Canadian deep geological repository. *Science of The Total Environment*, *828*, 153944. https://doi.org/10.1016/j.scitotenv.2022.153944

Rauschenbach, I., Posternak, V., Cantarella, P., McConnell, J., Starovoytov, V., and Häggblom, M. M. (2013). *Seleniivibrio woodruffii* gen. nov., sp. nov., a selenate- and arsenate-respiring bacterium in the *Deferribacteraceae*. *International Journal of Systematic and Evolutionary Microbiology*, 63 (Pt_10), 3659-3665 https://doi.org/10.1099/ijs.0.043547-0

Reitz, T., Rossberg, A., Barkleit, A., Selenska-Pobell, S., and Merroun, M.L. (2014). Decrease of U^{VI} Immobilization Capability of the Facultative Anaerobic Strain *Paenibacillus* sp. JG-TB8 under Anoxic Conditions Due to Strongly Reduced Phosphatase Activity. *PLOS ONE*, 9, e102447. https://doi.org/10.1371/journal.pone.0102447

Renninger, N., Knopp, R., Nitsche, H., Clark, D.S., and Keasling, J.D. (2004). Uranyl Precipitation by *Pseudomonas aeruginosa* via Controlled Polyphosphate Metabolism. *Applied and Environmental Microbiology*, 70, 7404–7412. https://doi.org/10.1128/AEM.70.12.7404-7412.2004

Rogiers, T., Houdt, R.V., Williamson, A., Leys, N., Boon, N., and Mijnendonckx, K. (2022). Molecular Mechanisms Underlying Bacterial Uranium Resistance. *Frontiers in Microbiology*, 13, 822197. https://doi.org/10.3389/fmicb.2022.822197

Roh, C., Kang, C.K., and Lloyd, J.R. (2015). Microbial bioremediation processes for radioactive waste. *Korean Journal of Chemical Engineering.* 32, 1720–1726. https://doi.org/10.1007/s11814-015-0128-5

Rosa, E.A., Tuler, S.P., Fischhoff, B., Webler, T., Friedman, S.M., Sclove, R.E. *et al.* (2010). Nuclear Waste: Knowledge Waste? Science, 329 (5993), 762-763. https://doi.org/10.1126/science.1193205

Rui, X., Kwon, M. J., O'Loughlin, E. J., Dunham-Cheatham, S., Fein, J. B., Bunker, B., *et al.* (2013). Bioreduction of hydrogen uranyl phosphate: Mechanisms and U(IV) products. *Environmental Science and Technology*, 47(11), 5668-5678. https://doi.org/10.1021/es305258p

Ruiz Fresneda, M. A., Delgado Martín, J., Gómez Bolívar, J., Fernández Cantos, M. v., Bosch-Estévez, G., Martínez Moreno, M. F., and Merroun, M. L. (2018). Green synthesis and biotransformation of amorphous Se nanospheres to trigonal 1D Se nanostructures: Impact on Se mobility within the concept of radioactive waste disposal. *Environmental Science: Nano*, *5*(9), 2103–2116. https://doi.org/10.1039/c8en00221e

Ruiz-Fresneda, M. A., Gomez-Bolivar, J., Delgado-Martin, J., del Mar Abad-Ortega, M., Guerra-Tschuschke, I., and Merroun, M. L. (2019). The bioreduction of selenite under anaerobic and alkaline conditions analogous to those expected for a deep geological repository system. *Molecules*, *24*(21). https://doi.org/10.3390/molecules24213868

Ruiz-Fresneda, M. A., Eswayah, A. S., Romero-González, M., Gardiner, P. H. E., Solari, P. L., and Merroun, M. L. (2020a). Chemical and structural characterization of SeIV biotransformations by *Stenotrophomonas bentonitica* into Se0 nanostructures and volatiles Se species. *Environmental Science: Nano*, *7*(7), 2140–2155. https://doi.org/10.1039/D0EN00507J

Ruiz-Fresneda, M. A., Lopez-Fernandez, M., Martinez-Moreno, M. F., Cherkouk, A., Ju-Nam, Y., Ojeda, J. J., *et al.* (2020b). Molecular Binding of EuIII/CmIIIby *Stenotrophomonas bentonitica* and Its Impact on the Safety of Future Geodisposal of Radioactive Waste. *Environmental Science and Technology*, *54*(23), 15180–15190. https://doi.org/10.1021/acs.est.0c02418

Ruiz-Fresneda, M. A., Fernández-Cantos, M. v., Gómez-Bolívar, J., Eswayah, A. S., Gardiner, P. H. E., Pinel-Cabello, M., Solari, P. L., and Merroun, M. L. (2023). Combined bioreduction and volatilization of Se^{VI} by *Stenotrophomonas bentonitica*: Formation of trigonal selenium nanorods and methylated species. *Science of the Total Environment*, *858* (Part 2), 160030. https://doi.org/10.1016/j.scitotenv.2022.160030

Sánchez-Castro, I., Martínez-Rodríguez, P., Jroundi, F., Solari, P.L., Descostes, M., and Merroun, M.L. (2020). High-efficient microbial immobilization of solved U^{VI} by the *Stenotrophomonas* strain Br8. *Water Research*, 183, 116110. https://doi.org/10.1016/j.watres.2020.116110

Sánchez-Castro, I., Martínez-Rodríguez, P., Abad, M.M., Descostes, M., and Merroun, M.L., (2021). Uranium removal from complex mining waters by alginate beads doped with cells of *Stenotrophomonas* sp. Br8: Novel perspectives for metal bioremediation. Journal of Environmental Management 296, 113411. https://doi.org/10.1016/j.jenvman.2021.113411

Sarikhani, M. R., Malboobi, M. a., Aliasgharzad, N., and Greiner, R. (2019). Identification of two novel bacterial phosphatase-encoding genes in *Pseudomonas putida* strain P13. *Journal of Applied Microbiology*, 127, 1113–1124. https://doi.org/10.1111/jam.14376

Sepulveda-Medina, P., Katsenovich, Y., Musaramthota, V., Lee, M., Lee, B., Dua, R., *et al.* (2015). The effect of uranium on bacterial viability and cell surface morphology using atomic force microscopy in the presence of bicarbonate ions. *Research in Microbioly*. 166, 419–427. https://doi.org/10.1016/j.resmic.2015.03.003

Shrestha, R., Cerna, K., Spanek, R., Bartak, D., Cernousek, T., and Sevcu, A. (2022). The effect of low-pH concrete on microbial community development in bentonite suspensions as a model for microbial activity prediction in future nuclear waste repository. *Science of The Total Environment*, *808*, 151861. https://doi.org/10.1016/J.SCITOTENV.2021.151861

Shrestha, R., Černoušek, T., Stoulil, J., Kovářová, H., Sihelská, K., Špánek, R., *et al.* (2021). Anaerobic microbial corrosion of carbon steel under conditions relevant for deep geological repository of nuclear waste. *Science of The Total Environment*, *800*, 149539. https://doi.org/10.1016/j.scitotenv.2021.149539

Shukla, A., Parmar, P., and Saraf, M. (2017). Radiation, radionuclides and bacteria: An in-perspective review. *Journal of Environmental Radioactivity*, *180*(11), 27–35. https://doi.org/10.1016/j.jenvrad.2017.09.013

Sivaswamy, V., Boyanov, M.I., Peyton, B.M., Viamajala, S., Gerlach, R., Apel, W.A., *et al.* (2011). Multiple mechanisms of uranium immobilization by *Cellulomonas* sp. strain ES6. *Biotechnology Bioengineering*. 108, 264–276. https://doi.org/10.1002/bit.22956

Smart, N. R., Reddy, B., Rance, A. P., Nixon, D. J., Frutschi, M., Bernier-Latmani, R., and Diomidis, N. (2017). The anaerobic corrosion of carbon steel in compacted bentonite exposed to natural Opalinus Clay porewater containing native microbial populations. *Corrosion Engineering Science and Technology*, 52, 101–112. https://doi.org/10.1080/1478422X.2017.1315233

Smits, K.M., Sakaki, T., Howington, S.E., Peters, J.F., and Illangasekare, T.H. (2013). Temperature dependence of thermal properties of sands across a wide range of temperatures (30-70°C). *Vadose Zone Journal*, 138(4), 2256–2265. https://doi.org/10.2136/vzj2012.0033

Song, D., Li, X., Cheng, Y., Xiao, X., Lu, Z., Wang, Y., and Wang, F. (2017). Aerobic biogenesis of selenium nanoparticles by Enterobacter cloacae Z0206 as a consequence of fumarate reductase mediated selenite reduction. *Scientific Reports*, *7*(1). https://doi.org/10.1038/s41598-017-03558-3

Sreedevi, P. R., Suresh, K., and Jiang, G. (2022). Bacterial bioremediation of heavy metals in wastewater: A review of processes and applications. *Journal of Water Process Engineering*, *48*, 102884. https://doi.org/10.1016/J.JWPE.2022.102884

Staicu, L. C., Wójtowicz, P. J., Molnár, Z., Ruiz-Agudo, E., Gallego, J. L. R., Baragaño, D., *et al.* (2022). Interplay between arsenic and selenium biomineralization in Shewanella sp. O23S. *Environmental Pollution*, *306*, 119451. https://doi.org/10.1016/J.ENVPOL.2022.119451

Stylo, M., Neubert, N., Roebbert, Y., Weyer, S., and Bernier-Latmani, R. (2015). Mechanism of Uranium Reduction and Immobilization in *Desulfovibrio vulgaris* Biofilms. *Environmental Science and Technology*, 49(17), 10553-10561 https://doi.org/10.1021/acs.est.5b01769

Sun, W., and Nešic, S. (2007). A mechanistic model of H_2S corrosion of mild steel. Paper presented at the CORROSION 2007, Nashville, Tennessee, March 2007.

Suriya, J., Chandra Shekar, M., Nathani, N.M., Suganya, T., Bharathiraja, S., and Krishnan, M., 2017. Assessment of bacterial community composition in response to uranium levels in sediment samples of sacred Cauvery River. *Applied Microbiology and Biotechnology*, 101, 831–841. https://doi.org/10.1007/s00253-016-7945-2

Sutcliffe, B., Chariton, A.A., Harford, A.J., Hose, G.C., Greenfield, P., Elbourne, L.D.H., *et al.* (2017). Effects of uranium concentration on microbial community structure and functional potential. *Environmental Microbiology*. 19, 3323–3341. https://doi.org/10.1111/1462-2920.13839

Suzuki, Y., Kelly, S.D., Kemner, K.M., and Banfield, J.F. (2003). Microbial Populations Stimulated for Hexavalent Uranium Reduction in Uranium Mine Sediment. *Applied Microbiology and Biotechnolog*, 69, 1337–1346. https://doi.org/10.1128/AEM.69.3.1337-1346.2003

Tabak, H. H., Lens, P., van Hullebusch, E. D., and Dejonghe, W. (2005). Developments in bioremediation of soils and sediments polluted with metals and radionuclides - 1. Microbial processes and mechanisms affecting bioremediation of metal contamination and influencing metal toxicity and transport. In *Reviews in Environmental Science and Biotechnology*, 4, 115-156. https://doi.org/10.1007/s11157-005-2169-4

Tan, Y., Wang, Y., Wang, Y., Xu, D., Huang, Y., Wang, D., *et al.* (2018). Novel mechanisms of selenate and selenite reduction in the obligate aerobic bacterium *Comamonas testosteroni* S44. *Journal of Hazardous Materials*, *359*, 129-138. https://doi.org/10.1016/j.jhazmat.2018.07.014

Tan, Y., Yao, R., Wang, R., Wang, D., Wang, G., and Zheng, S. (2016). Reduction of selenite to Se(0) nanoparticles by filamentous bacterium *Streptomyces* sp. ES2-5 isolated from a selenium mining soil. *Microbial Cell Factories*, *15*(1). https://doi.org/10.1186/s12934-016-0554-z

Theodorakopoulos, N., Chapon, V., Coppin, F., Floriani, M., Vercouter, T., Sergeant, C., *et al.* (2015). Use of combined microscopic and spectroscopic techniques to reveal interactions between uranium and *Microbacterium* sp. A9, a strain isolated from the Chernobyl exclusion

zone. *Journal of Hazardous Materials*, 285, 285–293. https://doi.org/10.1016/j.jhazmat.2014.12.018

Tišáková, L., Pipíška, M., Godány, A., Horník, M., Vidová, B., and Augustín, J. (2013). Bioaccumulation of 137Cs and 60Co by bacteria isolated from spent nuclear fuel pools. *Journal of Radioanalytical and Nuclear Chemistry*, 295, 737-748 https://doi.org/10.1007/s10967-012-1932-6

Tripathy, S., Thomas, H. R., and Stratos, P. (2017). Response of compacted bentonites to thermal and thermo-hydraulic loadings at high temperatures. *Geosciences*, *7*(3), 53. https://doi.org/10.3390/geosciences7030053

Ullah, A., Yin, X., Wang, F., Xu, B., Mirani, Z. A., Xu, B., Chan, M. W. H., Ali, A., Usman, M., Ali, N., & Naveed, M. (2021). Biosynthesis of Selenium Nanoparticles (via Bacillus subtilis BSN313), and Their Isolation, Characterization, and Bioactivities. *Molecules*, *26*(18). https://doi.org/10.3390/molecules26185559

UNSCEAR. (2013), Sources, effects and risks of ionizing radiation: Report to the General Assembly with Scientific Annexes. UNSCEAR 2013 Report Volume I. New York, United Nations, 2014. Available from: http://www.unscear.org/unscear/en/publications/2013_1.html

Videla, H. A., and Herrera, L. K. (2009). Understanding microbial inhibition of corrosion. A comprehensive overview. *International Biodeterioration and Biodegradation*, 63(7), 896-900 https://doi.org/10.1016/j.ibiod.2009.02.002

Villar, M. V., Pérez del Villar, L., Martín, P. L., Pelayo, M., Fernández, A. M., Garralon, A., *et al.* (2006). The study of Spanish clays for their use as sealing materials in nuclear waste repositories: 20 years of progress. *Journal of Iberian Geology*, *32*(1), 15–36.

Vogel, M., Fischer, S., Maffert, A., Hübner, R., Scheinost, A. C., Franzen, C., *et al.* (2018). Biotransformation and detoxification of selenite by microbial biogenesis of selenium-sulfur nanoparticles. *Journal of Hazardous Materials*, *344*, 749–757. https://doi.org/10.1016/j.jhazmat.2017.10.034

Waite, T.D., Davis, J.A., Payne, T.E., Waychunas, G.A., and Xu, N. (1994). Uranium^{VI} adsorption to ferrihydrite: Application of a surface complexation model. *Geochimica et Cosmochimica Acta*, 58, 5465–5478. https://doi.org/10.1016/0016-7037(94)90243-7

Wang, T., Yang, L., Zhang, B., and Liu, J. (2010). Extracellular biosynthesis and transformation of selenium nanoparticles and application in H_2O_2 biosensor. *Colloids and Surfaces B: Biointerfaces*, *80*(1), 94–102. https://doi.org/10.1016/j.colsurfb.2010.05.041

Wang, Y., Shu, X., Zhou, Q., Fan, T., Wang, T., Chen, X., *et al.* (2018). Selenite reduction and the biogenesis of selenium nanoparticles by *Alcaligenes faecalis* se03 isolated from the gut of *Monochamus alternatus* (Coleoptera: Cerambycidae). *International Journal of Molecular Sciences*, 19(9), 2799. https://doi.org/10.3390/ijms19092799

Wang, M., Jiang, D., and Huang, X. (2022). Selenium nanoparticle rapidly synthesized by a novel highly selenite-tolerant strain *Proteus penneri* LAB-1. *IScience*, *25*(9), 104904. https://doi.org/10.1016/J.ISCI.2022.104904

Xu, Y., Zeng, Z., and Lv, H. (2019). Temperature dependence of apparent thermal conductivity of compacted bentonites as buffer material for high-level radioactive waste repository. *Applied Clay Science, 174*, 10-14. https://doi.org/10.1016/j.clay.2019.03.017

Xu, C., Zhang, Y., Cheng, G., and Zhu, W. (2008). Pitting corrosion behavior of 316L stainless steel in the media of sulfate-reducing and iron-oxidizing bacteria. *Materials Characterization*, 59, 245–255. https://doi.org/10.1016/j.matchar.2007.01.001

Yang, T., Chen, M. L., and Wang, J. H. (2015). Genetic and chemical modification of cells for selective separation and analysis of heavy metals of biological or environmental significance. *TrAC - Trends in Analytical Chemistry*, 66, 90-102. https://doi.org/10.1016/j.trac.2014.11.016

You, W., Peng, W., Tian, Z., and Zheng, M., 2021. Uranium bioremediation with U^{VI}-reducing bacteria. *Science of Total Environment*, 798, 149107. https://doi.org/10.1016/j.scitotenv.2021.149107

Yun, J., Malvankar, N.S., Ueki, T., and Lovley, D.R. (2016). Functional environmental proteomics: elucidating the role of a c-type cytochrome abundant during uranium bioremediation. *The ISME Journal*, 10, 310–320. https://doi.org/10.1038/ismej.2015.113

Yung, M.C., and Jiao, Y., 2014. Biomineralization of Uranium by PhoY Phosphatase Activity Aids Cell Survival in Caulobacter crescentus. *Applied and Environmental Microbiology*. 80, 4795–4804. https://doi.org/10.1128/AEM.01050-14

Zambonino, M. C., Quizhpe, E. M., Jaramillo, F. E., Rahman, A., Santiago Vispo, N., Jeffryes, C., *et al.* (2021). Green Synthesis of Selenium and Tellurium Nanoparticles: Current Trends, Biological Properties and Biomedical Applications. *International Journal of Molecular Sciences*, *22*(3). https://doi.org/10.3390/ijms22030989

Zhang, J., Song, H., Chen, Z., Liu, S., Wei, Y., Huang, J., *et al.* (2018). Biomineralization mechanism of U(VI) induced by *Bacillus cereus* 12-2: The role of functional groups and enzymes. *Chemosphere*, 206, 682-692. https://doi.org/10.1016/j.chemosphere.2018.04.181

Zhang, X., Gu, P., and Liu, Y. (2019). Decontamination of radioactive wastewater: State of the art and challenges forward. *Chemosphere*, *215*, 543–553. https://doi.org/10.1016/j.chemosphere.2018.10.029

Zheng, L., Rutqvist, J., Xu, H., and Birkholzer, J.T. (2017). Couple THMC models for bentonite in an argillite repository for nuclear waste: Illitization and its effect on swelling stress under high temperature. *Engineering Geology*, *230*, 118–129. https://doi.org/10.1016/j.enggeo.2017.10.002

Zhong, J., Hu, X., Liu, X., Cui, X., Lv, Y., Tang, C., *et al.* (2021). Isolation and Identification of Uranium Tolerant Phosphate-Solubilizing Bacillus spp. and Their Synergistic Strategies to U(VI) Immobilization. *Frontiers in Microbiology*, *12*. https://doi.org/10.3389/fmicb.2021.676391


Modified from iStock
Credit: magann

Objectives

OBJECTIVES

The main aim of this PhD Thesis is to study and explore the impact of the microorganisms present in the Spanish bentonite on the biogeochemical processes that may occur at bentonite/copper canister/selenium interface within the context of Deep Geological Repositories (DGR) for radioactive waste. The proposed use of this bentonite as a backfill and sealing material underscores the need to comprehend the role of the inherent microorganisms to ensure the long-term integrity of DGR system. This study will provide valuable knowledge that will contribute to assess the safety performance and long-term stability of this type of disposal system.

Therefore, the specific objectives of this PhD Thesis are:

1) To evaluate the effect of bentonite compaction at dry density (1.7 g cm^{-3}) on microbial diversity and, consequently, the role of the inherent microorganisms in the bentonite stability and corrosion of copper canister.
2) To explore the effect of the high temperature (tyndallization and incubation at 60 ºC) on the microbial communities, mineralogical stability of the bentonite, and corrosion of copper material.
3) To study the effect of lactate, acetate and sulfate, spiked to water hyper-saturated bentonite slurry microcosms (used as model systems), on bacterial diversity and biogeochemical processes, including copper corrosion mechanisms.
4) To investigate the effect of selenite [Se(IV)] on microbial communities in hyper-saturated bentonite slurry microcosms and the associated biogeochemical processes, determining how microorganisms affect selenium speciation.

Obtained from iStock

Credit: Yassine Khalfalli

Materials and Methods

MATERIALS AND METHODS

This section describes the general Materials and Methods for the different experimental setups. For more detailed information about the development of the experiments, including compacted bentonite blocks and hypersaturated bentonite microcosms, and the preparation of their components, as well as the specific techniques used, please refer to the *Materials and Methods* section in each independent chapter (Chapters I - IV).

1_ Bentonite location, collection and storage

The bentonite was aseptically collected in February 2020 at the 'Cortijo de Archidona' site (Almeria, Spain) at a maximum depth of 80 cm (**Fig. 1**). It was then manually defragmented in the laboratory and dried for a minimum of five days at room temperature inside a laminar flow cabinet to remove excess moisture. To obtain a homogeneous powder, the bentonite was ground using a disinfected stainless-steel roller and a mortar. Finally, it was stored at 4 ºC until the preparation of the different experimental designs.

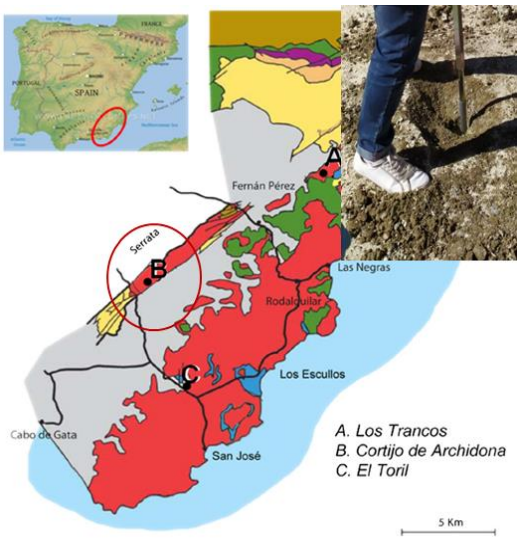

Fig. 1. Bentonite sampling location and collection. Modified from Lopez-Fernandez et al., 2015.

2_ Copper material

Oxygen Free High Conductivity (OFHC) copper disks (**Fig. 2A**) were obtained from Goodfellow Company (UNS number C10100; goodfellow.com). The dimensions of the disks were 4.0 ± 10 % mm thick and 10.0 ± 0.5 mm in diameter. The elemental composition consisted of 99.9 % - 100 % pure copper, with small impurities (in data sheet) of S (< 0.0015 %), Pb (< 0.0005 %), Sb (< 0.0004 %), P (< 0.0003 %) and Zn (< 0.0001 %). Prior to use, the Cu disks were autoclaved for 15 min at 121 °C.

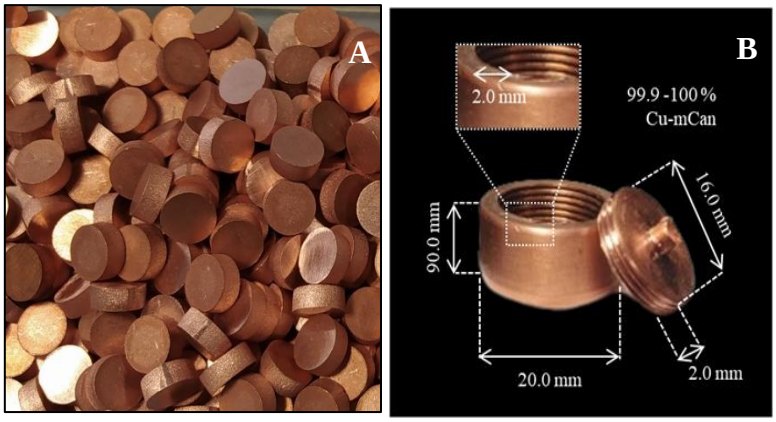

Fig 2. A) OFHC copper disks, and B) dimension of the high-purity copper mini-canisters (Cu-mCan).

For the preparation of copper mini canisters (Cu-mCan) (**Fig. 2B**), copper rods (purity: 99. 9 - 100 %) from the same company was obtained, Goodfellow (UNS number C10100), containing small impurities (in data sheet) of Cr (< 1 ppm), Fe (2 ppm), Ag (70 ppm), Al (1 ppm), Mg (1 ppm), Mn (< 1 ppm), Ni (2 ppm), Na (< 1 ppm), Sn (1 ppm), Pb (2 ppm), Si (2 ppm), Bi (1 ppm) and Ca (1 ppm). Two bars of different diameters (20.6 ± 0.05 and 16.0 ± 0.5 mm) were used for the fabrication of the Cu-mCan. The Cu-mCan were manufactured in the mechanical workshop of the Centro de Instrumentación Científica (University of Granada, Spain). The Cu-mCan were sterilized by autoclaving for 15 min at 121 ºC.

3_ Spectroscopic and chemical characterization of bentonite

X-Ray Diffraction (XRD)

X-ray powder diffraction (XRD) is an analytical and non-destructive method primarily used to identify the phases of crystalline substances. XRD involves constructive interference of a monochromatic X-ray beam with the lattice planes of a crystalline sample, following Bragg's Law ($n\lambda=2d\ sin\ \theta$) (**Fig. 3**). This law connects the wavelength of radiation, diffraction angle, and lattice spacing. By rotating the sample through various angles, different diffraction directions are achieved due to the random orientation of the powdered material. The detected diffracted X-rays, which vary in intensity based on atomic positions, create a unique XRD pattern, serving as a material's fingerprint. This pattern, compared against standard database references, facilitates the identification of various crystalline samples.

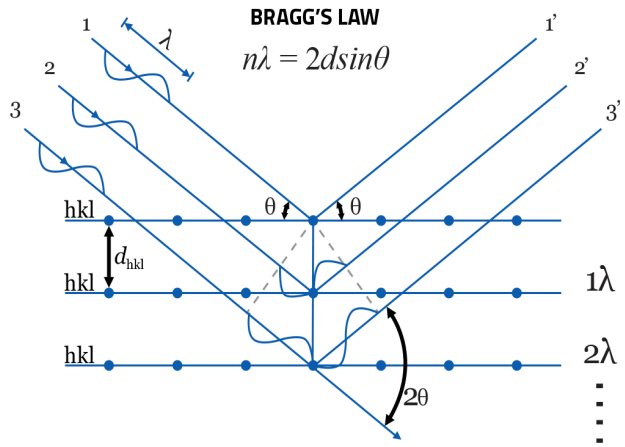

Fig. 3. Bragg's law on which X-Ray Diffraction (XRD) analysis are based (https://www.veqter.co.uk/residual-stress-measurement/x-ray-diffraction).

In this study, Oriented Aggregates (OA) of the bentonite were carried out to study the behavior of smectite basal reflections by XRD. Air-dried AOs were analyzed using a PANalytical X'Pert Pro diffractometer (CuKα radiation, 45 kV, 40 mA)

equipped with an X'Celerator solid-state linear detector. A step increment of 0.008º 2θ and a counting time of 10 s/step was used. Subsequently, the samples were exposed to ethylene glycol (EG) vapor at 60 °C for 24 h and reanalyzed with the diffractometer. HighScore software was used to analyze the diffractograms.

X-Ray Fluorescence (XRF)

XRF is an analytical technique that can be used to determine the chemical composition of a wide variety of sample types, including solids and powders. XRF provides qualitative and quantitative environmental sample´s information. This method is based on atomic emission that measures the wavelength and intensity of X-rays emitted by energized atoms in a given sample (**Fig. 4**). The primary X-ray beam from an X-ray tube causes the emission of fluorescent X-rays with discrete energies characteristic of the elements present in the sample. The major element composition of the bentonite was determined by XRF analysis using a PANalytical Zeltium with a rhodium anode ceramic X-ray tube with a high transmission beryllium ultrathin front window.

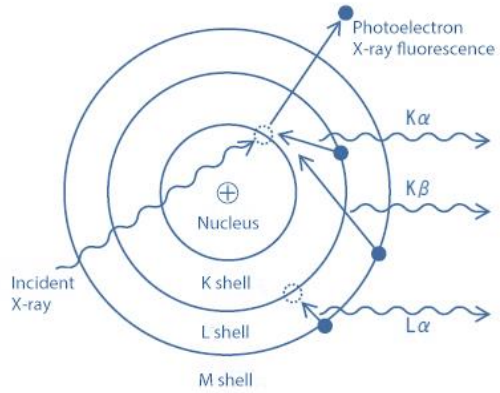

Fig. 4. Principle of Fluorescent X-rays emission (modified from: https://www.matsusada.com/column/words-xrf.html)

pH

The pH of the samples was measured in triplicate with an Advanced Digital Handheld Portable Meter HQ40D pH meter (Hach) previously calibrated with commercial reference solutions (4.00 and 7.00). The bentonite from the compacted blocks was ground and homogenized with 0.01 M $CaCl_2$ at a 1:15 w:v ratio. In the case of hypersaturated microcosms, supernatant was sampled and filtered through sterile 0.22 µm filters.

4_ High Pressure Ion Chromatography (HPIC)

Acetate, lactate, and sulfate concentrations in the supernatants from hypersaturated microcosms were quantified by High Pressure Ion Chromatography (HPIC) (**Fig. 5**). This technique involves using a buffered aqueous solution, known as the mobile phase, to transport the sample from the loop to the chromatography column. The column contains a stationary phase analyte which is covalently bonded to charged functional groups, such as a cation exchange resin. The target analytes, whether anions or cations, are retained in the stationary phase but can be eluted by increasing the concentration of similarly charged species, which displaces the analyte ions.

The concentrations of acetate, lactate, and sulfate in supernatants were determined by a HPIC Methrom Hispania 925 Eco ICE system (Herisau, Switzerland). This system was equipped with an IC conductivity detector, Metrohm Suppressor Module (MSM), a 250 µL injection loop with a peristaltic pump, a high-pressure pump with a purge valve from Metrohm, and a 919 UF autosampler. Samples were filtered through a 0.22 µm membrane and diluted in ultrapure water prior to injection. The analysis was carried out at room temperature using a Metrosep A 5-250/4.0 column (250 x 4.0 mm) with a Metrosep A Supp 5 Guard/4.0 pre-column. The flow rate was maintained at 0.7 mL min-1, with a mobile phase of 3.2 mM Na_2CO_3 / $NaHCO_3$ 1 mM. Chemical suppression was achieved using a MSM-

Metrohm Suppressor Module with a solution of 250 mM H_2SO_4, 10 mM oxalic acid, and 10 % acetone. Calibration was performed using standard solutions of the target compounds. Data was processed using MagIC Net 3.1 basic software. Standard solutions of acetate, sulfate, and lactate (1,000 mg L^{-1}).

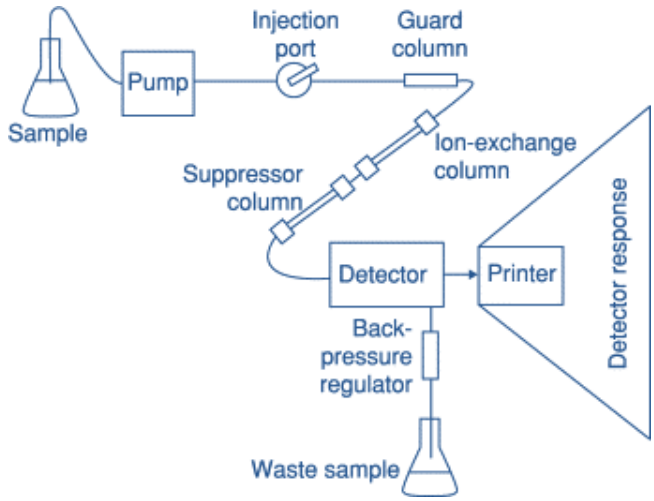

Fig. 5. Essential components of an ion-exchange chromatograph (HPIC). Modified from R.H. Worden, in Encyclopedia of Geology, 2005.

5_ Molecular characterization of microbial diversity

DNA extraction and sequencing

All DNA extractions from bentonite samples were based on the extraction protocol described in Povedano-Priego et al. (2021). Some modifications of this protocol due to the difficulty of extraction in these samples are described in Chapter III. Total DNA quantification was performed using a Qubit 3.0 fluorometer (Life Technology, Invitrogen™).

The amplification, sequencing, and subsequent bioinformatics analyses were performed at STAB VIDA (Caparica, Portugal; https://www.stabvida.com). For library construction, primers 341F (5′-CCTACGGGNGGCWGCAG-3′) and 785R (5′-GACTACHVGGGTATCTAATCC-3′) were used, targeting the V3 – V4

variable regions of the 16S rRNA gene. Sequencing was carried out on the Illumina MiSeq platform, a Next-Generation Sequencing (NGS) technology, employing the MiSeq Reagent Kit v3 for 300bp paired-end reads. MiSeq System takes advantage of the chemical process sequencing by synthesis (SBS) technology from Illumina. Quality control of the sequencing data was conducted using FastQC software.

For the hypersaturated microcosm experiments, the analysis and sequencing of the extracted DNA were carried out in collaboration with the Department of Gastroenterology at the University of Magdeburg (Germany). For the library preparation, each sample underwent two sequential PCR reactions using a mix of standard and barcoded fusion primers. The primers 807F (5′-GGATTAGATACCCBRGTAGTC-3′) and 1050R (5′-AGYTGDCGACRRCCRTGCA-3′), were chosen for targeting the V5 – V6 regions of the 16S rRNA gene. The completed libraries were sequenced on the MiSeq Illumina platform, (2 × 250 bp, Hayward, California, USA).

Bioinformatics and statistical analysis

For sequencing carried out in STAB VIDA, the raw sequences were then processed using QIIME2 v2021.4, where the DADA2 plugin was used to trim and truncate low-quality areas, dereplicate reads, and remove chimeras. To assess the adequacy of the read numbers, alpha rarefaction curves were constructed. The reads were grouped into operational taxonomic units (OTUs) and taxonomically classified using the scikit-learn classifier and the SILVA database (release 138 QIIME), with a clustering threshold set at 99% similarity.

In the case of the sequencing carried out at the University of Magdeburg, FastaQ files were processed and normalized using the "dada2" and "phyloseq" packages, respectively, in R 4.2.1 software. Bayesian classification was used to assign phylotypes to taxonomic affiliation (pseudo-bootstrap threshold of 80%).

Relative abundances and alpha diversity indices were performed using Explicet 2.10.5. To evaluate similarity between samples at the genus level, a matrix based on the Bray-Curtis algorithm was used, and subsequent similarity between samples was carried out by Principal Coordinate Analysis (PCoA) using Past4 software. In addition, a HeatMap was performed to visualize taxa with higher relative abundance.

6_ Molecular identification of bacterial isolates and culture-dependent techniques

DNA extraction and sequencing

The DNA was extracted from pure colonies using 100 µL of PrepMan™ Ultra Sample Preparation Reagent (Thermo Fisher), followed by a 10-minute thermal lysis at 95 ºC. Amplification of 16S rRNA gene fragments was carried out using primers 341F (5'-TCGTCGGCAGCGTCAGATGTGTATAAGAGACAGCCTACGGGNGGCWGCAG-3') and 785R (5'-GTCTCGTGGGCTCGGAGATGTGTATAAGAGACAGGACTACHVGGGTATCTAATCC-3'). The PCR products were then purified using the Wizard® SV Gel and PCR Clean-Up System (Promega), and the purified samples were subjected to Sanger Sequencing at Eurofins Genomics, Germany. This process includes electrophoresis and relies on the random integration of chain-terminating dideoxynucleotides by DNA polymerase during the replication of DNA in vitro. The sequenced data were then classified by The RDP Classifier and compared with those available in the GenBank database using BLAST (Basic Local Alignment Search Tool) analysis.

Most Probable Number (MPN) method

The quantification of sulfate-reducing bacteria was estimated by the Most Probable Number (MPN) method (**Fig. 6**). This method was conducted following the MPN method of Biotechnology Solutions (Houston, USA, biotechnologysolutions.com), based on serial dilutions in triplicate, using Postgate's medium (DSMZ_Medium63, dsmz.de) with Na-thioglycolate replaced by Cysteine-HCl (0.5 g L^{-1}). The MPN of sulfate-reducing bacteria was estimated by comparing the positive bottles (presence of black precipitates) with a reference table (MPN Method, biotechnologysolutions.com).

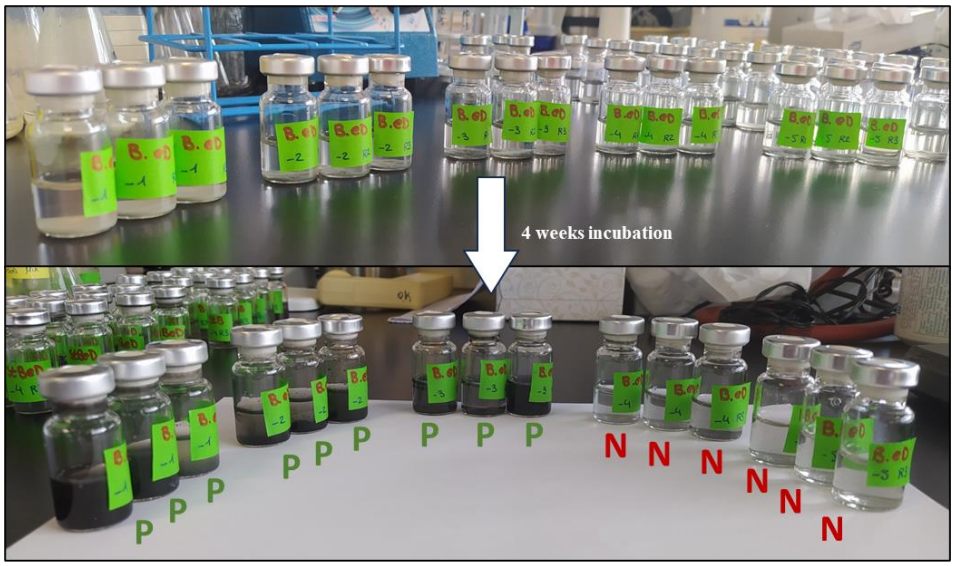

Fig. 6. Examples of bottles from the Most Probable Number (MPN) experiment of sample B.eD from compacted bentonite blocks before and after 4-week incubation. P: bottle considered positive, N: bottles considered negative.

7_ Microscopic and spectroscopic analysis

Variable Pressure Field Emission Scanning Electron Microscopy (VP-FESEM)

Surface visualization of the copper disks was carried out using a Zeiss SUPRA40VP variable pressure field emission scanning electron microscope (VP-FESEM) equipped with SE (InLens) and BSE detectors (**Fig. 7A**). For chemical

analyses, the energy dispersive X-ray (EDX) detector consisted of a 50 mm^2 XMAX silicon drift detector that allowed the detection of elements with Z4 ≥ (Be) and high-count rates.

High Resolution Scanning Electron Microscopy (HRSEM)

The base of the Cu-mCan were analyzed using an AURIGA Carl Zeiss SMT high-resolution scanning microscope (HRSEM) equipped with SE, SE-inLens, BSE, EsB and STEM (BF/DF) detectors (**Fig. 7B**). Qualitative and quantitative energy dispersive X-ray microanalysis (EDX) was used for elements analyses of atomic number greater than Be.

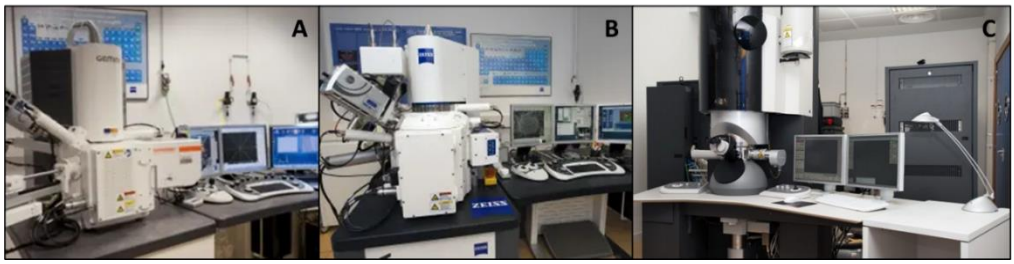

Fig. 7. A) Zeiss SUPRA40VP variable pressure field emission scanning electron microscope (VP-FESEM), B) AURIGA Carl Zeiss SMT high-resolution scanning microscope (HRSEM), and C) high-angle annular dark-field scanning transmission electron microscope (HAADF-STEM, FEI TITAN G2 80-300). Obtained from: https://cic.ugr.es/servicios/

High-Angle Annular Dark Field Scanning Transmission Electron Microscope (HAADF-STEM)

For the characterization of the selenium precipitates a high-angle annular dark-field scanning transmission electron microscope (HAADF-STEM, FEI TITAN G2 80-300) was used (**Fig 7C**). EDX microanalyses were performed at 300 kV. In addition, selected area electron diffraction (SAED) and HRTEM combined with Fast Fourier Transform (FFT) were used for allotropic characterization of selected precipitates.

Micro-Fourier Transform Infrared Spectroscopy (micro-FTIR)

The detection of organic compounds, present on the surfaces of the copper disks, was analyses by reflectance micro-Fourier Transform Infrared Spectroscopy (micro-FTIR). The basic principle of this technique is based on the excitation of molecular groups by a beam of infrared light that generates vibrational shifts in the bonds of the molecule. The vibrational motions are distinguished by the type of displacement generated in the bonds. The micro-FTIR analyses were carried out using a PerkinElmer Spotlight micro-FTIR spectroscope, which is equipped with a mercury-cadmium-telluride detector featuring 16 gold-wired infrared detector elements. The reflectance micro-FTIR images were collected with a per-pixel aperture size of 25 μm x 25 μm, four scans per pixel, and a spectral resolution of 16 cm^{-1}.

X-Ray Photoelectron Spectroscopy (XPS)

XPS is a method used for analyzing surface chemistry of different samples including minerals, microbes, materials, etc. It involves measuring the energy of photoelectrons released from a surface when it is exposed to X-rays in a vacuum environment. This method yields comprehensive insights into the elemental composition and chemical state of elements, and molecules in a sample. XPS was used in this study to identify the chemical composition of the corrosion compounds present on the surface of the copper materials by a Kratos AXIS Supra photoelectron spectrometer. The X-ray source was a monochromatic Al Kα (1486.6 eV) operating at an X-ray emission current of 20 mA and a high anode voltage of 15 kV. The acquisition angle was set at 90° with respect to the sample plane. The analysis comprised a broad probe scan (160 eV step energy, 1.0 eV step size) and a high-resolution scan (20 eV step energy, 0.1 eV step size) for component speciation. The integral Kratos charge neutralizer served as a source of electrons to counteract the differential charge. The binding energy scale was calibrated using the Au $4f_{5/2}$ (83.9 eV), Cu $2p_{3/2}$ (932.7 eV) and Ag $3d_{5/2}$ (368.27 eV) lines of clean gold, copper and silver standards from the National Physical

Laboratory (NPL), UK. CasaXPS 2.3.22 software was used to fit the peaks of the XPS spectra. The effect of surface charge was compensated for all binding energies by referencing the adventitious carbon C 1s peak at 285 eV.

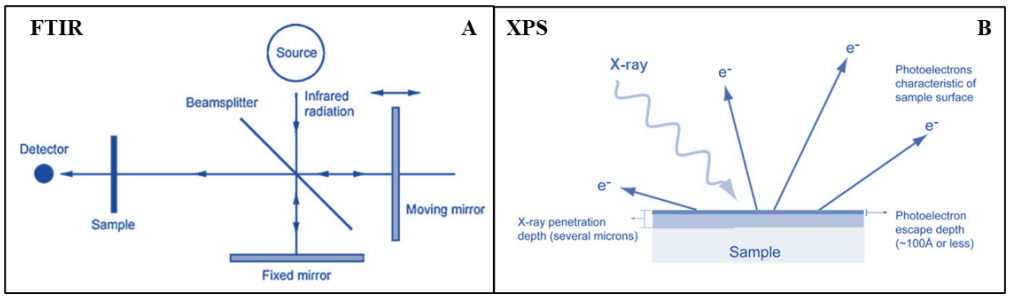

Fig. 8. Principle of A) Micro-Fourier Transform Infrared Spectroscopy (micro-FTIR), and B) X-Ray Photoelectron Spectroscopy (XPS). Images modified from https://www.findlight.net/blog/ftir-principles-applications/, and https://www.eag.com/techniques/spectroscopy/x-ray-photoelectron-spectroscopy-xps-esca/; respectively.

EDX maps associated with electron images from the Cu disc

Chapter I:

Impact of compacted bentonite microbial community on the clay mineralogy and copper canister corrosion: a multidisciplinary approach in view of a safe Deep Geological Repository of nuclear wastes

Authors

Marcos F. Martinez-Moreno[a]*, Cristina Povedano-Priego[a], Mar Morales-Hidalgo[a], Adam D. Mumford[b], Jesus J. Ojeda[b], Fadwa Jroundi[a], Mohamed L. Merroun[a]

[a]Department of Microbiology, Faculty of Sciences, University of Granada, Granada, Spain

[b]Department of Chemical Engineering, Faculty of Science and Engineering, Swansea University, Swansea, United Kingdom

This chapter has been published in Journal of Hazardous Materials: Martinez-Moreno, M.F., et al. (2023). J. Hazard. Mater., 131940. https://doi.org/10.1016/j.jhazmat.2023.131940

IF: 13.6 / **Q**1 / **D**1

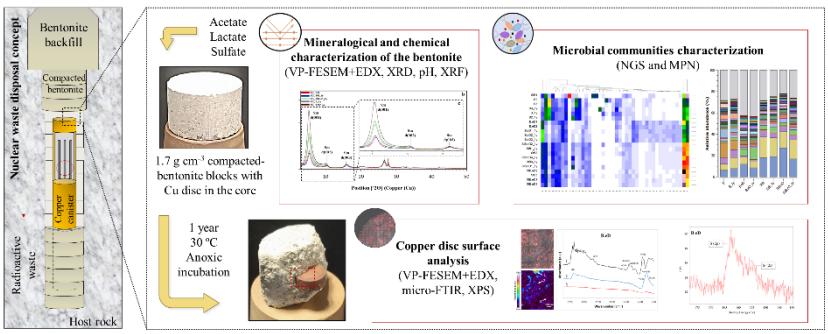

Abstract

The Deep Geological Repository (DGR) is the preferred option for the final disposal of high-level radioactive waste. Microorganisms could affect the safety of the DGR by altering the mineralogical properties of the compacted bentonite or inducing the corrosion of the metal canisters. In this work, the impact of physicochemical parameters (bentonite dry density, heat shock, electron donors/acceptors) on the microbial activity, stability of compacted bentonite and corrosion of copper (Cu) discs was investigated after one-year anoxic incubation at 30 ºC. No-illitization in the bentonite was detected confirming its structural stability over 1 year under the experimental conditions. The microbial diversity analysis based on 16S rRNA Next Generation Sequencing showed slight changes between the treatments with an increase of aerobic bacteria belonging to Micrococcaceae and *Nocardioides* in heat-shock tyndallized bentonites. The survival of sulfate-reducing bacteria (the main source of Cu anoxic corrosion) was demonstrated by the most probable number method. The detection of Cu_xS precipitates on the surface of Cu metal in the bentonite/Cu metal samples amended with acetate/lactate and sulfate, indicate an early stage of Cu corrosion. Altogether, the outputs of this study help to better understand the predominant biogeochemical processes at the bentonite/Cu canister interface upon DGR closure.

Keywords: *DGR, compacted bentonite, microbial diversity, sulfate-reducing bacteria, copper corrosion*

1_ Introduction

One of the most relevant issues in the nuclear energy industry is the final disposal and management of high-level radioactive waste (HLW). These waste products generate significant amounts of heat due to the radioactive decay process, whilst also containing large quantities of long-lived radionuclides with a half-life of hundreds to millions of years (Betandiieva et al., 2009). For this reason, HLW must be properly and safely confined for at least 100,000 years in suitable facilities until the radiotoxicity decreases to levels comparable to natural ones (Ojovan and Steinmetz, 2022). The most internationally accepted option for this final disposal is the Deep Geological Repository (DGR), based on a multi-barrier system that isolates the waste from the biosphere. HLW will be stored in corrosion-resistant metal canisters, surrounded by a filling and sealing buffer material (the engineered barriers), and the whole system will be hosted a few hundred meters depth in a stable geological formation (the natural barrier) (WNA, 2021).

The nature of the canisters would depend on the DGR concept adopted by each country. Canada, Korea, and Sweden propose copper as external coating material for metal canisters. Finland has already proceeded to implement Cu as material for metal canisters (POSIVA, n.d.). Other alternatives include steel-based materials (e.g., Belgium, Czech Republic), titanium (e.g., Japan, United Kingdom), and nickel alloys (e.g., United States of America) (Hall et al., 2021). The buffer material in most countries typically consist of highly compacted bentonite clay, which could minimize the groundwater flow, and retard the migration of the radionuclides. Bentonite presents favorable mechanical support providing stability for canisters, low permeability which reduces the groundwater infiltration, high ion exchange that helps with radionuclide retention and retardation in case of containment breach, high plasticity and swelling capacity in order to allow self-sealing of canister cracks, good thermal conductivity, and optimal properties for compaction (García-Romero et al., 2019). In Spain, bentonite from “El Cortijo de

Archidona" (Almería) has been widely studied as a potential buffer material, for DGR use, characterizing its geochemical, mineralogical properties (Huertas et al., 2021; Villar et al., 2006). The impact of the microbial community processes in this bentonite, under different relevant DGR conditions, has only began to be studied in the last few years, (Povedano-Priego et al., 2021; Lopez-Fernandez et al., 2014).

The determination of the structure and composition of the microbial community in the bentonite buffer is crucial to highlight the impact that their activities would have on the long-term stability of the DGR. For instance, microorganisms could affect the integrity of the metal canisters through microbially influenced corrosion (MIC) promoted by biofilm formation on the metal surface or the production of corrosive metabolites. Moreover, in the case of canister cracks or fissures, bacteria could interact with, and mobilize radionuclides, increasing their migration through the different barriers. Another implication is related to the microbial metabolism that could contribute to gas phase liberation within the DGR (Guo and Fall, 2021). The main gases produced by microorganisms are in the form of hydrogen (H_2), methane (CH_4), and carbon dioxide (CO_2). These gases would increase the pressure within the DGR, compromising the clay barrier integrity (Bagnoud et al., 2016). However, certain aspects related to this disposal technology (e.g., compaction density of the buffer material, anoxic conditions, heat produced by the radionuclide waste, etc.) would hinder the activity and viability of the bacterial communities. Upon DGR closure, oxygen will be gradually consumed due to, for example, microbial activity or corrosion of metal canister (e.g., rock bolts or other steel construction materials), then enhancing an anoxic environment to prevail in the repository (Payer et al., 2019; Keech et al., 2014). Some groups of anaerobic bacteria such as sulfate-reducing (SRB) and iron-reducing bacteria (IRB) can potentially be active under these conditions. Detrimental effects of the activity of these bacteria include the induction of MIC processes, the reduction of Fe(III) to Fe(II) in the smectite (the main mineral in bentonites), as well as the reduction of sulfate to sulfide (as the main corrosion agent of copper). In addition, some SRB

(e.g., *Desulfovibrio vulgaris* and *Desulfitobacterium frappieri*) could cause MIC by reducing the structural Fe(III) in smectite (Pentráková et al., 2013; Liu et al., 2012; Shelobolina et al., 2003) and producing sulfide, providing sulfate is available in the repository. Sulfide production through reduction of sulfate is kinetically hindered under temperature and pressure standard abiotic conditions (Cross et al., 2004). Therefore, the potential presence of sulfide would be originated by the SRB activity (Bengtsson and Pedersen, 2017), which increases at greater distances from the canisters as favorable conditions prevail (e.g., decrease of temperature and increase of water activity). These products could diffuse through the biologically inactive portion of the sealing materials and affect the type and rate of copper corrosion at the container surface. However, diffusion modeling studies suggest that only a small amount of sulfide would actually reach the canisters surface, resulting in a limited impact on container corrosion (King 2002, Wersin et al., 1994, King et al., 2003).

Compaction density of the bentonite is another important issue to be addressed, since the viability and activity of the bacterial communities could be reduced at high dry densities (Pedersen, 2010). Nevertheless, microbes are able to survive in a metabolically nearly inactive state or as spores (Bengtsson and Pedersen, 2017, 2016). Maanoja et al. (2020) reported that the organic matter naturally present in compacted bentonites can sustain biological sulfate reduction by SRB. Accordingly, Povedano-Priego et al. (2021) demonstrated the resistance of the microbial communities to high compaction densities (1.5 and 1.7 g cm^{-3}) of the acetate-treated Spanish bentonite, since no significant differences in the bacterial diversity observed after two years of anaerobic incubation. In addition, SRB groups such as *Pseudomonas*, *Desulfuromonas*, *Desulfosporosinus*, and *Desulfovibrio* were identified. For this reason, the present study is focused on assessing whether the stimulation of microbial activity in highly compacted bentonite (1.7 g cm^{-3}) by the addition of electron donors and acceptors could affect the biogeochemical processes at bentonite/Cu disc surface interface. Thus, metal-

canister corrosion and the mineralogical stability of the clay for long-time periods are crucial to be characterized.

Hence, the main aim of the present work was to investigate the bio-geochemical and physicochemical processes at the Cu canister/bentonite clay barrier interface-based microcosm and to characterize the biocorrosion products on the metal surface. The studies were focused on assessing the possible one-year-term shifts in the microbial communities of highly-compacted Spanish bentonite containing a copper disc in their core, after one-year anaerobic incubation at 30 ºC. To stimulate the activity of indigenous anaerobic bacteria (e.g., SRB), bentonite was amended with electron donors (acetate and lactate) and an electron acceptor (sulfate), which participate in redox reactions relevant for DGR safety studies (Povedano-Priego et al., 2021; Matschiavelli et al., 2019, Grigoryan et al., 2018). Microscopic and spectroscopic state-of-the-art techniques were performed to determine the stability of the bentonite and the potential corrosion on the copper disc. Moreover, the most probable number (MPN) technique was carried out to determine viability and quantify the approximate number of SRB per gram in the bentonite samples. Several studies have reported the effect of microbial activity on canister materials or on the stability of commercial bentonites such as MX-80, Opalinus Clay or FEBEX (Pedersen, 2010; Smart et al., 2017; Madina et al., 2005). Moreover, to the best of our knowledge, this is the first work that collectively describes the impact of indigenous bacteria, from the highly-compacted Spanish bentonite, on the clays' mineralogical stability and the corrosion of copper, whilst also considering the effect of different physiochemical parameters on the bentonite microbial community. Thus, this study lays the baseline to define the microbial effects on both the compacted Spanish bentonite properties, and the initial steps related to long-term corrosion of copper canisters, all of which could affect the safety of nuclear waste storage within the DGR.

2_ Material and methods

2.1_ Elaboration of compacted bentonite blocks containing a copper disc

2.1.1_ Bentonite collection

Bentonite samples were collected aseptically from El Cortijo de Archidona (Almeria, Spain) in February 2020, at a maximum depth of ~ 80 cm. In addition to its safety-related properties, this bentonite has been selected as a reference sealing material for the future Spanish DGR, due to its low carbonate and colloidal contents and a high degree of plasticity and compressibility (Villar et al., 2006). Once in the laboratory, bentonite was stored at 4 ºC until further used.

Bentonites were manually disaggregated and dried under sterile conditions in a laminar flow cabinet for at least 5 days. Then, they were ground with a sterile stainless-steel roller to obtain a homogeneous powder.

2.1.2_ Copper disc material

Oxygen-Free High Conductivity (OFHC) copper discs (Cu disc) were obtained from Goodfellow (UNS number C10100; goodfellow.com). The discs dimensions were 4.0 ± 10% mm of thickness and 10.0 ± 0.5 mm of diameter. The elemental composition was 99.9% – 100% Cu, with small impurities of S (< 0.0015%), Pb (< 0.0005%), Sb (< 0.0004%), P (< 0.0003%), and Zn (< 0.0001%). Prior to their use, the Cu discs were sterilized by autoclaving 15 min. at 121 ºC.

2.1.3_ Pre-treatment, compaction process, and incubation conditions

In order to stimulate the microbial activity of anaerobic bacteria (e.g., SRB), the bentonites were sprayed, until a mud-like consistency was obtained, with a sterile mixture solution of sodium acetate (30 mM) and sodium lactate (10 mM) as electron donors. In addition, sodium sulfate (20 mM) was added as a final electron acceptor. Since the addition of electron donors/acceptor in the bentonite does not represent a real DGR scenario, bentonite was amended with the electron donors/acceptor to be able to observe changes in the physico-chemical properties

of the clay on a laboratory timescale, as MIC processes would occur too slowly to be observed over the course of our study (1 year incubation). Control samples were only amended with sterile distilled water. The mixture was then dried under sterile conditions in a laminar flow cabinet at room temperature and, afterwards, bentonite samples were ground to a homogeneous fine powder. Additionally, other bentonite series were heat-shocked by tyndallization (110 ºC for 45 min, 3 consecutive days) to reduce the presence and activity of bentonite autochthonous bacteria. A summary of the different treatments is shown in **Table 1**.

Table 1.

Nomenclature and summary of the different treatments of bentonite blocks. All samples were compacted to 1.7 g cm^{-3} dry density and contained an OFHC copper disc (Cu disc) in the core.

Sample name	Characteristics	
	Bentonite	Treatment
B.eD	Non-tyndallized	Acetate:Sulfate:Lactate 30:20:10 mM
B	Non-tyndallized	Distilled water
StB.eD	Tyndallized	Acetate:Sulfate:Lactate 30:20:10 mM
StB	Tyndallized	Distilled water

Glossary: **B**: non-tyndallized bentonite, **StB**: tyndallized ('Sterile') bentonite, **eD**: treated with electron Donors and sulfate.

The compaction of the bentonite was conducted in the Laboratorio de Mecánica de Suelos (CIEMAT. Madrid, Spain) following the procedure of Povedano-Priego et al. (2021) with some modifications. The amount of bentonite required to compact the blocks to a dry density of 1.7 g cm^{-3} was calculated, taking into account the percentage of the initial moisture, the volume of the cylindrical steel mold (diameter x height: 30.3 x 20.0 mm) and the volume of the copper discs (0.31 cm^3). The initial moisture content (of 12%) was calculated by weighing 2 g from treated bentonite samples before and after desiccation at 110 ºC for 24 hours. The procedure (**Supplementary Fig. S1**) consisted of weighing 13.5 g of dry bentonite, pouring it into the aseptic steel mold, placing the Cu disc in the center of the mold,

and then adding another 13.5 g of dry bentonite. Finally, a hydraulic press was used at a pressure of 25-30 MPa to obtain the block.

The compacted bentonite blocks were incubated anaerobically simulating repository-relevant conditions. To provide this anoxic atmosphere, samples were placed into anaerobic jars with anaerobiosis generator sachets (AnaeroGen™, Thermo Scientific), and then incubated at 30 ºC for one year.

2.2_ Topographical, mineralogical, and chemical characterization of compacted bentonite blocks

After one year of incubation, the blocks were taken out from the anaerobic jar. Samples were shattered with the help of a sterilized stainless-steel spatula, and ground to a homogeneous powder with an aseptic mortar, to study the possible changes in the bentonite, as well as in the copper surface. Variable Pressure Field Emission Scanning Electron Microscopy (VP-FESEM) Zeiss SUPRA40VP equipped with an Energy Dispersive X-Ray Microanalysis (EDX) system with a large-area X-Max 50 mm detector was used for the visualization of possible pores or fractures in the compacted bentonite and the analysis of its elemental composition, respectively. The samples were previously prepared for observation by carbon metallization.

Mineralogical characterization and composition of major element analyses were carried out on a homogeneous powder of bentonite by using X-Ray Diffraction (XRD), and X-Ray Fluorescence (XRF), respectively.

XRD was performed using Oriented Aggregates (OA) to study the behavior of the basal reflections of smectite under diverse treatments. Samples were prepared using 0.3 g of bentonite in 3 mL of distilled water (Moore and Reynolds, 1989). The clay suspension was dispersed by sonication (2 times of 5 minutes each) Air-dried OA were studied employing a powder X-ray diffraction on a PANalytical

X'Pert Pro diffractometer (CuKα radiation, 45 kV, 40 mA) equipped with an X'Celerator solid-state linear detector. A step increment of 0.008º 2Θ and a counting time of 10 s/step were used. Afterwards, the samples were exposed to ethylene-glycol (EG) vapor at 60 ºC for 24 h and re-analyzed with the diffractometer. HighScore software enabled the analysis of the XRD diffractograms.

The bentonite composition in major elements was determined by XRF analysis using PANalytical Zeltium with a rhodium anode ceramic X-ray tube with an ultra-thin high transmission beryllium front window.

The pH of the bentonite samples was measured in triplicate as described in Povedano-Priego et al. (2019). The ground bentonite was mixed and homogenized with 0.01 M $CaCl_2$ in a ratio of 1:15.

2.3_ Microbial community study

After one year of anaerobic incubation, the compacted bentonite blocks were stored at -20 ºC for the total microbial community analysis by culture-independent techniques and at 4 ºC for the culture-dependent techniques. For these analyses, the bentonite blocks were aseptically broken into small fragments, and homogeneously ground with a mortar.

2.3.1_ DNA extraction protocol and sequencing

DNA extractions were performed in triplicate for each treatment (B.eD, B, StB.eD, StB). The optimized DNA extraction protocol for compacted bentonites was followed in detail as described in Povedano-Priego et al. (2021). Briefly, 0.3 g of ground bentonite was added in 2 mL screw-cap tubes with sterilized glass beads (one of 3 mm diameter and 0.25 g of 0.3 mm diameter). Depending on the samples, a total of 2.4 – 3.6 g of bentonite per replicate was used to reach enough final DNA concentration for sequencing. Subsequently, 400 µL of Na_2HPO_4 (0.12 M pH 8)

was added to each tube and vortexed at maximum speed to help DNA desorption from the clay particles. After the extraction, the quantification of the total DNA was performed on a Qubit 3.0 Fluorometer (Life Technology, Invitrogen™).

Amplification, sequencing, and bioinformatics analyses of the extracted DNA were conducted at STAB VIDA (Caparica, Portugal, stabvida.com). The library construction was performed using the primers 341_F (5′-CCTACGGGNGGCWGCAG-3′) and 785_R (5′-GACTACHVGGGTATCTAATCC-3′) whose molecular target is the V3 – V4 variable region of 16S rRNA gene (Thijs et al., 2017). The sequencing was carried out with Illumina MiSeq platform, using MiSeq Reagent Kit v3 and 300bp paired-end. After the sequencing, FastQC software was used to perform the quality controls. The generated raw sequence data were analysed using QIIME2 v2021.4 (Caporaso et al., 2010). The reads were denoised using DADA2 plugin in order to trim and truncate low quality regions, dereplicate the reads, and filter chimeras (Callahan et al., 2016). Alpha rarefaction curves were constructed to determine whether the obtained number of reads reached a reasonable amount. The reads were organized in operational taxonomic units (OTUs) and classified by taxon using the scikit-learn classifier with the SILVA (release 138 QIIME) database (clustering threshold: 99% similarity). The sequence read archive (SRA) of the raw data was submitted at the National Center for Biotechnology Information (NCBI) with the BioProject ID PRJNA947581.

Alpha diversity indices and relative abundance analysis of the annotated OTUs (taxa) were carried out using Explicet 2.10.5 (Robertson et al., 2013). In order to compare the similarity between samples at genus level, a matric based on Bray-Curtis algorithm were grouped by PCoA (Principal Coordinate Analysis) using Past4 software (Hammer et al., 2001). Moreover, a heatmap was constructed to visualise OTUs with more than 0.50% of relative abundance. For that, the function ‘heatmap.2’ and the packages “phyloseq”, “gplots” and “RcolorBrewer” were used

in R 4.2.1 software (McMurdie and Holmes, 2013; Warnes et al., 2022; Neuwirth, 2022; R Core Team, 2022).

2.3.2_ Most probable number of sulfate-reducing bacteria

To determine the effect of acetate, lactate, and sulfate on the microbial community of bentonite, the approximate number of culturable SRB per gram of clay was calculated using the Most Probable Number (MPN) enumeration (Haynes et al., 2018) inoculating the Postgate medium (DSMZ_Medium63, dsmz.de) and following the MPN Method of Biotechnology Solutions (Houston, USA, biotechnologysolutions.com). This technique is based on serial dilutions in triplicate. For this purpose, 1 g of bentonite from each treatment was ground under N_2 atmosphere (mixed from 3 block replicates) and added to 10 mL of a N_2-degassed 0.9% NaCl solution. This mixture was shaken at 180 rpm for 24 h to disaggregate the clay and separate the bacterial cells from the bentonite particles. Afterwards, 1 mL of this suspension was transferred to 9 mL of Postgate Medium in previously N_2-degassed serum bottles until the 10^{-5} dilution. The whole process was carried out in an anaerobic glove box to maintain anoxic conditions. Then, the bottles were sealed and incubated at 30 ºC in static and darkness. After 4 weeks, the presence of black precipitates indicated a positive result. The MPN of SRB was estimated by comparing positive bottles to a reference table (MPN Method, biotechnologysolutions.com), taking into account the correction for the initial dilution.

2.4_ Copper disc surface analysis

Copper discs extracted from the bentonite blocks were prepared for their observation by VP-FESEM coupled with EDX. The samples were fixed in a 2.5% glutaraldehyde solution in 0.1 M PBS buffer, pH=7.4 for 24 hours at 4°C. The samples were then washed in the same buffer (3 times for 15 minutes each at 4°C) before being post-fixed in 1% osmium tetroxide in darkness for 1 hour at room

temperature. The samples were washed again in distilled water (3 times for 5 minutes each), then dehydrated in an increasing concentration gradient of ethanol (from 50% to 100%). Finally, the samples were dried using the Critical Point Drying (CPD) method (Anderson, 1951) with carbon dioxide in a Leica EM CPD300 and coated with carbon by evaporation in an EMITECH K975X Carbon Evaporator.

To determine organic compounds, present on the surface of the Cu discs, samples were removed from the bentonites blocks and analyzed with reflectance micro-Fourier Transform Infrared Spectroscopy (micro-FTIR). The samples were not previously prepared or cleaned (unmodified) in order to preserve any potential corrosion compounds or biofilm formation after 1-yer incubation. Reflectance micro-FTIR images were obtained using a PerkinElmer Spotlight micro-FTIR spectroscope, equipped with a mercury–cadmium–telluride detector (consisting of 16 gold-wired infrared detector elements). A per-pixel aperture size of 6.25 μm x 6.25 μm was used with two co-added scans per pixel and a spectral resolution of 16 cm^{-1}.

Subsequently, the unmodified copper discs were analysed by XPS. The XPS measurements for surface chemistry were made on a Kratos AXIS Supra Photoelectron Spectrometer. The X-ray source was a monochromated Al Kα source (1486.6 eV), operated with an X-ray emission current of 20 mA and an anode high tension (acceleration voltage) of 15 kV. The take-off angle was fixed at 90° relative to the sample plane. The data were collected from three randomly selected locations and the area corresponding to each acquisition was a rectangle of approximately 110 μm x 110 μm (FOV2 lens). Each analysis consisted of a wide survey scan (pass energy 160 eV, 1.0 eV step size) and high-resolution scan (pass energy 20 eV, 0.1 eV step size) for component speciation. The integral Kratos charge neutralizer was used as an electron source to eliminate differential charging. The binding energy scale was calibrated using the Au $4f_{5/2}$ (83.9 eV), Cu $2p_{3/2}$

(932.7 eV) and $Ag3d_{5/2}$ (368.27 eV) lines of cleaned gold, copper and silver standards from the National Physical Laboratory (NPL), UK. The software CasaXPS 2.3.22 (Fairley, 2019) was used to fit the XPS spectra peaks. To compensate for the effect of surface charging, all the binding energies were referenced to the C1s adventitious carbon peak at 285 eV. No additional constraint was applied to the initial binding energy values.

3_ Results

3.1_ Mineralogical and chemical analysis of the bentonite

After one year of anoxic incubation, the inner Cu disc embedded in the compacted bentonite amended with electron donors (B.eD) was collected, fragmented, and analyzed by VP-FESEM. As shown in **Fig. 1**, few cracks near the interface Cu disc – compacted bentonite area (**Fig. 1a-b**) and small fissures on the bentonite surface (**Fig. 1c**) were observed. At high magnification, smectite showed the common leaf-like morphology (Povedano-Priego et al., 2021) (**Fig. 1d**). These irregularities (fissures and cracks) could be due to the fracturing of the bentonite block.

EDX maps showed the presence and distribution of the elements at the interface compacted bentonite – Cu disc (**Supplementary Fig. S2**). The major elements in

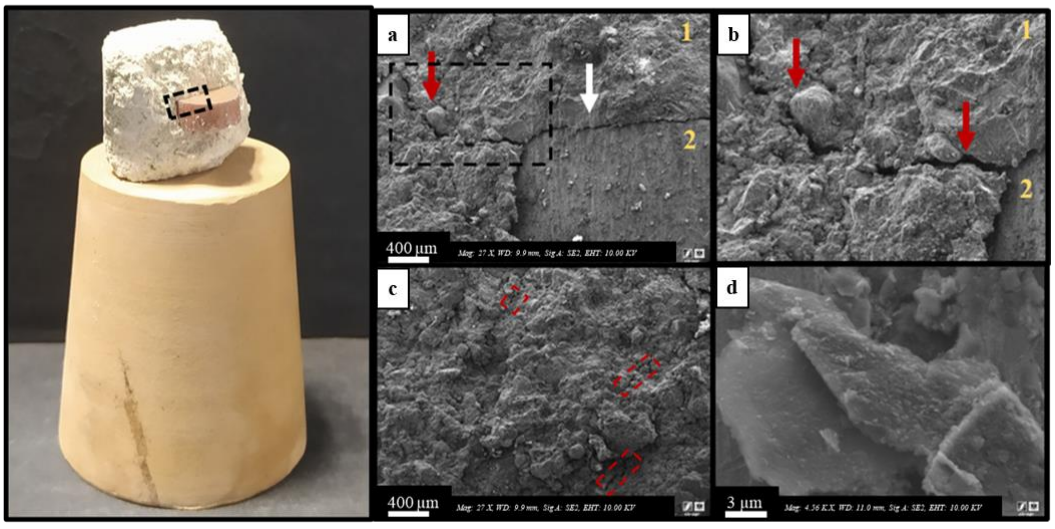

Fig. 1. Left: plowed B.eD bentonite block with copper disc image after one year of anaerobic incubation. (a) SEM images of the selected area in left image, and (b) a magnification of the selected area in (a) showing the topography of the block at the bentonite (1) - copper disc (2) interface (white arrow) and cracks (red arrows). (c) Small fissures in the compacted bentonite (red squares). (d) Leaf-like smectites at high magnification.

bentonite (**Supplementary Fig. S2_a1**) were Si, Al, Fe, and Mg (**Supplementary Fig. S2_d-g**). While no signal of Cu was observed in the bentonite phase, it was entirely detected on the Cu disc (**Supplementary Fig. S2 b**). Geochemical analyses evidenced no apparent changes among the treatments (**Supplementary Table S1**). However, the dominant oxides obtained by XRF showed some slight variation after one year of incubation, where SiO_2 indicated a decrease of ~ 3.11%, while Fe_2O_3 and Al_2O exhibited an increase of ~ 1.27% and ~ 1.16%, respectively. In addition, the values of the pH ranged between 7.7 and 8.2 showing a decrease of ~ 0.42 on average, after one year of incubation (**Supplementary Table S1**).

The oriented aggregates (OA) technique was performed to identify potential changes in the illite/smectite interstratified clay minerals. XRD patterns of the OA before and after the exposure to ethylene glycol treatment showed no differences between samples (**Fig. 2b**). Moreover, XRD patterns indicated that smectite (montmorillonite) was the dominant mineral phase, in addition to minority mineral phases such as quartz and plagioclases.

3.2_ Effect of the different treatments on microbial communities

3.2.1_ Comparison of bacterial diversity after one year of anaerobic incubation

The total DNA from the different treatments, including compacted bentonite blocks prior to the incubation (time 0) and after one year of anaerobic incubation (1y), was extracted and sequenced in triplicate. Enough sequencing depth was

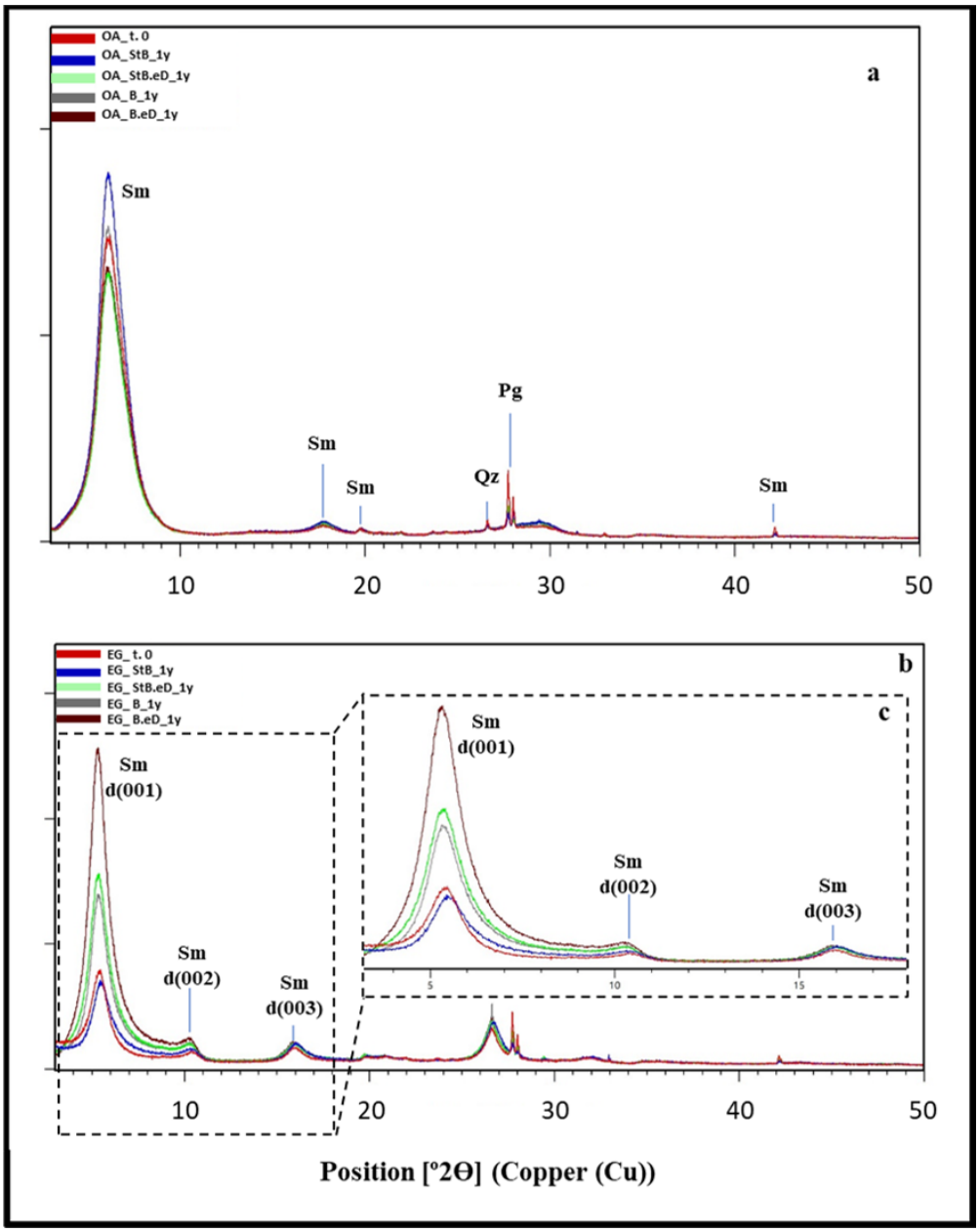

Fig. 2. (a) Oriented aggregates (OA) X-ray diffraction (XRD) patterns of samples t. 0 and after one year of anaerobic incubation (1y). B: non-tyndallized bentonite blocks, StB: tyndallized bentonite, eD: treated with acetate, sulfate and lactate. Sm: smectite; Qz: quartz; Pg: plagioclase. (b) OA XRD patterns after 24h at 60 ºC exposure with ethylene glycol (EG) and (c) smectite-illite zone magnification.

achieved as shown by rarefaction curves (**Supplementary Fig. S3**), and the Good's coverage index (**Table 2**). A range of 63,546 to 431,964 sequence reads was obtained from most samples. Some replicates (i.e.: StB2_1y, B1, and B.eD3) were not included in the analysis due to the low sequencing quality (< 1,500).

Richness (Sobs), diversity (ShannonH and SimpsonD), and evenness (ShannonE) indices of the samples are presented in **Table 2**. An increase in the richness values was observed in the non-tyndallized samples after the incubation period (B_1y and B.eD_1y), while in the tyndallized samples (StB_1y and StB.eD_1y) the value of this parameter decreased. ShannonH and SimpsonD indices indicated a high diversity in all the samples (values > 3 and close to 1, respectively), showing no taxa dominance. However, slightly higher diversity was observed in the non-tyndallized samples, with respect to the tyndallized ones.

Table 2.
Good's coverage values, Richness (Sobs), diversity (ShannonH. and SimpsonD), and evenness (ShannonE) indices of the bacterial communities from 1.7 g cm^{-3} compacted bentonite blocks. B: non-tyndallized bentonite, StB: tyndallized bentonite, eD: treated with electron donors and sulfate, 1y: after one year of anaerobic incubation.

	Good's cov.	Sobs	ShannonH	SimpsonD	ShannonE
B	1.00	437	6.80	0.98	0.78
B_1y	1.00	471	5.82	0.96	0.65
B.eD	1.00	299	5.62	0.96	0.68
B.eD_1y	1.00	562	6.59	0.97	0.72
StB	1.00	273	4.98	0.92	0.62
StB_1y	1.00	266	5.30	0.92	0.66
StB.eD	1.00	488	5.04	0.89	0.56
StB.eD_1y	1.00	310	5.41	0.93	0.65

A total of 742 OTUs were detected (**Supplementary Table S2**) and classified in 34 phyla. Of the 34 total phyla, 3 belonged to the Archaea (0.01%), and 31 to the Bacteria domain (99.99%). The Archaea phyla included Aenigmarchaeota in

sample B, and Crenarchaeota and Thermoplasmota in sample B.eD, representing ≤ 0.01% within each treatment (**Supplementary Table S3**). On the other hand, bacterial phyla such as Actinobacteriota (59.48%) and Proteobacteria (24.18%) were the most dominant followed by Chloroflexi (6.05%), Gemmatinomonadota (1.82%), Bacteriroidota (1.77%), and Firmicutes (1.59%). No remarkable differences were found at phylum level between treatments or incubation times (**Fig. 3**).

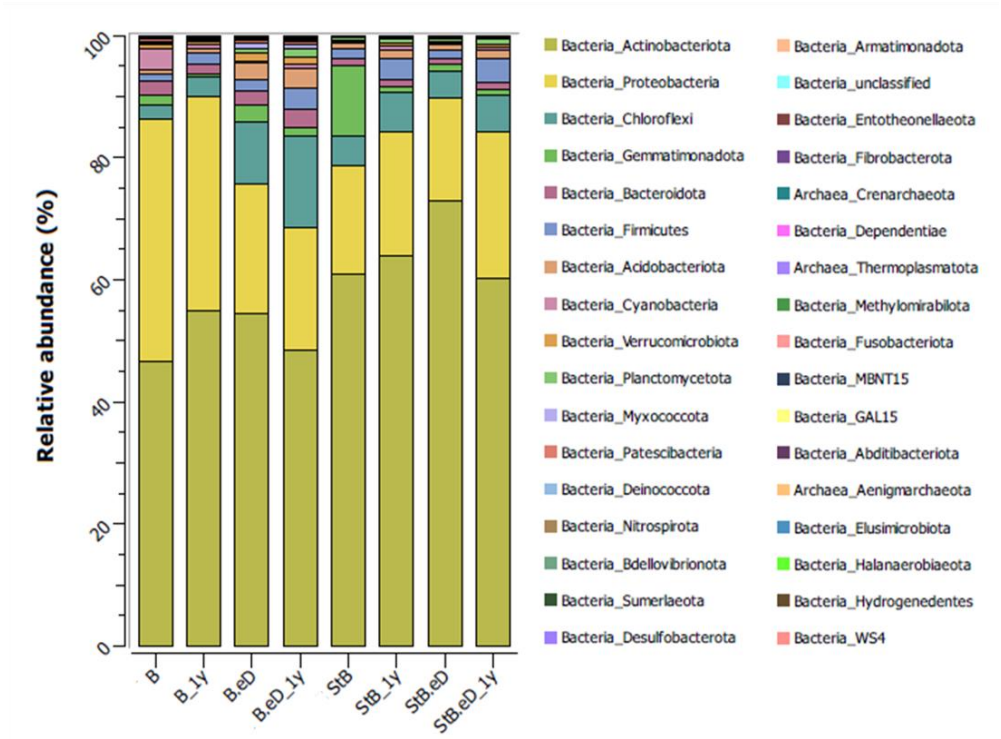

Fig 3. Phyla relative abundance of the bacterial and archaeal communities from 1.7 g cm^{-3} compacted bentonite blocks. Stacked bars show averages of biological triplicates (duplicates in StB.eD, B and B.eD) B: non-tyndallized bentonite, StB: tyndallized bentonite, eD: treated with electron donors and sulfate, 1y: after one year of anaerobic incubation.

At the genus level, principal coordinate analysis (PCoA), based on the Bray-Curtis distance, showed the dissimilarity of the communities among the different samples (**Fig. 4**). A clear distinction between tyndallized (StB and StB.eD) and non-tyndallized (B and B.eD) samples was observed. Moreover, non-tyndallized

samples were split into two well-differentiated clusters, electron donors/sulfate treated (B.eD), and untreated (B) samples. This last difference between samples B and B.eD (time 0) was potentially due to the fact that after the treatment addition, samples were dried at room temperature for some days until the compaction process was achieved, possibly affecting the bacterial growth. This separation was not observed between the tyndallized samples (StB and StB.eD). Additionally, no dissimilarities were found between the samples before and after one year of anaerobic incubation (1y). These results were supported by the heatmap establishing a clear difference between the tyndallized and non-tyndallized samples and, within this last group, between the acetate:lactate:sulfate treated and non-treated samples (**Fig. 5**).

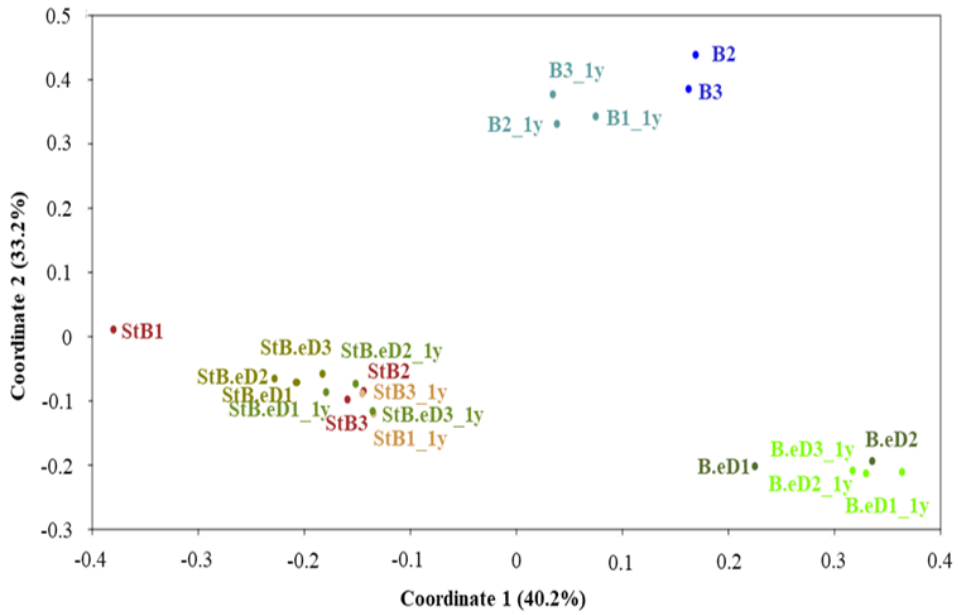

Fig. 4. PCoA (Principal Coordinate Analysis) plot revealing the dissimilarity of microbial genera communities of the 1.7 g cm^{-3} compacted bentonite blocks in triplicate (duplicates in StB.eD, B and B.eD). The distance is based on Bray-Curtis algorithm. B: non-tyndallized bentonite, StB: tyndallized bentonite, eD: treated with electron donors and sulfate, 1y: after one year of anaerobic incubation.

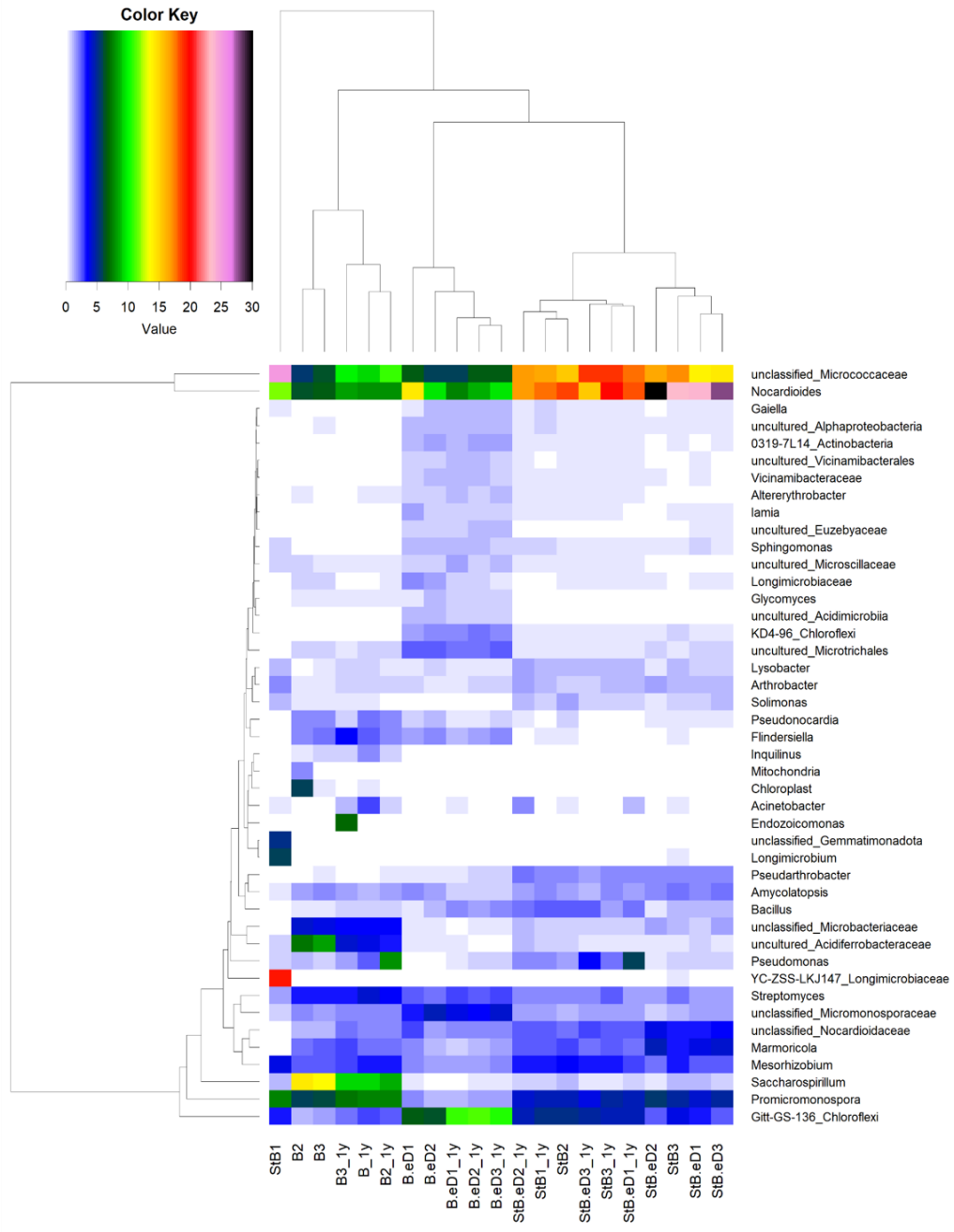

Fig. 5. Heatmap of the relative abundance of the samples at genus level of the 1.7 g cm^{-3} compacted bentonite blocks in triplicate (duplicates in StB.eD, B and B.eD). Cut off: 0.5% of r.a. Different colors show the relative abundance of each genus (the warmer the color, the greater relative abundance). B: non-tyndallized bentonite, StB: tyndallized bentonite, eD: treated with electron donors and sulfate, 1y: after one year of anaerobic incubation.

The microbial communities were mostly represented by *Nocardioides*, unclassified Micrococcaceae, *Promicromonospora* and *Saccharospirilum* (16.32%, 9.77%, 3.97% and 3.93%, respectively). A slight increase (Δ) in the abundance of *Pseudomonas* was observed in B and StB.eD after one year of incubation (Δ 2.98% and Δ 3.04%, respectively) (**Fig. 6, Supplementary Table S2**). In relation to the heat-shock tyndallization process, unclassified Micrococcaceae and *Nocardioides* were more abundant in the tyndallized samples (StB, StB.eD, StB_1y, and StB.eD_1y) (17.47% and 20.26%, on average) than in the non-tyndallized ones (B, B.eD, B_1y and B.eD_1y) (7.13% and 8.69%, in average), while *Saccharospirillum* and Chloroflexi (Gitt-GS-136) were less abundant after the heat-shock treatment (in average from 5.93% to 0.90%, and from 5.32% to 4.03%, respectively) (**Fig. 5** and **6**, **Supplementary Table S2**). Within the non-tyndallized samples, an increase in the presence of Chloroflexi (Gitt-GS-136, and KD4-96), and unclassified Micromonosporaceae was detected in the bentonite amended with electron donors and sulfate. Moreover, some representatives of uncultured Acidimicrobiia, *Sphingomonas*, uncultured Euzebyaceae, *Iamia*, *Vicinamibacteraceae* or *Gaiella* were only detected in the acetate:lactate:sulfate amended treatment within the non-tyndallized samples. In addition, genera such as *Promicromonospora*, *Saccharospirillum*, and *Streptomyces* were slightly more abundant in the unamended treatment within the non-tyndallized samples (**Fig. 5** and **Fig**. **6**, **Supplementary Table S2**).

Regarding bacteria involved in sulfate reduction (SRB), *Desulfosporosinus*, *Desulfotomaculum*, *Desulfuromonas*, *Desulfovibrio*, *Desulfurivibrio*, *Desulfovirga*, and members of the families Desulfurivibrionaceae, Desulfomonadia and Desulfuromonadaceae, among others, were detected in the samples in a very low relative abundance (< 0.2%) (**Supplementary Fig. S4** and **Table S2**). These SRB showed no differences in terms of the addition of acetate:lactate:sulfate after one year of incubation. The most remarkable aspect

lays in the enrichment of *Desulfosporosinus* in all the treatments after the incubation (**Supplementary Fig. S4** and **Table S2**).

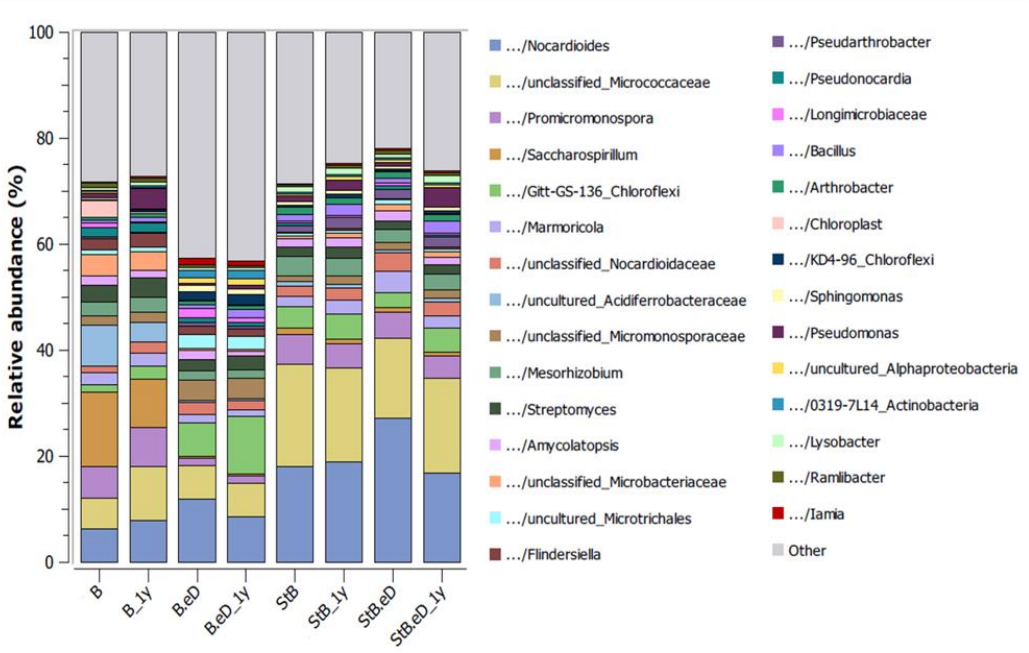

Fig 6. OTU relative abundance of the bacterial and archaeal communities from 1.7 g cm^{-3} compacted bentonite blocks. Cut-off: 0.6 % of relative abundance. Stacked bars show averages of biological triplicates (duplicates in StB.eD, B and B.eD) B: non-tyndallized bentonite, StB: tyndallized bentonite, eD: treated with electron donors and sulfate, 1y: after one year of anaerobic incubation.

3.2.2_ Viability and most probable number of sulfate-reducing bacteria

The MPN results demonstrated the presence and survival of viable and cultivable SRB in all the treatments (**Table 3**). The values varied in a range of 2 x 10^1 and 2.5 x 10^3 MPN g^{-1} of bentonite (B_1y and B.eD_1y, respectively). This group of microorganisms could be capable of surviving despite the harsh environmental conditions in the bentonite blocks (i.e.: high compaction density and dry environment). Moreover, it was evidenced that SRB are even able to withstand the heat shock produced by the tyndallization process (110 ºC for 45 min, 3 consecutive days) as shown in the StB_1y (1.5 x 10^3 MPN g^{-1} bentonite), and StB.eD_1y (9.5 x 10^2 MPN g^{-1} bentonite) samples. In addition, a slight increase in

the acetate:lactate:sulfate amended samples after one year of anaerobic incubation (B.eD_1y) was detected (**Table 3**). A remarkable decrease was observed in sample B (untreated sample) after the incubation time (B_1y). Nonetheless, a slight decrease was detected in the tyndallized amended samples (StB.eD_1y) in comparison to the non-tyndallized (B.eD_1y) after the incubation period.

Table 3.

Most probable number (MPN) of sulfate-reducing bacteria per gram of three-mixed replicates sample from 1.7 g cm^{-3} compacted bentonite blocks. The value was estimated following the protocol of MPN method from Biotechnology Solutions based in serial dilutions in triplicate in Postgate medium. MPN g^{-1} of bentonite was calculated taking into account the initial pre-dilution to disperse the cells (1 g of bentonite powder in 10 mL of 0.9% NaCl). t. 0: initial bentonite. B: non-tyndallized bentonite, StB: tyndallized bentonite, eD: treated with electron donors and sulfate, 1y: after one year of anaerobic incubation.

Sample	XYZ pattern*	MPN reading**	3PB dilution***	MPN mL-1	MPN g-1 bentonite
t.0	330	25.0	100	2.50 x 101	250
B_1y	211	2.00	100	2.00 x 100	20
B.eD_1y	330	25.0	101	2.50 x 102	2500
StB_1y	210	1.50	102	1.50 x 102	1500
StB.eD_1y	320	9.50	101	9.50 x 101	950

*XYZ pattern: number of positive bottles after 3PB dilution

**MPN reading: MNP value from the refence table

***3PB dilution: dilution with 3 positive bottles prior to XYZ pattern

3.3_ Characterization of the Cu-discs surface

VP-FESEM analyses were carried out on a selection of Cu discs removed from the blocks of each treatment. The data obtained are presented in **Fig. 7**. Five adjacent areas of ~ 560 x 430 µm were selected from the edge to the center of the disc. The composition of the 5 images from samples B and B.eD showed the distribution of Cu, Fe, Ti, S, Si, Al, O, and C on the surface of the Cu disc (**Fig. 7**). Micrographs

of the discs from tyndallized bentonite and the untreated copper disc (t. 0) indicated no notable changes in the surface of the discs (**Supplementary Fig. S5**).

The metal surfaces appeared to be practically unaltered. Some damages were observed possibly due to the pressure exerted by some fraction of the bentonite

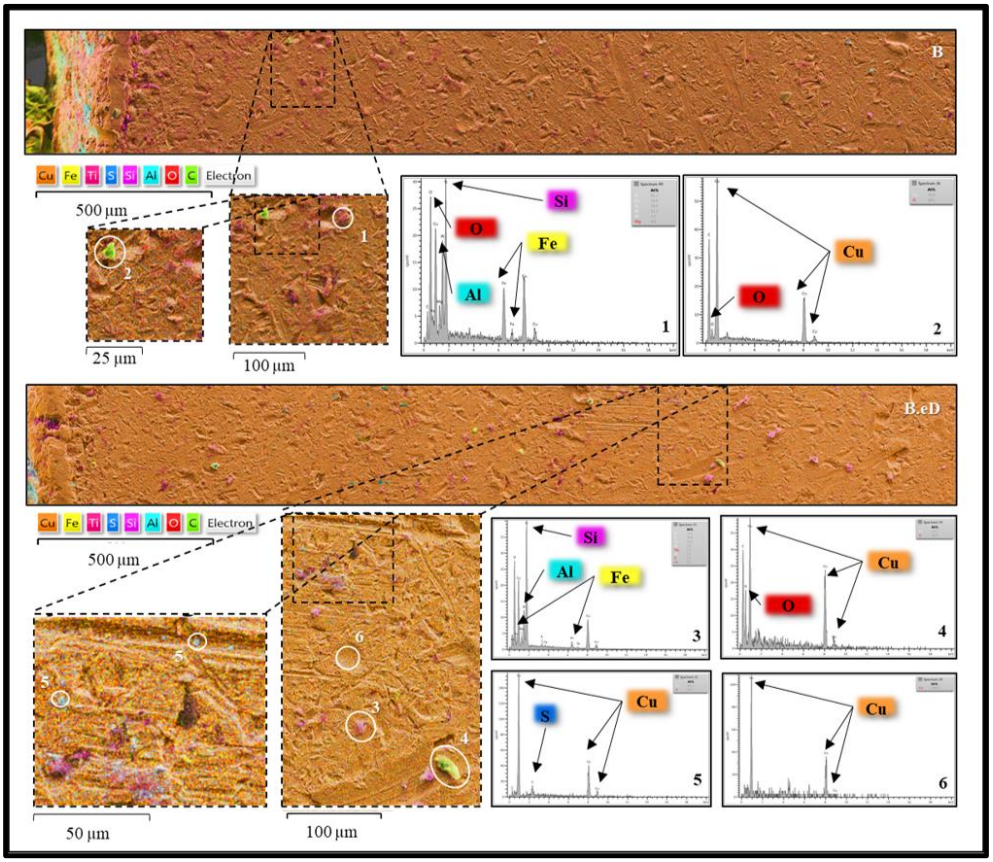

Fig. 7. EDX maps associated with electron images from a selected area (from edge to center) of Cu disc from B and B.eD treatments, respectively. EDX show the distribution of Cu, Fe, Ti, S, Si, Al, O and C in the studied area. White circle and EDX analysis show the presence of bentonite (Si, Al, Fe) adhered to the surface (1 and 3), precipitates related to CuxO (2 and 4), CuxS (5), and unaltered copper (6).

during the bentonite block compaction process. Bentonite traces adhering to the surface of the discs (pink, and blue-green areas) showed Si, Fe, and Al peaks in the EDX spectra (**Fig. 7_1** and **7_3**). In addition, some yellow-orange areas were possibly related to the presence of small copper oxides confirmed by Cu and O peaks (**Fig. 7_2** and **7_4**). On the other hand, small blue-almost-white precipitates

presented Cu and S peaks may be related to small size copper sulfides (< 1 µm) (**Fig. 7_5**). An example of unaltered copper zone is shown in **Fig. 7_6**. The presence of carbon in the spectra was related to previous carbon treatment of the samples during their preparation for microscopy analyses.

Reflectance micro-FTIR was used to identify the presence or absence of organic substances on the copper samples. **Fig. 8** shows the results obtained from samples B.eD and B (non-tyndallized) with this technique. Areas of the bentonite discs with different treatments were observed using the optical microscope, and then scanned using the infrared microscope. A false-color image is generated showing the locations of infrared-absorbing molecules. An absorbance scale indicates the areas where there is higher abundance of organic or IR-active compounds (red color), or low absorbance regions (dark blue), where usually no IR-absorbing functional groups are present. In all samples, the areas with no IR absorbing molecules presented a relatively flat spectrum, and this is usually superimposed with exposed copper regions in the discs (as seen in the optical microscope). The presence of bentonite was observed on the samples, and when analyzed with micro-FTIR the spectra of these regions usually showed the typical spectra of Si-O, Si-O-Si, AlOH and other inorganic compounds expected on the bentonite-associated regions. Bands related to proteins, lipids and polysaccharides were only detected in sample B.eD, indicating the presence of organic compounds usually associated with the presence of microbial cells or microbial activity in this sample (as shown in **Fig. 8**).These spectra are very well documented, especially for bacteria related samples (Ojeda and Dittrich, 2012; Jiang et al., 2004; Orsini et al., 2000; Naumann et al., 1991). The bands around 3000 cm^{-1} in Spectrum 1 in sample B.eD (**Fig. 8**) can be attributed to the stretching of oxygen-hydrogen (νO-H). The peaks around 2800 cm^{-1} are normally attributed to methyl (CH_3) and >CH_2 functional groups (νC-H). The signals around 1640 and 1540 cm^{-1} corresponded to the amide I and II bands,

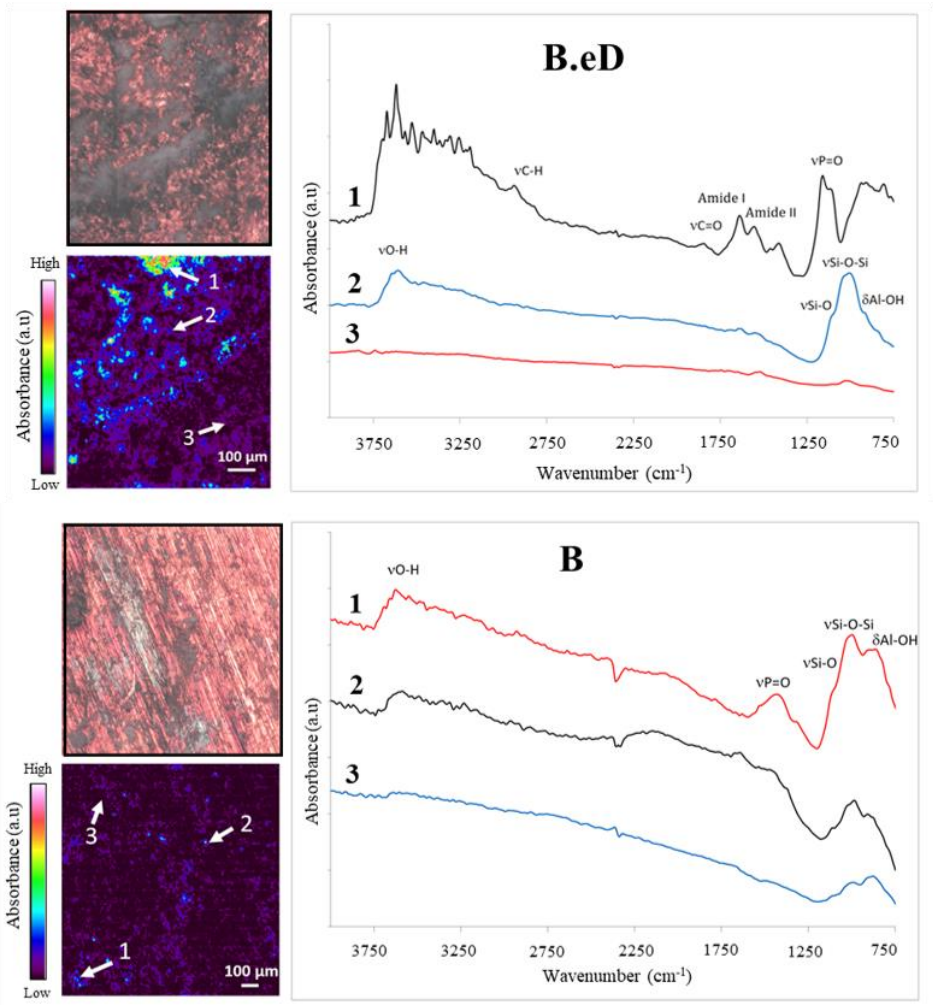

Fig. 8. Reflectance micro-FTIR spectroscopy for the study of microbial presence on the copper disc from sample B.eD and B after 1 year of incubation. Left: optical image of the scanned regions and false-colour image of the sample scanned using reflectance micro-FTIR spectroscopy. Right: infrared spectra of 3 different regions on the samples.

respectively. The amide I band is due to the stretching carbon-oxygen double bonds (νC=O) within amides associated with proteins and the amide II band is a combination of bending N-H bonds (δN-H) within amides and contributions from stretching C-N (νC-N) groups. The peak around 1400 cm^{-1} is due to the symmetric stretching C-O bond of carboxylate groups (ν_{sym} COO-), while the asymmetric stretching (ν_{asym} COO-) is concealed by the amine II band. The signal around 1760 cm^{-1} corresponds to the vibrational C=O stretching (νC=O) of carboxylic acids.

The double bond stretching of phosphate-oxygen >P=O (νP=O), which is connected to phosphodiesters of nucleic acids and general phosphoryl groups, is observed at 1240 cm^{-1}. Tyndallized samples (StB.eD and St.B) showed FTIR spectra similar to sample B where no presence of proteins, lipids or polysaccharides was detected (**Supplementary Fig. S6**).

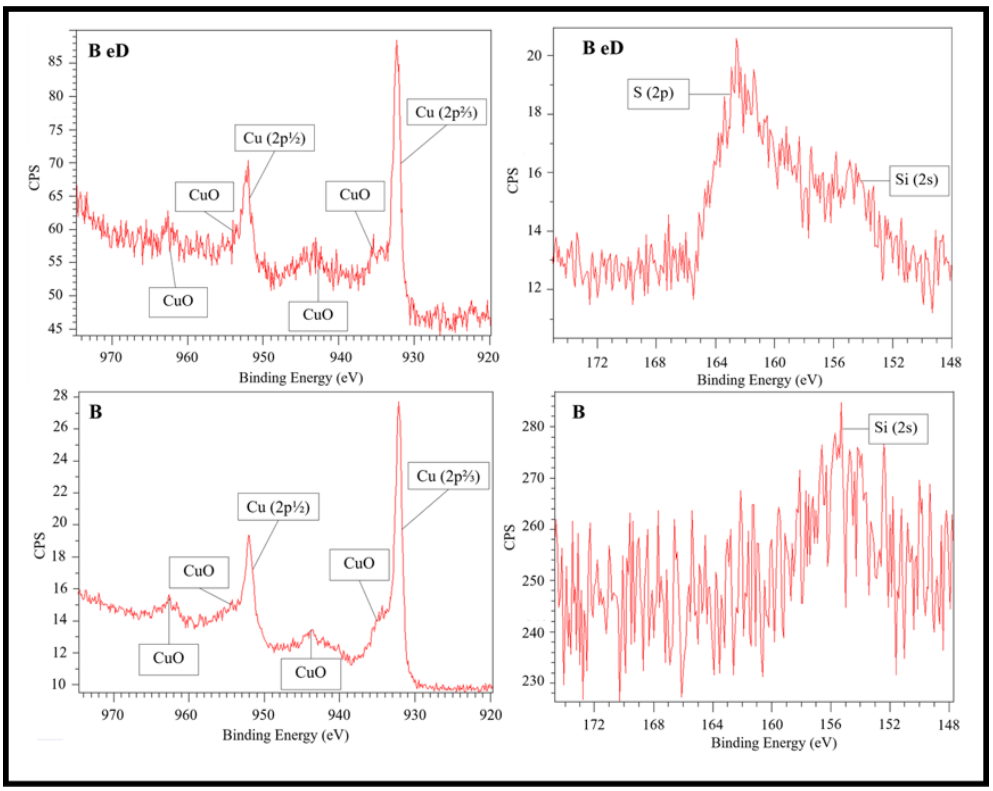

Fig. 9. High resolution XPS scan for the copper 2p region (left), between 975-920 eV and for the sulfur 2p region (right), between 175-148 eV for sample B.eD (top) and B (bottom) after one year of anaerobic incubation.

XPS analysis was undertaken to assess the surface chemistry of each sample, with wide scans showing the presence of Cu, C, O, Si, Na, P, Fe, Mg and Al on the majority of the samples. The presence of these elements (except for Cu) was likely due to bentonite residues still present on the surface of the discs. The peaks of the Cu $2p_{3/2}$ and Cu $2p_{1/2}$ in the Cu 2p high-resolution scans suggested a combination of elemental copper alongside copper oxide in all samples. As shown in **Fig. 9** and

Supplementary Fig. S7, the Cu $2p_{3/2}$ peaks were observed at 932.4 eV, and the peaks of Cu $2p_{1/2}$ were observed at 952.1 eV, corresponding to elemental Cu and in agreement with tabulated data (Wagner et al., 1979). However, the presence of peaks likely attributed to CuO were also evident in all samples, as additional peaks were detected around 933.8 eV and 953.5 eV for the Cu $2p_{3/2}$ and Cu $2p_{1/2}$, respectively. No sulfur signal was detected in samples B, StB and St.eD. The peak observed around 155.3 eV in all samples corresponds to Si 2s (Clarke and Rizkalla, 1976). In sample B.eD, in addition to the Si 2s signal, a peak at 162.2 eV was observed, indicating the presence of sulfur (**Fig. 9**).

4_ Discussion

4.1_ Mineralogical and chemical stability of the bentonite

Although the present work does not focus on an in-depth study of the stability of the physico-chemical properties of bentonite, it is crucial to take into account the impact of microorganisms on the safety-relevant properties of the clay. Meleshyn (2011) described how microbial activity could influence these clay properties including the swelling pressure, specific surface area, cation exchange capacity, anion sorption capacity, porosity, permeability, and fluid pressure or plasticity. Microbial processes that could compromise the clay buffer included reduction and dissolution of clay minerals, formation of biofilm, hydrogen sulfide attack produced by sulfate-reducing bacteria, and microbial gas production.

Bentonite from El Cortijo de Archidona (also called FEBEX, Spanish or “Serrata” clay) has been selected by ENRESA (Spanish national radioactive waste company) as the most suitable backfilling and sealing material for a future DGR in Spain. This clay has been widely studied and characterized since the 90’s within the FEBEX project (Full-scale Engineered Barriers Experiment) (Huertas et al., 2021). The mineralogical composition of the bentonite from El Cortijo de Archidona site was previously described by Lopez-Fernandez et al. (2015) and consist of

smectites (montmorillonite) as the dominant mineral phase (~ 84%) followed by plagioclase (albite), and quartz (~ 12% and ~ 3%, respectively). In addition, this bentonite has a very low organic carbon content, in the range of 0.12 – 0.03%, comparing with other clays such as Opalinus Clay (~ 0.6%) or Boom Clay (1 – 5%) (Nagra 2002, Van Geet et al., 2003). The chemical composition of the studied bentonite (**Supplementary Table S1**) is very similar to sample BI-2 site reported by Lopez-Fernandez et al. (2014) with a decrease in the content of Fe_2O_3 and an increase in the CaO content. Despite the extensive physicochemical characterization of this bentonite, the impact of microbial processes within the DGR concept is still unknown. Therefore, the necessity to elucidate how microorganisms could alter the different DGR barriers is increasing. In the last years, several studies on the microbial communities present in bentonite from El Cortijo de Archidona have been performed (Povedano-Priego et al., 2023, 2022, 2021, 2019; Lopez-Fernandez et al., 2018, 2015, 2014).

Povedano-Priego et al. (2021) focused on studying the impact dry density of compacted bentonite (1.5 and 1.7 g cm^{-3}), amended with acetate after 2-years anaerobic incubation, has on the stability of this clay mineral. The study showed the presence of several cracks and small fissures and, at high magnification, several pores in the 1.5 g cm^{-3}. In general, it is well documented that the more the compaction density of clays increases, the smaller the size and number of pores is (Meleshyn 2021, Matusewicz and Olin 2021, Villar et al., 2012). In the present study, no pores have been observed, which could retard the water diffusion and, therefore, compromise the growth of bacteria (Masurat et al., 2010). Major elements composition and pH showed no important variations in the bentonite samples, similar to those previously found in uncompacted bentonite samples collected from the same site (Povedano-Priego et al., 2019; Lopez-Fernandez et al., 2015). The stability of bentonite properties is one of the most important issues related to the safety in a DGR (Villar et al., 2006). A common concern within the

DGR environment is the irreversible smectite-to-illite transformation that would affect the swelling capacity of bentonites (Kaufhold and Dohrmann, 2010). This process depends on many factors such as, for example, high temperatures (100 - 200 °C) and time. However, some studies have shown that this process can occur at lower temperatures (< 50 °C) (Ohazuruike and Lee, 2023). The illitization process may be caused by the attachment of K^+ ions, possibly from the K-feldspars of the bentonite, into the smectite interlayer creating covalent bonds with oxygen. Nonetheless, microorganisms can potentially stimulate this transformation. Microbial metabolism can cause changes in the geochemical conditions of the environment, promoting the smectite-to-illite transformation. The activity of some methanogens and sulfate-reducing bacteria could utilize the structural Fe(III) present in smectite as an electron acceptor coupled with the oxidation of H_2 and/or organic matter, leading to the formation of illite (Kim et al., 2019). However, no evidence of illitization process has been observed within our experimental conditions (e.g., effect of the addition of electron donors and acceptor for the stimulation of microorganisms, heat shock, anoxic conditions, etc.) according to the mineralogical and chemical analyses.

4.2_ Shifts in bacterial diversity and viability of SRB after one year of anaerobic incubation

Dry and highly compacted bentonite could suppose a stressful, confined, and starving environment for microorganisms. These conditions could repress microbial activity but not destroy the cells. Therefore, it is important to identify the microbial communities in bentonite and their changes under different DGR relevant conditions. The microbial diversity analyses based on 16S rRNA Next Generation Sequencing showed slight changes between tyndallized (StB and StB.eD) and non-tyndallized (B and B.eD) samples. Moreover, non-tyndallized samples were split into two well-differentiated clusters, electron donors/sulfate treated (B.eD), and untreated (B) samples. The heat-shock produced by the

tyndallization process stimulated an increase of aerobic bacteria belonging to Micrococcaceae and *Nocardioides*. The increase of these aerobic bacteria could be related to the ability of the bentonite to "trap" oxygen molecules that may eventually become available for such bacteria (Burzan et al., 2022). Additionally, the tyndallization process resulted in non-detectable presence of bacteria such as *Glycomyces* (growth temperature range 15-37 ºC; Labeda et al., 2004) or uncultured Acidimicrobiia, while others with growth temperature ranging between 10-42 ºC decreased their relative abundance as *Flindersiella*, *Inquilinus*, *Saccharospirillum* or *Promicromonospora* (Kaewklat and Franco, 2011; Coenye et al., 2002; Choi et al., 2011; Zheng et al., 2017). This could be explained by the fact that some mesophilic bacteria cannot recover from the exposure to high temperatures, producing thus a pronounceable effect on the bacterial diversity (Gilmour et al., 2022). Despite the potential applications of *Promicromonospora* species, a limited number of reports investigated genomic and phenotypic aspects of these genus members such as multi-resistance to extreme conditions (radiation, desiccation, oxidative stress, etc.) (Guesmi et al., 2021). Therefore, the decrease in relative abundance of the less copious mesophilic bacteria in the samples can cause the more representative ones to increase their presence. An increase in the relative abundance of Chloroflexi members, as well as *Gaiella*, *Sphingomonas*, and *Iamia* has been observed in the acetate:lactate:sulfate amended non-tyndallized samples (B.eD). Although scarce information is available about *Gaiella*, its ability to assimilate acetate and lactate has been reported in *G. occulta* (Albuquerque et al., 2011). Similarly, the genus *Sphingomonas* has been proved to assimilate lactate and acetate (Vaïtilingom et al., 2010). Interestingly, some members were able to contribute to the biogeochemical cycle of sulfur through bio-desulfurization (a process for the removal of sulfur from different materials), and in the MIC of copper cold-water pipes (Cui et al., 2016, White et al., 1996). On another hand, it is important for the safety of DGR barriers to consider the presence and activity of SRB, since this bacterial group is the main source of

copper corrosion in anoxic conditions through the sulfide production (Bengtsson and Pedersen, 2017). As shown in this study by metagenomic analyses, several SRB members (e.g., *Desulfosporosinus*, *Desulfotomaculum*, and *Desulfovibrio*) have been detected with a very low relative abundance (< 0.2%). According to Povedano-Priego et al. (2021), less sequences related to this group were detected in the acetate-amended compacted bentonite. Here, in addition to acetate, lactate and sulfate were incorporated to the compacted blocks, which could have stimulated the growth and detection of more SRB. Additionally, previous studies have shown that species belonging to this group of bacteria were capable of facing these harsh conditions by spore formation in species of *Desulfosporosinus* and *Desulfotomaculum* (Grigoryan et al., 2018), or by forming desiccated dormant cells in dry bentonite (Masurat et al., 2010b). Therefore, it is worthy to determine the ability of SRB to become active once growth conditions turn favorable (e.g., rewetting and enrichment of organic matter of compacted bentonite through infiltration of groundwater in the repository).

Here by the MPN of SRB, the presence and subsistence of viable and cultivable cells were demonstrated. SRB could be able to withstand the heat shock produced by the tyndallization process as shown in the StB and StB.eD samples. Masurat et al. (2010b) also observed the resistance of SRB to high temperatures (75 – 120 ºC), showing cell viability after being enriched again in brackish SRB culture medium. In addition, bacterial cells face water loss during desiccation, enhanced by the strong affinity of the bentonite taking the water from the cells leading to cell inactivation and spore formation. The formation of biofilms and sporulation are also well-known strategies used by bacteria to survive desiccation (Laskowska and Kuczyńska-Wiśnik, 2020). Yet, the metabolic activity can be restored when water is in contact with the cell again (Potts, 1994). The compaction at high density (1.7 g cm^{-3}) and the absence of a renewal water flow and/or organic compounds are conditions that make the bentonite blocks a hostile environment for the bacterial growth and viability over time. Previous studies have demonstrated that the

increase in the density of the bentonite compaction has a negative effect on the viability of SRB (Bengtsson and Pedersen, 2017; Stroes-Gascoyne et al., 2006). Nevertheless, it should be noted that the MPN method is only an approximation of the potentially viable SRB cells present per gram of bentonite and the results could depend on several variables, e.g. the samples' storage time at 4 ºC, that could decrease the number of viable anaerobic cells (Maanoja et al., 2020). Thus, these results should be complemented, in future studies, by quantifying specific genes involved in sulfate reduction (e.g., *dsrA* and *aspA*) by qPCR of the bentonite extracted DNA.

4.3_ Alteration and corrosion compounds characterization of copper disc

VP-FESEM from sample B.eD and B showed signals related to the presence of the bentonite adhered on the surface of the copper disc (Si, Fe, Al, etc.), supported by XRF analysis (**Fig. 7**, **Supplementary Table S1**). The presence of oxygen on the copper surface could be due to the high affinity of copper for oxygen molecules. This oxygen can remain trapped in the bentonite (Burzan et al., 2022) and could participate in the copper oxidation. In sample B.eD, the detection of small precipitates of S associated to copper were detected. This could be related to an initial step of MIC of the copper surface. The increase in the number of SRB found in the MPN experiment may be related to the presence of these precipitates. Under anoxic conditions, SRB are capable of oxidizing lactate (electron donor) coupled to the reduction of sulfate as terminal electron acceptor (Thauer et al., 2007). The resulting HS^- metabolite could be combined with H^+ to form H_2S. The mechanism of copper corrosion influenced by bacteria is explained elsewhere (Dou et al. 2020). Briefly, the H_2S secreted by the SRB can dissociate to H^+ and HS^-. The latter could diffuse to the Cu surface and react with the metal to produce Cu_2S. Several studies have reported copper corrosion mediated by sulfide produced by SRB. Chen et al. (2014) showed that, under anaerobic conditions, SRB are able to adhere onto copper surfaces (biofilm) and form a Cu_2S film as the main corrosion

product. The production of EPS from the SRB biofilm and, subsequently the Cu_2S film, reduces the toxicity of copper towards SRB. When Cu_2S is removed from the copper surface, the presence of small pits caused by the corrosion effect of SRB could be observed on the material surface. Kurmakova et al. (2019) in an experiment with copper and different strains of SRB, showed that these bacteria were responsible for the formation of Cu_2S corrosion products, with *Desulfovibrio* sp. M.4.1 exhibiting the highest corrosive impact on the metal surface. Corrosion of high purity copper in the presence of SRB in groundwater borehole or in MX-80 clay has been demonstrated in other studies where the presence of Cu_2S precipitates have been detected (Pedersen, 2010; Masurat et al., 2010; Johansson et al., 2017). Pedersen et al. (2010) in experiments on copper corrosion in compacted bentonite reported the relationship between the sulfur (^{35}S) diffusion coefficient and the compaction density of the clay. This relationship consists of a decrease in the rate of corrosion in the copper material (1.20 $m^2\ s^{-1}$ to 0.30 $m^2\ s^{-1}$) as the density increased (1750 Kg m^{-3} to 2000 Kg m^{-3}, respectively) due to, among other factors, the geochemical parameters (e.g., presence of the ferrous iron, capable of immobilizing the sulfide) or the growth conditions of the SRB (e.g., bioavailability of sulphate, electron donors and carbon sources). Accordingly, Johaness et al. (2017) in the post-test examination of three MiniCan test series of copper-cast iron canisters reported similar results. The cast iron showed an integrated corrosion rate of several hundred micrometers per year (μm y^{-1}). Regarding copper, the integrated corrosion rate also decreased as the dry density of MX-80 bentonite clay increased (0.15 to 0.02 μm y^{-1} in 1300 to 1600 Kg m^{-3}, respectively).

Micro-FTIR spectroscopy was used to assess the potential presence of microorganisms on the surface of the samples. The occurrence of microorganisms was detected only on sample B.eD. As shown in **Fig. 8**, the presence of infrared absorption bands corresponding to amides, phosphoryl groups, carboxylic and carboxylate compounds suggested that in this sample the presence of

microorganisms could be possible. The distribution of the microorganisms, according to the false-color image in **Fig. 8**, was not homogeneous or uniform. The IR-absorbing molecules associated with bacteria were localized at discrete locations on the sample, and usually next to areas with spectra that could be attributed to bentonite. Spectrum 2 in B.eD sample (**Fig. 8**) shows an example of the typical dioctahedral smectite bands from bentonite adhered to the surface of the discs. The band at 3620 cm^{-1} corresponds to the OH stretching for dioctahedral smectites with octahedral sheets rich in Al (Zviagina et al., 2004). Bands related to Si-O and Si-O-Si stretching vibrations bands are detected at 1110 cm^{-1} and 980 cm^{-1}, respectively (Gaggiano et al., 2013). The bands around 850 cm^{-1} correspond with bending vibrations of AlOH (Bishop et al., 2002). Areas showing no IR-absorption bands correspond to the surface of copper only (as can be seen in spectrum 3 in both samples, **Fig. 8**) and indicate the absence of organic-absorbing molecules above the detection limit of this technique. No evidence of bands related to proteins, lipids or polysaccharides were detected in the samples B, StB and St.BeD (**Fig. 8** and **Supplementary Fig. S6**). In these samples, flat spectra showing no-IR absorbing molecules correspond to the copper surface (dark blue areas in the false-color image), and spectra of bentonite, sulfur-containing compounds (e.g., sulfate) or phosphates; the latter likely to belong to the added electron donors or naturally present in the bentonite.

X-ray photoelectron spectroscopy (XPS) provides a direct chemical characterization of the surface of samples (2-5 nm depth), and has been applied to investigate the composition of the copper discs under the different treatments. In all samples, the presence of elemental copper was evident as shown in **Fig. 9** and **Supplementary Fig. S7**. Sharp peaks were observed at 932.4 eV and 952.1 eV a separation of 19.7 eV). These peaks have previously been associated with the presence of elemental copper (Wagner et al., 1979), and the binding energies corresponding to Cu $2p_{3/2}$ and Cu $2p_{1/2}$ were observed at 952.1 eV at 932.4 eV, and the peaks of Cu $2p_{3/2}$ peaks Cu $2p_{1/2}$ were observed at 932.1 eV, corresponding to

elemental Cu and in agreement with tabulated data (Wagner et al., 1979). Evidence of anaerobic bio-corrosion on copper surfaces usually involves the presence of Cu_xS compounds. Peaks of CuS in the Cu 2p high resolution region have been previously reported at 932.2 eV for $Cu2p_{3/2}$ (Krylova and Andrulevičius, 2009). However, as can be seen in **Fig. 9**, the peaks of elemental Cu in all samples were observed at 932.1 eV, meaning that any potential presence of CuS compounds would have been masked and unable to be detected in these spectra. Therefore, high resolution scans in the region 148-175 eV were performed to assess the presence of sulfur, as this is the region where the S2p peak would appear if present on the surface of the sample.

High resolution scans in the region between 148-175 eV were performed to assess the presence of sulfur and its potential complexation environment. However, no sulfur signal was detected in samples B, StB and St.BeD (**Fig. 9** and **Supplementary Fig. S7**). The peak observed around 155.3 eV in all samples corresponds to Si 2s, previously attributed to silica (Clarke and Rizkalla, 1976), likely due to bentonite. In sample B.eD, in addition to the Si 2s signal, a peak at 162.2 eV was observed, indicating the presence of sulfur in the form of sulfide. Peaks with binding energy around 162.2 eV have previously been reported as CuS and Cu_2S (Scheer and Lewerenz, 1994; Krylova and Andrulevičius, 2009). No peak corresponding to sulfate was detected, as these would have been appeared at binding energies of around 169 eV (Krylova and Andrulevičius, 2009).

The addition of relatively high concentrations of electron donors/acceptor in the bentonite does not represent a real DGR scenario due to the oligotrophic nature of such subsurface environment. However, these nutrients would be able to stimulate the activity of indigenous SRB mainly responsible of the metal surface corrosion on a laboratory timescale, helping to better understand this process in case of enrichment of the bacteria present in the bentonite. The main source of copper corrosion under DGR relevant conditions will be related to the production of

hydrogen sulfide. The potential presence of this compound would be originated by the SRB activity (Bengtsson and Pedersen, 2017). In this study, combining the observations from VP-FESEM, the reflectance micro-FTIR data and the results from XPS, the sample B.eD showed both Cu_xS compounds and the presence of organic compounds, probably of microbial cell origin, on its surface. The infrared spectra of microorganisms were usually in proximity with the bentonite, which could suggest these bacteria could be associated to the bentonite and not directly on the copper surface. The evidence of sulfide-associated compounds also suggests microbial activity of SRB, which could potentially affect the copper surface; however, further tests are needed to verify this hypothesis.

The results presented here shed light for the first time on the microbial activity, bentonite stability, and corrosion of Cu canisters under repository-relevant conditions (e.g., high-density compaction of bentonite, anoxic conditions). This study showed that the mineralogical stability of bentonite was not affected by biotic or abiotic factors. The presence and viability of SRB in all the bentonite blocks, regardless of the treatment, demonstrated the capacity of this bacterial group to survive once the conditions become favorable (i.e., water infiltration). The observed presence of Cu_xS species in the electron donor/sulfate-amended sample (B.eD_1y) could suggest the presence of an early stage corrosion on the copper surface. This study also highlighted the need for further investigation into the bentonite porosity, in order to assess the possible presence of bacterial cells within the pores. In addition, the use of molecular biology techniques, such as qPCR, could provide insights into the activity of SRB by the quantification of the genes involved in sulfate reduction.

5_ Conclusions

The present study describes the impact of physicochemical parameters (dry density of bentonite, heat shock, electron donors, and sulfates) on the microbial activity,

bentonite stability, and the corrosion of Cu canisters within the concept of DGR. Based on the results of this work, no illitization of smectite was observed in compacted bentonite throughout a year of anoxic incubation at 30 ºC regardless of the treatment. Thus, the stability of bentonite was not affected by biotic (microorganisms), nor abiotic factors (addition of acetate-lactate-sulfate or heat-shock tyndallization process) along the incubation time. Regarding the presence of fractures/pores in the blocks in our study, since this was merely observational, complementary techniques such as mercury intrusion porosimetry test (MIP), atomic force microscopy or permeability studies would be necessary to determine and quantify the porosity of the samples. The addition of acetate, lactate, and sulfate solutions seem to stimulate certain bacterial groups capable of introducing these compounds into their metabolism. In addition, the heat-shock produced by the tyndallization of bentonite seems to slightly shape the bacterial diversity with the enrichment of aerobic bacteria belonging to Micrococcaceae and *Nocardioides*. It is worth noting the presence and viability of SRB in all the bentonite blocks regardless of the treatment. This demonstrated the capacity of this bacterial group to survive despite the harsh conditions in the compacted bentonite and turn functional once the conditions become favorable. SRB are of special importance upon DGR closure since they are the main source of anoxic corrosion of metal canisters. The observed presence of small amounts of Cu_xS species in the non-tyndallized electron donor/sulfate (B.eD) sample could suggest the presence of an early stage of corrosion on the copper surface. The detection of Cu_xS species in the non-tyndallized electron donor/sulfate (B.eD) sample shown minor indication of the corrosion process, as expected given the conditions of the experiment (addition of electron donors and sulfate). In addition, the study aims to understand the long-term behavior of copper corrosion related to DGR, so early detection of corrosion is valuable information for understanding this mechanism in the long term.

Altogether, the results obtained provide new insights in understanding the predominant biogeochemical processes at the bentonite/Cu canister interface upon repository gallery closure.

Funding

The present work was supported by the grant RTI2018-101548-B-I00 from MCIN/AEI/10.13039/501100011033 "ERDF A way of making Europe" to MLM from the "Ministerio de Ciencia, Innovación y Universidades" (Spanish Government). ADM acknowledges funding from the UK Engineering and Physical Sciences Research Council (EPSRC) DTP scholarship (project reference: 2748843).

Declaration of Competing Interest

The authors declare that they have no known competing financial interest or personal relationships that could have appeared to influence the work reported in this paper.

Acknowledgements

The authors acknowledge the assistance of Dr. F. Javier Huertas (IACT, Spain) for his guidance and help in collecting the bentonite from the deposit of Almería. Dr. María Victoria-Villar group (CIEMAT, Spain) for the facilities and help during the elaboration of the compacted blocks. Prof. Antonio Sánchez-Navas (Department of Mineralogy and Petrology, University of Garanada, Spain) for his help and training on the diffractometer. Moreover, Concepción Hernández-Castillo and Dr. Isabel Guerra-Tschuschke (Centro de Instrumentación Cientifica, University of Granada, Spain) for the sample preparation and microscopy assistance, respectively.

CRediT authorship contribution statement

Marcos F. Martinez-Moreno: Conceptualization, Methodology, Validation, Investigation, Formal analysis, Visualization, Writing − original draft, Writing − review & editing. Cristina Povedano-Priego: Methodology, Validation, Investigation, Formal analysis, Visualization, Writing − review & editing. Mar Morales-Hidalgo: Writing − review & editing. Adam Mumford: Validation, Formal analysis, Investigation, Writing − original draft, Writing − review & editing. Fadwa Jroundi: Methodology, Formal Analysis, Writing − review & editing. Jesus Ojeda: Validation, Formal analysis, Investigation, Writing − original draft, Writing − review & editing. Mohamed L. Merroun: Conceptualization, Methodology, Formal analysis, Resources, Writing − original draft, Writing − review & editing, Supervision, Project administration, Funding acquisition.

References

Albuquerque, L., França, L., Rainey, F. A., Schumann, P., Nobre, M. F., da Costa, M. S. 2011. *Gaiella occulta* gen. nov., sp. nov., a novel representative of a deep branching phylogenetic lineage within the class Actinobacteria and proposal of Gaiellaceae fam. nov. and Gaiellales ord. nov. Syst. Appl. Microbiol. 34, 595-599. https://doi.org/10.1016/j.syapm.2011.07.001

Anderson, T.F. 1951. Techniques for the preservaation of three-dimensional structure in preparing specimens for the electron microscope. Trans. N.Y. Acad. Sci. 13, 130 - 134 https://doi.org/10.1111/j.2164-0947.1951.tb01007.x

Bagnoud, A., de Bruijn, I., Andersson, A.F., Diomidis, N., Leupin, O.X., Schwyn, B., Bernier-Latmani, R. 2016. A minimalistic microbial food web in an excavated deep subsurface clay rock. FEMS Microbiol. Ecol. 92:fiv138. https://doi.org/10.1093/femsec/fiv138

Batandjieva, B., Delcheva, T., Duhovnik, B. 2009. Classification of radioactive waste: safety guide: IAEA General Safety Guide GSG-1. Vienna. International Atomic Energy Agency.

Bengtsson, A., Pedersen, K. 2017. Microbial sulphide-producing activity in water saturated Wyoming MX-80, Asha and Calcigel bentonites at wet densities from 1500 to 2000 kg m^{-3}. Appl. Clay Sci. 137, 203-212. https://doi.org/10.1016/j.clay.2016.12.024

Bengtsson, A., Pedersen, K. 2016. Microbial sulphate-reducing activity over load pressure and density in water saturated Boom Clay. Appl. Clay Sci. 132, 542-551. https://doi.org/10.1016/j.clay.2016.08.002

Bishop, J., Madejová, J., Komadel, P., and Fröschl, H. 2002. The influence of structural Fe, Al and Mg on the infrared OH bands in spectra of dioctahedral smectites. Clay Miner. 37(4), 607-616. https://doi.org/10.1180/0009855023740063

Burzan, N., Lima, R. M., Frutschi, M., Janowczyk, A., Reddy, B., Rance, A., Diomidis, N., Bernier-Latmani, R. 2022. Growth and Persistence of an Aerobic Microbial Community in Wyoming Bentonite MX-80 Despite Anoxic in situ Conditions. Front. Microbiol. 13: 858324 https://doi.org/10.3389%2Ffmicb.2022.858324

Callahan, B.J., McMurdie, P.J., Rosen, M.J., Han, A.W., Johnson, A.J.A., Holmes, S.P. 2016. DADA2: High-resolution sample inference from Illumina amplicon data. Nat. Methods. 13, 581-583. https://doi.org/10.1038/nmeth.3869

Caporaso J.G., Kuczynski J., Stombaugh J., Bittinger K., Bushman F.D., Costello E.K., Fierer, N., Gonzalez Peña, A., Goodrich, J.K., Gordon, J.I., Huttley, G.A., Kelley, S.T., Knights, D., Koening, J.E., Ley, R.E., Lozupone, C.A., McDonald, D., Muegge, B.D., Pirrung, M., Reeder, J., Sevinsky, J.R., Turnbaugh, P.J., Walters, W.A., Widmann, J., Yatsuneko, T., Zaneveld, J., Knight, R. 2010. QIIME allows analysis of high-throughput community sequencing data. Nat. Methods. 7, 335–336.

Chen, S., Wang, P., Zhang, D. 2014. Corrosion behavior of copper under biofilm of sulfate-reducing bacteria. Corros. Sci. 87, 407 – 415. http://dx.doi.org/10.1016/j.corsci.2014.07.001

Choi, A., Oh, H.M., Cho, J.C. 2011. *Saccharospirillum aestuarii* sp. nov., isolated from tidal flat sediment, and an emended description of the genus *Saccharospirillum*Int. J. Syst. Evol. Microbiol. 61, 487-492. https://doi.org/10.1099/ijs.0.022996-0

Coenye, T., Goris, J., Spilker, T., Vandamme, P., LiPuma, J.J. 2002. Characterization of unusual bacteria isolated from respiratory secretions of cystic fibrosis patients and description of *Inquilinus limosus* gen. nov., sp. nov. J. Clin. Microbiol. 40, 2062-2069. https://doi.org/10.1128/JCM.40.6.2062-2069.2002

Clarke, T.A., Rizkalla, E.N. 1976. X-ray photoelectron spectroscopy of some silicates. Chem. Phys. Lett. 37, 523-526. https://doi.org/10.1016/0009-2614(76)85029-4

Cross, M.M., Manning, D.A., Bottrell, S.H., Worden, R.H. 2004. Thermochemical sulphate reduction (TSR): experimental determination of reaction kinetics and implications of the

observed reaction rates for petroleum reservoirs. Org. Geochem. 35, 393-404. https://doi.org/10.1016/j.orggeochem.2004.01.005

Cui, X., Zhao, S., Wang, B. 2016. Microbial desulfurization for ground tire rubber by mixed consortium-*Sphingomonas* sp. and *Gordonia* sp. Polym. Degrad. Stab. 128, 165-171. https://doi.org/10.1016/j.polymdegradstab.2016.03.011

Dou, W., Pu, Y., Han, X., Song, Y., Chen, S., Gu, T. 2020. Corrosion of Cu by a sulfate reducing bacterium in anaerobic vials with different headspace volumes. Bioelectrochemistry, 133, 107478. https://doi.org/10.1016/j.bioelechem.2020.107478

Fairley, N. CasaXPS, 2.3.22 ed.; Casa Software Ltd.: 2019.

Gaggiano, R., De Graeve, I., Mol, J.M.C., Verbeken, K., Kestens, L.A.I. and Terryn, H. 2013. An infrared spectroscopic study of sodium silicate adsorption on porous anodic alumina. Surf Interface Anal. 45: 1098-1104. https://doi.org/10.1002/sia.5230

García-Romero, E., María Manchado, E., Suárez, M., and García-Rivas, J. 2019. Spanish bentonites: a review and new data on their geology, mineralogy, and crystal chemistry. Fortschr. Mineral. 9:696. https://doi.org/10.3390/min9110696

Gilmour, K.A., Davie, C.T., Gray, N. 2022. Survival and activity of an indigenous iron-reducing microbial community from MX80 bentonite in high temperature/low water environments with relevance to a proposed method of nuclear waste disposal. Sci. Total Environ. 814, 152660. https://doi.org/10.1016/j.scitotenv.2021.152660

Guesmi, S., Nouioui, I., Pujic, P., Dubost, A., Najjari, A., Ghedira, K., Igual, J.M., Cherif, A., Klenk, H., Sghaier, H., Normand, P. 2021. Draft genome sequence of *Promicromonospora panici* sp. nov., a novel ionizing-radiation-resistant actinobacterium isolated from roots of the desert plant *Panicum turgidum*. Extremophiles. 25, 25-38. https://doi.org/10.1007/s00792-020-01207-8

Guo, G. Fall, M. 2021. Advances in modelling of hydro-mechanical processes in gas migration within saturated bentonite: A state-of-art review. Eng. Geol. 287, 106123. https://doi.org/10.1016/j.enggeo.2021.106123

Grigoryan, A.A., Jalique, D.R., Medihala, P., Stroes-Gascoyne, S., Wolfaardt, G.M., McKelvie, J., Korber, D.R. 2018. Bacterial diversity and production of sulfide in microcosms containing uncompacted bentonites. Heliyon. 4, e00722. https://doi.org/10.1016/j.heliyon.2018.e00722

Haavisto, J.M., Lakaniemi, A.M., Puhakka, J.A. 2019. Storing of exoelectrogenic anolyte for efficient microbial fuel cell recovery. Environ. Technol. 40, 1467-1475. https://doi.org/10.1080/09593330.2017.1423395

Hall, D.S., Behazin, M., Binns, W.J., and Keech, P.G. 2021. An evaluation of corrosion processes affecting copper-coated nuclear waste containers in a deep geological repository. Prog. Mater. Sci. 118, 100766. https://doi.org/10.1016/j.pmatsci.2020.100766

Hammer, O. 2001. PAST: paleontological statistics software package for education and data analysis. Palaeontol. Electron. *http://palaeo-electronicaorg*

Haynes, H.M., Pearce, C.I., Boothman, C., Lloyd, J.R. 2018. Response of bentonite microbial communities to stresses relevant to geodisposal of radioactive waste. Chem. Geol. 501, 58-67. https://doi.org/10.1016/j.chemgeo.2018.10.004

Huertas, F., Fariña, P., Farias, J., García-Siñeriz, J.L., Villar, M.V., Fernández, A.M., Martin, P.L., Elorza, F.J., Gens, A., Sánchez, M., Lloret, A., Samper, J., Martínez, M. Á. 2021. Full-scale Engineered Barriers Experiment. Updated Final Report 1994-2004.

Huttunen-Saarivirta, E., Rajala, P., Carpén, L. 2016. Corrosion behavior of copper under biotic and abiotic conditions in anoxic ground water: electrochemical study. Electrochim. Acta. 203, 350-365. https://doi.org/10.1016/j.electacta.2016.01.098

Jiang, W., Saxena, A., Song. S., Ward, B.B., Beveridge, T.J., Myneni, S.C.B. 2004. Elucidation of Functional Groups on Gram-Positive and Gram-Negative Bacterial Surfaces Using Infrared Spectroscopy. Langmuir 20, 11433-11442. https://doi.org/10.1021/la049043

Johansson, A.J., Lilja, C., Sjögren, L., Gordon, A., Hallbeck, L., Johansson, L. 2017. Insights from post-test examination of three packages from the MiniCan test series of coppercast iron canisters for geological disposal of spent nuclear fuel: impact of the presence and density of bentonite clay. Corros. Eng. Sci. Technol. 52, 54-60. https://doi.org/10.1080/1478422X.2017.1296224

Kaewkla, O., Franco, C.M. 2011. *Flindersiella endophytica* gen. nov., sp. nov., an endophytic actinobacterium isolated from the root of Grey Box, an endemic eucalyptus tree. Int. J. Syst. Evol. 61, 2135-2140. https://doi.org/10.1099/ijs.0.026757-0

Kaufhold, S., Dohrmann, R. 2010. Stability of bentonites in salt solutions: II. Potassium chloride solution — Initial step of illitization? Appl. Clay Sci. 49, 98-107. https://doi.org/10.1016/j.clay.2010.04.009

Kim, J., Dong, H., Yang, K., Park, H., Elliott, W. C., Spivack, A., ... and Heuer, V. B. 2019. Naturally occurring, microbially induced smectite-to-illite reaction. Geol. Soc. Am. Bull. 47, 535-539.

King, F. 2002. Status of the copper corrosion model for a deep geologic repository. Ontario Power Generation, Nuclear Waste Management Division Report, 06819-REP-01300-10043-R00.

King, F., M. Kolar, S. Stroes-Gascoyne, and P. Maak. 2003. Model for the microbiological corrosion of copper containers in a deep geologic repository. MRS Online Proceedings Library (OPL), 807, 811.

Krylova, V., Andrulevičius, M. 2009. Optical, XPS and XRD studies of semiconducting copper sulfide layers on a polyamide film. Int. J. Photoenergy. https://doi.org/10.1155/2009/304308

Kurmakova, I, Kupchyk, O, Bondar, O, Demchenko, N, Vorobyova, V. 2019. Corrosion of copper in a medium of bacteria sulfate reduction proceeding. J. Chem. Technol. Metall. 54, 416 – 422.

Labeda, D.P., Kroppenstedt, R.M. 2004. Emended description of the genus *Glycomyces* and description of *Glycomyces algeriensis* sp. nov., *Glycomyces arizonensis* sp. nov. and *Glycomyces lechevalierae* sp. nov. Int. J. Syst. Evol. 54, 2343-2346. https://doi.org/10.1099/ijs.0.63089-0

Laskowska, E., Kuczyńska-Wiśnik, D. 2020. New insight into the mechanisms protecting bacteria during desiccation. Curr. Genet. 66, 313-318. https://doi.org/10.1007/s00294-019-01036-z

Liu, D., Dong, H., Bishop, M.E., Zhang, J., Wang, H., Xie, S., Wang, S., Huang, L., Eberl, D.D. 2012. Microbial reduction of structural iron in interstratified illite-smectite minerals by a sulfate-reducing bacterium. Geobiology, 10, 150-162. https://doi.org/10.1111/j.1472-4669.2011.00307.x

Lopez-Fernandez, M., Vilchez-Vargas, R., Jroundi, F., Boon, N., Pieper, D., Merroun, M.L. 2018. Microbial community changes induced by uranyl nitrate in bentonite clay microcosms. Appl. Clay Sci. 160, 206-216. https://doi.org/10.1016/j.clay.2017.12.034

Lopez-Fernandez, M., Cherkouk, A., Vílchez-Vargas, R., Jauregui, R., Pieper, D., Boon, N., Sanchez-Castro, I., Merroun, M.L. 2015. Bacterial diversity in bentonites, engineered barrier for deep geological disposal of radioactive wastes. Microb. Ecol. 70, 922-935. https://doi.org/10.1007/s00248-015-0630-7.

Lopez-Fernandez, M., Fernández-Sanfrancisco, O., Moreno-García, A., Martín-Sánchez, I., Sánchez-Castro, I., Merroun, M.L. 2014. Microbial communities in bentonite formations

and their interactions with uranium. Appl. Geochem. 49, 77-86. https://doi.org/10.1016/j.apgeochem.2014.06.022

Maanoja, S., Lakaniemi, A.M., Lehtinen, L., Salminen, L., Auvinen, H., Kokko, M., Palmroth, M, Muuri, E, Rintala, J. 2020. Compacted bentonite as a source of substrates for sulfate-reducing microorganisms in a simulated excavation-damaged zone of a spent nuclear fuel repository. Appl. Clay Sci. 196, 105746. https://doi.org/10.1016/j.clay.2020.105746

Madina, V., Insausti, M., Azkarate, I., Garmendia, I., and Cuñado, M. A. 2005. Corrosion behaviour of container candidate materials for HLW disposal in granite-bentonite media. Afinidad, 62(519), 383-387.

Masurat, P., Eriksson, S., Pedersen, K. 2010. Microbial sulphide production in compacted Wyoming bentonite MX-80 under in situ conditions relevant to a repository for high-level radioactive waste. Appl. Clay Sci. 47, 58-64. https://doi.org/10.1016/j.clay.2009.01.004

Masurat, P., Eriksson, S., Pedersen, K. 2010b. Evidence of indigenous sulphate-reducing bacteria in commercial Wyoming bentonite MX-80. Appl. Clay Sci. 47, 51-57. https://doi.org/10.1016/j.clay.2008.07.002

Matschiavelli, N., Kluge, S., Podlech, C., Standhaft, D., Grathoff, G., Ikeda-Ohno, A., Warr, L.N., Chukharkina, A., Arnold, T., & Cherkouk, A. 2019. The year-long development of microorganisms in uncompacted bavarian bentonite slurries at 30 and 60 ºC. Environ. Sci. Technol. 2019, 53, 10514−10524. https://doi.org/10.1021/acs.est.9b02670

Matusewicz, M., Olin, M. 2019. Comparison of microstructural features of three compacted and water-saturated swelling clays: MX-80 bentonite and Na-and Ca-purified bentonite. Clay Miner. 54, 75-81. https://doi.org/10.1180/clm.2019.1

McMurdie, P.J., Holmes, S. 2013. Phyloseq: a R package for reproducible interactive analysis and graphics of microbiome census data. PLoS One. 8, e61217. https://doi.org/10.1371/journal.pone.0061217

Meleshyn, A.Y., Zakusin, S.V., Krupskaya, V.V. 2021. Swelling pressure and permeability of compacted bentonite from 10th khutor deposit (Russia). Minerals. 11, 742. https://doi.org/10.3390/min11070742

Meleshyn, A. 2011. Microbial processes relevant for long-term performance of radioactive waste repositories in clays. GRS-291. ISBN 978-3-939355-67-0. Available from: https://www.grs.de/sites/default/files/pdf/GRS-291.pdf

Moore, D., Reynolds, R. 1989. X-ray Diffraction and the Identification and Analysis of Clay Minerals. Oxford University Press (OUP). p. 332.

Nagra. 2002. Project Opalinus Clay-safety report: demonstration of disposal feasibility for spent fuel, vitrified high-level waste and long-lived intermediate level waste (Entsorgungsnachweis). Nagra Technical Report NTB 02-05. Available from: https://inis.iaea.org/collection/NCLCollectionStore/_Public/50/053/50053802.pdf?r=1

Naumann, D., Helm, D., Labischinski, H. 1991. Microbiological characterizations by FT-IR spectroscopy. Nature 351, 81-82. https://doi.org/10.1038/351081a0

Neuwirth E. 2022. _RColorBrewer: ColorBrewer Palettes_. R package version 1.1-3, < https://CRAN.R-project.org/package=RColorBrewer >.

Ohazuruike, L., and Lee, K. J. 2023. A comprehensive review on clay swelling and illitization of smectite in natural subsurface formations and engineered barrier systems. Nuclear Engineering and Technology. Nucl. Eng. Technol. 55, 1495 – 1506. https://doi.org/10.1016/j.net.2023.01.007

Ojeda, J.J. and Dittrich, M. 2012. Fourier transform infrared spectroscopy for molecular analysis of microbial cells. J. Microbiol. Methods. 187-211. https://doi.org/10.1007/978-1-61779-827-6_8

Ojovan, M.I.; Steinmetz, H.J. 2022. Approaches to Disposal of Nuclear Waste. Energies, 15, 7804. https://doi.org/10.3390/en15207804

Orsini, F.; Ami, D.; Villa, A. M.; Sala, G.; Bellotti, M.G.; Doglia, S.M. 2000. FT-IR microspectroscopy for microbiological studies. J. Microbiol. Meth. 42 , 17. https://doi.org/10.1016/S0167-7012(00)00168-8

Payer, J. H., Finsterle, S., Apps, J.A., Muller, R.A. 2019. Corrosion performance of engineered barrier system in deep horizontal drillholes. Energies. 12, 1491. https://doi.org/10.3390/en12081491

Pedersen, K. 2010. Analysis of copper corrosion in compacted bentonite clay as a function of clay density and growth conditions for sulfate-reducing bacteria. J. Appl. Microbiol., 108, 1094-1104. https://doi.org/10.1111/j.1365-2672.2009.04629.x

Pentráková, L., Su, K., Pentrák, M., Stucki, J.W. 2013. A review of microbial redox interactions with structural Fe in clay minerals. Clay Miner. 48, 543-560. https://doi.org/10.1180/claymin.2013.048.3.10

POSIVA. Final Disposal. https://www.posiva.fi/en/index/finaldisposal.html (accessed 16 May 2023).

Potts, M. 1994. Desiccation tolerance of prokaryotes. Microbiol. Rev. 58, 755-805.

Povedano-Priego, C., Jroundi, F., Solari, P.L., Guerra-Tschuschke, I., del Mar Abad-Ortega, M., Link, A., Vilchez-Vargas, R., Merroun, M.L. 2023. Unlocking the bentonite microbial diversity and its implications in selenium bioreduction and biotransformation: Advances in deep geological repositories. J. Hazard. Mater. 445, 130557. https://doi.org/10.1016/j.jhazmat.2022.130557

Povedano-Priego, C., Jroundi, F., Lopez-Fernandez, M., Morales-Hidalgo, M., Martin-Sánchez, I., Huertas, F.J., Dopson, M. Merroun, M.L. 2022. Impact of anoxic conditions, uranium(VI) and organic phosphate substrate on the biogeochemical potential of the indigenous bacterial community of bentonite. Appl. Clay Sci. 216, 106331. https://doi.org/10.1016/j.clay.2021.106331

Povedano-Priego, C., Jroundi, F., Lopez-Fernandez, M., Shrestha, R., Spanek, R., Martín-Sánchez, I., Villar, M.V., ˇSevců, A., Dopson, M. Merroun, M.L. 2021. Deciphering indigenous bacteria in compacted bentonite through a novel and efficient DNA extraction method: Insights into biogeochemical processes within the Deep Geological Disposal of nuclear waste concept. J. Hazard. Mater. 408, 124600. https://doi.org/10.1016/j.jhazmat.2020.124600

Povedano-Priego, C., Jroundi, F., Lopez-Fernandez, M., Sánchez-Castro, I., Martin-Sánchez, I., Huertas, F.J., Merroun, M.L. 2019. Shifts in bentonite bacterial community and mineralogy in response to uranium and glycerol-2-phosphate exposure. Sci. Total Environ. 692, 219-232. https://doi.org/10.1016/j.scitotenv.2019.07.228

Pusch, R., Carlsson, T. 1985. The physical state of pore water of Na smectite used as barrier component. Eng. Geol. 21, 257-265. https://doi.org/10.1016/0013-7952(85)90016-X

Keech, P.G., Ramamurthy, P.Vo.S., Chen, J., Jacklin, R., & Shoesmith, D.W. 2014. Design and development of copper coatings for long term storage of used nuclear fuel. Corros. Eng. Sci. Technol. 49, 425-430. https://doi.org/10.1179/1743278214Y.0000000206

R Core Team. 2022. R: A language and environment for statistical computing. R Foundation for Statistical Computing, Vienna, Austria. URL https://www.R-project.org/.

Robertson, C.E., Harris, J.K., Wagner, B.D., Granger, D., Browne, K., Tatem, B., Feazel, L.M., Park, K., Pace, N.R., Frank, D.N. 2013. Explicet: graphical user interface software for

metadata-driven management, analysis and visualization of microbiome data. Bioinformatics, 29, 3100-3101. https://doi.org/10.1093/bioinformatics/btt526

Scheer, R., Lewerenz, H.J. 1994. Photoemission study of evaporated $CuInS_2$ thin films. II. Electronic surface structure. J. Vac. Sci. Technol. A: Vac. Surf. Films. 12, 56-60. https://doi.org/10.1116/1.578858

Shelobolina, E.S., VanPraagh, C.G., Lovley, D.R. 2003. Use of ferric and ferrous iron containing minerals for respiration by *Desulfitobacterium frappieri*. Geomicrobiol. J. 20, 143-156. https://doi.org/10.1080/01490450303884

Smart, N. R., Reddy, B., Rance, A. P., Nixon, D. J., Frutschi, M., Bernier-Latmani, R., and Diomidis, N. 2017. The anaerobic corrosion of carbon steel in compacted bentonite exposed to natural Opalinus Clay porewater containing native microbial populations. Corros. Eng. Sci. Technol., 52(sup1), 101-112. https://doi.org/10.1080/1478422X.2017.1315233

Stroes-Gascoyne, S., Hamon, C.J., Dixon, D.A., Kohle, C.L., Maak, P. 2006. The effects of dry density and porewater salinity on the physical and microbiological characteristics of compacted 100% bentonite. Mater. Res. Soc. Symp. Proc. Vol. 985. https://doi.org/10.1557/PROC-985-0985-NN13-02

Thauer, R.K., Stackebrandt, E., Hamilton, W.A. 2007. Energy metabolism and phylogenetic diversity of sulphate-reducing bacteria. Sulphate-reducing bacteria. 1-38. https://doi:10.1017/cbo9780511541490.002

Thijs, S., Op De Beeck, M., Beckers, B., Truyens, S., Stevens, V., Van Hamme, J. D., Weyens, N. Vangronsveld, J. 2017. Comparative evaluation of four bacteria-specific primer pairs for 16S rRNA gene surveys. Front. Microbiol. 8, 494. https://doi.org/10.3389/fmicb.2017.00494

Vaïtilingom, M., Amato, P., Sancelme, M., Laj, P., Leriche, M., Delort, A.M. 2010. Contribution of microbial activity to carbon chemistry in clouds. Appl. Environ. Microbiol. 76, 23-29. https://doi.org/10.1128/AEM.01127-09

Van Geet, M., Maes, N., Dierckx, A. 2003. Characteristics of the Boom Clay organic matter, a review. Geological Survey of Belgium, Professional paper. 298, 1-23

Villar, M.V., Gómez-Espina, R., Campos, R., Barrios, I., Gutiérrez, L. 2012. Porosity changes due to hydration of compacted bentonite. Unsaturated Soils: Research and Applications. Volume 1 (pp. 137-144). Springer. https://doi.org/10.1007/978-3-642-31116-1_18

Villar, M.V., Fernández-Soler, J.M., Delgado Huertas, A., Reyes, E., Linares, J., Jiménez de Cisneros, C., Linares, J., Reyes, E., Delgado, A., Fernandez-Soler, J.M., Astudillo, J. 2006. The study of Spanish clays for their use as sealing materials in nuclear waste repositories: 20 years of progress. J. Iber. Geol. 32, 15-36.

Wagner, C.D., Riggs, W.M., Davis, L.E., Moulder, J.F., Muilenberg, G.E. 1979. Handbook of x-ray photoelectron spectroscopy: a reference book of standard data for use in x-ray photoelectron spectroscopy. Perkin-Elmer Corporation: Eden Prairie, MN.

Warnes G, Bolker B, Bonebakker L, Gentleman R, Huber W, Liaw A, Lumley T, Maechler M, Magnusson A, Moeller S, Schwartz M, Venables, B. 2022. _gplots: Various R Programming Tools for Plotting Data_. R package version 3.1.3, https://CRAN.R-project.org/package=gplots

Wersin, P., K. Spahiu, and J. Bruno. 1994. Kinetic modelling of bentonite-canister interaction: Long-term predictions of copper canister corrosion under oxic and anoxic conditions. (No. SKB-TR--94-25). Swedish Nuclear Fuel and Waste Management Co.

White, D.C., Sutton, S.D., Ringelberg, D. B. (1996). The genus *Sphingomonas*: physiology and ecology. Curr. Opin. Biotechnol. 7, 301-306. https://doi.org/10.1016/S0958-1669(96)80034-6

WNA. World Nuclear Association. 2021. Storage and disposal of radioactive waste. https://www.world-nuclear.org/

Zheng, W., Li, D., Zhao, J., Liu, C., Zhao, Y., Xiang, W., Wang, X. 2017. Promicromonospora soli sp. nov., a novel actinomycete isolated from soil. Int. J. Syst. Evol. Microbiol. 67, 3829-3833. https://doi.org/10.1099/ijsem.0.002207

Zviagina, B.B., McCarty, D.K., Środoń, J., and Drits, V.A. 2004. Interpretation of infrared spectra of dioctahedral smectites in the region of OH-stretching vibrations. Clays Clay Miner. 52, 399–410. https://doi.org/10.1346/CCMN.2004.0520401

Supplementary material for:

Impact of compacted bentonite microbial community on the clay mineralogy and copper canister corrosion: a multidisciplinary approach in view of a safe Deep Geological Repository of nuclear wastes

Marcos F. Martinez-Moreno[1,*], Cristina Povedano-Priego[1], Mar Morales-Hidalgo[1], Adam D. Mumford[2], Jesus J. Ojeda[2], Fadwa Jroundi[1], Mohamed L. Merroun[1]

[1]*Faculty of Sciences, Department of Microbiology, University of Granada, Granada, Spain.*

[2]*Department of Chemical Engineering, Faculty of Science and Engineering, Swansea University, Swansea, United Kingdom*

Supplementary Table S1.

pH and chemical composition (%) by X-ray fluorescence (XRF) of the initial samples and one year of anaerobic incubation (1y).

Treatment	pH	SiO2	Al2O3	Fe2O3	MnO	MgO	CaO	Na2O	K2O	TiO2	P2O5	LOI
B.eD	8.08	61.91	17.12	3.89	0.04	3.72	3.54	1.94	1.63	0.27	0.08	5.83
B.eD_1y	7.74	57.96	17.65	5.20	0.03	3.55	3.94	3.11	1.39	0.32	0.08	6.17
B	8.16	61.93	16.95	3.84	0.04	4.70	3.10	1.43	1.17	0.19	0.05	6.56
B_1y	7.71	57.38	17.80	5.25	0.02	3.53	3.80	3.01	1.37	0.32	0.07	7.35
StB.eD	8.20	60.51	16.49	3.92	0.05	3.80	4.80	1.87	1.53	0.30	0.07	6.64
StB.eD_1y	7.81	58.61	17.91	5.00	0.02	4.15	2.92	2.60	1.05	0.27	0.04	6.78
StB	8.13	59.64	16.49	3.90	0.05	3.82	5.18	1.81	1.52	0.28	0.07	7.23
StB_1y	7.73	57.60	17.88	5.19	0.03	3.55	3.86	2.97	1.34	0.32	0.06	6.70
Average t. 0	8.14 ± 0.05	61.00 ± 1.12	16.76 ± 0.32	3.89 ± 0.03	0.05 ± 0.01	4.01 ± 0.46	4.16 ± 0.99	1.76 ± 0.20	1.46 ± 0.20	0.26 ± 0.05	0.07 ± 0.01	6.51 ± 0.57
Average t. 1y	7.72 ± 0.07	57.89 ± 0.54	17.81 ± 0.12	5.16 ± 0.11	0.03 ± 0.01	3.70 ± 0.30	3.63 ± 0.48	2.92 ± 0.22	1.29 ± 0.16	0.31 ± 0.03	0.06 ± 0.02	6.75 ± 0.48

*LOI: Loss on ignition

Supplementary Table S2.

Phyla relative abundance of the bacterial and archaeal communities from 1.7 g cm-3 compacted bentonite blocks in triplicate (duplicates in StB.eD, B and B.eD). B: non-tyndallized bentonite, StB: tyndallized bentonite, eD: treated with electron donors and sulfate, 1y: after one year of anaerobic incubation.

	Relative abundance (%)								
	Total	B	B_1y	B.eD	B.eD_1y	StB	StB_1y	StB.eD	StB.eD_1y
Bacteria_Actinobacteriota	59.48	46.53	54.98	54.53	48.47	60.81	64.01	72.93	60.30
Bacteria_Proteobacteria	24.18	39.81	34.88	21.04	20.16	17.85	20.29	16.86	23.88
Bacteria_Chloroflexi	6.05	2.27	3.26	10.36	14.93	4.90	6.39	4.38	6.02
Bacteria_Gemmatimonadota	1.82	1.55	0.54	2.64	1.37	11.43	0.85	1.22	0.93
Bacteria_Bacteroidota	1.77	2.27	1.62	2.32	2.95	1.13	1.20	0.87	1.27
Bacteria_Firmicutes	1.59	1.28	1.83	1.83	3.49	1.76	3.55	1.37	3.91
Bacteria_Acidobacteriota	1.52	0.71	0.71	2.69	3.31	0.82	1.35	0.93	1.36
Bacteria_Cyanobacteria	1.04	3.42	0.73	0.36	0.61	0.27	0.61	0.17	0.47
Bacteria_Verrucomicrobiota	0.72	0.60	0.31	1.30	1.18	0.26	0.51	0.28	0.47
Bacteria_Planctomycetota	0.57	0.42	0.38	0.74	1.31	0.42	0.62	0.47	0.75
Bacteria_Myxococcota	0.44	0.24	0.14	0.90	0.84	0.09	0.24	0.17	0.23
Bacteria_Patescibacteria	0.28	0.33	0.18	0.42	0.36	0.09	0.08	0.12	0.11
Bacteria_Deinococcota	0.15	0.26	0.17	0.16	0.15	0.06	0.09	0.07	0.09
Bacteria_Nitrospirota	0.12	0.09	0.08	0.21	0.40	0.03	0.07	0.04	0.07
Bacteria_Bdellovibrionota	0.07	0.12	0.01	0.12	0.04	0.00	0.00	0.01	0.02
Bacteria_Sumerlaeota	0.05	0.03	0.10	0.05	0.11	0.06	0.11	0.04	0.10
Bacteria_Desulfobacterota	0.05	0.02	0.03	0.09	0.25	0.01	0.01	0.01	0.02
Bacteria_Armatimonadota	0.04	0.01	0.01	0.09	0.02	0.01	0.01	0.03	0.02
Bacteria_unclassified	0.02	0.01	0.03	0.06	0.00	0.00	0.00	0.01	0.00
Bacteria_Entotheonellaeota	0.01	0.00	0.00	0.01	0.02	0.00	0.02	0.01	0.00
Bacteria_Fibrobacterota	0.01	0.02	0.00	0.01	0.01	0.00	0.00	0.00	0.01
Bacteria_Dependentiae	0.01	0.01	0.00	0.01	0.01	0.00	0.00	0.00	0.00

Archaea_Crenarchaeota	0.01	0.00	0.00	0.01	0.00	0.00	0.00	0.00	0.00
Bacteria_Methylomirabilota	0.00	0.00	0.00	0.00	0.00	0.00	0.00	0.00	0.00
Bacteria_Elusimicrobiota	0.00	0.01	0.00	0.00	0.00	0.00	0.00	0.00	0.00
Bacteria_MBNT15	0.00	0.01	0.00	0.00	0.01	0.00	0.00	0.00	0.00
Bacteria_Hydrogenedentes	0.00	0.00	0.00	0.00	0.00	0.00	0.00	0.00	0.00
Bacteria_GAL15	0.00	0.01	0.00	0.00	0.00	0.00	0.00	0.00	0.00
Bacteria_Abditibacteriota	0.00	0.00	0.00	0.01	0.00	0.00	0.00	0.00	0.00
Archaea_Thermoplasmatota	0.00	0.00	0.00	0.01	0.00	0.00	0.00	0.00	0.00
Bacteria_Halanaerobiaeota	0.00	0.00	0.00	0.01	0.01	0.00	0.00	0.00	0.00
Bacteria_Fusobacteriota	0.00	0.00	0.00	0.01	0.00	0.00	0.00	0.00	0.00
Archaea_Aenigmarchaeota	0.00	0.01	0.00	0.00	0.00	0.00	0.00	0.00	0.00
Bacteria_WS4	0.00	0.00	0.00	0.01	0.00	0.00	0.00	0.00	0.00

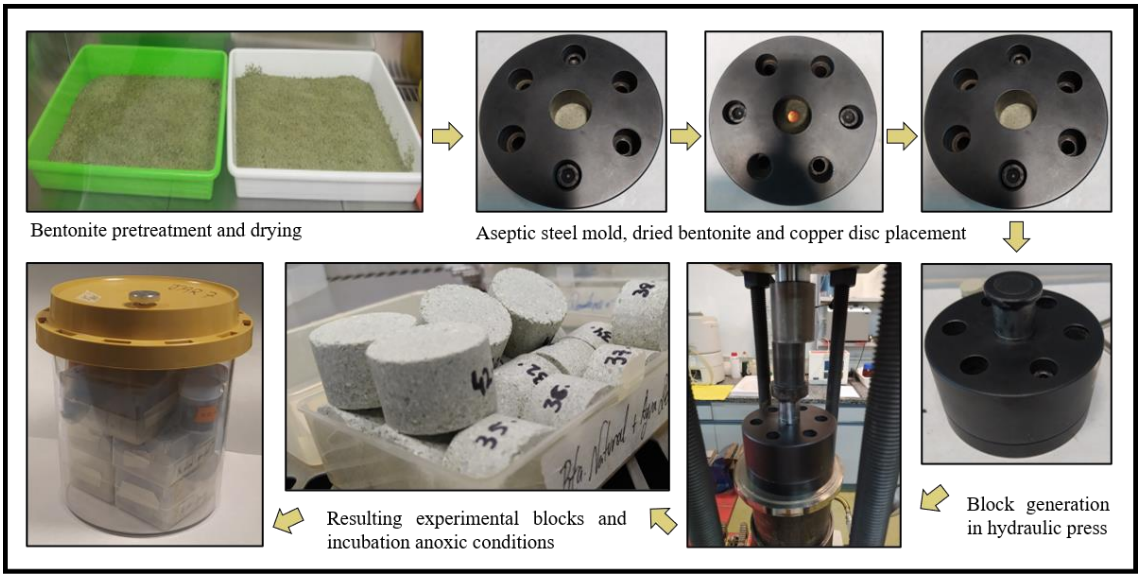

Supplementary Fig. S1. Compaction process of the experimental bentonite blocks.

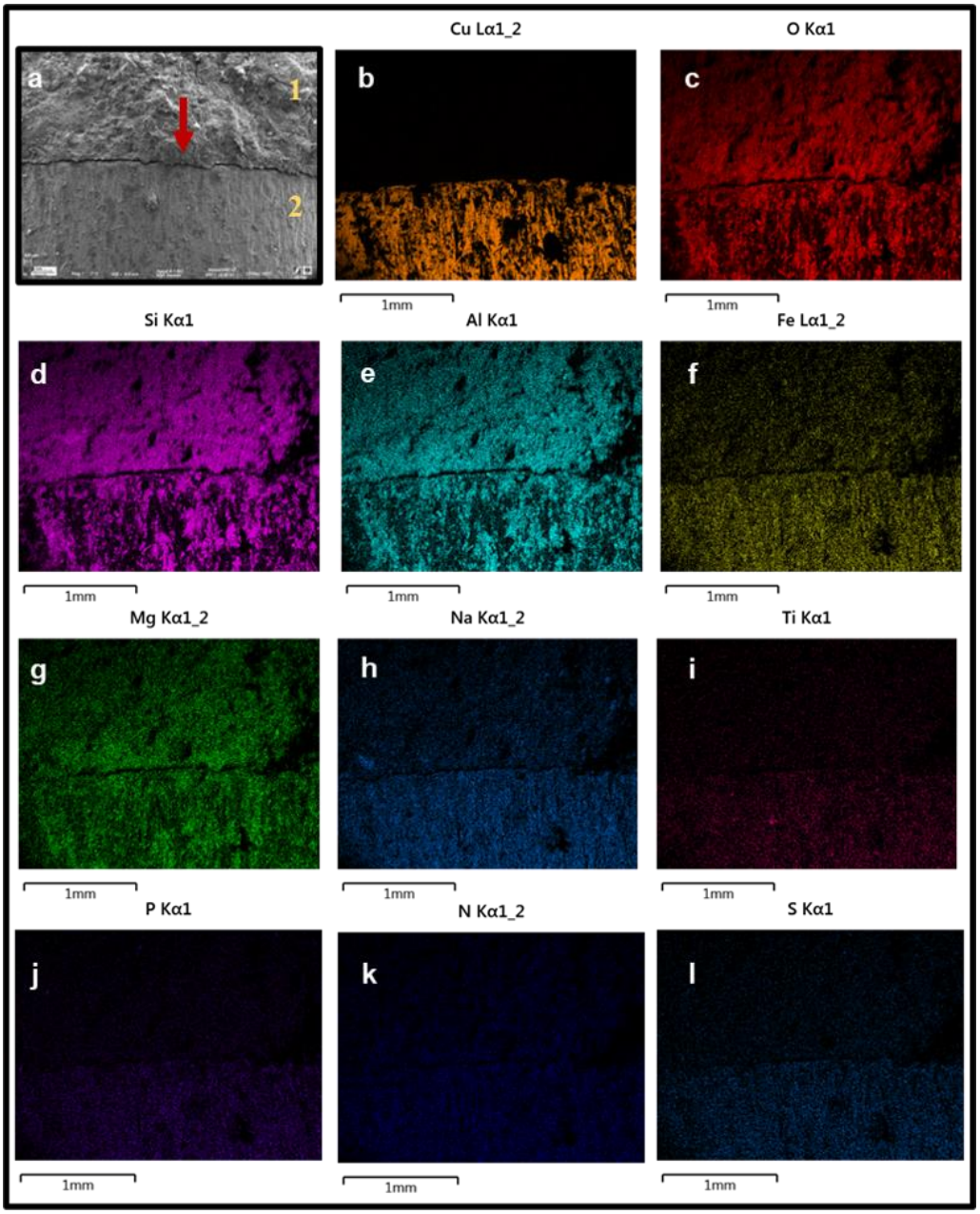

Supplementary Fig. S2. Cross sections of B.eD after one-year of anaerobic incubation showing the (a) topography of the block at the bentonite (1) - copper disk (2) interface (red arrow). (b-l) EDX maps indicating the elements distribution of Cu, O, Si, Al, Fe, Mg, Na, Ti, P, N and S.

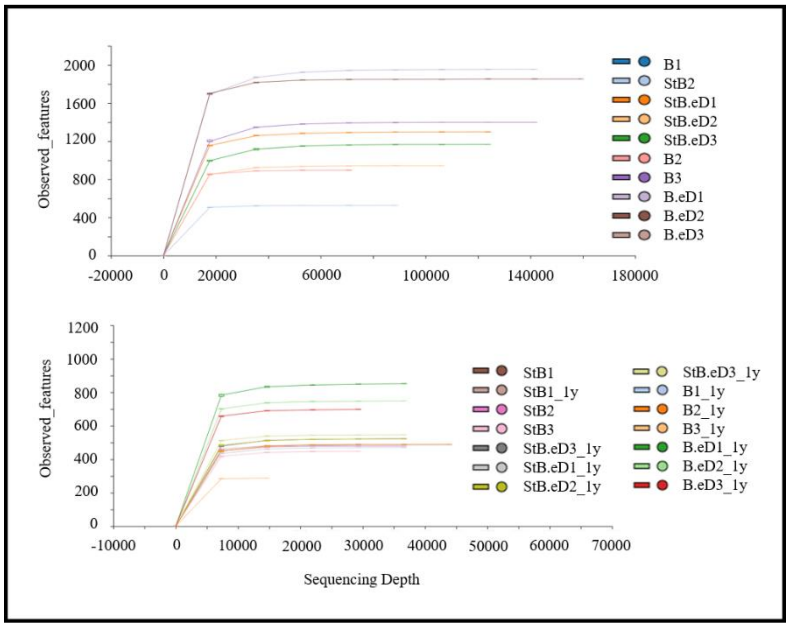

Supplementary Fig. S3. Rarefaction curves of the sequenced samples representing the richness and sample size. B: non-tyndallized bentonite, StB: tyndallized bentonite, eD: treated with electron donors and sulfate, 1y: after one year of anaerobic incubation.

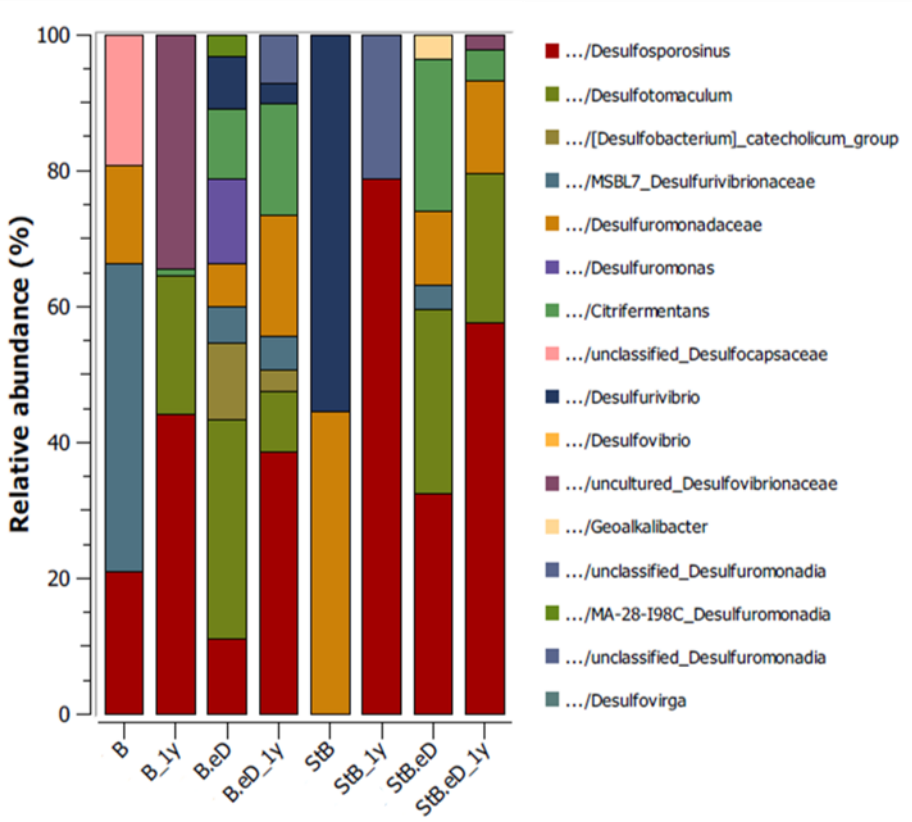

Supplementary Fig. S4. OTU relative abundance within a selected SRB group of the bacterial communities from 1.7 g cm^{-3} compacted bentonite blocks. Stacked bars show averages of biological triplicates (duplicates in StB.eD, B and B.eD) B: non-tyndallized bentonite, StB: tyndallized bentonite, eD: treated with electron donors and sulfate, 1y: after one year of anaerobic incubation.

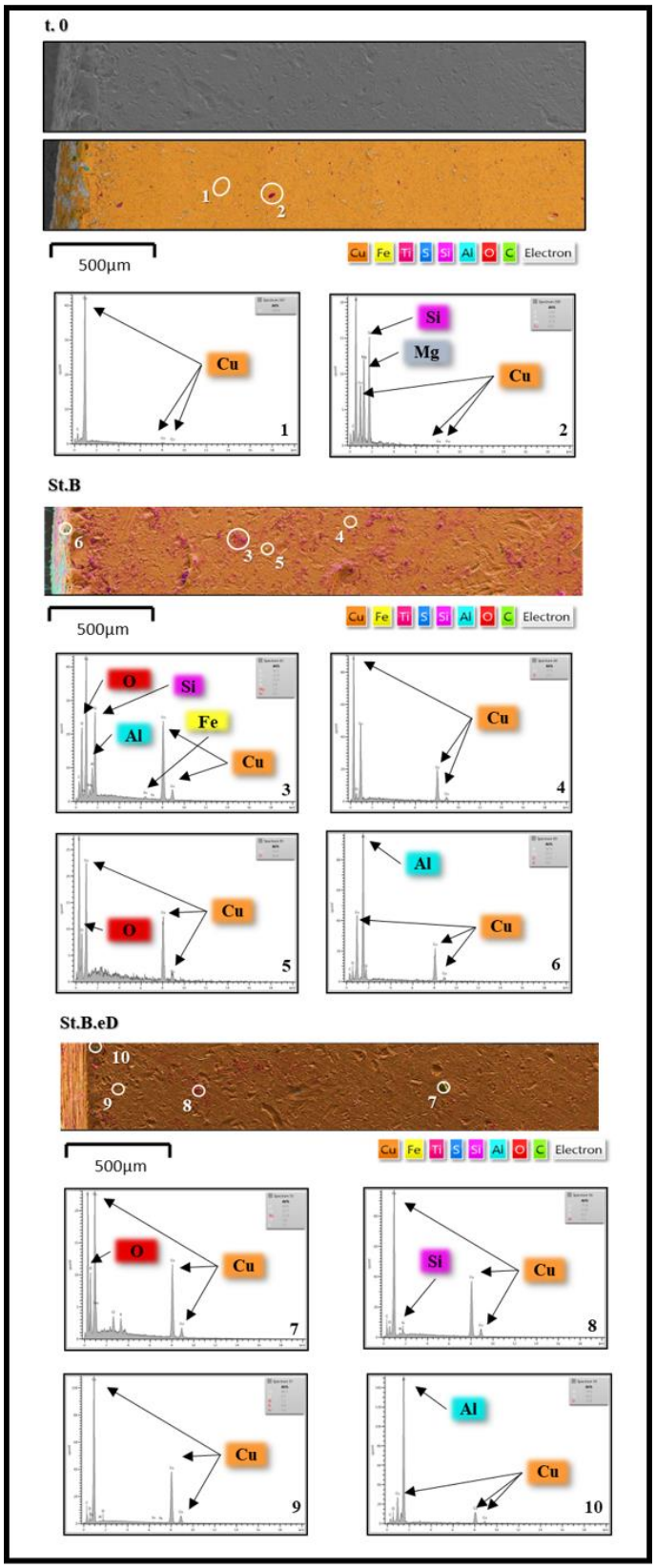
t. 0
1
2
500µm
Cu Fe Ti S Si Al O C Electron
Cu
1
Si
Mg
Cu
2
St.B
6
3
5
4
500µm
Cu Fe Ti S Si Al O C Electron
O
Si
Al
Fe
Cu
3
Cu
4
Cu
O
5
Al
Cu
6
St.B.eD
10
9
8
7
500µm
Cu Fe Ti S Si Al O C Electron
O
Cu
7
Si
Cu
8
Cu
9
Al
Cu
10

Supplementary Fig. S5. EDX maps associated with electron images from a selected area (from edge to center) of Cu disc from t. 0, StB and StB.eD treatments. EDX show the distribution of Cu, Fe, Ti, S, Si, Al, O and C in the studied area. White circle and EDX analysis show the presence of bentonite (Si, Al, Fe) adhered to the surface (3, 6, 8 and 10), precipitates related to Cu_xO (5 and 7), and unaltered copper (1, 4 and 9). A possible cross contamination was observed in t. 0 (2) since the sample was not in contact with bentonite.

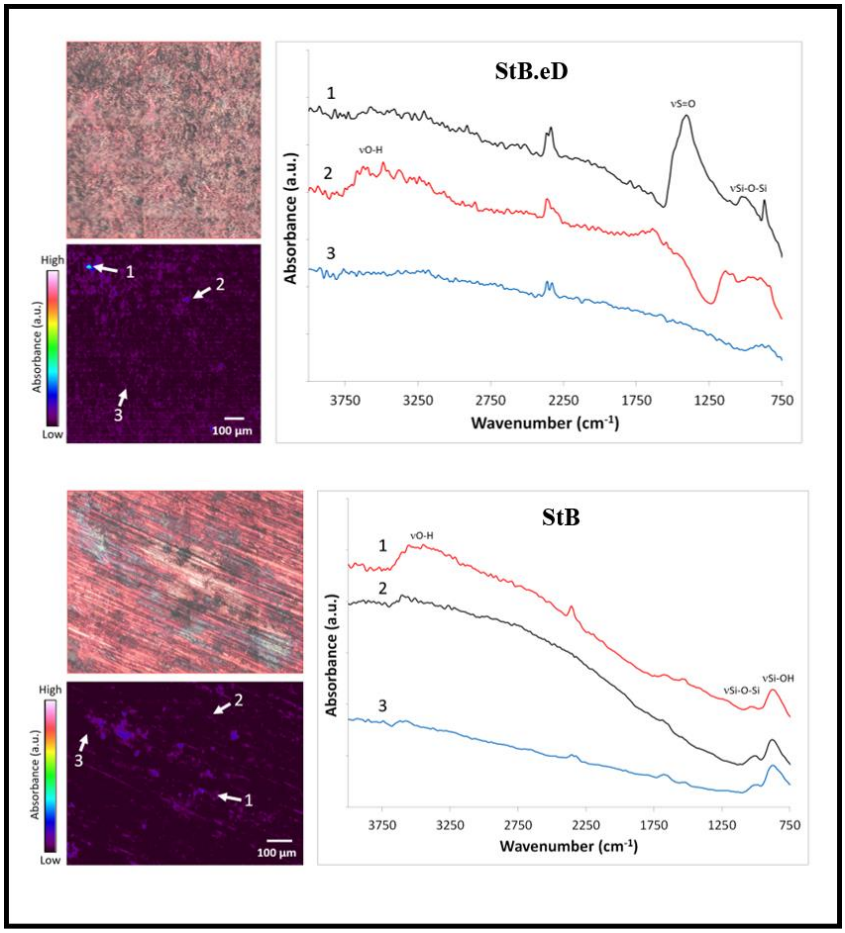

Supplementary Fig. S6. Reflectance micro-FTIR spectroscopy for the study of microbial presence on the copper disc from sample StB.eD and StB after one year of incubation. Left: optical image of the scanned regions and false-colour image of the sample scanned using reflectance micro-FTIR spectroscopy. Right: infrared spectra of three different regions on the samples.

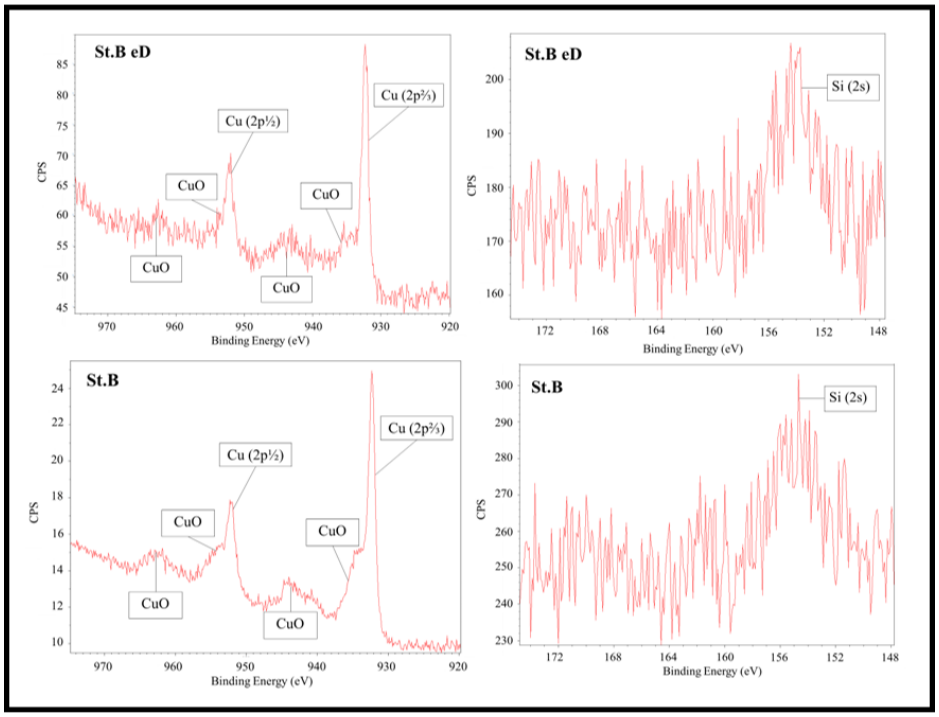

Supplementary Fig. S7. High resolution XPS scan for the copper 2p region (left), between 975-920 eV and for the sulfur 2p region (right), between 175-148 eV for sample StB.eD (top) and StB (bottom) after one year of anaerobic incubation.

Supplementary Data S1. OTU relative abundance of the bacterial and archaeal communities from 1.7 g cm^{-3} compacted bentonite blocks in triplicate (duplicates in StB.eD, B and B.eD). This table only represents a cut-off > 0.5% of the total relative abundance. B: non-tyndallized bentonite, StB: tyndallized bentonite, eD: treated with electron donors and sulfate, 1y: after one year of anaerobic incubation.

Genera	Relative abundance (%)								
	Total	B	B_1y	B.eD	B.eD_1y	StB	StB_1y	StB.eD	StB.eD_1y
Nocardioides	16.32	6.33	7.97	11.93	8.51	18.00	18.94	27.23	16.85
unclassified_Micrococcaceae	9.77	5.85	10.10	6.24	6.32	19.30	17.72	15.04	17.81
Promicromonospora	3.97	5.97	7.37	1.40	1.41	5.70	4.62	4.91	4.21
Saccharospirillum	3.93	13.96	9.04	0.37	0.34	1.18	0.80	0.88	0.75
Gitt-GS-136_Chloroflexi	3.80	1.36	2.56	6.43	10.94	4.02	4.82	2.74	4.54
Marmoricola	2.71	2.31	2.45	1.50	1.19	2.05	2.50	4.16	2.39
unclassified_Nocardioidaceae	2.45	1.22	2.05	2.28	1.79	1.80	2.38	3.47	2.58
uncultured	2.31	7.76	3.78	0.44	0.32	0.83	0.60	0.57	0.76
unclassified	2.28	1.71	1.79	3.73	3.85	1.18	1.64	1.37	1.48
Mesorhizobium	2.28	2.58	2.96	1.76	1.66	3.57	3.28	2.48	3.04
Streptomyces	2.22	3.20	3.65	2.22	2.68	1.85	2.13	1.54	1.77
Amycolatopsis	1.77	1.72	1.39	1.69	0.82	1.47	1.79	1.94	1.41
unclassified	1.68	4.16	3.55	0.43	0.36	0.69	0.83	1.26	1.00
uncultured_Microtrichales	1.37	0.82	0.72	2.50	2.34	0.43	0.64	0.78	0.59
Flindersiella	1.23	2.04	2.73	1.73	1.42	0.23	0.33	0.24	0.29
Pseudarthrobacter	1.00	0.33	0.24	0.55	0.67	1.27	1.96	1.82	1.87
Pseudonocardia	1.00	1.86	1.68	0.99	0.65	0.44	0.15	0.53	0.31
Longimicrobiaceae	0.96	0.84	0.22	1.63	0.78	0.30	0.36	0.54	0.41
Bacillus	0.87	0.60	0.83	0.81	1.70	1.30	2.09	0.99	2.33

Arthrobacter	0.85	0.49	0.77	0.62	0.64	1.31	1.16	1.26	1.23
Chloroplast	0.83	3.17	0.33	0.15	0.20	0.07	0.04	0.02	0.10
KD4-96_Chloroflexi	0.82	0.19	0.26	1.67	1.93	0.44	0.61	0.46	0.57
Sphingomonas	0.70	0.27	0.21	1.20	0.99	0.64	0.72	0.54	0.65
Pseudomonas	0.70	0.90	3.88	0.32	0.74	1.10	1.96	0.69	3.74
uncultured_Alphaproteobacteria	0.68	0.32	0.26	1.17	1.27	0.29	0.66	0.46	0.57
0319-7L14_Actinobacteria	0.66	0.22	0.27	1.29	1.46	0.29	0.39	0.37	0.40
Lysobacter	0.65	0.49	0.77	0.64	0.57	1.09	1.22	0.72	1.26
Ramlibacter	0.63	0.84	0.67	0.47	0.31	0.38	0.54	0.66	0.65
Iamia	0.62	0.21	0.25	1.22	0.96	0.27	0.41	0.40	0.38
Caenimonas	0.59	0.92	0.99	0.52	0.31	0.36	0.53	0.46	0.64
JG30-KF-CM45_Thermomicrobiales	0.58	0.32	0.25	0.86	0.91	0.25	0.47	0.52	0.43
uncultured	0.56	0.61	0.53	0.74	1.20	0.59	0.43	0.30	0.47
Vicinamibacteraceae	0.55	0.29	0.13	0.98	1.05	0.26	0.51	0.34	0.44
uncultured_Acidimicrobiia	0.55	0.22	0.05	1.27	0.84	0.10	0.06	0.18	0.05
Kribbella	0.55	0.74	0.56	0.37	0.34	0.42	0.68	0.59	0.57
Glycomyces	0.52	0.62	0.49	0.89	0.88	0.12	0.16	0.12	0.13
67-14_Solirubrobacterales	0.52	0.28	0.27	0.80	0.91	0.27	0.50	0.43	0.41
Pelagibius	0.52	0.29	0.27	0.59	0.83	0.47	0.64	0.59	0.56
Gaiella	0.51	0.17	0.27	0.92	1.22	0.55	0.62	0.34	0.54
Solimonas	0.51	0.57	0.38	0.06	0.07	1.14	0.73	0.87	1.03

Deep Geological Repository

Personal illustration

Chapter II:

Microbial responses to elevated temperature: Evaluating bentonite mineralogy and copper canister corrosion within the long-term stability of deep geological repositories of nuclear waste

Authors

Marcos F. Martinez-Moreno[a]*, Cristina Povedano-Priego[a], Adam D. Mumford[b], Mar Morales-Hidalgo[a], Kristel Mijnendonckx[c], Fadwa Jroundi[a], Jesus J. Ojeda[b], Mohamed L. Merroun[a]

[a]Faculty of Sciences, Department of Microbiology, University of Granada, Granada, Spain
[b]Department of Chemical Engineering, Faculty of Science and Engineering, Swansea University, Swansea, United Kingdom
[c]Microbiology Unit, Belgian Nuclear Research Centre, SCK CEN, Mol, Belgium

This chapter has been published in the journal Science of the Total Environment:
Martinez-Moreno, M.F., et al. (2024). Sci. Total Environ., 170149. https://doi.org/10.1016/j.scitotenv.2024.170149

IF: 9.8 / **Q**1 / **D**1

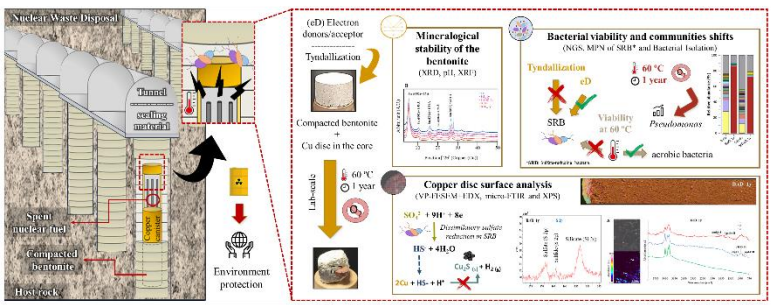

Abstract

Deep Geological Repositories (DGRs) consist of radioactive waste contained in corrosion-resistant canisters, surrounded by compacted bentonite clay, and buried few hundred meters in a stable geological formation. The effects of bentonite microbial communities on the long-term stability of the repository should be assessed. This study explores the impact of harsh conditions (60 ºC, highly-compacted bentonite, low water activity), and acetate:lactate:sulfate addition, on the evolution of microbial communities, and their effect on the bentonite mineralogy, and corrosion of copper material under anoxic conditions. No bentonite illitization was observed in the treatments, confirming its mineralogical stability as an effective barrier for future DGR. Anoxic incubation at 60 ºC reduced the microbial diversity, with *Pseudomonas* as the dominant genus. Culture-dependent methods showed survival and viability at 60 ºC of moderate-thermophilic aerobic bacterial isolates (e.g., *Aeribacillus*). Despite the low presence of sulfate-reducing bacteria in the bentonite blocks, we proved their survival at 30 ºC but not at 60 ºC. Copper disk´s surface remained visually unaltered. However, in the acetate:lactate:sulfate-treated samples, sulfide/sulfate signals were detected, along with microbial-related compounds. These findings offer new insights into the impact of high temperatures (60ºC) on the biogeochemical processes at the compacted bentonite/Cu canister interface post-repository closure.

Keywords: *Nuclear repository, compacted bentonite, high temperature, microbial diversity, sulfate-reducing bacteria, copper corrosion*

1_ Introduction

The management and safe disposal of high-level waste (HLW) containing long-lived radionuclides is a critical concern within the nuclear energy industry. To address this, HLW must be confined for over 100,000 years until it reaches natural radiation levels (Ojovan and Steinmetz, 2022). The internationally accepted option for their final disposal is the Deep Geological Repository (DGR). It consists of storing HLW in corrosion-resistant metal canisters and surrounded by a buffer material (e.g., highly compacted bentonite), as engineered barrier, and placed a few hundred meters depth within a stable geological formation, acting as natural barrier (WNA, 2021). The material of the metal canisters would depend on the DGR concept implemented by each country. Canada, Korea, Sweden or Finland have opted for, or already implemented, copper as external coating material for metal canisters (Hall et al., 2021). Compacted bentonite clay is the preferred buffer material due to its mechanical support, low permeability, strong ion exchange capabilities, self-sealing capacity, good thermal conductivity, and ideal compaction properties (García-Romero et al., 2019). Extensive geochemical, mineralogical and microbiological based research has been conducted in Spain on the bentonite from El Cortijo de Archidona site (commercialized as FEBEX) for its use in future DGRs (Martinez-Moreno et al., 2023; Povedano-Priego et al., 2021; Huertas et al., 2021; Lopez-Fernandez et al., 2014; Villar et al., 2006).

Understanding the structure and composition of the microbial community in the bentonite buffer is crucial to ensure the DGR safety. Microorganisms could impact the long-term stability of the repository, e.g., by causing microbially influenced corrosion (MIC) of the metal canisters. MIC results from processes such as biofilm formation and the production of corrosive metabolites (e.g., HS^-). This process could induce corrosion in the canisters that would allow bacteria to interact with and mobilize radioactive materials, increasing their migration through DGR

barriers (Meleshyn, 2011). Nonetheless, factors such as dry density of compacted bentonites, and heat from radioactive waste, can limit the bacterial activity.

Once the DGR is sealed, an anoxic environment will prevail due to the consumption of oxygen by microorganism or canister corrosion (Payer et al., 2019; Keech et al., 2014). The DGR microenvironment within the bentonite surrounding the metal canister will differ significantly from the host rock, transitioning from warm, dry, and oxidizing to cool, wet, and anoxic conditions (Hall et al., 2021). This microenvironment will be predominantly shaped by the thermal behavior of the canisters, which is determined by the DGR layout and the decay characteristics of the radionuclide inventory in the used nuclear fuel bundles (King et al., 2017). Under cool, wet and anoxic conditions, certain anaerobic bacteria (e.g., sulfate-reducing, SRB; and iron-reducing bacteria, IRB) can be potentially active. These bacteria could induce MIC, reduce the structural iron in smectite (the main mineral in bentonites), and metabolize sulfate to sulfide (the main corrosion agent of copper). For instance, *Desulfovibrio vulgaris* and *Desulfitobacterium frappieri* cause MIC by reducing the structural Fe(III) in smectite, and generating sulfide, through sulfate reduction (Pentráková et al., 2013; Liu et al., 2012; Shelobolina et al., 2003). The presence of sulfide in the DGR will be primarily due to SRB activity (Bengtsson and Pedersen, 2017). Sulfide can diffuse through the buffer materials, reaching the canister surface and resulting in the corrosion of copper. Another important aspect to consider is the compaction density of the bentonite. While there is no clear dry-compaction density threshold for the presence of SRB, research indicated that their growth and multiplication are more pronounced at lower compaction densities compared to higher densities, surviving in a metabolically inactive or spore-forming state to cope with the harsh environmental conditions (Bengtsson and Pedersen, 2017, 2016). Previous studies have reported that no significant differences at the microbial community level were observed between 1.5 and 1.7 g cm^{-3} of dry density in the Spanish bentonite after two years of anaerobic incubation, while detecting SRB such as *Desulfuromonas*,

Desulfosporosinus, and *Desulfovibrio* (Povedano-Priego et al., 2021). Moreover, Martinez-Moreno et al. (2023) demonstrated the survival of SRB in bentonite with a dry compaction density of 1.7 g cm^{-3} after one year of anoxic incubation at 30 ºC and their potential effect on the corrosion of copper material. Previous studies have investigated the impact of microbial activity on canister materials and the stability of commercial bentonites such as MX-80, Opalinus Clay, and FEBEX (Pedersen, 2010; Smart et al., 2017; Martinez-Moreno et al., 2023; Madina et al., 2005). Temperature is another critical physical parameter to be considered in the DGR safety studies. The temperature evolution on the surface of the canisters will depend on the DGR concept, location, and the materials used as engineered barriers. The Canadian program (based on copper-coated canister) predicts a temperature evolution rising to a maximum peak of around 100 ºC within several decades, followed by a gradual decrease to ambient temperature (King et al., 2017).

Therefore, the present study attempts to explore the impact of high temperature (60 ºC) and bentonite dry-compaction density on the evolution of microbial communities, corrosion of copper surface, and the stability of the bentonite's mineralogy at the copper canister/compacted bentonite interface under anoxic conditions. To approach a more realistic scenario, simulating a post-closure DGR stage, highly compacted bentonite blocks (1.7 g cm^{-3}), with high-purity copper disks in the core, were elaborated. The study examined the one-year anaerobic evolution of microbial communities at 60 ºC, with one set of bentonites supplemented with acetate, lactate, and sulfate as electron donors and acceptor to stimulate indigenous bentonite bacteria (e.g., SRB). State-of-the-art microscopic and spectroscopic techniques were employed to assess the stability of the bentonite and the potential corrosion of copper disks. The survival of SRB was quantified through the most probable number (MPN) method. However, to the best of our knowledge, this is the first study to comprehensively describe the behavior of indigenous bacteria from highly compacted Spanish bentonite on the mineralogical

stability of clay and copper corrosion at high temperatures (60 ºC) simulating the first period in the DGR.

2_ Material and methods

2.1_ Bentonite source and pre-treatment

The bentonite used in this work was collected from El Cortijo de Archidona located in the southeastern region of Spain, specifically in Almeria. Samples were aseptically collected in February 2020, at a maximum depth of ~ 80 cm. Once in the laboratory, bentonite was manually disaggregated and dried in a laminar flow cabinet for at least 5 days at room temperature. Following the removal of excess moisture, the bentonite was meticulously ground using a sterile stainless-steel roller and mortar to achieve a homogeneous powder. Subsequently, it was carefully stored at 4 ºC until it was needed for further analysis.

The samples' treatments were previously described in Martinez-Moreno et al. (2023). Briefly, sterile solutions of sodium acetate (30 mM), sodium lactate (10 mM), and sodium sulfate (20 mM) were sprayed on the bentonite to stimulate the activity of anaerobic bacteria, such as SRB. Control samples were only supplemented with sterile distilled water. The solutions were gradually added until reaching a bentonite with mud-like consistency. Then, they were dried at room temperature and ground under sterile conditions until homogeneous powder was achieved. In addition, another set of bentonite samples underwent a heat-shocking process known as tyndallization (110 ºC for 45 min, 3 consecutive days), hereinafter referred to as "sterilized bentonite", aimed at reducing the presence and activity of indigenous bacteria within the bentonite. The description of the different treatments is summarized in **Table 1**.

2.2_ Assembly of compacted bentonite blocks with copper disks

The bentonite blocks assembly was conducted in the Laboratorio de Mecánica de Suelos (CIEMAT. Madrid, Spain) as explained in detail by Martinez-Moreno et al. (2023). In order to achieve a dry density of 1.7 g cm^{-3}, the quantity of bentonite was determined considering the initial moisture percentage (12%), the volume of the cylindrical steel mold (dimensions of 30.3 x 20.0 mm), and the volume of the copper disks (0.31 cm^3). The initial degree of saturation of the bentonite was approximately 55%, based on the initial moisture content (12%), the dry density (1.7 g cm-3), and the specific gravity of the FEBEX bentonite (2.7 g cm-3). The saturated moisture content was estimated to be around 21%, corresponding to a water activity (aw) of 0.94–0.95 or a Relative Humidity (RH) of 94 – 95% (Fernández, 2004). Then, a pressure of 25-30 MPa was applied with a hydraulic press to achieve the desired compaction.

Table 1.

Sample ID and description of the treatments of the bentonite blocks. All samples were compacted to 1.7 g cm^{-3} dry density containing an oxygen-free high conductivity (OFHC) copper disk (Cu disk) in the core. Bentonite blocks were incubated 1 year at 60 ºC under anaerobic conditions.

Sample ID	Treatment
B.eD_1y	Bentonite amended with acetate, lactate and sulfate (30:10:20 mM)
B_1y	Bentonite amended with distilled water
StB.eD_1y	Sterilized bentonite amended with acetate, lactate and sulfate (30:10:20 mM)
StB_1y	Sterilized bentonite amended with distilled water

Glossary: B: bentonite, StB: sterilized bentonite, eD: treated with electron donors and sulfate.

Oxygen-free high conductivity (OFHC) copper disks were acquired from Goodfellow company (goodfellow.com). The copper grade was C101 (purity: 99.9 – 100%) with dimension of 4.0 ± 10% mm thickness and 10.0 ± 0.5 mm diameter. Cu disks were sterilized by autoclaving for 15 min at 121 ºC and placed in the core of the bentonite blocks. The resulting blocks were placed into an anaerobic jar containing an anaerobiosis generator sachet (AnaeroGen™, Thermo Scientific),

and were incubated at 60 ºC for one year to simulate the early stages within the DGR after its closure.

2.3_ Mineralogical and geochemical analyses of the bentonite

After incubation, the samples were shattered using a sterilized stainless-steel spatula and ground with an aseptic mortar until a homogeneous powder was achieved.

Mineralogical characterization was carried out by XRD analysis through oriented aggregates (OA) technique to examine the behavior of the basal reflections of smectite under different treatments. The sample preparation (a mixture of the three replicates) was performed following the procedure described in Martinez-Moreno et al. (2023). OA samples were analyzed by a powder X-ray diffraction by a PANalytical X'Pert Pro diffractometer equipped with an X'Celerator solid-state linear detector, employing CuKα radiation at 45 kV and 40 mA. Data collection involved a step increment of 0.008º 2Θ and a counting time of 10 s/step. Subsequently, the samples were exposed to ethylene-glycol (EG) vapor at 60 ºC for 24 h, and re-analyzed using the same parameters. The XRD diffractograms were analyzed utilizing the HighScore software.

The elemental composition of the bentonite from the different treatments (a mixture of the three replicates) was assessed through X-ray fluorescence (XRF) analysis using a PANalytical Zeltium instrument. The analysis employed a rhodium anode ceramic X-ray tube equipped with an ultra-thin high transmission beryllium front window.

The pH of the bentonite samples was determined in triplicate following the method described in Povedano-Priego et al. (2019). The bentonite was mixed and homogenized with 0.01 M $CaCl_2$ at a ratio of 1:15.

2.4_ Characterization of bentonite microbial communities

Following a year of anaerobic incubation, the bentonite samples were preserved at -20 ºC for the investigation of the bacterial diversity. Simultaneously, for culture-dependent techniques, separate samples were maintained at 4 ºC. To perform these analyses, the bentonite blocks were first broken into small fragments, and then finely ground into a homogeneous mixture using a sterile mortar.

2.4.1_ Total DNA extraction and 16S rRNA gene sequencing

DNA extractions were conducted, in triplicate for each treatment (B.eD, B, StB.eD, StB) and incubation time (t. 0 and after 1-year incubation at 60 ºC), following the optimized phenol-chloroform-based protocol described by Povedano-Priego et al. (2021), with some modifications. In the first steps, bentonite powder was moistened with sterile milliQ water in a ratio of 1:3 w/v and stored at 4 ºC for at least 3 days. Subsequently, 0.3 g of the bentonite sample was placed into 2 mL screw-cap tubes, along with sterilized glass beads. The total amount of bentonite used per replicate varied depending on the samples, ranging from 3.6 g to 10.8 g, in order to achieve good DNA yields for sequencing purposes. Afterwards, 400 µL of Na_2HPO_4 (0.12 M) was added to each tube and then vortexed at a maximum speed. Subsequently, the chemical lysis was achieved by adding 650 µL lysis buffer, 28 µL lysozyme (10 mg/mL), and 4 µL proteinase K (20 mg/mL). After performing the bead beating at a speed of 5.5 m s^{-1} for 45 s three times, the samples were incubated 45 min at 37 ºC followed by an incubation at 60 ºC for 75 min. Finally, the next steps of the protocol were followed in detail as described in Povedano-Priego et al. (2021). The total DNA obtained was quantified on a Qubit 3.0 Fluorometer (Life Technology, Invitrogen™).

Amplification of the extracted DNA, sequencing, and the bioinformatics analyses were performed at STAB VIDA (Caparica, Portugal, stabvida.com) and are detailed in Martinez-Moreno et al. (2023). For library construction, the primers

pair 341F - 785R were employed, targeting the V3-V4 variable regions of 16S rRNA gene (Thijs et al., 2017). Sequencing was performed on the Illumina MiSeq platform and the resulting raw sequence data were then analysed using QIIME2 v2023.2 (Caporaso et al., 2010). The reads were grouped into operational taxonomic units (OTUs) and taxonomically classified using the scikit-learn classifier with the SILVA database (release 138 QIIME). The raw data were submitted to the sequence read archive (SRA) at the National Center for Biotechnology Information (NCBI) under the BioProject accession number PRJNA1044717.

Explicet 2.10.5 (Robertson et al., 2013) was used to obtain alpha diversity indices and conduct analysis of the relative abundance of the annotated different taxa. To assess the similarity between samples at the genus level, a matrix based on the Bray-Curtis algorithm was generated and then subjected to PCoA (Principal Coordinate Analysis) using the Past4 software (Hammer et al., 2001).

2.4.2_ Determination of the most probable number of sulfate-reducing bacteria

In order to assess the impact of the temperature and the electron donors/acceptor addition on bacteria involved in copper corrosion, the number of culturable SRB was estimated by the most probable number (MPN) enumeration method. This method was performed following the MPN Method of Biotechnology Solutions (Houston, USA, biotechnologysolutions.com), based on serial dilution in triplicate, in Postgate medium (DSMZ_Medium63, https://www.dsmz.de) replacing Na-thioglycolate with Cysteine-HCl (0.5 g L^{-1}). The procedure was conducted under anoxic conditions within an Argon-atmosphere glove box. For each treatment, 10 mL of N_2-degassed phosphate-buffered saline solution (PBS) was mixed with 1 g of anoxically-ground bentonite from the 3 block replicates per treatment. To facilitate the detachment of bacterial cells from the bentonite particles, the mixtures were shaken at 180 rpm for 24 h. Subsequently, 0.5 mL of

the suspension was transferred to 4.5 mL of the modified Postgate medium in N_2-degassed septum bottles until the 10^{-5} dilution. Afterwards, the septum bottles were sealed and incubated at 30 ºC and 60 ºC in static and darkness conditions for 4 weeks. This process was carried out in triplicate for each treatment. The MPN of SRB was estimated by comparing positive bottles (presence of black precipitates) to a reference table (MPN Method, biotechnologysolutions.com), considering the initial pre-dilution for the cell's dispersion (1 g of bentonite in 10 mL of PBS).

2.4.3_ Isolation and molecular identification of thermophilic-aerobic bacteria and anaerobic bacteria

For the aerobic bacterial isolation, 1 g of ground bentonite (a mixture of the three replicates) was added to 10 mL of PBS and shaken to facilitate the cell separation. For thermophilic bacteria, oligotrophic R2A medium (Reasoner and Geldreich, 1985) and 10% Luria-Bertani (LB) medium (Miller, 1972) were used. Subsequently, 100 µL from the mixtures (bentonite + PBS) and from the positive MPN bottles, for the isolation of anaerobic bacteria, were spread on their corresponding agar media, which were sealed with parafilm, and incubated at 60 ºC. The modified-Postgate agar plates were incubated at 30 ºC and 60 ºC under anoxic conditions within an anaerobic jar. Once growth was detected, isolated colonies were regrown until pure cultures were obtained by morphological and microscopic observation of the colonies.

DNA extraction from the pure cultures was performed with 100 µL of PrepMan™ Ultra Sample Preparation Reagent (Thermo Fisher) heating the samples 10 min at 95 ºC. The 16S rRNA gene fragments amplification was performed using the primer pair 341F (5'-TCGTCGGCAGCGTCAGATGTGTATAAGAGACAGCCTACGGGNGGCWGCAG-3') and 785R (5'-GTCTCGTGGGCTCGGAGATGTGTATAAGAGACAGGACTACHVGGGTATCTAATCC-3'). The PCR (Polymerase Chain Reaction) reaction

proceeded as one initial cycle at 94 ºC for 2 minutes, followed by 30 cycles of 94 °C for 30 seconds, 56 °C for 30 seconds, and 72 °C for 2 minutes. Concluding, there was a final extension step at 72 °C for 10 minutes. The PCR products were purified using Wizard® SV Gel and PCR Clean-Up System (Promega). The purified products were sequenced to Sanger Sequencing (Eurofins Genomics, Germany). The resulting sequences were classified with The RDP Classifier and compared with those available in the GenBank by BLAST (Basic Local Alignment Search Tool) analysis. The nucleotide sequences reported here were submitted to the sequence read archive (SRA) at the National Center for Biotechnology Information (NCBI) under the BioProject accession number PRJNA1045398.

2.5_ Assessment of the copper disk surface corrosion

The copper disks were extracted from the bentonite blocks and prepared for VP-FESEM (Variable Pressure-Field Emission Scanning Electron Microscopy) coupled with EDX (Energy-Dispersive X-ray) analysis. The preparation was conducted as described in Martinez-Moreno et al. (2023). Briefly, the disks were immersed in 2.5% glutaraldehyde in 0.1 M PBS buffer (24 h at 4 ºC), washed in the same buffer 3 times (15 min. each), and post-fixed in 1% osmium tetroxide (1 h at room temperature). Lastly, they were subjected to Critical Point Drying technique (Anderson, 1951) employing carbon dioxide in a Leica EM CPD300 instrument followed by carbon coating through evaporation utilizing an EMITECH K975X Carbon Evaporator.

For the spectroscopic analyses of the Cu surface, samples were removed from the bentonite blocks without further preparation or cleaning of the copper surface (unmodified). Reflectance micro-Fourier Transform Infrared Spectroscopy (micro-FTIR) was employed for the detection of organic compounds on the copper disk surfaces, using a PerkinElmer Spotlight micro-FTIR spectroscope equipped with a mercury-cadmium-telluride detector (16 gold-wired infrared detector

elements). Reflectance micro-FTIR images were collected using a per-pixel aperture size of 25 μm x 25 μm, four scans per pixel, and a spectral resolution of 16 cm^{-1}.

Additionally, the surfaces of the unmodified copper disks were chemically analysed by X-ray Photoelectron Spectroscopy (XPS) using a Kratos AXIS Supra Photoelectron Spectrometer. The X-ray source was a monochromated Al Kα (1486.6 eV) operating at an X-ray emission current of 20 mA and an anode high tension (acceleration voltage) of 15 kV. The take-off angle was fixed at 90º relative to the sample plane. Data was gathered from three randomly selected positions, with each acquisition area forming an approximately 110 μm x 110 μm rectangle (FOV2 lens). Analysis comprised a broad survey scan (pass energy of 160 eV, step size of 1.0 eV) and a high-resolution scan (pass energy of 20 eV, step size of 0.1 eV) for component speciation. The integral Kratos charge neutralizer served as an electron source to counteract differential charging. The binding energy scale was calibrated using the Au $4f_{5/2}$ (83.9 eV), Cu $2p_{3/2}$ (932.7 eV) and Ag $3d_{5/2}$ (368.27 eV) lines of cleaned gold, copper and silver standards from the National Physical Laboratory (NPL), UK. CasaXPS 2.3.22 (Fairley, 2019) software was employed to fit the XPS spectra peaks. The effect of surface charging was compensated for all the binding energies by referring to the C 1s adventitious carbon peak at 285 eV. There were no further restrictions applied on the initial binding energy values.

3_ Results and discussion

3.1_ Analyses of the mineralogical and chemical stability of the bentonite

The Spanish bentonite from El Cortijo de Archidona, commercialized as FEBEX clay, has been chosen by ENRESA, the Spanish national radioactive waste company, as the preferred backfilling and sealing material the future DGR in Spain. This clay has been extensively studied under the FEBEX project since the 90s (Huertas et al., 2021). Despite the comprehensive physicochemical

characterization of this bentonite, there is a growing necessity to unravel the ways by which microorganisms could impact the safety of the different DGR barriers.

The pH values and the chemical characterization by XRF are shown in **Supplementary Table S1.** The pH from the different treatments showed no remarkable differences after one year of anoxic incubation at 60 ºC. The chemical characterization showed that the dominant oxides were SiO_2 and Al_2O_3 with no important differences among the treatments. After one year of incubation, slight increases (Δ) were detected in the percentage of Fe, Na, and Al oxides (Δ 1.27%, Δ 1.25%, and Δ 1.04%, respectively) and decreases (negative Δ) in the concentration of Si and Mg oxides (Δ -3.27% and Δ -0.47%, respectively), on average. The chemical composition of the bentonite from this study closely aligns with the BI-2 sampling site in Cortijo de Archidona reported by Lopez-Fernandez et al. (2014).

Although the aim of this study does not delve into an exhaustive examination of the stability of the physico-chemical parameters of bentonite samples, it is important to consider the impact of microorganisms on the safety-relevant characteristics of the clay. Meleshyn (2011) outlined the potential influence of microbial activity on clay properties (e.g., swelling pressure, specific surface area, cation exchange capacity, anion sorption capacity, among others), affecting the stability of bentonite and, in consequence, the DGR safety. Microbial processes that could compromise the integrity of the clay encompassed actions such as the reduction and dissolution of clay minerals, the formation of biofilms, a hydrogen sulfide attack by SRB, and the generation of microbial gases. One concern is the irreversible smectite-to-illite transformation, which impacts the swelling capacity (Kaufhold and Dohrmann, 2010). This transformation is often driven by high temperatures (100 – 200 ºC) and time, but can also occur at lower temperatures (< 50 °C) (Ohazuruike and Lee, 2023). Illitization could be triggered by K^+ (possibly from K-feldspars of the clay) that attach to the smectite interlayer and

bond covalently with oxygen (Kaufhold and Dohrmann, 2010). However, the smectite-to-illite transformation process could be stimulated by microbial activity affecting the geochemical conditions. Certain bacteria, i.e., IRB and SRB could use the structural Fe(III) in smectite as electron acceptor associated with the oxidation of organic matter or H_2, leading to the illite formation (Kim et al., 2019).

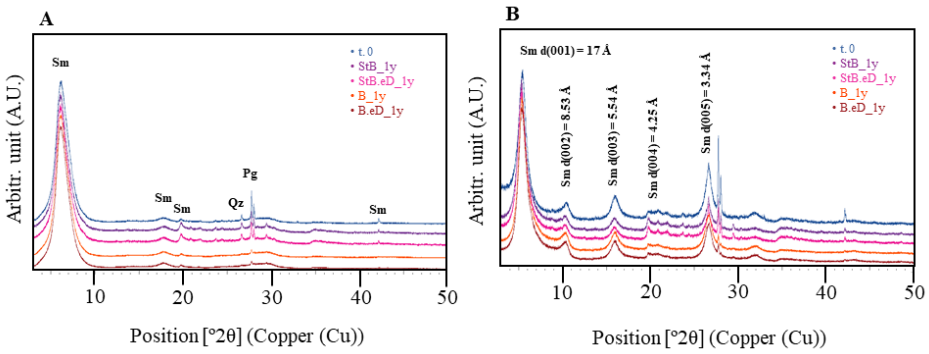

Fig. 1. (A)**:** Oriented aggregates (OA) X-ray diffraction (XRD) patterns of samples at t. 0 and after one year of anaerobic incubation at 60 ºC (1y). (B): OA XRD spectra after 24 h of exposure to ethylene glycol (EG) at 60 ºC. Glossary: B: bentonite, StB: sterilized bentonite, eD: addition of acetate, sulfate, and lactate. Sm: smectite; Qz: quartz; Pg: plagioclase.

In our study, XRD patterns showed that the dominant mineral phase was smectite (montmorillonite), besides minor mineral phases as quartz and plagioclases (**Fig. 1_A**). These results are in agreement with those of previous studies which reported that the mineral composition of this bentonite consists of smectites (montmorillonite) as the dominant mineral phase (~ 84%), followed by plagioclase (albite) and quartz (about 12% and 3%, respectively) (Lopez-Fernandez, 2015; Povedano-Priego et al., 2019). The dioctahedral smectites maintain bentonite ability to expand, as indicated for all samples by the (001) reflection at around 17 Å in the ethylene glycol (EG) pattern (**Fig. 1_B**), confirming the full expansion of interlayer sites without undergoing illitization (Fernández et al., 2022). Indeed, under the essayed conditions (e.g., addition of electron donors/acceptor, tyndallization process, anoxic conditions, incubation at 60 ºC, etc.), no illite was

detected. Moreover, no appreciable differences in the mineralogy were observed between treatments after one year of incubation. Hence, the stability of the smectite remained unaffected by both biotic and abiotic factors at 60 ºC. Although one year might be considered a relatively short time for detecting the conversion from smectite to illite in the samples, it remains essential to investigate its presence in the bentonite samples, particularly when considering longer timeframes.

3.2_ Assessment of the viability and survival of culturable bacteria

The compaction dry density of bentonite inversely correlates with bacterial activity, primarily attributable to the reduced water activity (a_w). Investigations on MX-80 bentonite, compacted at 1.6 g cm^{-3}, indicated that an a_w below 0.96 inhibited bacterial activity, leading to spore formation or bacterial dormancy (Stroes-Gayscone et al., 2010). In our study, the initial dry density of 1.7 g cm^{-3} corresponded to an a_w of 0.94-0.95, slightly below the threshold for suppressing bacterial activity. Therefore, the survival, viability and activity of specific bacterial groups has to be considered. The quantification of SRB within each treatment was determined by the Most Probable Number (MPN) method at 30 ºC (one optimal growth temperature for SRB), and at 60 ºC. Moreover, a molecular-level identification was conducted from the bacterial isolates, focusing on moderate-thermophilic bacteria able to grow at 60 ºC and some anaerobic bacteria involved in the biogeochemical cycle of sulfur and iron.

3.2.1_ Quantification of the most probable number of SRB

All bottles incubated at 60 ºC, including negative controls (uninoculated Postgate media), exhibited the black precipitate that we would count as positive for SRB growth in the MPN enumeration. To check whether the precipitate was due to abiotic factors (e.g., high temperature) or to bacterial growth, selected dilutions from the different treatments were plated on agar-Postgate dishes and incubated anaerobically at 60 ºC. After 4 weeks of anaerobic incubation, no colonies were

detected. Therefore, it was assumed that the presence of black precipitates in the bottles was mediated by unknown abiotic factors (e.g., reaction of some of the components of the medium to the high temperature of 60 ºC).

However, the MPN enumeration showcased the viability and survival of culturable SRB across all treatments at 30 ºC (**Table 2**). The values ranged between 9.5 x 10^1 and 2.5 x 10^3 MPN g^{-1} of bentonite (samples StB_1y and B.eD_1y, respectively). The growth detection of this group of bacteria showed their ability to survive despite the harsh incubation conditions within the bentonite blocks after one-year incubation (e.g., high dry-density compaction and temperature). Moreover, it was evidenced that SRB are even able to withstand the heat shock produced by the tyndallization process as shown in the StB_1y (9.5 x 10^1 MPN g^{-1} bentonite) and StB.eD_1y (1.5 x 10^2 MPN g^{-1} bentonite).

Table 2.

Most probable number (MPN) of SRB per gram of bentonite (MPN g^{-1}). The values were obtained taking into account the initial pre-dilution for the cell's dispersion (1 g of bentonite in 10 mL of PBS). Glossary: t. 0: initial bentonite sample; B: bentonite; StB: sterilized bentonite; eD: addition of acetate, lactate, and sulfate; _1y: after one year of anaerobic incubation at 60 ºC.

Sample	XYZ pattern*	MPN reading**	3PB dilution***	MPN mL-1	MPN g-1 bentonite
t. 0	330	25.0	10^0	25.0 x 10^0	2.5 x 10^2
B_1y	210	1.5	10^{-2}	1.5 x 10^2	1.5 x 10^3
B.eD_1y	330	25.0	10^{-1}	25.0 x 10^1	2.5 x 10^3
StB_1y	320	9.5	10^0	9.5 x 10^0	9.5 x 10^1
StB.eD_1y	210	1.5	10^{-1}	1.5 x 10^1	1.5 x 10^2

*XYZ pattern: number of positive bottles after 3PB dilution

**MPN reading: MNP value from the reference table

***3PB dilution: dilution with 3 positive bottles prior to XYZ pattern

Following one-year incubation, the bentonite samples that were sterilized (StB_1y and StB.eD_1y) showed a decrease in the number of SRB compared to the preincubation bentonite (t. 0), while the unsterilized samples (B_1y and B.eD_1y)

increased in SRB number (**Table 2**). Moreover, samples amended with electron donors/acceptor (B.eD_1y and StB.eD_1y) exhibited a slight increase compared to unamended samples (B_1y and StB_1y). Hence, it can be assumed that the tyndallization process had a slight long-term negative impact on the number of SRB, while the addition of acetate, lactate, and sulfate had a positive effect. Martinez-Moreno et al. (2023) demonstrated that the addition of electron donors/acceptor before (t. 0) and after one-year anaerobic incubation at 30 ºC stimulated the number of SRB in highly compacted bentonite blocks. Additionally, in our study, a lower number of SRB was observed in the sterile samples (StB_1y and StB.eD_1y) after the incubation at 60 ºC compared to those incubated at 30 ºC. Moreover, the bentonite compaction at high density (1.7 g cm^{-3}) and the absence of a renewal water flow and/or organic compounds are adverse conditions making the bentonite blocks a hostile environment for the bacterial growth and viability over time. Previous studies have demonstrated that the increase in the density of the bentonite compaction has a negative effect on the viability of bacteria (e.g., SRB) (Bengtsson & Pedersen, 2017; Stroes-Gascoyne et al., 2006). Some SRB such as *Desulfosporosinus* and *Desulfotomaculum* could cope with harsh environments by spore formation, or by entering in a dormant state (desiccated cells) in dry bentonite (Grigoryan et al., 2018; Masurat et al., 2010). Groundwater infiltration into the repository could rewet and enrich the bentonite with organic matter, creating a less harsh environment for SRB. Consequently, it is important to know the ability of this group of bacteria to become active after periods of harshness within the DGR environment. Some studies have also observed the ability of SRB to withstand high temperatures (75 – 120 ºC) and recover their cell viability after being enriched (Martinez-Moreno et al., 2023; Masurat et al., 2010). However, it should be noted that the MPN method provides approximate information about the number of SRB per gram of bentonite. Nonetheless, it is important to isolate and identify molecularly the bacteria of

interest to further explore how incubation conditions affect their viability and potential long-term influence on DGR safety.

3.2.2_ Isolation and molecular identification of moderate-thermophilic aerobic and anaerobic bacteria

Modified-Postgate agar medium was employed to isolate anaerobic bacteria from the positive bottles of the MPN experiment at 30 ºC and 60 ºC. In addition, oligotrophic culture medium R2A and 10% LB were used to isolate microbial strains capable of withstanding and growing at 60 ºC. No colonies were detected in agar-Postgate and R2A media incubated at 60 ºC. As previously mentioned, the absence of colony formation on agar-Postgate incubated at 60 °C from the MPN bottles confirmed that this bacterial group was unable to exhibit activity at 60 ºC. However, 9 pure cultures of anaerobic bacteria on modified Postgate were isolated at 30°C. In addition, 13 pure cultures of aerobic bacteria were isolated on 10% LB medium at 60 ºC.

Table 3.

Affiliation of the 16S rRNA gene sequences of the isolates. RDP Classifier shows taxa (G: genera / O: order) and ID with a 100 % of confidence threshold (C.T.) based on a naive Bayesian classifier providing an accurate taxonomic placement of rRNA gene sequences. BLAST shows the closet phylogenetic relative strain, their percentage of identity and the accession number.

			RDP Classifier	BLAST		
Isolate	Medium	Incubation	Taxa 100% C.T.	Closet Phyl. Relative	Ident. (%)	Accession no.
B.eD_8	LB	Aerob. / 60 ºC	G_ *Aeribacillus*	*A. composti* N.8	99.92	NR_159152.1
B.eD_1	LB	Aerob. / 60 ºC	G_ *Staphylococcus*	*S. epidermidis* Fussel	99.91	NR_036904.1
Pg_1	Postgate	Anaerob. / 30 ºC	G_ *Pseudomonas*	*P. lurida* P513/18	99.71	NR_042199.1
Pg_2	Postgate	Anaerob. / 30 ºC	O_ Clostridiales	*C. thermarum* GA15002	98.13	NR_178823.1
Pg_3	Postgate	Anaerob. / 30 ºC	G_ *Anaerosolibacter*	*A. carboniphilus* IRF19	99.72	NR_178620.1
Pg_5	Postgate	Anaerob. / 30 ºC	G_ *Sporacetigenium*	*S. mesophilum* ZLJ115	99.50	NR_043101.1
Pg_6	Postgate	Anaerob. / 30 ºC	G_ *Pelosinus*	*P. fermentans* DSM 17108 R7	98.95	NR_043577.1

Four out of the 9 anaerobic bacterial colonies belonged to the genus *Anaerosolibacter* followed by *Pseudomonas, Sporacetigenium, Pelosinus,* and the

order Clostridiales (**Table 3**). Among the 13 aerobic bacterial isolates, 10 strains belonged to the genus *Aeribacillus* (99.92% identity related to *A. composti* N.8) and 3 belonged to the genus *Staphylococcus* (99.91% identity related to *S. epidermidis* Fussel) (**Table 3**).

Regarding the strains isolated from the modified-Postgate medium, the closest phylogenetic relative for *Pseudomonas* was *P. lurida* EOO26. It was reported that this strain exhibited high metal tolerance, including Cu, and was associated to the anaerobic biocorrosion of steel-based metal canisters related to the DGR (Kumar et al., 2021; Jia et al., 2017). The strain Pg_2 belonged to the order Clostridiales, which encompass only strict anaerobic bacteria. The closest phylogenetic relative of this strain was the spore-forming *Clostridium thermarum* isolated from hot spring of Yunnan (China) presenting a temperature growth range of 28 – 50 ºC (Liu et al., 2020). Another isolated strain was Pg_3, which was closely related to *Anaerosolibacter carboniphilus*, a strictly anaerobic, sulfate and iron-reducing bacterium that grows in a temperature range of 20 – 45 ºC, and was previously isolated from coal contaminated soil of Republic of Korea (Hong et al., 2015). Regarding S*poracetigenium*, although this bacterium has no sulfate-reducing capacity, it is also spore-forming and an obligate anaerobic bacterium with a growth range between 20 and 42 ºC (Chen et al., 2006). Moreover, *S. mesophilum* is able to produce acetate, ethanol, hydrogen and carbon dioxide from glucose as major fermentation products that may be available for other microorganisms in the bacterial community of the bentonite. Finally, the closest phylogenetic strain for Pg_6 was *Pelosinus fermentans*. This is a spore-forming iron-reducing bacterium, able to use acetate and lactate as carbon sources and grow between 4 – 36 ºC (Shelobolina et al., 2007). Some of the strains isolated in this study using the agar modified-Postgate medium for SRB do not exhibit the ability to reduce sulfate based on the cited literature for each genus (Kumar et al., 2021; Jia et al., 2017; Liu et al., 2020; Chen et al., 2006; Chen et al., 2006). The growth ability of these

strains in the agar modified-Postgate may be associated with the capability of use some reagent from the medium but without using the sulfate as electron acceptor.

Aeribacillus composti is an obligate aerobic, spore-forming bacterium isolated from olive mill pomace compost that grows in a temperature range between 50 - 65 ºC (Finore et al., 2017). Moreover, *Staphylococcus epidermidis* is a commensal bacterium of human skin that may be an opportunistic microorganism. Strains belonging to this facultative anaerobe have been isolated in hostile environments such as hot springs in Taporan area (India), showing growth capacity at temperatures between 20 ºC – 70 ºC (Pandey et al., 2015). The presence of *Staphylococcus* in the bentonite samples could be related to anthropogenic activities in the El Cortijo de Archidona's sampling site. The presence and survival of these aerobic bacteria could be related to the presence of oxygen molecules trapped in the bentonite before or during the compaction process (Burzan et al., 2022; Stroes-Gayscone et al., 2010).

These findings clearly demonstrated that the isolated strains exhibited the capability to tolerate elevated temperatures (moderate-thermophilic bacteria), as well as specific metals such as copper. They are also actively participating in processes related to acetate and lactate consumption/production. Moreover, their capacity to be involved in iron and sulfate reduction was of particular significance. The isolation and taxonomic identification of bacteria form the studied samples are crucial for determining their potential impact on the materials' alteration within the DGR, especially their role in influencing the corrosion of future metal canisters.

3.3_ Microbial diversity responses to incubation conditions

Samples before (t. 0) and after one year of anaerobic incubation at 60 ºC were subjected to DNA extraction in triplicate. Despite multiple attempts, none of the three replicates of unamended samples (electron donors/acceptor free samples)

incubated at 60 ºC for one year under anaerobic conditions (B_1y and StB_1y) yielded enough DNA of satisfactory quality for sequencing. The use of highly compacted bentonite blocks (1.7 g cm^3 dry density), along with its low permeability, high swelling capacity, and incubation conditions (anaerobiosis and high temperature), created a harsh environment for the presence and survival of indigenous bacteria (Martinez-Moreno et al., 2023). These extreme conditions could affect and decrease drastically the yield of the DNA extracted due to the possible low number of bacterial cells in the samples (Povedano-Priego et al., 2021). As previously mentioned, electron donors and sulfate were added to stimulate indigenous bacteria (Matschiavelli et al., 2019, Grigoryan et al., 2018), thereby enhancing DNA extraction post-incubation. Accordingly, this section will focus on analyzing the impact of temperature (60 ºC), compaction density (1.7 g cm^{-3}), and sterilization (tyndallization) on the microbial community within the amended compacted bentonite under anoxic conditions after one year incubation (B.eD, StB.eD, B.eD_1y, StB.eD_1y).

For these samples, enough sequencing depth was achieved as shown by the rarefaction curves (**Supplementary Fig. S1**). The sequence reads ranged from 2,868 to 431,964. Some replicates were not included in this study because of a failure in the library preparation or sequencing step (B.eD_1y_R3, StB.eD_R3, and StB.eD_1y_R1). Alpha-diversity indices of the treatments are shown in **Table 4** (**Supplementary Table S2** for individual samples). After one-year incubation, a drastic decrease in the Richness values (Sobs and Chao1) of both bentonite (B.eD_1y) and sterile bentonite (StB.eD_1y) samples was evidenced. Furthermore, it was notable that this reduction in richness was more pronounced in the sterilized bentonite sample (StB.eD_1y). The diversity indices (ShannonH and SimpsonD) followed the same pattern. Pre-incubation samples (B.eD and StB.eD) indicated high diversity (> 3 and close to 1, respectively), while after-incubation samples (B.eD_1y and StB.eD_1y) showed low values (< 3 and far from 1, respectively) indicating taxa dominance.

Table 4.
Richness (Sobs/Chao1), diversity (ShannonH. and SimpsonD), and evenness (ShannonE) indices. Glossary: B: bentonite; StB: sterilized bentonite; eD: addition of acetate, lactate, and sulfate; 1y: after one year of anaerobic incubation at 60 ºC.

	Sobs/Chao1	ShannonH	SimpsonD	ShannonE
B.eD	523	5.04	0.89	0.56
B.eD_1y	198	1.41	0.27	0.17
StB.eD	582	6.60	0.97	0.72
StB.eD_1y	126	2.12	0.47	0.30

As a result of amplifying V3-V4 variable regions of 16S rRNA gene, a total of 779 OTUs were identified (**Supplementary Data S1**) and classified into 32 different phyla (**Supplementary Table S3**). Among these, 2 phyla were attributed to the Archaea domain (representing 0.01% of the total relative abundance), while the remaining 30 were associated to 29 Bacteria domain (99.99% of the total) and 1 OTU was unassigned. The most dominant phyla were Actinobacteriota (47.52%) and Proteobacteria (37.62%), followed by Chloroflexi (5.19%), Firmicutes (3.68%), Gemmatimonadota (1.38%), and Acidobacteriota (1.26%).

Principal coordinate analysis (PCoA) at genus level, using Bray-Curtis distance, revealed the dissimilarity of microbial communities between different treatments (**Fig. 2**). A distinct separation was evidenced between the samples after (B.eD_1y and StB.eD_1y) and before (B.eD and StB.eD) incubation. Moreover, the samples prior to incubation showed a division into two different clusters: bentonite (B.eD) and sterile bentonite (StB.eD). Moreover, no dissimilarities were found between the samples after the incubation, irrespective of whether the bentonite was sterilized or not (B.eD_1y and StB.eD_1y). PCoA suggested that the bentonite tyndallization affected the microbial diversity before incubation. However, this conditioning factor is not observed after one year of anaerobic incubation at 60 ºC.

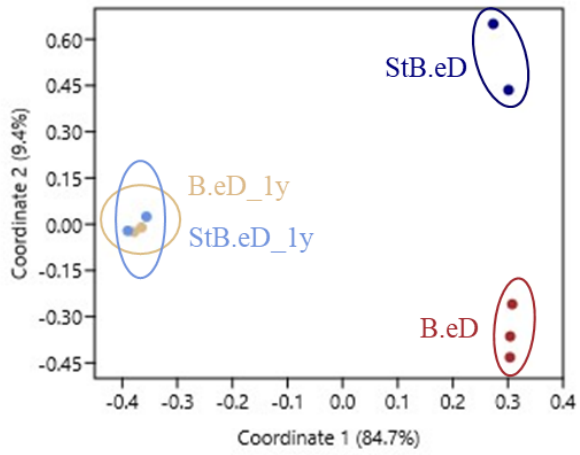

Fig. 2. PCoA (Principal Coordinate Analysis) plot revealing the dissimilarity of microbial genera communities of the bentonite samples in duplicates (triplicates in B.eD). Distance based on Bray-Curtis. Glossary: B: bentonite, StB: sterilized bentonite, eD: addition of acetate, sulfate, and lactate; 1y: after one year of anaerobic incubation at 60 ºC.

In general, the most representative OTUs were *Pseudomonas*, *Nocardioides*, and unclassified Micrococcaceae (23.00%, 14.67%, and 8.40%, respectively), followed by Chloroflexi Gitt-GS-136, *Promicromospora*, *Marmoricola*, and unclassified Nocardioidaceae (3.22%, 2.39%, 2.13%, and 2.12%, respectively) (**Fig. 3**, **Supplementary Data S1**). In the pre-incubation samples (B.eD and StB.eD), the prevailing OTUs were *Nocardioides* (27.23% and 11.92%), unclassified *Micrococcaceae* (15.04% and 6.23%), and Chloroflexi Gitt-GS-136 (2.74% and 6.42%), which exhibited a substantial reduction in their relative abundance after the incubation, even disappearing (0.03% and 0.00%; 1.78% and 0.70%; 0.08% and 0.00%; respectively) (**Fig. 3** and **Supplementary Data S1**). However, in the post-incubation samples (B.eD_1y and StB.eD_1y), the taxa dominance observed in the alpha-diversity values (**Table 4**) corresponded to an evident increase (Δ) in the relative abundance of the genus *Pseudomonas* with respect to the pre-incubation samples (Δ 84.92% in B.eD_1y, and Δ 72.23% in StB.eD_1y).

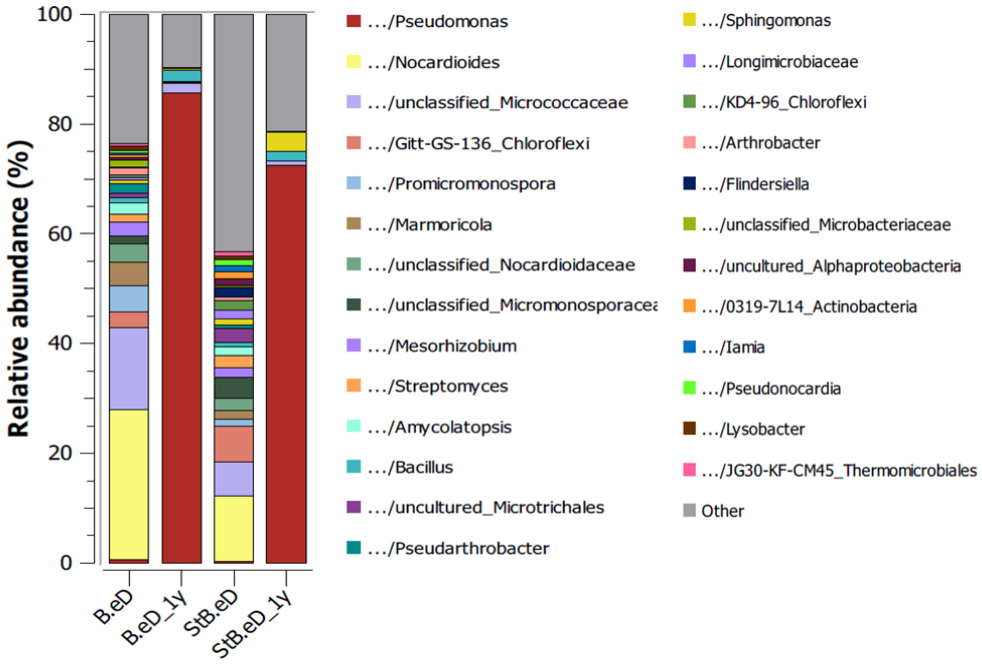

Fig. 3. OTU relative abundance (%) of the bacterial and archaeal communities of the bentonite samples in duplicates (triplicate in B.eD). Bar plot representing a cut off ≥ 0.50%. Glossary: B: bentonite, StB: sterilized bentonite, eD: addition of acetate, sulfate, and lactate; 1y: after one year of anaerobic incubation at 60 ºC.

Previous research conducted at 30 ºC, demonstrated that microbial communities exhibited only slight changes after one year of anaerobic incubation (Martinez-Moreno et al., 2023). In contrast, the present study revealed that the incubation temperature of 60 ºC seems to be a clear limiting factor, reducing the microbial diversity of the bentonite and resulting in the predominance of the genus *Pseudomonas* in the samples. This is a facultative anaerobe bacterium that may use acetate and lactate as electron donor under anaerobic conditions (Chen et al., 2020; Essén et al., 2007; Eschbach et al., 2004). The experimental conditions of this study, i.e., high compaction and dry density, anaerobic conditions, and 60 ºC incubation temperature, greatly restrict the potential presence and activity of bacteria. In situations of limited energy and physicochemical stress, microorganisms might significantly reduce their size and morphological

characteristics to enhance their survival. Species of the genus *Pseudomonas* such as *P. syringae* have been demonstrated to decrease their size under harsh conditions (Monier and Lindow, 2003). Furthermore, previous research reported on the capacity of *Pseudomonas* spp. to be involved in the corrosion of carbon steel and copper materials within the context of DGR, through the reduction of iron and nitrates, respectively (Shrestha et al., 2022; Jia et al., 2017; Dou et al., 2022).

Next to *Pseudomonas* (85.62% and 72.55%), the dominant taxa in the post-incubation samples (B.eD_1y and StB.eD_1y), were *Bacillus* (2.01% and 1.74%, respectively), unclassified Micrococcaceae (1.78% and 0.70%, respectively), *Anaerosolibacter* (1.06% and 1.50%), and *Sphingomonas* (0.21% and 3.55%). The genus *Bacillus* encompasses a broad number of species known for their remarkable resistance and adaptability to a wide range of extreme environmental conditions (e.g., formation of endospores, metabolic versatility or cellular protection strategies). Hence, the occurrence in the post-incubation samples could be attributed to the aforementioned mechanisms. Moreover, *Anaerosolibacter* is an obligate anaerobe, mesophilic bacterium, able to use Fe(III), elemental sulfur, thiosulfate and sulfate as electron acceptors and demonstrated the capability to tolerate temperatures reaching up to 45 ºC (Hong et al., 2015). Regarding *Sphingomonas*, this genus can assimilate lactate and acetate (Vaïtilingom et al., 2010). Interestingly, certain strains within *Sphingomonas* have been found to play a role in the sulfur biogeochemical cycle through a process known as bio-desulfurization, which involves the removal of sulfur from various materials. They were also reported to be implicated in the MIC of copper cold-water pipes (Cui et al., 2016, White et al., 1996).

In this study, SRB were detected in the samples B.eD, B.eD_1y, and StB.eD, represented by the phylum Desulfobacterota with low relative abundances (0.01%, 0.02%, and 0.03% in total, respectively) (**Supplementary Table S3**). Moreover, genera such as *Desulfosporosinus*, *Desulfotomaculum*, *Pelosinus*, and

Sporacetigenium were detected in a very low relative abundance in samples B.eD_1y, StB.eD and StB.eD_1y (≤ 0.03%), being *Anaerosolibacter* more represented in sample B.eD_1y and StB.eD_1y (1.06% and 1.50%, respectively) (**Supplementary Data S1**). Despite the limited occurrence of this bacterial group in the samples, delving into their study remains crucial due to their important role in the long-term anaerobic corrosion of copper canisters within the DGR context (Bengtsson and Pedersen, 2017).

3.4_ Surface characterization of copper disks

The main corrosive agent of copper under DGR relevant conditions will be biogenic hydrogen sulfide generated by SRB (Bengtsson and Pedersen, 2017). Under anaerobic conditions, these bacteria have the ability to oxidize lactate (as an electron donor) while simultaneously reducing sulfate as terminal electron acceptor (Thauer et al., 2007). This process yields HS^- as a metabolic product, which may subsequently combine with H^+ to generate H_2S. The H_2S released by SRB can dissociate into H^+ and HS^-. The latter can migrate to the surface of the copper and react with the metal, resulting in the formation of Cu_2S (Dou et al., 2020). Chen et al. (2014) demonstrated that in anaerobic environments, SRB possess the capability to attach to copper surfaces, forming a biofilm, and generating Cu_2S as the main corrosion product. The generation of extracellular polymeric substances (EPS) from the SRB biofilm, and subsequently from the Cu_2S film, serves to diminish copper's toxicity for SRB.

In our study, VP-FESEM analyses were conducted on Cu disks taken from the blocks from each treatment after one-year incubation. **Fig. 4** shows a composition of five adjacent areas of approximately 560 x 430 µm each selected from the edge to the center of the disk. The resulting five-images composition from Cu blank (copper disk before experimental setup), previously characterized in Martinez-Moreno et al. (2023), B.eD_1y, and B_1y samples revealed the surface distribution

of Cu, Fe, Ti, S, Si, Al, O, and C, and the general EDX and quantification of these elements in the study area as a sum of the EDX spectra in more than 10 selected points in each disk. Microscopy images from the sterilized bentonite treatments are not shown since no alterations or differences were observed with respect to the samples in **Fig. 4**.

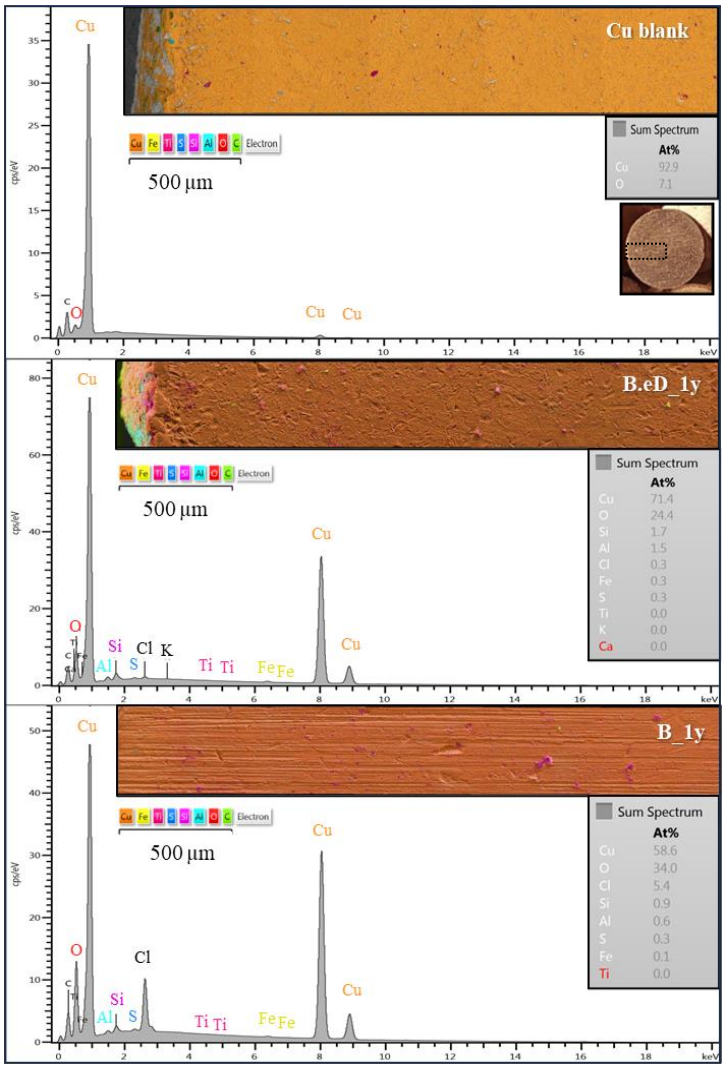

Fig. 4. Sum EXD spectrum associated with elemental quantification of VP-FESEM five-micrographs composition from a selected area (edge to center) of Cu disks blank, and from samples B.eD_1y and B_1y.

The metal surfaces seemed to be nearly unaltered. However, certain irregularities on the surface were detected, potentially resulting from the pressure applied by fractions of the bentonite during the compaction process of the blocks' assembly. Residual bentonite presented on the copper surface was observed, shown as pink and yellow areas in **Fig. 4**, and corresponding to the presence of Si, Fe, Ti, and Al in the EDX spectrum. According to the sum spectrum in **Fig. 4**, the presence of S was very low in the studied areas in both B.eD_1y and B_1y samples. No copper sulfide (Cu_xS) precipitates were observed.

Complementarily, to assess and compare the surface compositions of each copper disks, XPS was employed. Wide scans revealed the presence of Cu, C, O, Si, Na, Fe, Mg and Al on the surface of the samples. Excluding Cu, these elements were likely due to bentonite adhered to the surface of the disks. High resolution scans for the Cu 2p region displayed elemental copper peaks on all samples and also revealed the probable existence of CuO. **Fig. 5** shows the high resolution scans for the Cu 2p region on samples B_1y and B.eD_1y. Two sharp peaks, corresponding to Cu $2p_{3/2}$ and Cu $2p_{1/2}$, were seen at 934.21 eV and 954.17 eV, respectively. These peaks are in accordance with previously reported data attributed to elemental copper (Wagner et al., 1979) and were evident on every sample. The high-resolution scan of this region also unveiled the presence of CuO on the surface of all samples (**Fig. 5**). The peaks observed at 943.49 eV and 962.89 eV, and the distance between Cu $2p_{1/2}$ and Cu $2p_{3/2}$ peaks (of 19.96 eV), presented clear evidence for the presence of CuO (Wagner et al., 1979). High resolution spectra of the Cu 2p region of untreated copper disks (blanks) did not show the presence of CuO (**Supplementary Fig. S2**). The presence of oxygen on the surface of the samples may be due to the high affinity of the copper for oxygen molecules. Some oxygen particles can remain trapped in the bentonite (Burzan et al., 2022) and could participate in the oxidation of copper.

As mentioned before, anaerobic MIC on copper surfaces should also reveal the presence of Cu_xS. Previous studies have shown that peaks for CuS are observed at approximately 932.2 eV in the high-resolution Cu 2p scans (Krylova and Andrulevičius, 2009). However, if this was present, it would have been overshadowed by the Cu $2p_{3/2}$ peak and therefore any presence of CuS could not be confirmed from the Cu 2p high resolution spectra. Therefore, in order to investigate further, high resolution scans on the S 2p region between 143-180 eV were conducted.

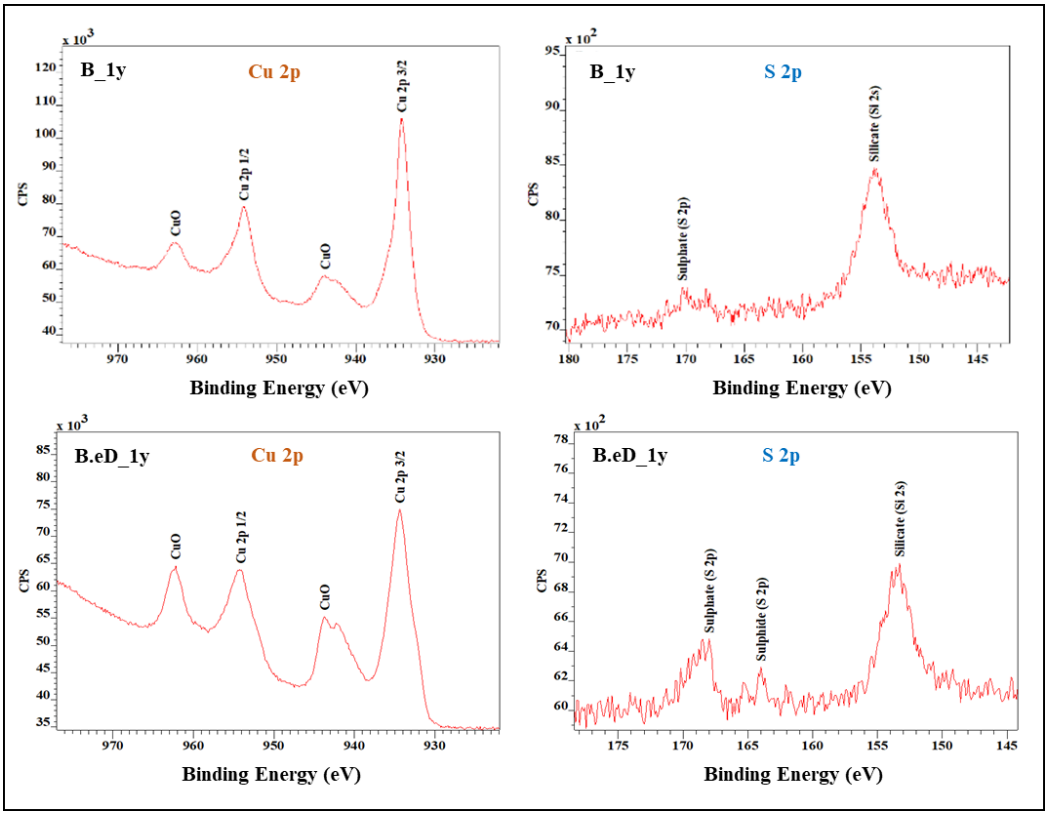

Fig. 5. High resolution XPS spectra of: Cu 2p (region between 922-977eV), left, and S 2p (region between 143-180eV), right, for samples B_1y (top) and BeD_1y (bottom).

The XPS spectra in the S 2p region between 143-180eV (**Fig. 5**) revealed a peak around 155.3eV corresponding to Si 2s on all samples, due to bentonite adhered on the scanned area of the sample (Clarke and Rizkalla, 1976). In conjunction with

the Si 2s peak, samples from different treatments showed the presence of sulfur on the surface in at least two different moieties: sulfate and sulfide. Sulfate was detected on all samples (**Fig. 5** and **Supplementary Fig. S3**) with peaks at roughly 169 eV (Fantuzzi et al., 2015). However, sulfide was only detected on samples B.eD_1y and StB.eD_1y (**Fig. 5** and **Supplementary Fig. S3**) with a very small peak around 163.5 eV. This binding energy has been previously observed for metal sulfides and disulfides, with reported values between 162.9-164.5 eV, respectively (Hussain et al., 2018). According to the literature, the binding energies reported for CuS and Cu_2S peaks are around 162.2 eV (Krylova and Andrulevičius, 2009; Scheer and Lewerenz, 1994), however, these signals were less evident from the acquired spectra.

Reflectance micro-FTIR spectroscopic analysis was employed to investigate the possible existence of microbial biofilm on the sample surfaces. The results obtained for samples B.eD_1y and B_1y are shown in **Fig. 6**. An optical microscope was used to inspect sections of the discs, whilst the infrared microscope was employed for scanning. False-color images were produced to reveal the location of IR-active functional groups. The absorbance scale on the left indicates the abundance of molecules absorbing the infrared radiation on a specific area, with regions with a greater concentration of organic or IR-active compounds depicted in red, and regions with low absorbance areas depicted in dark blue, indicating the absence of IR-absorbing functional groups. The regions lacking IR-absorbing molecules exhibited a generally flat spectrum, often corresponding with exposed copper areas observed on the discs (**Fig. 6**).

The presence of proteins, lipids, and polysaccharides bands in a spectrum can normally be correlated to the presence of microbial macromolecules on the surface of the samples, within the detection limits of this technique. Remains of bentonite adhered to the disks surface were also identified on the samples. The spectra obtained from these areas displayed the characteristic spectral features of Si-O, Si-

O-Si, Al-OH, and other inorganic compounds commonly associated with bentonite (blue spectra, **Fig. 6**). Bands for Al-OH bending vibrations are located at around 850 cm^{-1} (Bishop et al., 2002). Si-O and Si-O-Si stretching vibrations demonstrate bands at 1,110 cm^{-1} and 980 cm^{-1}, respectively (Gaggiano et al., 2013). Bands associated with proteins, lipids, and polysaccharides were identified on samples B_1y and B.eD_1y, supporting the existence of organic substances typically linked with microbial cells or their metabolites (**Fig. 6**). The signals at approximately 1,640 cm^{-1} and 1,540 cm^{-1} were attributed to the amide I and II bands, respectively. Stretching of the carbon-oxygen double bonds (νC—O) was the primary contributor to the amide I band whereas a combination of bending N-H bonds (δN-H) and stretching C-N (νC-N) groups within amides were responsible for the amide II band. These spectral bands have been extensively reported in the literature for

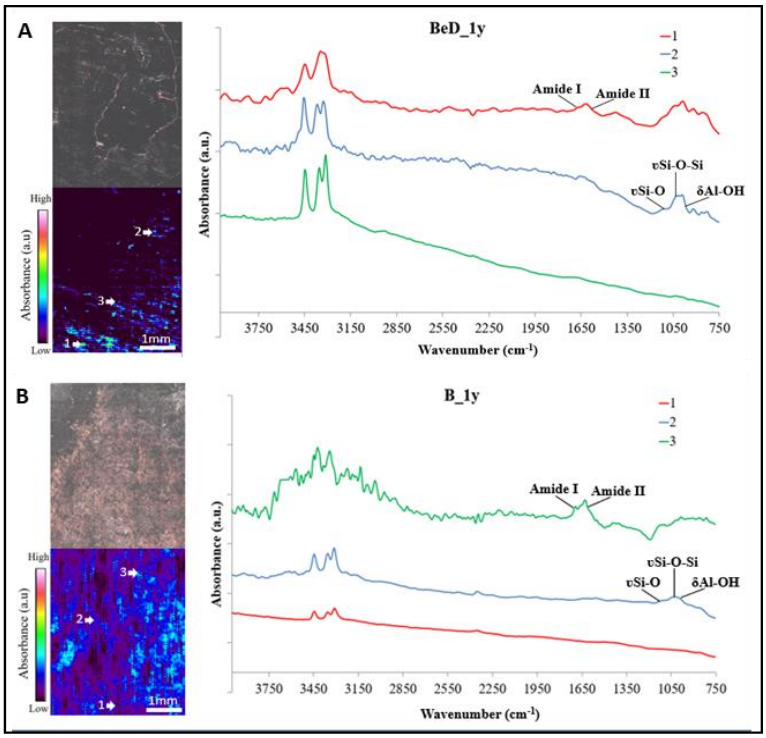

Fig. 6. Reflectance micro-FTIR spectroscopy from B.eD_1y (A) and B_1y (B) samples. Top left: optical image of the scanned region. Bottom left: false-color image of the sample scanned using reflectance micro-FTIR spectroscopy. Right: infrared spectra of 3 different regions on the sample.

samples associated with bacteria (Jiang et al., 2004; Nauman et al., 1991; Ojeda and Dittrich, 2012; Orsini et al., 2000).

The detection of sulfur on the surface of copper disks could be related to bacterial activity (Pedersen, 2010). Martinez-Moreno et al. (2023) observed small sized precipitates of Cu_xS on the surface of copper disks incubated at 30ºC. In contrast, no precipitates were observed by microscopy in this study after one year of incubation at 60 ºC. However, the sulfur was detected in the form of sulfate and sulfide. The presence of sulfate in the sample B.eD_1y could be related to the addition of this electron aceptor during the pretreatment of the bentonite, which was in direct contact with the copper disk during the incubation time. While SRB growth was not observed at 60 ºC in the modified-Postgate medium, it is possible that some bacteria within this group could exhibit activity at this temperature.

A deep characterization of the copper surface was performed in this study. The microorganism's infrared spectra were frequently found in close proximity to the bentonite, implying a potential association between these microorganisms and the bentonite rather than direct contact with the copper surface. The identification of sulfide further suggests the possibility of SRB activity, which could potentially influence the condition of the copper surface. However, it is essential to conduct additional investigations to substantiate this hypothesis since no precipitates related to the formation of Cu_xS were observed by microscopy.

4_ Conclusions

The current study investigated the effect of physicochemical factors, including high temperature (60ºC), high dry-compaction density of bentonite, the addition of electron donors/acceptor, the pre-sterilization of bentonite, and anoxic conditions after one year, on the microbiology of highly compacted bentonite. It further explores the resulting impacts of the microbial communities on the mineralogical stability of the bentonite and the corrosion of copper materials related to the

engineering barriers of future DGR of nuclear waste. The results show that no illitization of smectite was observed under different conditions, indicating the mineralogical stability of the bentonite and its key role as effective barrier for future DGR. Our study demonstrated that the applied tyndallization procedure to sterilize the bentonite was not sufficient to eradicate SRB as viable species since showed growth after one year in amended and unamended samples with electron donors and acceptor. During the tyndallization, the temperature does not exceed 110 ºC to prevent any alteration of the bentonite properties. This temperature could be not enough to destroy all the bacteria. Other hypothesis could be the effect of bentonite, which could protect some bacteria from the tyndallization heat-shock due to its role as buffer, but this needs more research. Moreover, in the non-sterilized samples, the addition of electron donors/acceptor was beneficial for the viability of SRB. Interestingly, we were able to isolate species with the ability to grow at 60 °C but only under aerobic conditions. For the anaerobic species, the conditions needed to be lowered to 30 °C to observe growth. Therefore, although they remain viable, these species are probably not highly active at 60 °C. This was further confirmed by the presence of sulfide, which indicated sulfate reduction, but not in sufficient amounts to observe visual changes on the surface of copper disks. Furthermore, the isolated strains were also observed in the sequencing results, which showed a decreased bacterial diversity after one year of anaerobic incubation with *Pseudomonas* becoming the dominant genus and, to a lesser extent, some bacterial groups adapted to extreme conditions.

These findings provide new perspectives on understanding the biogeochemical processes at the interface bentonite/Cu canister after repository closure. Specifically, this study provides new insights about how the gradual increase of temperature, due to the heat produced by the decay process of the waste, within the DGR could impact the microbial communities and, subsequently, affects the stability of the bentonite and the copper-based metal canisters.

Funding

The present work was supported by the grant RTI2018–101548-B-I00 "ERDF A way of making Europe" to MLM from the "Ministerio de Ciencia, Innovación y Universidades" (Spanish Government). The project leading to this application has received funding from the European Union's Horizon 2020 research and innovation programme under grant agreement No 847593 to MLM. ADM acknowledges funding from the UK Engineering and Physical Sciences Research Council (EPSRC) DTP scholarship (project reference: 2748843). MFM-M acknowledges the Federation of European Microbiological Societies (FEMS) for the award of a Research and Training Grant (FEMS-GO-2021-077) at the SCK CEN (Belgium).

Acknowledgements

The authors acknowledge the assistance of Dr. F. Javier Huertas (IACT, Spain) for his guidance and help in collecting the bentonite from the El Cortijo de Archidona site (Almería, Spain). Dr. María Victoria-Villar group (CIEMAT, Spain) for the facilities and help during the setup of the compacted bentonite samples. Prof. Antonio Sánchez-Navas (Department of Mineralogy and Petrology, University of Garanada, Spain) for his help and training on the DRX equipment. Daniel García Muñoz Bautista Cerro and Dr. Isabel Guerra-Tschuschke (Centro de Instrumentación Cientifica, University of Granada, Spain) for the sample preparation and microscopy assistance, respectively. Moreover, Carla Smolders for her guidance and training on the facilities at the Belgian Nuclear Research Centre - SCK CEN.

References

Anderson, T.F. 1951. Techniques for the preservaation of three-dimensional structure in preparing specimens for the electron microscope. Trans. N.Y. Acad. Sci. 13, 130 - 134 https://doi.org/10.1111/j.2164-0947.1951.tb01007.x

Batandjieva, B., Delcheva, T., Duhovnik, B. 2009. Classification of radioactive waste: safety guide: IAEA General Safety Guide GSG-1. Vienna. International Atomic Energy Agency.

Bengtsson, A., Pedersen, K. 2017. Microbial sulphide-producing activity in water saturated Wyoming MX-80, Asha and Calcigel bentonites at wet densities from 1500 to 2000 kg m^{-3}. Appl. Clay Sci. 137, 203-212. https://doi.org/10.1016/j.clay.2016.12.024

Bengtsson, A., Pedersen, K. 2016. Microbial sulphate-reducing activity over load pressure and density in water saturated Boom Clay. Appl. Clay Sci. 132, 542-551. https://doi.org/10.1016/j.clay.2016.08.002

Bishop, J., Madejová, J., Komadel, P., and Fröschl, H. 2002. The influence of structural Fe, Al and Mg on the infrared OH bands in spectra of dioctahedral smectites. Clay Miner. 37(4), 607-616. https://doi.org/10.1180/0009855023740063

Burzan, N., Lima, R. M., Frutschi, M., Janowczyk, A., Reddy, B., Rance, A., Diomidis, N., Bernier-Latmani, R. 2022. Growth and Persistence of an Aerobic Microbial Community in Wyoming Bentonite MX-80 Despite Anoxic in situ Conditions. Front. Microbiol. 13: 858324 https://doi.org/10.3389%2Ffmicb.2022.858324

Callahan, B.J., McMurdie, P.J., Rosen, M.J., Han, A.W., Johnson, A.J.A., Holmes, S.P. 2016. DADA2: High-resolution sample inference from Illumina amplicon data. Nat. Methods. 13, 581-583. https://doi.org/10.1038/nmeth.3869

Caporaso J.G., Kuczynski J., Stombaugh J., Bittinger K., Bushman F.D., Costello E.K., Fierer, N., Gonzalez Peña, A., Goodrich, J.K., Gordon, J.I., Huttley, G.A., Kelley, S.T., Knights, D., Koening, J.E., Ley, R.E., Lozupone, C.A., McDonald, D., Muegge, B.D., Pirrung, M., Reeder, J., Sevinsky, J.R., Turnbaugh, P.J., Walters, W.A., Widmann, J., Yatsuneko, T., Zaneveld, J., Knight, R. 2010. QIIME allows analysis of high-throughput community sequencing data. Nat. Methods. 7, 335–336.

Chen, Z., Jiang, Y., Chang, Z., Wang, J., Song, X., Huang, Z., Chen, S., Li, J. 2020. Denitrification characteristics and pathways of a facultative anaerobic denitrifying strain, *Pseudomonas denitrificans* G1. J. Biosci. Bioeng., 129(6), 715-722. https://doi.org/10.1016/j.jbiosc.2019.12.011

Chen, S., Wang, P., Zhang, D. 2014. Corrosion behavior of copper under biofilm of sulfate-reducing bacteria. Corros. Sci. 87, 407 – 415. http://dx.doi.org/10.1016/j.corsci.2014.07.001

Chen, S., Song, L., Dong, X. 2006. *Sporacetigenium mesophilum* gen. nov., sp. nov., isolated from an anaerobic digester treating municipal solid waste and sewage. Int. J. Syst. Evol. Microbiol., 56(4), 721-725. https://doi.org/10.1099/ijs.0.63686-0

Clarke, T.A., Rizkalla, E.N. 1976. X-ray photoelectron spectroscopy of some silicates. Chem. Phys. Lett. 37, 523-526. https://doi.org/10.1016/0009-2614(76)85029-4

Cui, X., Zhao, S., Wang, B. 2016. Microbial desulfurization for ground tire rubber by mixed consortium-*Sphingomonas* sp. and *Gordonia* sp. Polym. Degrad. Stab., 128, 165-171. https://doi.org/10.1016/j.polymdegradstab.2016.03.011

Dou, W., Pu, Y., Han, X., Song, Y., Chen, S., Gu, T. 2020. Corrosion of Cu by a sulfate reducing bacterium in anaerobic vials with different headspace volumes. Bioelectrochemistry, 133, 107478. https://doi.org/10.1016/j.bioelechem.2020.107478

Eschbach, M., Schreiber, K., Trunk, K., Buer, J., Jahn, D., Schobert, M. 2004. Long-term anaerobic survival of the opportunistic pathogen *Pseudomonas aeruginosa* via pyruvate fermentation. J. Bacteriol., 186(14), 4596-4604. https://doi.org/10.1128/jb.186.14.4596-4604.2004

Essén, S. A., Johnsson, A., Bylund, D., Pedersen, K., Lundström, U. S. 2007. Siderophore production by *Pseudomonas stutzeri* under aerobic and anaerobic conditions. Appl. Environ. Microbiol., 73(18), 5857-5864. https://doi.org/10.1128/AEM.00072-07

Fantauzzi, M., Elsener, B., Atzei, D., Rigoldi, A., Rossi, A. 2015. Exploiting XPS for the identification of sulfides and polysulfides. RSC adv., 5(93), 75953-75963. https://doi.org/10.1039/C5RA14915K

Fernández, A.M. (2004). Caracterización y modelización del agua intersticial de materiales arcillosos: Estudio de la bentonita de Cortijo de Archidona. Editorial Ciemat. ISBN84-7834-479-9, 505 pp.

Fernández, A. M., Marco, J. F., Nieto, P., León, F. J., Robredo, L. M., Clavero, M. Á., Cardona, A. I., Fernández, S, Svensson, D, Sellin, P. 2022. Characterization of Bentonites from the in situ ABM5 Heater Experiment at Äspö Hard Rock Laboratory, Sweden. Minerals, 12(4), 471. https://doi.org/10.3390/min12040471

Finore, I., Gioiello, A., Leone, L., Orlando, P., Romano, I., Nicolaus, B., Poli, A. 2017. *Aeribacillus composti* sp. nov., a thermophilic bacillus isolated from olive mill pomace compost. Int. J. Syst. Evol. Microbiol., 67(11), 4830-4835. https://doi.org/10.1099/ijsem.0.002391

Gaggiano, R., De Graeve, I., Mol, J.M.C., Verbeken, K., Kestens, L.A.I. and Terryn, H. 2013. An infrared spectroscopic study of sodium silicate adsorption on porous anodic alumina. Surf Interface Anal. 45: 1098-1104. https://doi.org/10.1002/sia.5230

García-Romero, E., María Manchado, E., Suárez, M., and García-Rivas, J. 2019. Spanish bentonites: a review and new data on their geology, mineralogy, and crystal chemistry. Fortschr. Mineral. 9:696. https://doi.org/10.3390/min9110696

Grigoryan, A.A., Jalique, D.R., Medihala, P., Stroes-Gascoyne, S., Wolfaardt, G.M., McKelvie, J., Korber, D.R. 2018. Bacterial diversity and production of sulfide in microcosms containing uncompacted bentonites. Heliyon. 4, e00722. https://doi.org/10.1016/j.heliyon.2018.e00722

Hall, D.S., Behazin, M., Binns, W.J., and Keech, P.G. 2021. An evaluation of corrosion processes affecting copper-coated nuclear waste containers in a deep geological repository. Prog. Mater. Sci. 118, 100766. https://doi.org/10.1016/j.pmatsci.2020.100766

Hong, H., Kim, S. J., Min, U. G., Lee, Y. J., Kim, S. G., Roh, S. W., Kim, J. G., Na J. G., Rhee, S. K. 2015. *Anaerosolibacter carboniphilus* gen. nov., sp. nov., a strictly anaerobic iron-reducing bacterium isolated from coal-contaminated soil. Int. J. Syst. Evol. Microbiol., 65(Pt_5), 1480-1485. https://doi.org/10.1099/ijs.0.000124

Huertas, F., Fariña, P., Farias, J., García-Siñeriz, J.L., Villar, M.V., Fernández, A.M., Martin, P.L., Elorza, F.J., Gens, A., Sánchez, M., Lloret, A., Samper, J., Martínez, M. Á. 2021. Full-scale Engineered Barriers Experiment. Updated Final Report 1994-2004.

Hussain, S., Lalla, N. P., Kuo, Y. K., Lakhani, A., Sathe, V. G., Deshpande, U., Okram, G. S. 2018. Thermoelectric properties of Ag-doped CuS nanocomposites synthesized by a facile polyol method. Phys. Chem. Chem. Phys., 20, 5926-5935. https://doi.org/10.1039/C7CP07986A

Jia, R., Yang, D., Xu, D., Gu, T. 2017. Anaerobic corrosion of 304 stainless steel caused by the *Pseudomonas aeruginosa* biofilm Front. Microbiol., 8, 2335. https://doi.org/10.3389/fmicb.2017.02335

Jiang, W., Saxena, A., Song. S., Ward, B.B., Beveridge, T.J., Myneni, S.C.B. 2004. Elucidation of Functional Groups on Gram-Positive and Gram-Negative Bacterial Surfaces Using Infrared Spectroscopy. Langmuir 20, 11433-11442. https://doi.org/10.1021/la049043

Kaufhold, S., Dohrmann, R. 2010. Stability of bentonites in salt solutions: II. Potassium chloride solution — Initial step of illitization? Appl. Clay Sci. 49, 98-107. https://doi.org/10.1016/j.clay.2010.04.009

Keech, P. G., Vo, P., Ramamurthy, S., Chen, J., Jacklin, R., Shoesmith, D. W. 2014. Design and development of copper coatings for long term storage of used nuclear fuel. Corros. Eng. Sci. Technol., 49(6), 425-430. https://doi.org/10.1179/1743278214Y.0000000206

Kim, J., Dong, H., Yang, K., Park, H., Elliott, W. C., Spivack, A., ... and Heuer, V. B. 2019. Naturally occurring, microbially induced smectite-to-illite reaction. Geol. Soc. Am. Bull. 47, 535-539.

King, F., Hall, D. S., Keech, P. G. 2017. Nature of the near-field environment in a deep geological repository and the implications for the corrosion behaviour of the container. Corros. Eng. Sci. Technol., 52(sup1), 25-30. https://doi.org/10.1080/1478422X.2017.1330736

Krylova, V., Andrulevičius, M. 2009. Optical, XPS and XRD studies of semiconducting copper sulfide layers on a polyamide film. Int. J. Photoenergy. https://doi.org/10.1155/2009/304308

Kumar, A., Voropaeva, O., Maleva, M., Panikovskaya, K., Borisova, G., Rajkumar, M., Bruno, L. B. 2021. Bioaugmentation with copper tolerant endophyte *Pseudomonas lurida* strain EOO26 for improved plant growth and copper phytoremediation by *Helianthus annuus*. Chemosphere, 266, 128983. https://doi.org/10.1016/j.chemosphere.2020.128983

Madina, V., Insausti, M., Azkarate, I., Garmendia, I., and Cuñado, M. A. 2005. Corrosion behaviour of container candidate materials for HLW disposal in granite-bentonite media. Afinidad, 62(519), 383-387.

Martinez-Moreno, M.F., Povedano-Priego, C., Morales-Hidalgo, M., Mumford, A.D., Ojeda, J.J., Jroundi, F., Merroun, M. L. 2023. Impact of compacted bentonite microbial community on the clay mineralogy and copper canister corrosion: a multidiskiplinary approach in view of a safe Deep Geological Repository of nuclear wastes. J. Hazard. Mater. 131940. https://doi.org/10.1016/j.jhazmat.2023.131940

Masurat, P., Eriksson, S., Pedersen, K. 2010. Evidence of indigenous sulphate-reducing bacteria in commercial Wyoming bentonite MX-80. Appl. Clay Sci. 47, 51-57. https://doi.org/10.1016/j.clay.2008.07.002

Matschiavelli, N., Kluge, S., Podlech, C., Standhaft, D., Grathoff, G., Ikeda-Ohno, A., Warr, L.N., Chukharkina, A., Arnold, T., & Cherkouk, A. 2019. The year-long development of microorganisms in uncompacted bavarian bentonite slurries at 30 and 60 ºC. Environ. Sci. Technol. 2019, 53, 10514−10524. https://doi.org/10.1021/acs.est.9b02670

Meleshyn, A. 2011. Microbial processes relevant for long-term performance of radioactive waste repositories in clays. GRS-291. ISBN 978-3-939355-67-0. Available from: https://www.grs.de/sites/default/files/pdf/GRS-291.pdf

Miller, J.H. 1972. Experiments in Molecular Genetics. Cold Spring Harbor

Monier, J. M., Lindow, S. E. 2003. *Pseudomonas syringae* responds to the environment on leaves by cell size reduction. Phytopathology, 93(10), 1209-1216. https://doi.org/10.1094/PHYTO.2003.93.10.1209

Naumann, D., Helm, D., Labischinski, H. 1991. Microbiological characterizations by FT-IR spectroscopy. Nature 351, 81-82. https://doi.org/10.1038/351081a0

Laboratory, Cold Spring Harbor, New York, pp. 352–355.

Liu, L., Jiao, J. Y., Fang, B. Z., Lv, A. P., Ming, Y. Z., Li, M. M., Salam, N., Li, W. J. 2020. Isolation of *Clostridium* from Yunnan-Tibet hot springs and description of *Clostridium thermarum* sp. nov. with lignocellulosic ethanol production. Syst. Appl. Microbiol., 43(5), 126104. https://doi.org/10.1016/j.syapm.2020.126104

Liu, D., Dong, H., Bishop, M.E., Zhang, J., Wang, H., Xie, S., Wang, S., Huang, L., Eberl, D.D. 2012. Microbial reduction of structural iron in interstratified illite-smectite minerals by a sulfate-reducing bacterium. Geobiology, 10, 150-162. https://doi.org/10.1111/j.1472-4669.2011.00307.x

Lopez-Fernandez, M., Cherkouk, A., Vílchez-Vargas, R., Jauregui, R., Pieper, D., Boon, N., Sanchez-Castro, I., Merroun, M.L. 2015. Bacterial diversity in bentonites, engineered barrier for deep geological disposal of radioactive wastes. Microb. Ecol. 70, 922-935. https://doi.org/10.1007/s00248-015-0630-7.

Lopez-Fernandez, M., Fernández-Sanfrancisco, O., Moreno-García, A., Martín-Sánchez, I., Sánchez-Castro, I., Merroun, M.L. 2014. Microbial communities in bentonite formations and their interactions with uranium. Appl. Geochem. 49, 77-86. https://doi.org/10.1016/j.apgeochem.2014.06.022

Ohazuruike, L., and Lee, K. J. 2023. A comprehensive review on clay swelling and illitization of smectite in natural subsurface formations and engineered barrier systems. Nuclear Engineering and Technology. Nucl. Eng. Technol. 55, 1495 – 1506. https://doi.org/10.1016/j.net.2023.01.007

Ojeda, J.J. and Dittrich, M. 2012. Fourier transform infrared spectroscopy for molecular analysis of microbial cells. J. Microbiol. Methods. 187-211. https://doi.org/10.1007/978-1-61779-827-6_8

Ojovan, M.I.; Steinmetz, H.J. 2022. Approaches to Disposal of Nuclear Waste. Energies, 15, 7804. https://doi.org/10.3390/en15207804

Orsini, F.; Ami, D.; Villa, A. M.; Sala, G.; Bellotti, M.G.; Doglia, S.M. 2000. FT-IR microspectroscopy for microbiological studies. J. Microbiol. Meth. 42, 17. https://doi.org/10.1016/S0167-7012(00)00168-8

Pandey, A., Dhakar, K., Sharma, A., Priti, P., Sati, P., Kumar, B. 2015. Thermophilic bacteria that tolerate a wide temperature and pH range colonize the Soldhar (95 C) and Ringigad (80 C) hot springs of Uttarakhand, India. Ann. Microbiol, 65(2), 809-816. https://doi.org/10.1007/s13213-014-0921-0

Payer, J. H., Finsterle, S., Apps, J.A., Muller, R.A. 2019. Corrosion performance of engineered barrier system in deep horizontal drillholes. Energies. 12, 1491. https://doi.org/10.3390/en12081491

Pedersen, K. 2010. Analysis of copper corrosion in compacted bentonite clay as a function of clay density and growth conditions for sulfate-reducing bacteria. J. Appl. Microbiol., 108, 1094-1104. https://doi.org/10.1111/j.1365-2672.2009.04629.x

Pentráková, L., Su, K., Pentrák, M., Stucki, J.W. 2013. A review of microbial redox interactions with structural Fe in clay minerals. Clay Miner. 48, 543-560. https://doi.org/10.1180/claymin.2013.048.3.10

POSIVA. Final Disposal. https://www.posiva.fi/en/index/finaldisposal.html (accessed 16 May 2023).

Povedano-Priego, C., Jroundi, F., Lopez-Fernandez, M., Shrestha, R., Spanek, R., Martín-Sánchez, I., Villar, M.V., ˇSevců, A., Dopson, M. Merroun, M.L. 2021. Deciphering indigenous bacteria in compacted bentonite through a novel and efficient DNA extraction method: Insights into biogeochemical processes within the Deep Geological Disposal of nuclear waste concept. J. Hazard. Mater. 408, 124600. https://doi.org/10.1016/j.jhazmat.2020.124600

Povedano-Priego, C., Jroundi, F., Lopez-Fernandez, M., Sánchez-Castro, I., Martin-Sánchez, I., Huertas, F.J., Merroun, M.L. 2019. Shifts in bentonite bacterial community and mineralogy

in response to uranium and glycerol-2-phosphate exposure. Sci. Total Environ. 692, 219-232. https://doi.org/10.1016/j.scitotenv.2019.07.228

Reasoner, D.J., Geldreich, E., 1985. A new medium for the enumeration and subculture of bacteria from potable water. Appl. Environ. Microbiol. 49, 1–7.

Scheer, R., Lewerenz, H.J. 1994. Photoemission study of evaporated CuInS2 thin films. II. Electronic surface structure. J. Vac. Sci. Technol. A: Vac. Surf. Films. 12, 56-60. https://doi.org/10.1116/1.578858

Shelobolina, E. S., Nevin, K. P., Blakeney-Hayward, J. D., Johnsen, C. V., Plaia, T. W., Krader, P., Woodard, T., Holmes, D. E., VanPraagh, C. G., Lovley, D. R. 2007. *Geobacter pickeringii* sp. nov., *Geobacter argillaceus* sp. nov. and *Pelosinus fermentans* gen. nov., sp. nov., isolated from subsurface kaolin lenses. Int. J. Syst. Evol. Microbiol., 57(1), 126-135. https://doi.org/10.1099/ijs.0.64221-0

Shelobolina, E.S., VanPraagh, C.G., Lovley, D.R. 2003. Use of ferric and ferrous iron containing minerals for respiration by Desulfitobacterium frappieri. Geomicrobiol. J. 20, 143-156. https://doi.org/10.1080/01490450303884

Shrestha, R., Cerna, K., Spanek, R., Bartak, D., Cernousek, T., & Sevcu, A. 2022. The effect of low-pH concrete on microbial community development in bentonite suspensions as a model for microbial activity prediction in future nuclear waste repository. Sci. Total Environ., 808, 151861. https://doi.org/10.1016/j.scitotenv.2021.151861

Smart, N. R., Reddy, B., Rance, A. P., Nixon, D. J., Frutschi, M., Bernier-Latmani, R., and Diomidis, N. 2017. The anaerobic corrosion of carbon steel in compacted bentonite exposed to natural Opalinus Clay porewater containing native microbial populations. Corros. Eng. Sci. Technol., 52(sup1), 101-112. https://doi.org/10.1080/1478422X.2017.1315233

Stroes-Gascoyne, S., Hamon, C. J., Maak, P., & Russell, S. 2010. The effects of the physical properties of highly compacted smectitic clay (bentonite) on the culturability of indigenous microorganisms. Appl. Clay Sci., 47(1-2), 155-162. https://doi.org/10.1016/j.clay.2008.06.010

Stroes-Gascoyne, S., Hamon, C.J., Dixon, D.A., Kohle, C.L., Maak, P., 2006. The effects of dry density and porewater salinity on the physical and microbiological characteristics of compacted 100% bentonite. Mater Res Soc Symp Proc Vol. 985. https://doi.org/10.1557/PROC-985-0985-NN13-02.

Thauer, R.K., Stackebrandt, E., Hamilton, W.A. 2007. Energy metabolism and phylogenetic diversity of sulphate-reducing bacteria. Sulphate-reducing bacteria. 1-38. https://doi:10.1017/cbo9780511541490.002

Thijs, S., Op De Beeck, M., Beckers, B., Truyens, S., Stevens, V., Van Hamme, J. D., Weyens, N. Vangronsveld, J. 2017. Comparative evaluation of four bacteria-specific primer pairs for 16S rRNA gene surveys. Front. Microbiol. 8, 494. https://doi.org/10.3389/fmicb.2017.00494

Vaïtilingom, M., Amato, P., Sancelme, M., Laj, P., Leriche, M., & Delort, A. M. (2010). Contribution of microbial activity to carbon chemistry in clouds. Appl. Environ. Microbiol., 76(1), 23-29. https://doi.org/10.1128/AEM.01127-09

Villar, M.V., Fernández-Soler, J.M., Delgado Huertas, A., Reyes, E., Linares, J., Jiménez de Cisneros, C., Linares, J., Reyes, E., Delgado, A., Fernandez-Soler, J.M., Astudillo, J. 2006. The study of Spanish clays for their use as sealing materials in nuclear waste repositories: 20 years of progress. J. Iber. Geol. 32, 15-36.

Wagner, C.D., Riggs, W.M., Davis, L.E., Moulder, J.F., Muilenberg, G.E. 1979. Handbook of x-ray photoelectron spectroscopy: a reference book of standard data for use in x-ray photoelectron spectroscopy. Perkin-Elmer Corporation: Eden Prairie, MN.

White, D. C., Sutton, S. D., Ringelberg, D. B. 1996. The genus *Sphingomonas*: physiology and ecology. Curr. Opin. Biotechnol., 7(3), 301-306. https://doi.org/10.1016/S0958-1669(96)80034-6

WNA. World Nuclear Association. 2021. Storage and disposal of radioactive waste. https://www.world-nuclear.org/

Yang, S., Li, S., Jia, X. 2019. Production of medium chain length polyhydroxyalkanoate from acetate by engineered Pseudomonas putida KT2440. J. Ind. Microbiol. Biotechnol., 46(6), 793-800. https://doi.org/10.1007/s10295-019-02159-5

Supplementary material for:

Microbial Responses to Elevated Temperature: Evaluating Bentonite Mineralogy and Copper Canister Corrosion within the Long-Term Stability of Deep Geological Repositories of Nuclear Waste

Marcos F. Martinez-Moreno[1,*], Cristina Povedano-Priego[1], Adam D. Mumford[2], Mar Morales-Hidalgo[1], Kristel Mijnendonckx[3], Fadwa Jroundi[1], Jesus J. Ojeda[2], Mohamed L. Merroun[1]

[1]*Faculty of Sciences, Department of Microbiology, University of Granada, Granada, Spain.*

[2]*Department of Chemical Engineering, Faculty of Science and Engineering, Swansea University, Swansea, United Kingdom*

[3]*Microbiology Unit, Belgian Nuclear Research Centre, SCK CEN, Mol, Belgium*

Supplemetary Table S1.

pH values and chemical composition (%) by X-ray fluorescence (XRF) before and after one year of anaerobic incubation at 60 ºC (1y).

Treatment	pH	SiO_2	Al_2O_3	Fe2O3	MnO	MgO	CaO	Na2O	K2O	TiO_2	P_2O_5	LOI
B.eD	8.07 ± 0.07	61.91	17.12	3.89	0.04	3.72	3.54	1.94	1.63	0.27	0.08	5.83
B.eD_1y	7.74 ± 0.04	58.23	17.63	5.09	0.03	3.53	3.84	2.97	1.35	0.32	0.07	6.06
B	8.10 ± 0.02	61.93	16.95	3.84	0.04	4.70	3.10	1.43	1.17	0.19	0.05	6.56
B_1y	7.59 ± 0.09	57.43	17.94	5.26	0.02	3.50	3.86	3.04	1.37	0.32	0.06	6.71
StB.eD	8.18 ± 0.05	60.51	16.49	3.92	0.05	3.80	4.80	1.87	1.53	0.30	0.07	6.64
StB.eD_1y	7.65 ± 0.06	57.48	17.85	5.15	0.02	3.52	3.94	3.06	1.33	0.31	0.06	6.83
StB	8.13 ± 0.06	59.64	16.49	3.90	0.05	3.82	5.18	1.81	1.52	0.28	0.07	7.23
StB_1y	7.59 ± 0.03	57.77	17.78	5.15	0.03	3.62	3.90	2.95	1.35	0.29	0.07	6.96

*LOI: Loss on ignition

Supplementary Table S2.
Richness (Sobs), diversity (ShannonH. and SimpsonD), and evenness (ShannonE) indices. Glossary: B: bentonite, StB: sterilized bentonite, eD: addition of acetate, sulfate, and lactate; 1y: after one year of anaerobic incubation at 60 ºC.

	Sobs	ShannonH	SimpsonD	ShannonE
B.eD_R1	326	5.35	0.91	0.64
B.eD_R2	275	4.66	0.87	0.58
B.eD_R3	288	4.94	0.89	0.61
BeD_1y_R1	137	1.85	0.37	0.26
BeD_1y_R2	107	0.85	0.15	0.13
StB.eD_R1	399	6.30	0.96	0.73
StB.eD_R2	413	6.74	0.98	0.78
StBeD_1y_R2	111	1.19	0.23	0.18
StBeD_1y_R3	25	2.62	0.65	0.56

Supplementary Table S3.

Phyla relative abundance of the bacterial and archaeal communities of the bentonite samples in duplicates (triplicate in B.eD). Glossary: B: bentonite, StB: sterilized bentonite, eD: addition of acetate, sulfate, and lactate; 1y: after one year of anaerobic incubation at 60 ºC.

	Total	B.eD	B.eD_1y	StB.eD	StB.eD_1y
Archaea	0.01	< 0.01	0.00	0.01	0.00
>Crenarchaeota	0.01	< 0.01	0.00	< 0.01	0.00
>Thermoplasmatota	< 0.01	< 0.01	0.00	< 0.01	0.00
Bacteria	99.99	39.35	20.42	33.14	7.08
>Abditibacteriota	< 0.01	0.00	0.00	< 0.01	0.00
>Acidobacteriota	1.26	0.37	0.00	0.89	0.00
>Actinobacteriota	47.52	28.69	0.66	18.08	0.09
>Armatimonadota	0.04	0.01	0.00	0.03	0.00
>Bacteroidota	1.13	0.34	0.03	0.77	< 0.01
>Bdellovibrionota	0.05	< 0.01	0.00	0.04	0.00

>Chloroflexi	5.19	1.72	0.04	3.43	0.00
>Cyanobacteria	0.23	0.07	0.03	0.12	0.01
>Deinococcota	0.08	0.03	< 0.01	0.05	0.00
>Dependentiae	< 0.01	< 0.01	0.00	< 0.01	0.00
>Desulfobacterota	0.06	0.01	0.02	0.03	0.00
>Entotheonellaeota	< 0.01	< 0.01	0.00	< 0.01	0.00
>Fibrobacterota	< 0.01	0.00	0.00	< 0.01	0.00
>Firmicutes	3.68	0.54	1.86	0.61	0.67
>Fusobacteriota	< 0.01	0.00	0.00	< 0.01	0.00
>Gemmatimonadota	1.38	0.49	0.01	0.89	0.00
>Halanaerobiaeota	0.01	0.00	0.01	< 0.01	< 0.01
>MBNT15	< 0.01	< 0.01	0.00	< 0.01	0.00
>Methylomirabilota	0.00	< 0.01	0.00	< 0.01	0.00
>Myxococcota	0.37	0.07	0.01	0.30	< 0.01
>Nitrospinota	0.00	< 0.01	0.00	0.00	0.00
>Nitrospirota	0.08	0.02	< 0.01	0.07	0.00
>Patescibacteria	0.19	0.05	< 0.01	0.14	0.00
>Planctomycetota	0.45	0.18	0.01	0.24	0.02
>Proteobacteria	37.62	6.63	17.72	6.97	6.29
>Sumerlaeota	0.04	0.02	0.00	0.02	0.00
>Unclassified	0.02	< 0.01	0.00	0.02	< 0.01
>Verrucomicrobiota	0.54	0.11	0.00	0.43	0.00
>WS4	0.01	0.00	0.01	< 0.01	0.00
Unassigned	< 0.01	0.00	< 0.01	0.00	0.00

Supplementary Data S1.

OTU relative abundance of the bacterial and archaeal communities of the bentonite samples in duplicates (triplicate in B.eD). This table only represents a cut-off > 0.2 % of the total relative abundance Glossary: B: bentonite, StB: sterilized bentonite, eD: addition of acetate, sulfate, and lactate; 1y: after one year of anaerobic incubation at 60 ºC.

	Relative abundance (%)				
OTU	Total	B.eD	B.eD_1y	StB.eD	StB.eD_1y
Pseudomonas	23.00	0.69	85.62	0.31	72.55
Nocardioides	14.67	27.23	0.03	11.92	0.00

unclassified_Micrococcaceae	8.40	15.04	1.78	6.23	0.70
Gitt-GS-136_Chloroflexi	3.22	2.74	0.08	6.42	0.00
Promicromonospora	2.39	4.91	0.00	1.40	0.00
Marmoricola	2.13	4.16	0.00	1.49	0.00
unclassified_Nocardioidaceae	2.12	3.47	0.00	2.28	0.00
unclassified_Micromonosporaceae	1.78	1.37	0.05	3.73	0.01
Mesorhizobium	1.56	2.48	0.01	1.76	0.00
Streptomyces	1.37	1.54	0.14	2.22	0.01
Amycolatopsis	1.32	1.94	0.00	1.69	0.02
Bacillus	1.19	0.99	2.01	0.81	1.74
uncultured_Microtrichales	1.14	0.78	0.01	2.50	0.00
Pseudarthrobacter	0.93	1.82	0.14	0.55	0.00
Sphingomonas	0.90	0.54	0.21	1.20	3.55
Longimicrobiaceae	0.76	0.54	0.00	1.63	0.00
KD4-96_Chloroflexi	0.74	0.46	0.02	1.67	0.00
Arthrobacter	0.71	1.26	0.03	0.62	0.00
Flindersiella	0.67	0.24	0.00	1.73	0.00
unclassified_Microbacteriaceae	0.64	1.26	0.00	0.43	0.00
uncultured_Alphaproteobacteria	0.57	0.46	0.02	1.17	0.00
0319-7L14_Actinobacteria	0.57	0.37	0.00	1.29	0.00
Iamia	0.56	0.40	0.00	1.21	0.00
Pseudonocardia	0.54	0.53	0.01	0.99	0.01
Lysobacter	0.50	0.72	0.00	0.64	0.00
JG30-KF-CM45_Thermomicrobiales	0.50	0.52	0.06	0.86	0.00
uncultured_Acidimicrobiia	0.49	0.18	0.01	1.27	0.00
Saccharospirillum	0.47	0.88	0.00	0.37	0.00
Vicinamibacteraceae	0.46	0.34	0.00	0.98	0.00
Gaiella	0.44	0.34	0.00	0.91	0.00
67-14_Solirubrobacterales	0.43	0.43	0.00	0.80	0.00
Pelagibius	0.43	0.59	0.00	0.59	0.00
Ramlibacter	0.42	0.66	0.00	0.47	0.00
uncultured_Euzebyaceae	0.41	0.34	0.00	0.83	0.00
Solirubrobacter	0.39	0.45	0.03	0.61	0.00
Altererythrobacter	0.38	0.24	0.00	0.86	0.00
uncultured_Vicinamibacterales	0.37	0.30	0.00	0.76	0.00
uncultured_Acidiferrobacteraceae	0.37	0.57	0.00	0.44	0.00
Kribbella	0.36	0.59	0.00	0.37	0.00
Solimonas	0.36	0.87	0.00	0.06	0.00
uncultured_Microscillaceae	0.36	0.30	0.00	0.74	0.00
Caenimonas	0.35	0.46	0.00	0.52	0.00

Unclassified_Rhizobiaceae	0.34	0.43	0.00	0.52	0.00
Glycomyces	0.34	0.12	0.00	0.89	0.00
Unclassified_Sphingomonadaceae	0.33	0.26	0.01	0.67	0.00
Uncultured_bacterium	0.32	0.00	1.06	0.00	1.50
Unclassified_Methylophilaceae	0.27	0.61	0.00	0.08	0.00
Noviherbaspirillum	0.27	0.42	0.00	0.31	0.00
Acinetobacter	0.27	0.00	0.06	0.00	3.64
S0134_terrestrial_group	0.25	0.28	0.00	0.43	0.00
Steroidobacter	0.25	0.17	0.00	0.56	0.00
IMCC26256	0.24	0.14	0.00	0.55	0.00
Longispora	0.24	0.13	0.00	0.59	0.00
Acinetobacter	0.24	0.02	0.02	0.02	3.13
Myceligenerans	0.23	0.37	0.00	0.26	0.00
Actinophytocola	0.23	0.13	0.00	0.53	0.00
Uncultured_Gemmatimonadaceae	0.23	0.29	0.00	0.35	0.00
Uncultured_Xanthobacteraceae	0.23	0.13	0.00	0.54	0.00
AKYG1722	0.21	0.23	0.01	0.37	0.00
Ilumatobacter	0.21	0.20	0.00	0.39	0.00
Nitriliruptoraceae	0.20	0.10	0.00	0.50	0.00
Clostridium_sensu_stricto_13	0.20	0.03	0.61	0.11	0.36

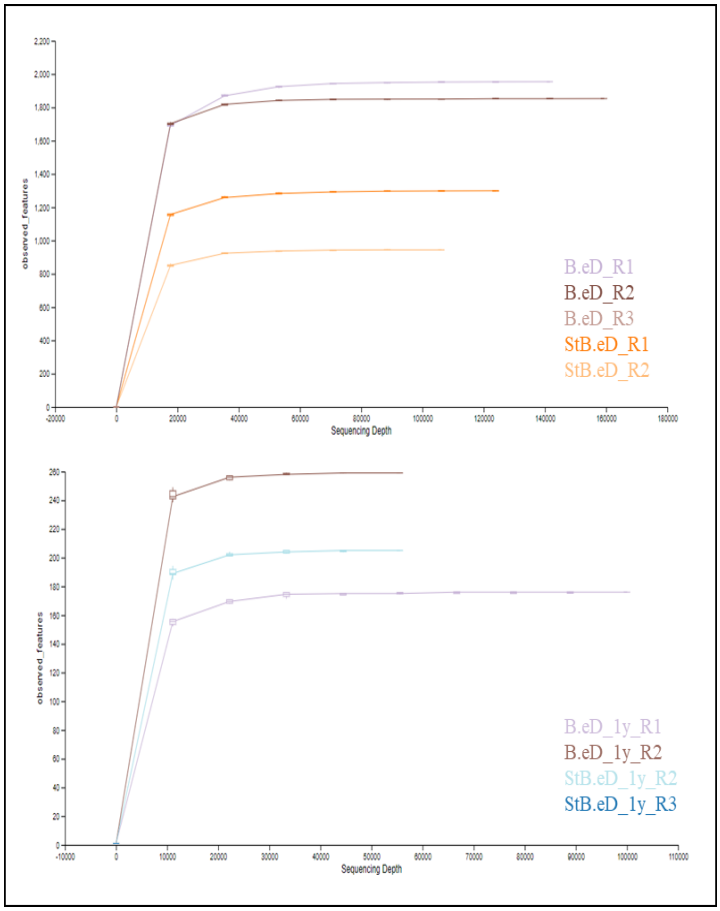

Supplementary Fig. S1. Rarefaction curves of the sequenced samples representing the richness and sample size. Glossary: B: bentonite, StB: sterilized bentonite, eD: addition of acetate, sulfate, and lactate; 1y: after one year of anaerobic incubation at 60 ºC.

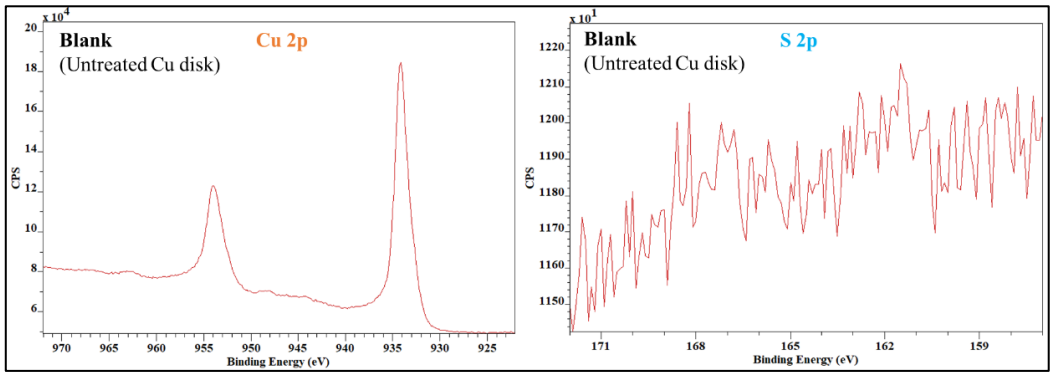

Supplementary Fig. S2. High resolution XPS spectra of Cu 2p, left, and S 2p, right, for untreated Cu disk (blank).

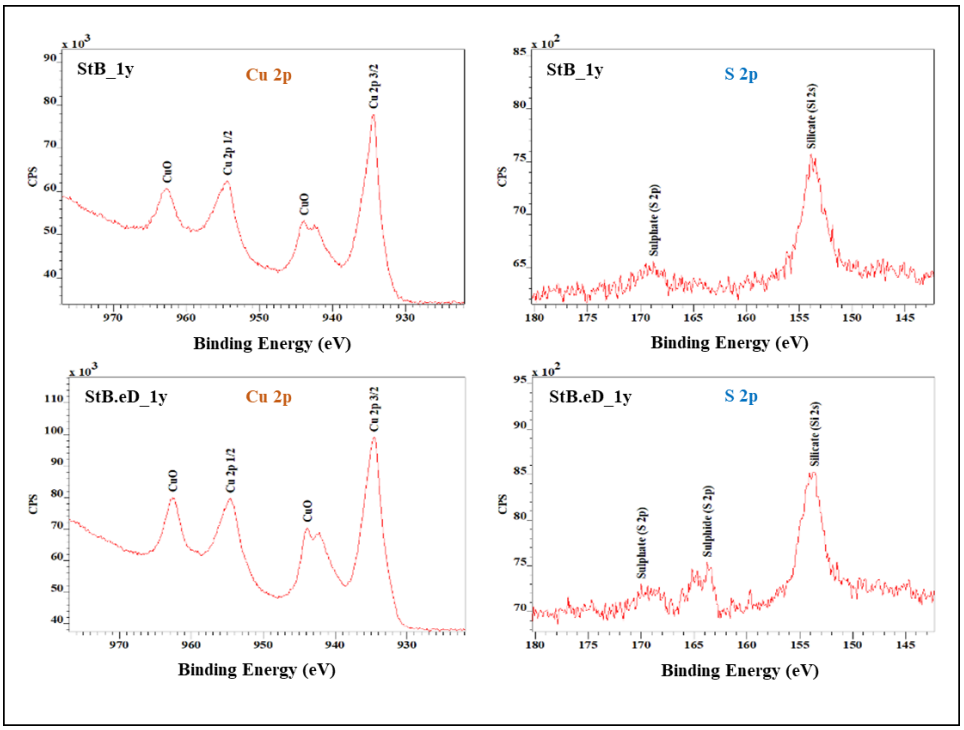

Supplementary Figure S3. High resolution XPS spectra of Cu 2p (region between 922-977eV), left, and S 2p (region between 143-180eV), right, for samples StB_1y (top) and StB.eD_1y (bottom)

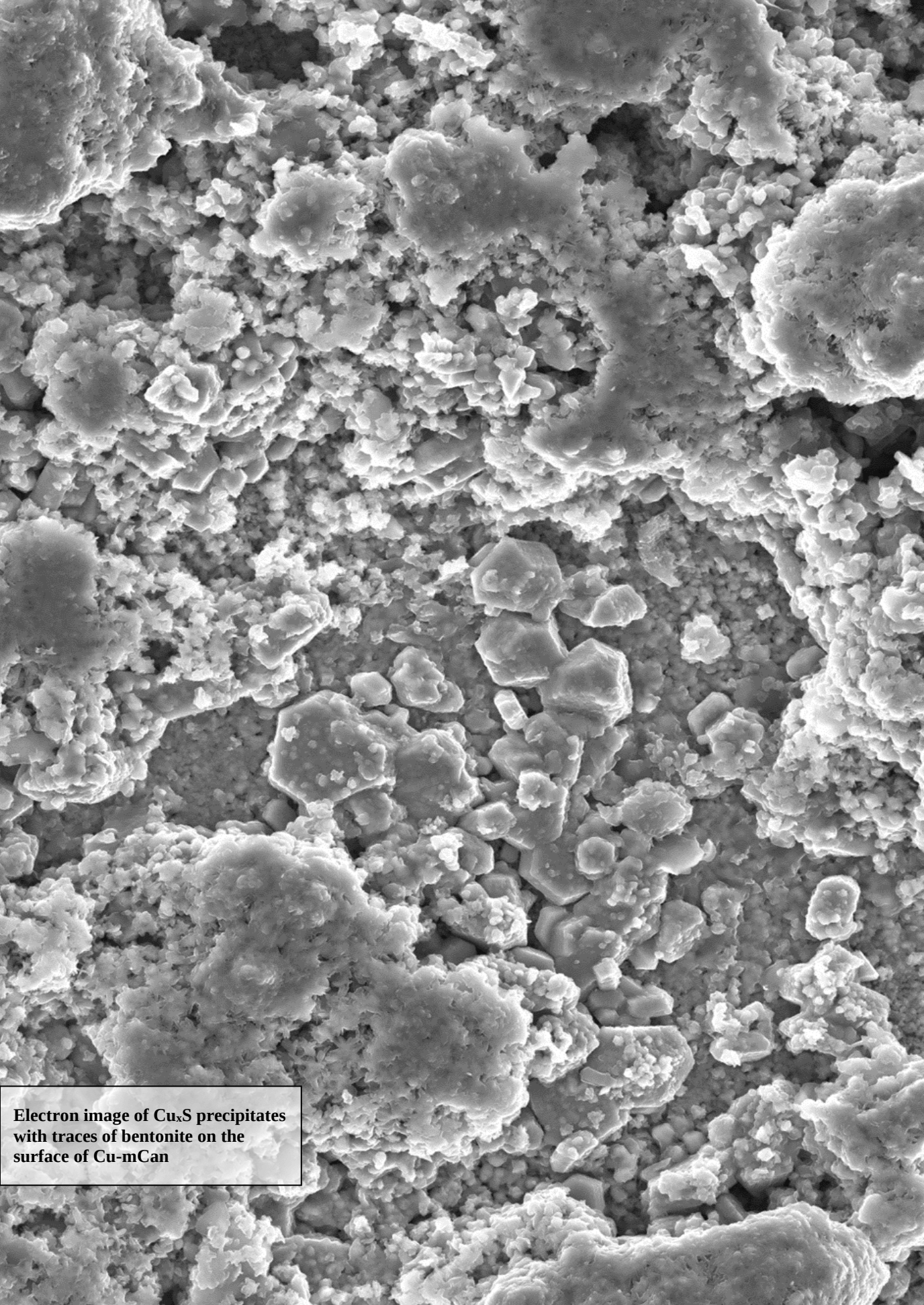

Electron image of Cu_xS precipitates with traces of bentonite on the surface of Cu-mCan

Chapter III:

Microbial influence in hyper-saturated Spanish bentonite microcosms: Unveiling a-year long geochemical evolution and early-stage copper corrosion related to nuclear waste repositories

Authors

Marcos F. Martinez-Moreno[1,*], Cristina Povedano-Priego[1], Mar Morales-Hidalgo[1], Adam d. Mumford[2], Elisabet Aranda[3], Jesus J. Ojeda[2], and Mohamed L. Merroun[1]

[1]Faculty of Sciences, Department of Microbiology, University of Granada, Granada, Spain.

[2]Department of Chemical Engineering, Faculty of Science and Engineering, Swansea University, Swansea, United Kingdom

[3]Institute of Water Research, Department of Microbiology, University of Granada, Granada, Spain

Abstract

The long-term confinement of radioactive waste within Deep Geological Repository (DGR) concept involves storing the waste in corrosion-resistant canisters, surrounded by compacted bentonite clay, and placed into a host rock. Microbial processes will likely play a key role in the safety assessment of repository. In the present study, uncompacted and hyper-saturated bentonite microcosms amended with electron donors (acetate-lactate)/acceptor (sulfate) were set up to investigate their geochemical evolution over a year of anaerobic incubation. In addition, the influence of microbial communities on the corrosion of copper in an early-stage (45 days) was assessed. The microbial communities partially oxidize lactate to acetate which is subsequently consumed when the lactate is depleted. The amended bacterial consortium and electron donors/acceptor accelerated the microbial activity, while bentonite's pre-sterilization had a retarding effect. Early-stage microbial communities showed that the bacterial consortium reduced microbial diversity with *Pseudomonas* and *Stenotrophomonas* dominating the community. However, certain sulfate-reducing bacteria such as *Desulfocurvibacter*, *Anaerosolibacter*, and *Desulfosporosinus* were stimulated by electron donors/acceptor, which favored the detected formation of corrosion compounds on the copper surface.

Keywords: *DGR, Spanish bentonite, microbial diversity, electron donors/acceptor, copper corrosion*

1_ Introduction

The global challenge of managing high-level radioactive waste (HLW) has led to the consideration of the Deep Geological Repository (DGR) as the internationally accepted option for this propose (WNA, 2023). The main objective is to preserve the long-term integrity and the safety performance of these repositories for periods spanning from several hundreds to millions of years, ensuring that no residual radioactive materials reach the surrounding environment (Betandiieva et al., 2009). The multi-barrier design of DGR consists of a buffering and sealing bentonite-based material surrounding the waste-containing metal canisters that will be placed several hundred meters underground in a stable geological formation (host rock) to ensure safety until the radiotoxicity diminishes to levels similar to natural ones (Ojovan and Steinmetz, 2022). The nature of the barriers depends on the particular strategy adopted by each country. Copper-coating metal canisters have been proposed, or already implemented, by countries such as Canada, Korea, Sweden, and Finland (Hall et al., 2021). In addition, bentonite clay was selected as the most appropriate buffer and sealing material. This clay provides mechanical support for canisters, prevents groundwater infiltration, retards radionuclides diffusion, and seals canisters in the event of rupture or cracks (García-Romero et al., 2019). In Spain, bentonite from Almeria (commercialized as FEBEX) has been proposed as buffer material for Spanish DGR (Huertas et al., 2021; Villar et al., 2006).

Since bentonites are not sterile, understanding the structure and composition of the microbial community within this clay could provide insights in its potential impact on the long-term stability and safety of the DGR (Meleshyn et al., 2011). Microorganisms may compromise the mineralogy and chemistry of the bentonite buffer, and the integrity of the metal canisters can be affected due to microbially influenced corrosion (MIC) via biofilm formation or corrosive metabolite production (Ruiz-Fresneda et al., 2023). Additionally, in case of canister cracks, bacteria could interact with and transport radionuclides, potentially increasing their

migration through the barriers to the environment. Moreover, microbial metabolism may contribute to the production of hydrogen, methane, and carbon dioxide, affecting the gas phase that would increase the pressure within the DGR (Guo & Fall, 2021; Bagnoud et al., 2016).

Once the DGR is sealed, the gradual depletion of oxygen will occur due to factors such as microbial activity and metal canister corrosion, leading to the establishment of an anoxic environment (Payer et al., 2019; Keech et al., 2014). In this context, certain anaerobic bacteria such as sulfate-reducing bacteria (SRB) and iron-reducing bacteria (IRB) could remain active. The activity of these groups of bacteria may have adverse consequences, including the promotion of MIC, the reduction of Fe(III) to Fe(II) in smectite (the major mineral in bentonites), and the reduction of sulfate to sulfide (a key agent in copper corrosion) (Pentráková et al., 2013; Liu et al., 2012; Shelobolina et al., 2003). Sulfide production, attributed to SRB activity, is more likely to occur further away from the canisters under conditions that favor SRB growth, such as lower temperatures and higher water activity (Bengtsson and Pedersen, 2017). This biogenic sulfide could diffuse through the biologically inactive section of the sealing materials and influence the nature and rate of copper corrosion on the canister surface.

To understand the impact of the activity of indigenous microorganisms in Spanish bentonite over the short term, optimal conditions for microbial growth, representing a worst-case scenario for a DGR, were simulated. In this study, hyper-saturated bentonite anaerobic microcosms were amended with acetate, lactate, and sulfate (electron donors and acceptor, respectively) to stimulate microbial activity. Hence, this study aims to comprehensively examine the impact of microorganisms on the geochemical evolution of a complex hyper-saturated bentonite system for one year of anaerobic incubation. Additionally, this work also focused on investigating the microbial communities and their influence on copper corrosion in an early state (45 days) of incubation within the microcosms.

Our results emphasize the role of the microorganisms present in the bentonite, which could provide optimal growth conditions in the event of an influx of nutrients due to the filtration of water in the bentonite.

2_ Materials and methods

2.1_ Bentonite sampling

The bentonite was collected from El Cortijo de Archidona site in Almeria (Spain). The samples were collected aseptically during February of 2020 from a maximum depth of ~ 80 cm. Subsequently, in the laboratory, the bentonite was manually disaggregated and dried for at least five days at room temperature within a laminar flow cabinet to eliminate excess moisture. The bentonite was ground using a sterile stainless-steel roller and mortar to achieve a uniform powder. Finally, it was stored at 4 ºC until the elaboration of the microcosms.

2.2_ Copper material and mini canisters (Cu-mCan) manufacturing

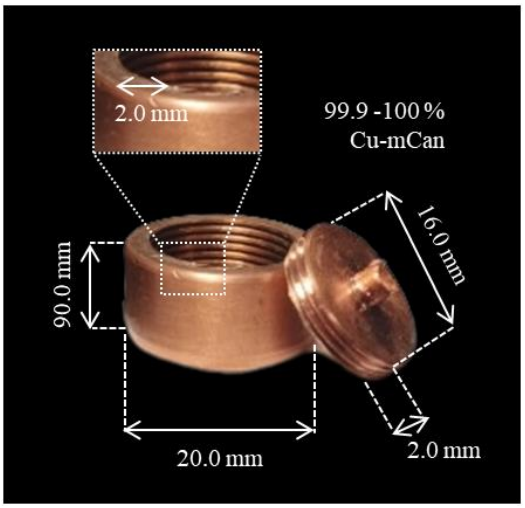

Fig. 1. Dimension of the high-purity copper mini-canisters (Cu-mCan).

Copper rods (99.9 – 100% Cu purity) were obtained from Goodfellow (UNS number C10100; goodfellow.com) containing small impurities of Cr (< 1 ppm), Fe

(2 ppm), Ag (70 ppm), Al (1 ppm), Mg (1 ppm), Mn (< 1 ppm), Ni (2 ppm), Na (< 1 ppm), Sn (1 ppm), Pb (2 ppm), Si (2 ppm), Bi (1 ppm), and Ca (1 ppm). Two different rods diameters (20.6 ± 0.05, and 16.0 ± 0.5 mm) were employed for the mini-canisters (Cu-mCan) manufacturing in the mechanical workshop of Centro de Instrumentación Científica (University of Granada, Spain) that were sterilized by autoclaving 15 min at 121 ºC. The final dimensions of the Cu-mCan are specified in **Fig. 1**.

2.3_ Elaboration of the equilibrium water and electron donors/acceptor solutions

Equilibrium water (EW) for the slurry preparation was performed by shaking bentonite powder in sterile distilled water in a 1:100 w/v ratio at 180 rpm for 24 h at room temperature. Subsequently, the mixture was centrifugated at 10,000 g for 5 min. The supernatant was recovered and autoclaved for 15 min at 121 ºC. The major elements composition of the EW was determined by Inductively Coupled Plasma-Mass Spectroscopy (ICP-MS) with a NexION 300D spectrometer (**Supplementary Table S1)**.

In order to stimulate the bacterial growth, stock solutions of 1 M sodium acetate ($C_2H_3NaO_2$) and 0.5 M sodium lactate (CH_3-CH(OH)-COONa) were previously prepared as electron donors. In addition, 0.5 M sodium sulfate (Na_2SO_4) stock solution was elaborated as electron acceptor. Electron donors/acceptor stock solutions were then sterilized by autoclaving.

2.4_ BPAS bacterial consortium and culture conditions

A consortium of four bacterial strains (BPAS) was added to the bacterial consortium-containing treatments (BC). These strains were detected in the microbial community of Spanish bentonite (Povedano-Priego et al., 2021; Lopez-Fernandez et al., 2018, 2014) and used in a previous study using water-saturated

microcosms detailed in Povedano-Priego et al., 2023. *Stenotrophomonas bentonitica* BII-R7 and *Bacillus* sp. BII-C3 were isolated from Spanish bentonite (Sanchez-Castro et al., 2017; Lopez-Fernandez et al., 2014). Additionally, *Pseudomonas putida* ATCC33015, and *Amycolatopsis ruanii* NCIMB14711 were purchased from ATCC (American Type Culture Collection; lgcstandards-atcc.org/), and NCIMB (National Collection of Industrial Food and Marine Bacteria; ncimb.com), respectively. *S. bentonitica, Bacillus* BII-C3, and *P. putida* were grown aerobically in Luria-Bertani (LB) medium consisting of tryptone (10 g L^{-1}), yeast extract (5 g L^{-1}), and NaCl (10 g L^{-1}); while *A. ruanii* was grown in YMG medium composed of yeast extract (4 g L^{-1}), malt extract (10 g L^{-1}), and D(+)-glucose monohydrate (4 g L^{-1}). After bacterial growth, the cells were recovered by centrifugation (10,000 rpm for 5 min) and washed twice with 0.9% NaCl. The final pellet was resuspended with the EW and the initial Optical Density was adjusted for each strain to 0.4 at 600 nm (OD_{600}) (Genesys 10 S UV-Vis - Thermo scientific).

2.5_ Microcosms assembly and sampling

Microcosms were set up following the procedure described by Povedano-Priego et al. (2023) with some modifications. 50 g of ground bentonite was added to 250 mL borosilicate glass bottles previously autoclaved. Solutions of electron donors and acceptor were supplemented in the electron donors/acceptor-containing (eD) microcosms with a final concentrations of acetate 30 mM, lactate 10 mM, and sulfate 20 mM. Additionally, the bacterial consortium-containing (BC) bottles were spiked with BPAS consortium with an initial OD_{600} of 0.4 for each bacterial strain. The volume of the different microcosms was calculated considering the addition of the solutions and then filled up to 230 mL with the EW. Finally, three sterilized Cu-mCan were deposited into each microcosm.

Different controls were considered in order to study four different parameters (sample code between brackets): i) bentonite and sterilized bentonite (B and StB), ii) acetate:lactate:sulfate addition (eD), and iii) the addition of a bacterial consortium (BC). The bentonite from the sterilized-bentonite (StB) microcosms was previously heat-shocked once in the bottles by tyndallization (110 ºC for 45 min, 3 consecutive days). A total of 24 microcosms were elaborated (8 treatments in triplicate). The sample ID and characteristic of the experimental conditions are summarized in **Table 1**.

Table 1.

Experimental conditions and sample ID of the different treatments. All free-oxygen microcosms incorporated three Cu mini-canisters (Cu-mCan) and elaborated in triplicate. A:L:S: acetate, lactate, and sulfate concentrations; BPAS: bacterial consortium; +: presence; -: absence.

Sample ID	Bentonite	A:L:S (mM)	BPAS
B.eD.BC	Non-sterilized	30:10:20	+
B.BC	Non-sterilized	-	+
B.eD	Non-sterilized	30:10:20	-
B	Non-sterilized	-	-
StB.eD.BC	Sterilized	30:10:20	+
StB.BC	Sterilized	-	+
StB.eD	Sterilized	30:10:20	-
StB	Sterilized	-	-

Once the microcosms were completed, the borosilicate bottles were sealed with butyl-rubber stoppers and degassed with N_2 to eliminate oxygen and create anaerobic conditions. Subsequently, microcosms were incubated at 28 ºC for one year. The workflow of the microcosms set-up is shown in **Fig. 2**. Samples from the different components (supernatant, bentonite slurry, and Cu-mCan) were recovered aseptically within a glovebox for the different analyses.

2.6_ Geochemical analyses of the microcosm supernatant

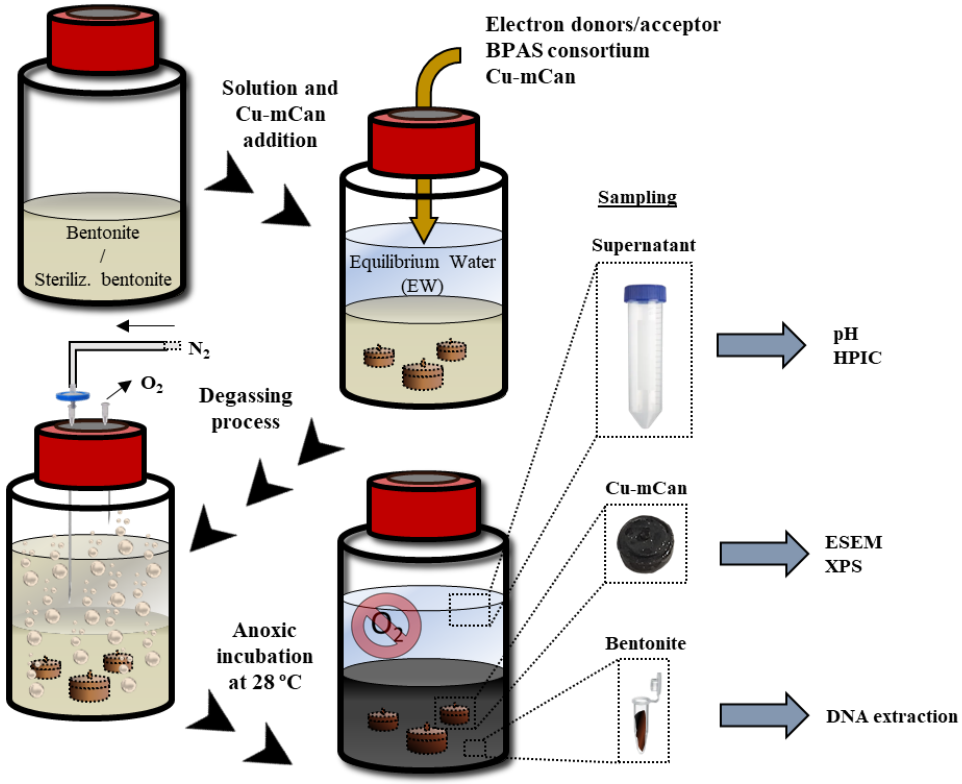

Fig. 2. Microcosms workflow, N_2 degassing process (anaerobic conditions), and sampling for the different analyses.

For the evolution of geochemical analysis, 5 mL of the supernatant (liquid phase) from each microcosm were collected at 45, 90, 135, and 365 days of incubation under anaerobic conditions, and filtered with 0.22 µm filter. The pH was measured by Advanced Digital Handheld Portable Meter HQ40D (Hach) previously calibrated with commercial reference solutions (4.00, and 7.00).

Acetate, lactate, and sulfate concentrations in the supernatants were quantified by High Pressure Ion Chromatography (HPIC). The analysis was performed in a 925 Eco ICE, Methrom Hispania (Herisau, Switzerland) coupled with an IC conductivity detector, a Metrohm Suppressor Module (MSM), 250 µL injection loop with peristaltic pump, Metrohm high pressure pump with purge valve and 919 UF autosampler. Before injection, samples were 0.22 µm filter-sterilized and

diluted in ultrapure water. The analyses of the target anions were investigated at room temperature, in suppressor mode using a column Metrosep A 5-250/4.0 (250 x 4.0 mm) with a pre-column Metrosep A Supp 5 Guard/4.0 (Methrom Hispania - Herisau, Switzerland) at a flow rate of 0.7 mL min^{-1}. The mobile phase used was 3.2 mM Na_2CO_3 / $NaHCO_3$ 1 mM. MSM-Metrohm Suppressor Module for chemical suppression was used with an aqueous solution of H_2SO_4 250 mM and 10 mM oxalic acid and 10% acetone. The calibration of the instrument was done by injecting standard solution of the target compounds. Data was analyzed with MagIC Net 3.1 basic software for ion chromatography. The standard solutions of acetate ($C_2H_3O_2^-$), sulfate (SO_4^{2-}), and lactate ($C_3H_5O_3^-$) with 1,000 mg L^{-1} concentration were provided from Sigma-Aldrich (Madrid, Spain) as well as oxalic acid and Na_2CO_3 / $NaHCO_3$. The H_2SO_4 and acetone were provided by VWR (Madrid, Spain).

2.7_ DNA extraction, sequencing, and computational procedure

DNA extraction was performed for each microcosm (total samples: 24) following the procedure detailed in Povedano-Priego et al. (2021). Subsequent, the extracted DNA concentration was determined using Qubit 3.0 Fluorometer (Life Technology, Invitrogen™).

For the library preparation, two consecutive PCR reactions were carried out for each sample using a combination of regular and barcoded fusion primers. To amplify the V5-V6 variable regions of the 16S rRNA gene, the following primers were used: 807F (5′-GGATTAGATACCCBRGTAGTC-3′) and 1050R (5′-AGYTGDCGACRRCCRTGCA-3′) as described by Bohorquez et al. (2012). The first PCR reaction proceeded as one initial cycle at 95 ºC for 15 minutes, followed by 35 cycles of 98 °C for 10 seconds, 55 °C for 10 seconds, and 72 °C for 45 seconds. Concluding, there was a final extension step at 72 °C for 2 minutes. The same conditions were applied for the second PCR reaction (barcoding step), with

only 10 PCR cycles. The quality of the library product was assessed through electrophoresis. To generate the FastaQ files, libraries were sequenced using the MiSeq Illumina platform (2 × 250 bp, Hayward, California, USA).

FastaQ files were processed and normalized employing “dada2” and “phyloseq” packages, respectively, in R 4.2.1 software (R Core Team, 2022). Bayesian classification was employed to assign the phylotypes to a taxonomic affiliation (80% pseudo-bootstrap threshold). The relative abundances and alpha diversity indices were conducted using Explicet 2.10.5 (Robertson et al., 2013). To assess the similarity between samples at genus level, a matrix based on the Bray-Curtis algorithm was used, and subsequent similarity between samples was performed through Principal Coordinate Analysis (PCoA) using Past4 software (Hammer et al., 2001). Furthermore, a heatmap was performed to visualize taxa with more than 0.50% relative abundance. For this purpose, the 'heatmap.2' function was employed in R software.

2.8_ Surface characterization of the copper mini canisters (Cu-mCan)

After 45 days of anoxic incubation, the Cu-mCan were removed from the microcosms, unscrewed, and dried under anaerobic atmosphere. To visualize corrosion compounds on the surface, the base of the Cu-mCan was metallized with a carbon coating through evaporation by an EMITECH K975X Carbon Evaporator for analysis by High Resolution Scanning Electron Microscopy (HRSEM) with an AURIGA Carl Zeiss SMT microscope associated with a qualitative and quantitative energy dispersive X-ray energy dispersive (EDX) microanalysis.

Moreover, no previous preparation was applied to the lids of the Cu-mCan for spectroscopic analysis. The chemical analysis by X-ray photoelectron spectroscopy (XPS) of the lid’s surface was conducted on a Kratos AXIS Supra Photoelectron Spectrometer. A monochromatic Al Kα (1486.6 eV) source operating at an X-ray emission current of 20 mA and a high anode voltage

(accelerating voltage) of 15 kV was used. The acquisition angle was set at 90° with respect to the sample plane. Data were collected from three randomly selected positions, with each acquisition area forming a rectangle of approximately 110 μm x 110 μm (FOV2 target). The analysis comprised a broad probe scan (160 eV pass energy, 1.0 eV step size) and a high-resolution scan (20 eV pass energy, 0.1 eV step size) for component speciation. To counteract the differential charge, an integral Kratos charge neutralizer was used. Au $4f_{5/2}$ (83.9 eV), Cu $2p_{3/2}$ (932.7 eV) and $Ag3d_{5/2}$ (368.27 eV) lines of clean gold, copper and silver standards from the National Physical Laboratory (NPL), UK, were employed for the calibration of the binding energy. Finally, CasaXPS 2.3.22 software (Fairley, 2019) was used to fit the peaks of the XPS spectra. All binding energies were offset by referencing the adventitious carbon C1s peak (285 eV). No further constraints were applied to the initial binding energy values.

3_ Results and discussion

3.1_ Water chemistry evolution

The pH values in the bentonite microcosm´s samples were slightly alkaline to neutral ranging between 9.09 and 7.43 (**Fig. 3**). The addition of nutrients (acetate, lactate, and sulfate) solutions and bacterial consortium (BC) decreased the initial pH value (time 0) compared to that of the control samples. Untreated bentonite is expected to have an initially alkaline pH around 9.00 due to its innate buffering capacity (Povedano-Priego et al., 2019; Rozalén et al., 2009). After one-year incubation, pH values tended to become less alkaline and stabilize between 7.51 and 8.37 in all treatments, in contrast to the initial values as seen in **Fig. 3**. The observed pH decrease could be due to leaching of the bentonite or microbial activity (Fernández-Díaz 2004; Povedano-Priego et al., 2019). Moreover, microorganisms may prompt the generation of gases such as hydrogen (H_2),

methane (CH_4), and carbon dioxide (CO_2) leading to the observed decrease in pH values (Bagnoud et al., 2016).

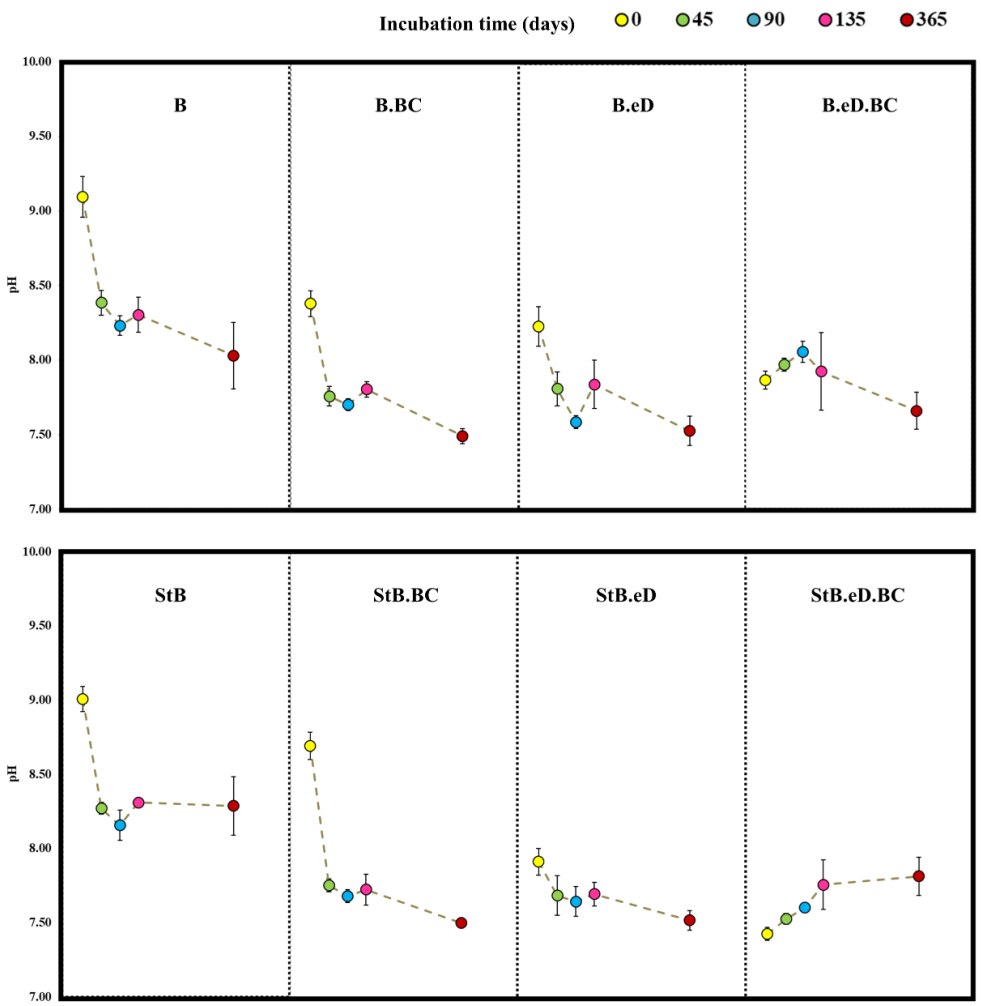

Fig. 3. pH evolution in hyper-saturated bentonite microcosms from time 0 to one-year incubation. Data were measured at time 0 (yellow), 45 (green), 90 (blue), 135 (pink) and 365 (red) days of incubation under anaerobic conditions. Data showed the mean values with standard derivations measured from three independent replicates. Glossary: Bentonite (B), Sterile bentonite (StB), amended with acetate, lactate and sulfate (eD); and with BPAS consortium (BC).

The evolution of the lactate, acetate and sulfate content of the amended samples (eD) are shown in **Fig. 4**. Lactate was the first electron donor to be consumed. In the microcosms spiked with bacterial consortium (B.eD.BC), lactate consumption

was completely achieved at 45 days of incubation (**Fig. 4A**), in contrast to the sterile counterpart (StB.eD.BC) where lactate consumption was achieved after 45 days. The microcosms lacking the bacterial consortium (B.eD and StB.eD) displayed a gradual lactate consumption, reaching the 100% at 135 days and 365 days, respectively. **Fig. 4B** represents the evolution of acetate content. Sample B.eD.BC showed a gradual consumption of acetate following lactate consumption, nearly exhausted after one year of incubation. In the remaining treatments, an increase in acetate content was observed, followed by a consumption that, depending on the treatment, reached 100% at one year of incubation as occurred in B.eD. However, the evolution of sulfate (as electron acceptor) showed slightly differences depending on the samples (**Fig. 4C**). Similar to the electron donors (lactate and acetate) observations, the sulfate consumption was higher in the non-sterilized samples containing the bacterial consortium (B.eD.BC). On the other hand, sulfate content in B.eD, StB.eD.BC, and StB.eD treatments remained relatively stable until reached a content of ~ 20-30% at one-year incubation.

The results clearly demonstrated that the addition of the bacterial consortium (BC samples) led to a faster depletion of acetate, lactate, and sulfate within the microcosms. In contrast, this process was slower in the sterile samples. Additionally, the increase in acetate content was correlated with the consumption of lactate and, to a lesser extent, sulfate. The conversion of lactate to acetate, CO_2, and H_2 can be mediated by SRB in the absence of sulfate and in presence of H_2O (Pankhania et al., 1988). Moreover, in our study, the gradual consumption of sulfate in the samples B.eD.BC and, after 135 days of incubation in the rest of the samples, in agreement with the results found by Matschiavelli et al. (2019). They observed a decrease in lactate and sulfate concentrations concomitant with acetate formation in B25 Bavarian bentonite microcosms. Their study deduced that lactate was metabolized through the reductive pathway of acetyl-CoA. This incomplete oxidation of lactate, coupled with the concurrent reduction of sulfate, gave rise to the formation of acetate and hydrogen sulfide. The presence of fissures in the

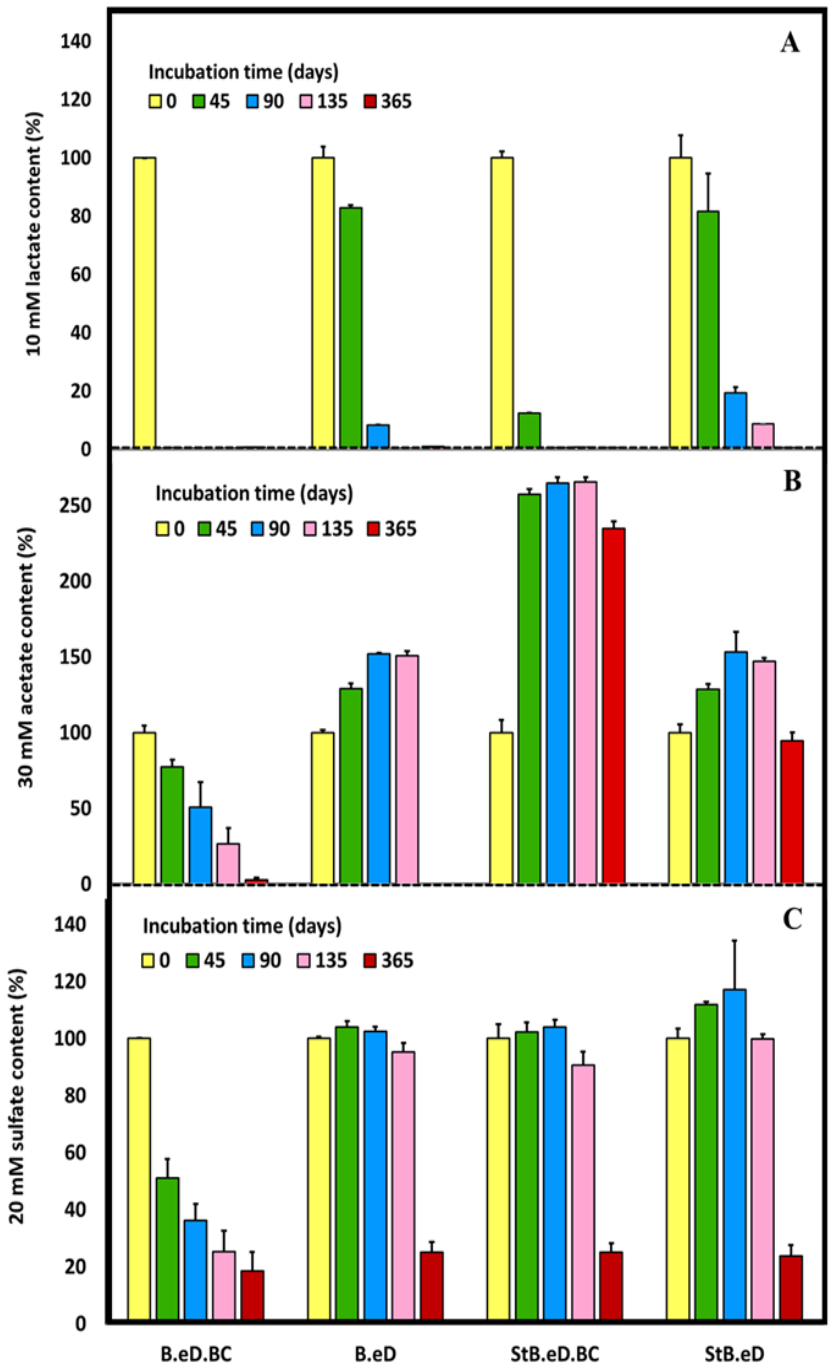

Fig. 4. Evolution of the initial concentration of 10 mM lactate (A), 30 mM acetate (B), and 20 mM sulfate (C) content recorded in Spanish bentonite microcosms incubated anaerobically at 30 ºC for 1 year. Data showed the mean values with standard derivations measured from three independent replicates. Glossary: Bentonite (B), Sterile bentonite (StB), amended with acetate, lactate and sulfate (eD); and with BPAS consortium (BC).

bentonite (white arrows in **Fig. 5**) and the formation of small bubbles in our microcosms could be related to gas generated from microbial activity. The rotten egg odor after sampling procedure could support also the hydrogen sulfide (H_2S) formation (He et al., 2011). The visual color changes reported in the bentonite microcosms during the incubation are also observed in **Fig. 5**. A shift towards black hues was evidenced in the treatment containing the bacterial consortium (B.eD.BC), with this transformation occurring at a slower rate when the bentonite was sterilized (StB.eD.BC). Subsequently, the treatments lacking the bacterial consortium (B.eD, and StB.eD) exhibited similar color changes, although with lower progression. The alteration in the color of the bentonite may be linked to the generation of H_2S, a byproduct of bacterial activity, which can react with iron and lead to the formation of black precipitates of reduced iron species (Miettinen et al., 2022; Matschiavelli et al., 2019).

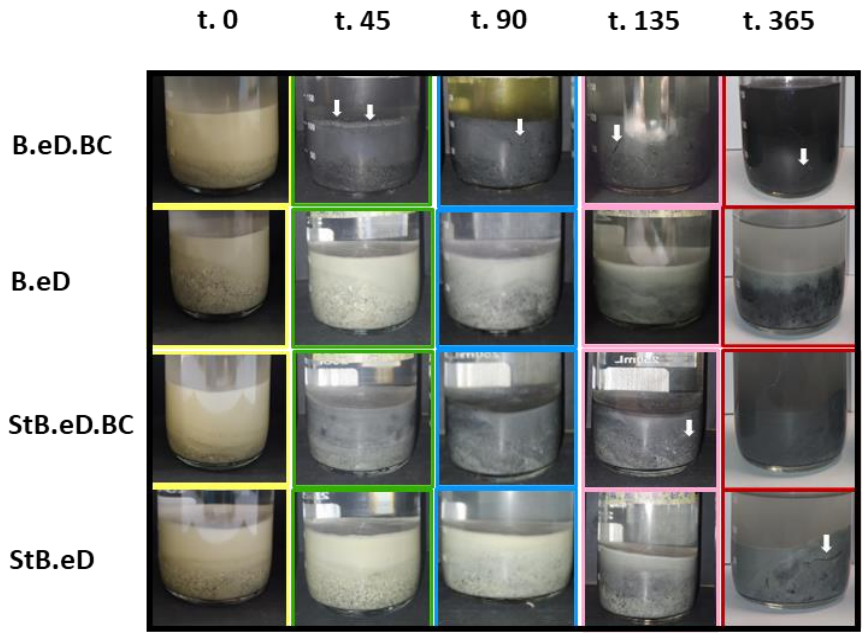

Fig. 5. Evolution of hyper-saturated Spanish bentonite microcosms before (yellow) and after 45 (green), 90 (blue), 135 (pink) and 365 (red) days of anaerobic incubation at 30 ºC. White arrows indicate the development of fissures and cavities attributed to gas formation. Glossary: Bentonite (B), Sterile bentonite (StB), amended with acetate, lactate and sulfate (eD); and with BPAS consortium (BC).

3.2_ Characterization of microbial communities in an early incubation stage

To get a thorough comprehension of early-stage geochemical changes and their influence on copper corrosion, it is necessary to characterize the microbial communities within each treatment. To achieve this, the total DNA from the different bentonite microcosms after 45 days of anaerobic incubation was extracted and sequenced in triplicate (duplicate in sample StB.eD). This section is focused on characterizing the structure and composition of bacterial communities in the different treatments: tyndallized (StB), presence of electron donors/acceptor (eD), and addition of the bacterial consortium (BC) in the early-stage of incubation (45 days) in view of study their early-stage influence in the corrosion of copper material (see 3.3. section).

For these samples, enough sequencing depth was achieved as shown by the rarefaction curves (**Supplementary Fig. S1**). A total of 412 phylotypes were detected and annotated in 13 phyla (98.06%) being Proteobacteria (74.63%), Firmicutes (19.74%), and Actinobacteria (2.67%) the most abundant phyla (**Supplementary Table S2**). At genus level, the phylotypes were annotated in 110 OTUs (**Supplementary Table S3**) with *Pseudomonas* (43.35%), *Stenotrophomonas* (13.41%), unclassified Clostridiales (4.75%), *Pseudoalteromonas* (4.64%), *Symbiobacterium* (4.24%), *Desulfocurvibacter* (3.08%), unclassified Firmicutes (2.98%), and *Desulfuromonas* (2.89%) presenting the higher relative abundance in the pool of the samples.

Richness (Sobs), diversity (ShannonH and SimpsonD), and evenness (ShannonE) indices at the genus level of the samples are presented in **Table 2**. The richness indices of unsterilized treatments reveal higher values in samples lacking bacterial consortium, and these values are greater in the absence of electron donors and sulfate (richness values B > B.eD > B.eD.BC > B.BC). In contrast, the dynamics in the sterilized treatments (StB) seem to be slightly different, with higher richness

values in the samples amended with electron donors and sulfate, while the presence of the consortium seemed to affect the richness indices diminishing the effect of electron donors (richness values StB.eD > StB.eD.BC > StB > StB.BC). These results are supported by the diversity indices (ShannonH and SimpsonD) showing the same trends in the samples (**Table 2**). The microcosms without bacterial consortium showed greater diversity values (ShannonH > 3, and SimpsonD close to 1) than those spiked with the bacterial consortium (BC), indicating that the addition of this consortium results in a displacement of the indigenous bentonite microbial community and the domination of specific taxa within the samples (ShannonH < 3, and SimpsonD further from 1).

Table 2.

Richness (Sobs), diversity (ShannonH. and SimpsonD), and evenness (ShannonE) indices. Glossary: Bentonite (B), Sterile bentonite (StB), amended with acetate, lactate and sulfate (eD); and with BPAS consortium (BC).

Sample ID	Sobs	ShannonH	ShannonE	SimpsonD
B.eD.BC	25.90	2.01	0.43	0.51
B.eD	29.26	3.35	0.69	0.86
B.BC	18.15	1.23	0.29	0.36
B	53.69	3.76	0.66	0.88
StB.eD.BC	39.68	2.03	0.38	0.59
StB.eD	41.00	3.31	0.62	0.82
StB.BC	15.39	1.65	0.42	0.58
StB	25.46	3.55	0.76	0.90

In order to analyze the dissimilarity and diversity distribution along different microcosms considering the relative abundance at genus level, samples were grouped by a Principal Coordinate Analysis (PCoA) based on Bray-Curtis distance (**Fig. 6**). The dissimilarity between samples containing the bacterial consortium and those lacking it was evidenced. The treatments containing bacterial consortium (BC samples) were grouped separately from the other treatments, indicating that the treatments lacking bacterial consortium showed a more heterogeneous distribution.

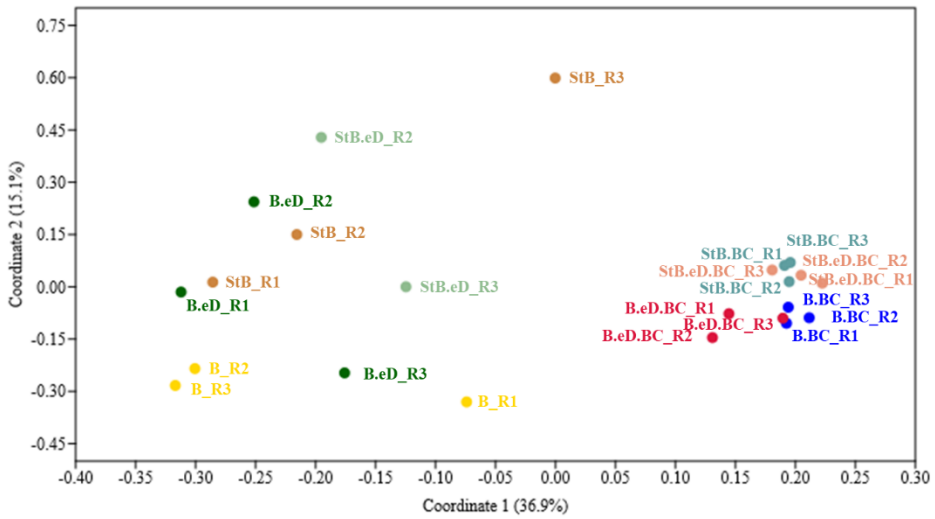

Fig. 6. Principal coordinate analysis (PCoA) plot showing the dissimilarity of bacterial communities at genus level from bentonite-slurry microcosms after 45 days of anaerobic incubation. Glossary: Bentonite (B), Sterile bentonite (StB), amended with acetate, lactate and sulfate (eD); and with BPAS consortium (BC).

Moreover, a heatmap was constructed to confirm the similarity between samples (**Fig. 7**). As observed, the clustering of BC samples is primarily attributed to the prevalence of bacterial genera from the BPAS consortium, notably *Pseudomonas* and *Stenotrophomonas*, which dominate the microbial communities of these microcosms. In contrast, for samples lacking a bacterial consortium, a slight differentiation was observed between samples with sterilized bentonite (StB) and those with non-sterilized bentonite (B) possibly due to the negative effect of the tyndallization process on the microbial diversity of the bentonite (Martinez-Moreno et al., 2023; Povedano-Priego et al., 2023). However, such differentiation was not observed concerning the absence or the presence (eD) of electron donors and sulfate. The main difference between microcosms amended with electron donors and sulfate (B.eD) and those without (B) resided in the presence of bacterial genera such as *Pseudoalteromonas* (24.17%), *Desulfocurvibacter* (22.72%), *Anaerosolibacter* (4.54%), *Desulfosporosinus* (4.54%), and unclassified microbes belonging to the highly diverse order Bacillaes (3.70%) in sample B.eD. Although *Pseudoalteromonas* is an aerobic bacterium, some strains isolated from deep-sea

sediments have adaptive mechanisms to tolerate low oxygen concentrations (Qin et al., 2011) which support the distribution of *Pseudoaltermonas* in the anoxic microcosms. Moreover, the strictly anaerobes *Desulfocurvibacter*, *Anaerosolibacter* and *Desulfosporosinus* can use sulfate and/or iron as electron acceptor to grow in the presence of organic substrates (e.g., lactate) (Spring et al., 2019; Hong et al., 2015; Hippe and Stackebrandt, 2015).

As shown in the heatmap (**Fig. 7**), the dominant genera in the consortium-spiked treatments (BC) were those of the consortium, *Pseudomonas* (54.59% - 78.88%) and *Stenotrophomonas* (34.96% - 8.10%) (**Supplementary Table S3** and **Figure 8**). *Amycolatopsis*, was detected in lower relative abundance in the BC microcosms exhibiting higher abundance in B.eD.BC and StB.eD.BC samples (2.31% and 2.05%, respectively). In contrast, the presence of *Amycolatopsis* was lower or undetectable in the samples without electron donors and sulfate: 0.12% and 0% (B.BC and StB.BC, respectively). Regarding *Bacillus* genera, was outside the detection range in the samples. *Pseudomonas putida* and *Stenotrophomonas bentonitica* are bacterial strains capable of growing or maintaining their activity under anaerobic conditions, while also exhibiting the ability to use acetate and/or lactate as a carbon source (Freikowski et al., 2010; Sanchez-Castro et al., 2017). *Pseudomonas* was also detected in the microcosms without bacterial consortium with a remarkable relative abundance of 9.80% (B.eD), 19.11% (B), 16.48 (StB.eD), and 9.91% (StB). On the other hand, *Stenotrophomonas* was only detected in the sterile controls (StB.eD and StB) with a 2.66% and 13.98% of relative abundance, respectively.

As observed in the chemical evolution data (**Fig. 4**), samples spiked with bacterial consortium (BC) showed the highest rate of lactate consumption after 45 days of incubation. Subsequently, these samples displayed the generation and subsequent consumption of acetate, dependent on whether the bentonite was pre-sterilized (StB) or not. *Pseudomonas* and *Stenotrophomonas* could be key contributors to the

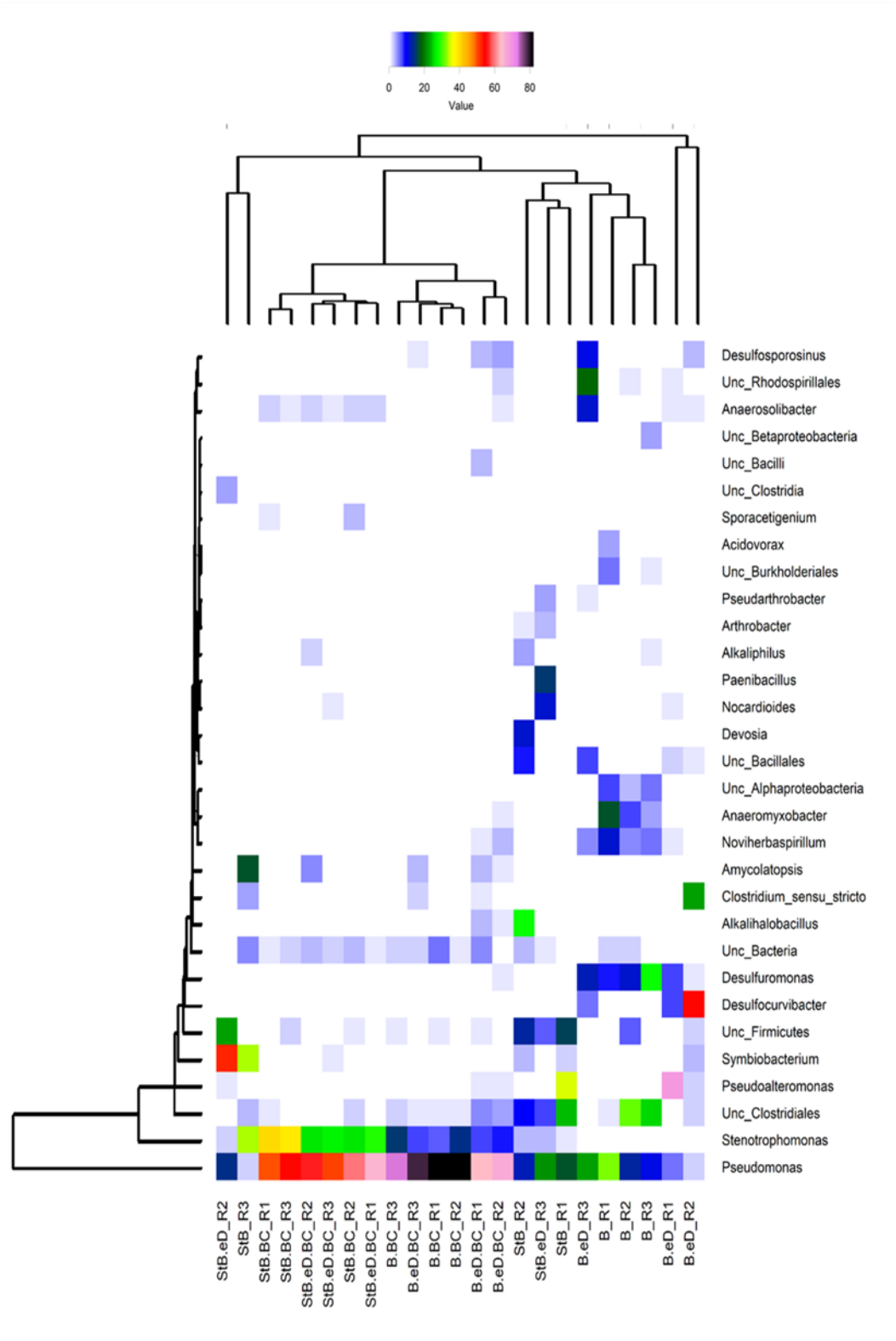
0
20
40
60
80
Value
Desulfosporosinus
Unc_Rhodospirillales
Anaerosolibacter
Unc_Betaproteobacteria
Unc_Bacilli
Unc_Clostridia
Sporacetigenium
Acidovorax
Unc_Burkholderiales
Pseudarthrobacter
Arthrobacter
Alkaliphilus
Paenibacillus
Nocardioides
Devosia
Unc_Bacillales
Unc_Alphaproteobacteria
Anaeromyxobacter
Noviherbaspirillum
Amycolatopsis
Clostridium_sensu_stricto
Alkalihalobacillus
Unc_Bacteria
Desulfuromonas
Desulfocurvibacter
Unc_Firmicutes
Symbiobacterium
Pseudoalteromonas
Unc_Clostridiales
Stenotrophomonas
Pseudomonas
StB.eD_R2
StB_R3
StB.BC_R1
StB.BC_R3
StB.eD.BC_R2
StB.eD.BC_R3
StB.BC_R2
StB.eD.BC_R1
B.BC_R3
B.eD.BC_R3
B.BC_R1
B.BC_R2
B.eD.BC_R1
B.eD.BC_R2
StB_R2
StB.eD_R3
StB_R1
B.eD_R3
B_R1
B_R2
B_R3
B.eD_R1
B.eD_R2

Fig. 7. Heatmap representing genus-level relative abundance and clustering based on Manhattan distance of the slurry-bentonite microcosms after 45 days of incubation. The 3.3% cut-off based on the maximums represents the 31 most abundant genera. The relative abundance of each genus is shows with different colors (the warmer the color, the greater relative abundance). Glossary: Bentonite (B), Sterile bentonite (StB), amended with acetate, lactate and sulfate (eD); and with BPAS consortium (BC).

observed trend of lactate consumption and acetate production/consumption in samples amended with electron donors/acceptor (eD) (Essén et al., 2007; Eschbach et al., 2004; Ruiz-Fresneda et al., 2019; Sanchez-Castro et al., 2017). Moreover, in sample B.eD.BC, the presence of the sulfate-reducing bacterium *Desulfosporosinus* (**Supplementary Table S3** and **Fig. 8**) was evidenced (2.62%). This bacterium is involved in the incomplete oxidation of substrates, such as lactate, to acetate, and in the use of sulfate as a terminal electron acceptor (Spring and Rosenzweig, 2006). This fact could be linked to the sulfate consumption (≈

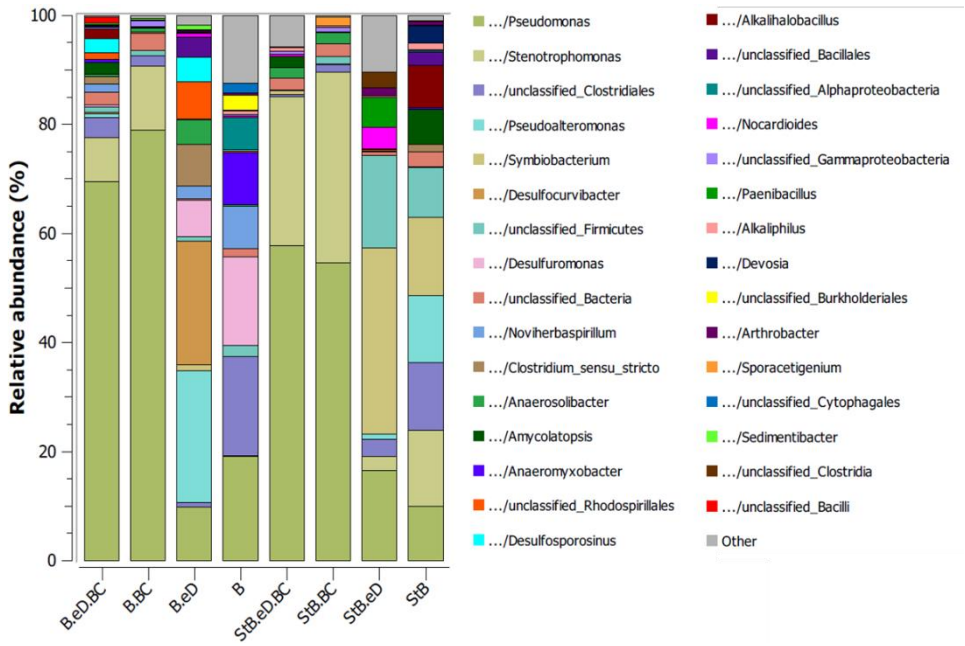

Fig. 8. OUT relative abundance of bacterial communities from the slurry-bentonite microcosms. Cutoff: 0.20% of relative abundance. Stacked bars show averages of biological replicates. Glossary: Bentonite (B), Sterile bentonite (StB), amended with acetate, lactate and sulfate (eD); and with BPAS consortium (BC).

50%) within this sample at the 45-day mark (**Fig. 4C**). In contrast, sample StB.eD.BC did not show sulfate reduction **(Fig. 4C**). This could be attributed to the absence of *Desulfosporosinus* in this treatment and the presence of the IRB and SRB *Anaerosolibacter* (1.83%; **Supplementary Table S3** and **Fig. 8**). The bioreduction of Fe(III) to Fe(II) occurs under less reducing conditions than sulfate. Therefore, the presence of this bacterial genus may indicate that the redox conditions are not yet optimal for sulfate reduction to occur.

The addition of electron donors and sulfate in samples not spiked with bacterial consortium appears to enhance the prevalence of bacterial genera such as *Desulfocurvibacter* (obligately anaerobic SRB that incompletely oxidize organic substrates to acetate), *Pseudoalteromonas* (IRB under low content of oxygen), *Anaerosolibacter* (IRB and SRB), and *Desulfosporosinus* (anaerobic bacteria that reduce sulfate through the incomplete oxidation of lactate to acetate) (Spring et al., 2019; Cheng et al., 2019; Stackebrandt et al., 1997). These genera exhibit high diversity in sample B.eD (22.72%, 24.17%, 4.54%, and 4.54%, respectively), whereas they were not detected, or detected in a very low abundance, in sample B (< 0.2%) (**Supplementary Table S3** and **Fig. 8**). Despite the presence of SRB in the B.eD treatment, no observable sulfate consumption was detected (**Fig. 4C**). This lack of consumption could be attributed to the limited time available for this process (45 days), as IRB such as *Pseudomonas* (9.80%), *Anaerosolibacter* (4.54%), and *Pseudoalteromonas* (24.17%) might be actively engaged in the reduction of Fe(III) to Fe(II). This reduction process may continue until the redox conditions within the microcosms become favorable for sulfate reduction. Moreover, the most abundant genera in sample B were *Pseudomonas* (19.11%), unclassified Clostridiales (18.25%), *Desulfuromonas* (16.37%), *Anaeromyxobacter* (9.57%), and *Noviherbaspirillum* (7.77%) being less abundant in the B.eD treatment (**Supplementary Table S3** and **Fig. 8**). *Desulfuromonas* has the capacity to use acetate and lactate as oxidizing agents, linking with the reduction of sulfate and acetate (Liesack and Finster 1994). The occurrence of

Pseudomonas, *Anaeromyxobacter*, and *Noviherbaspirillum*, all facultative anaerobes, indicated their capability to use acetate and/or lactate as carbon sources (Shrestha et al., 2022; Sanford et al., 2002; Ishii et al., 2017). On the other hand, *Symbiobacterium* was the most abundant genus within sterilized samples without bacterial consortium (StB.eD: 34.11%, and StB: 14.39%). Bacterial species within this genus, including *S. turbinis* and *S. terraclitae*, are moderately anaerobic and thermophilic, with the characteristic of occasional endospore formation. Furthermore, these bacteria are capable of producing acetate as an end product (Shiratori-Takano et al., 2014). The presence of this bacterial genus within the StB.eD.BC sample could suggest a contribution to the increase in acetate content observed in this treatment after 45 days of incubation (**Fig. 4B**). Moreover, in the sterilized sample without a bacterial consortium (StB), *Stenotrophomonas* (13.98%), unclassified Clostridiales (12.39%), *Pseudoalteromonas* (12.36%), *Pseudomonas* (9.91%), unclassified Firmicutes (9.12%), the facultatively anaerobic *Alkalihalobacillus* (7.81%), and *Amycolatopsis* (6.44%), were the most prevalent bacterial genera following *Symbiobacterium*.

In summary, the addition of the bacterial consortium had an impact on the shift of indigenous bentonite microbial community. However, it is noteworthy that only *Pseudomonas* and *Stenotrophomonas* managed to persist and prevail in the BC microcosms after 45 days of incubation, whereas *Amycolatopsis* and *Bacillus* exhibited lower abundances or fell below the detection threshold of the sequencing procedure. On the other hand, the tyndallization (bentonite's pre-sterilization method) exerts a detrimental effect on bacterial diversity within the bentonite contributing to a reduction in the microbial variability. Furthermore, the presence of specific bacterial genera was intricately linked to the consumption of lactate, acetate and sulfate within the samples at 45 days of anaerobic incubation. Some bacteria (e.g., *Desulfosporosinus*) are able to partially oxidize lactate, associated with sulfate reduction, leading to the production of acetate. This acetate, in turn, could serve as a carbon source for other bacterial groups. Conversely, the addition

of electron donors and sulfate appears to stimulate the presence of IRB and SRB (e.g., *Desulfocurvibacter*, *Pseudoalteromonas*, *Anaerosolibacter*, and *Desulfosporosinus*). These groups of bacteria are involved in the corrosion of metal canisters within the DGR (Schütz et al., 2015; Bengtsson and Pedersen, 2017). However, the sulfate consumption was only detected at 45 days of incubation in the sample B.eD.BC (≈ 50%). Hence, it is crucial to investigate the potential impact of these bacterial groups on the corrosion of copper material and characterize the resulting products.

3.3_ Characterization of the Cu-mCan surface in an early-incubation stage

In order to assess the influence of the microbial communities on the corrosion of the copper surface after 45-day incubation, the Cu-mCan were recovered from the studied microcosms. The metal surfaces were analyzed by microscopic and spectroscopic techniques (HRSEM, EDX, and XPS). Specifically, the analysis focused on Cu-mCan from microcosms with non-sterilized bentonite.

The Cu-mCan images of samples before (t. 0) and after 45 days and their HRSEM micrographs are shown in **Fig. 9**. The bentonite adhered to the copper surface was not removed to avoid the consequent displacement of copper alteration-related products. Visually, the samples exhibited a different coloration after the incubation comparing with the blank (t. 0). The sample B.eD.BC presented a marked color transformation, shifting to dark gray-black hues, as well as some zones on Cu-mCan B.BC (**Fig. 9_B,C)**. At microscopic level, the samples after the incubation exhibit a heterogenous topography (second column, **Fig. 9**). The sample t. 0 displayed a uniform topography, revealing only the presence of Cu and C (attributable to the metallization process during the sample preparation for HRSEM). Furthermore, elemental EDX map of Iron (Fe), Carbon (C), Aluminum (Al), Sulfur (S), Silicon (Si), Oxygen (O), and Copper (Cu) distribution of the selected areas is shown (**Fig. 9)**. The signal of Si (pink), Fe (yellow), and Al (cyan)

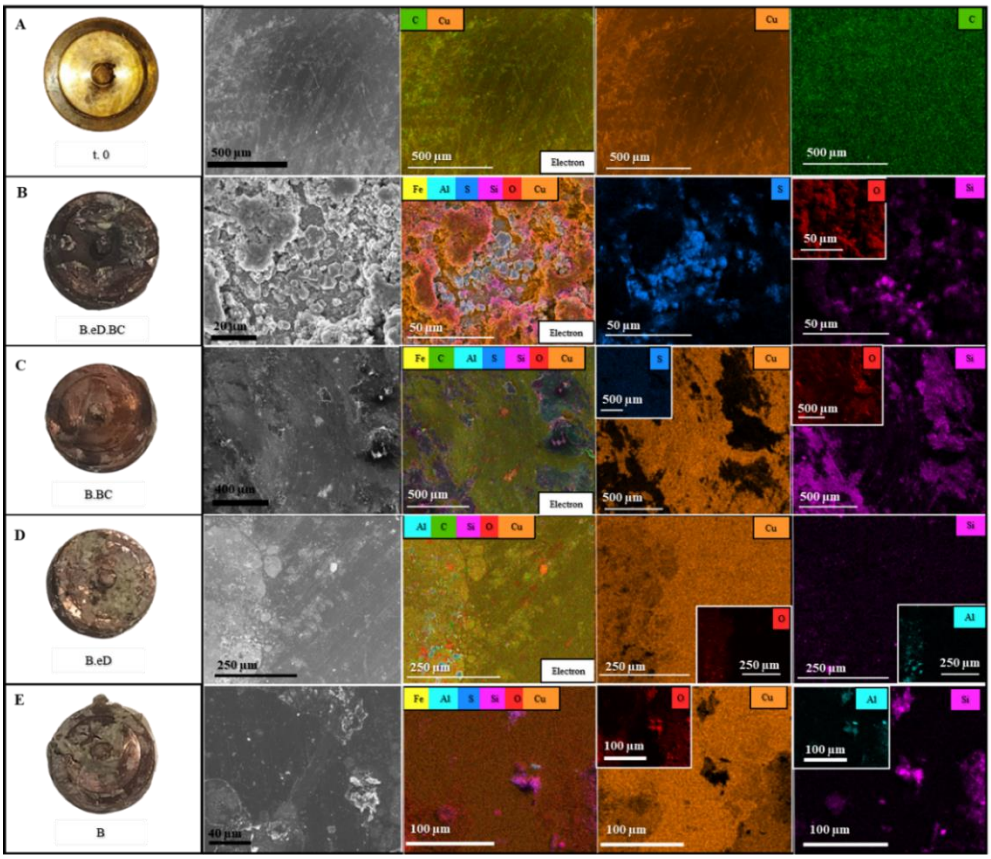

Fig. 9. Visual (first column), electron images (second column), and EDX maps of the Cu-mCan surface before experimental set-up (A) and after 45-days anoxic incubation from microcosms B.eD.BC (B), B.BC (C), B.eD (D), and B (E). EDX show the distribution of Cu (orange), Fe (yellow), S (dark blue), Si (pink), Al (cyan), O (red), and C (green) in the studied area. Glossary: Bentonite (B), amended with acetate, lactate and sulfate (eD); and with BPAS consortium (BC).

were attributed to the presence of bentonite adhered on the Cu surface. The detection of O (red) was mainly associated with Si (Si_xO) linking with the presence of bentonite. Moreover, O was also detected, to a lesser extent, on the copper surface (Cu_xO). Moreover, sulfur precipitates were only detected in the sample B.eD.BC, which may be related to Cu_xS (copper corrosion compounds) (**Fig. 9_B**) linking with the data of sulfate consumption (≈ 50%, **Fig. 4C**). Diffuse S accumulates distributed more dispersed manner were also detected in sample B.BC (**Fig. 9_C**). Furthermore, in sample B.eD, the presence of oxygen seemed to be

closely related to irregularities on the copper surface probably related to the presence of copper oxides (Cu_xO).

In order to identify the nature of the corrosion products, XPS analysis was undertaken in each Cu-mCan. Wide scans indicated the presence of Cu, C, O, Si, Na, Fe, Mg, and Al on all sample surfaces. With the exception of Cu, these elements were likely attributed to bentonite adhered to the Cu-mCan's surfaces. High-resolution scans of the Cu 2p region exhibited elemental copper peaks (sharp peaks at approximately 933 eV and 953 eV, corresponding to Cu $2p_{1/2}$ and Cu $2p_{3/2}$), alongside the likely presence of CuO (peaks around 943.49 eV and 962.89 eV) (Wagner et al., 1979), on all samples (**Fig. 10**). Further evidence for the existence of CuO included the separation of ≈ 20 eV between Cu $2p_{1/2}$ and Cu $2p_{3/2}$ (Wagner et al., 1979). It should be noted that no CuO was detected on the surface of the Cu-mCan prior to microcosms set up (time 0) as shown in the high-resolution spectra of the Cu2p (**Fig. 10**).

The main signal of MIC under anaerobic corrosion on copper materials are Cu_xS mediated by the activity of SRB (Hall et al., 2021). Previous studies indicate that peaks for CuS are typically observed around 932.2 eV in high-resolution Cu 2p scans (Krylova & Andrulevičius, 2009). In order to delve deeper into the overshadow of this peak by the Cu $2p_{3/2}$ peak, high-resolution scans were conducted in the S 2p region, spanning from 143 eV to 180 eV. This revealed the presence of sulfur on samples B.BC, B.eD.BC, and B.eD (**Fig. 10**). In samples B.BC and B.eD.BC, peaks related to the presence of Cu_2S (around 163 eV) were seen. This is a known corrosion product produced as a result of HS^- excretion from SRB activity (Martinez-Moreno et al., 2023; Yu et al., 1990). Moreover, the peak at 161.4 eV was assigned to CuS (Kutty, 1991). The peak around 154 eV, presented in all the Cu-mCan after 45-days incubation, was attributed to Si 2s in the form of SiO_2 (silicate) belonging to the presence of the bentonite adhered on the copper surface (Clarke & Rizkalla, 1976).

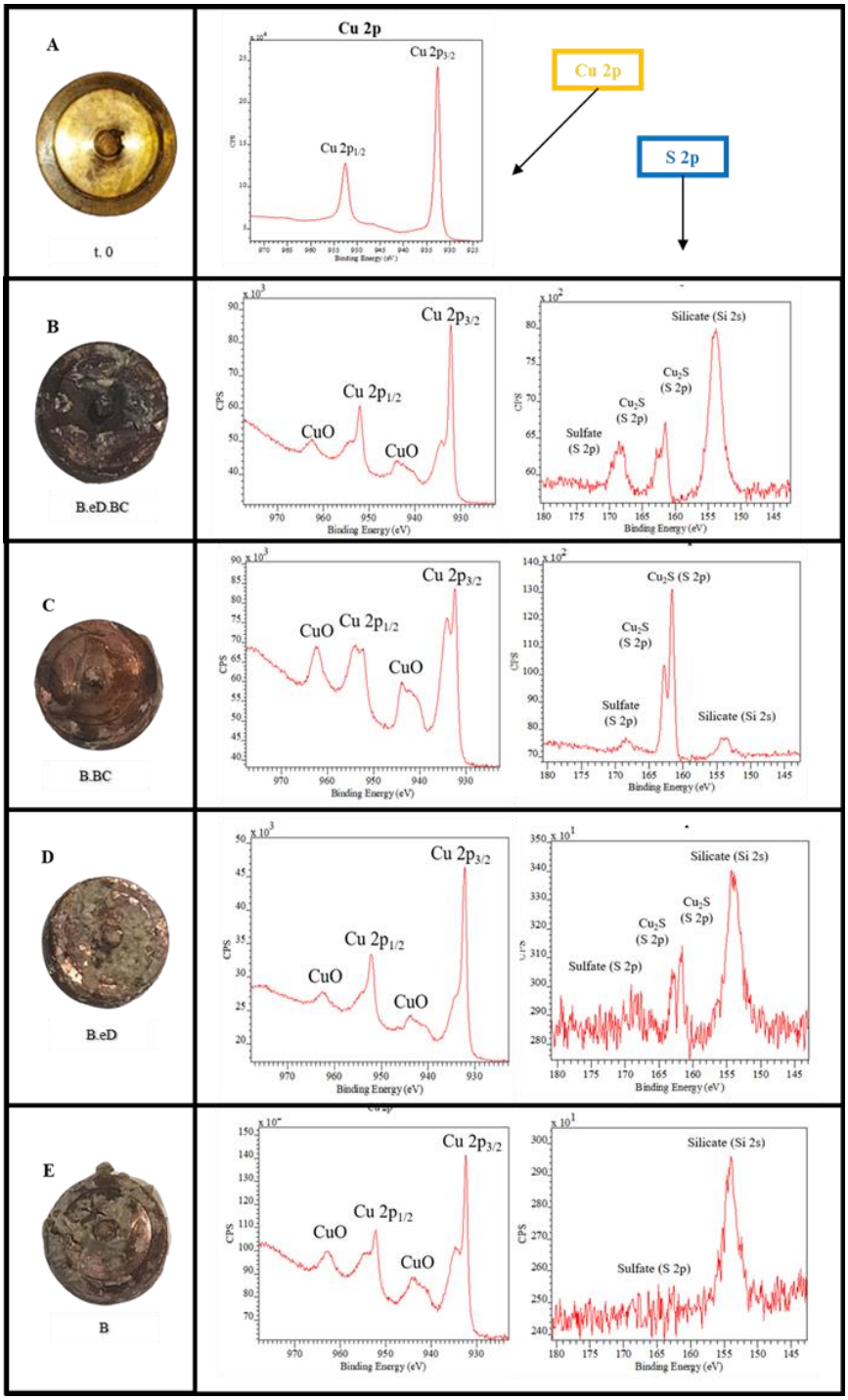

Fig. 10. High-resolution XPS spectra of the Cu 2p (977 eV – 922 eV) and S 2p (180 eV – 143 eV) regions of the Cu-mCan surface before experimental set-up (A) and after 45-days anoxic incubation from microcosms B.eD.BC (B), B.BC (C), B.eD (D), and B (E). Glossary: Bentonite (B), amended with acetate, lactate and sulfate (eD); and with BPAS consortium (BC).

Given that copper oxides (CuO) were identified on all Cu-mCan samples after 45 days of incubation, notably absent at t. 0, it can be inferred that the presence of oxygen, evidenced by CuO on the copper surface, occurred abiotically. The formation of the CuO species could be related to the oxygen molecules trapped in the bentonite or driven by the reduction of H_2O from the EW (Burzan et al., 2022; Huttunen-Saarivirta et al., 2016). Conversely, the identification of Cu_2S in the samples resulted from microbial influence. This observation was particularly pronounced on the surface of Cu-mCan from the treatment with electron donors/acceptor and the bacterial consortium (B.eD.BC), followed by the treatment only spiked with the bacterial consortium (B.BC). Additionally, a lesser extent of Cu_2S detection was detected in the treatment supplemented only with electron donors/acceptor (B.eD). In contrast, Cu_2S was not detected in treatment B (untreated bentonite) (**Fig. 9** and **Fig. 10**). Moreover, microscopic examination revealed the presence of precipitates of Cu_2S compounds exclusively in Cu-mCan from the treatment B.eD.BC (**Fig. 9**), aligning with the heightened presence of SRB within this treatment (**Fig. 8** and **Supplementary Table S3**).

The production of sulfide through the reduction of sulfate is kinetically hindered under standard abiotic conditions of temperature and pressure (Cross et al., 2004). Thus, the presence of sulfide is likely to be attributed to the activity of SRB (Bengtsson and Pedersen, 2017). Under anaerobic conditions SRB can oxidize lactate as electron donor coupled to sulfate reduction as terminal electron acceptor throw the dissimilatory sulfate reduction [**Eq. 1**: $SO_4^{2-} + 9H^+ + 8e^- \rightarrow HS^- + 4H_2O$] (Dou et al., 2020). The production of the sulfide in the microcosms was also inferred by the characteristic rotten egg smell in the microcosms (He et al., 2011). Interestingly, Salehi Alaei et al. (2023) observed the conversion of copper oxides (Cu_2O) to Cu_2S by a chemical substitution reaction between sulfide and the oxide [**Eq. 2**: $Cu_2O\ (s) + SH^-\ (aq) \rightarrow Cu_2S\ (s) + OH^-\ (aq)$]. Additionally, Dou et al. (2020) proposed that the resulting metabolite HS^-, from H_2S secreted by SRB, can diffuse to the surface and react with copper to form Cu_2S [**Eq. 3**: $2Cu + HS^- + H^+ \rightarrow Cu_2S$

(s) + H_2 (g)]. Chen et al. (2014) demonstrated that under anaerobic conditions, SRB can adhere to copper surfaces, forming a Cu_2S film as the primary corrosion product. The production of extracellular polymeric substances (EPS) from the SRB biofilm, and subsequently the Cu_2S film, mitigates the toxicity of copper toward SRB. In experiments with copper and different SRB strains, Kurmakova et al. (2019) found that these bacteria were accountable for Cu_2S corrosion products, with *Desulfovibrio* sp. M.4.1 showing the highest corrosive impact on the metal surface. The corrosion of high-purity copper in the presence of SRB in groundwater borehole or MX-80 clay has been demonstrated in other studies, where the presence of Cu_2S precipitates was detected (Johansson et al., 2017; Masurat et al., 2010). The addition of acetate, lactate, and sulfate to Spanish bentonite has been demonstrated to enhance bacterial activity, leading to the development of small corrosion compounds on copper discs within compacted bentonite blocks in the absence of water flow renewal after one year of anoxic incubation (Martínez-Moreno et al., 2023). The presence of an aqueous phase (EW) in this study accelerated this process, with corrosion compound formation observed in an early-stage of incubation (45 days).

4_ Study overview and conclusions

The surrounded environment of future DGR is considered hostile to organisms' survival (e.g., high temperature due to the decay process of the radionuclides, low water activity close to the canisters, high compaction of the bentonite, etc.). Thus, considering all possible scenarios is vital to prevent the release of radionuclides over periods of time spanning hundreds of thousands to millions of years and, therefore, to protect the biosphere and the future generations. The data presented in this work correspond to the elaboration of microcosms incubated in ideal conditions for microorganism's survival and activity: non-compacted bentonite, hyper-saturated, and amended with electron donors/acceptor. Although the DGR is designed to mitigate the diffusion of pore water into the canisters, the flow of

nutrients within the groundwater could be a possibility. Consequently, examining laboratory-scale models is crucial in generating insights under different scenarios.

This study described the geochemical evolution of the hyper-saturated bentonite microcosms over a year-long anaerobic incubation at 30 ºC, and in an early-stage microbial-community characterization and its influence in the corrosion of copper material. A trend towards pH stabilization was observed at less alkaline values ranging from 7.5 to 8.4, which could be linked to the effect of gas generation (e.g., H_2, CH_4, or CO_2) produced by microbial metabolism and the buffering properties of the bentonite. The consumption of lactate was the most pronounced, coupled with the formation of acetate and hydrogen sulfide in the microcosms. These finding were supported by the observation of fissures in the bentonite and the smell of rotten eggs after sampling. Moreover, the produced sulfide can react with the iron within the bentonite, causing their color change to grayish-blackish hues. It is important to highlight that the presence of a bacterial consortium, followed by the addition of electron donors/acceptor, significantly accelerated biogeochemical processes, whereas the pre-sterilization of the bentonite had a retarding effect.

The amended BPAS consortium was found to reduce the microbial diversity in the microcosms at the early stage (45 days), with *Pseudomonas* and *Stenotrophomonas* emerging as the predominant bacteria. Conversely, microcosms lacking BPAS consortium and amended with electron donors/acceptor or with pre-sterilized bentonite exhibited higher microbial diversity and heterogeneity. However, the addition of electron donors/acceptor helped with the stimulation of certain bacterial groups such as SRB, playing an important role in the formation of corrosion products on the copper surface.

Under anaerobic conditions, SRB are capable of oxidizing electron donors (e.g., lactate) coupled to sulfate reduction through dissimilatory sulfate reduction pathway. The produced sulfide could mediate the conversion of copper oxides

(possibly formed by trapped oxygen molecules on the bentonite or driven by the reduction of H_2O from the EW) to copper sulfide (Cu_2S) by a chemical substitution reaction between sulfides and oxides, or by the diffusion of and reaction of HS^- to copper.

Overall, microorganisms will play an important role in the geochemical evolution within the DGR and the stability of the different barriers could be compromised, emphasizing the impact of the SRB on the corrosion of the metal canisters, the gas generation, and the interaction with components of the bentonite.

Funding

The present work was supported by the grant RTI2018–101548-B-I00 "ERDF A way of making Europe" to MLM from the "Ministerio de Ciencia, Innovación y Universidades" (Spanish Government). The project leading to this application has received funding from the European Union's Horizon 2020 research and innovation program under grant agreement No 847593 to MLM. ADM acknowledges funding from the UK Engineering and Physical Sciences Research Council (EPSRC) DTP scholarship (project reference: 2748843).

Acknowledgements

The authors acknowledge the assistance of Dr. F. Javier Huertas (IACT, Spain) for his guidance and help in collecting the bentonite from the El Cortijo de Archidona site (Almería). Rahul (Instituto del Agua, University of Granada) for HPIC measurements. Moreover, Daniel García Muñoz Bautista Cerro and Alicia González Segura (Centro de Instrumentación Cientifica, University of Granada, Spain) for the sample preparation and microscopy assistance, respectively.

References

Bagnoud, A., De Bruijn, I., Andersson, A. F., Diomidis, N., Leupin, O. X., Schwyn, B., & Bernier-Latmani, R. 2016. A minimalistic microbial food web in an excavated deep subsurface clay rock. FEMS Microb. Ecol., 92(1), fiv138. https://doi.org/10.1093/femsec/fiv138

Batandjieva, B., Delcheva, T., Duhovnik, B. 2009. Classification of radioactive waste: safety guide: IAEA General Safety Guide GSG-1. Vienna. International Atomic Energy Agency.

Bengtsson, A., Pedersen, K. 2017. Microbial sulphide-producing activity in water saturated Wyoming MX-80, Asha and Calcigel bentonites at wet densities from 1500 to 2000 kg m^{-3}. Appl. Clay Sci. 137, 203-212. https://doi.org/10.1016/j.clay.2016.12.024

Bohorquez, L.C., Delgado-Serrano, L., López, G., Osorio-Forero, C., Klepac-Ceraj, V., Kolter, R., Junca, H., Baena, S., Zambrano, M.M. 2012. In-depth Characterization via Complementing Culture-Independent Approaches of the Microbial Community in an Acidic Hot Spring of the Colombian Andes. Micro Ecol. 63, 103–115. https://doi.org/10.1007/s00248-011-9943-3

Cheng, S., Li, N., Jiang, L., Li, Y., Xu, B., & Zhou, W. 2019. Biodegradation of metal complex Naphthol Green B and formation of iron–sulfur nanoparticles by marine bacterium *Pseudoalteromonas* sp CF10-13. Bioresour. Technol., 273, 49-55. https://doi.org/10.1016/j.biortech.2018.10.082

Chen, S., Wang, P., Zhang, D. 2014. Corrosion behavior of copper under biofilm of sulfate-reducing bacteria. Corros. Sci. 87, 407 – 415. http://dx.doi.org/10.1016/j.corsci.2014.07.001

Clarke, T. A., & Rizkalla, E. N. 1976. X-ray photoelectron spectroscopy of some silicates. Chem. Phys. Lett., 37(3), 523-526. https://doi.org/10.1016/0009-2614(76)85029-4

Cross, M.M., Manning, D.A., Bottrell, S.H., Worden, R.H. 2004. Thermochemical sulphate reduction (TSR): experimental determination of reaction kinetics and implications of the observed reaction rates for petroleum reservoirs. Org. Geochem. 35, 393–404. https://doi.org/10.1016/j.orggeochem.2004.01.005

Dou, W., Pu, Y., Han, X., Song, Y., Chen, S., Gu, T. 2020. Corrosion of Cu by a sulfate reducing bacterium in anaerobic vials with different headspace volumes. Bioelectrochemistry, 133, 107478. https://doi.org/10.1016/j.bioelechem.2020.107478

Eschbach, M., Schreiber, K., Trunk, K., Buer, J., Jahn, D., & Schobert, M. 2004. Long-term anaerobic survival of the opportunistic pathogen *Pseudomonas aeruginosa* via pyruvate

fermentation. J. Bacteriol., 186(14), 4596-4604. https://doi.org/10.1128/jb.186.14.4596-4604.2004

Essén, S. A., Johnsson, A., Bylund, D., Pedersen, K., & Lundström, U. S. 2007. Siderophore production by *Pseudomonas stutzeri* under aerobic and anaerobic conditions. Appl. Environ. Microbiol.73(18), 5857-5864. https://doi.org/10.1128/AEM.00072-07

Fairley, N. CasaXPS, 2.3.22 ed.; Casa Software Ltd.: 2019.

Fernández, A.M. (2004). Caracterización y modelización del agua intersticial de materiales arcillosos: Estudio de la bentonita de Cortijo de Archidona. Editorial Ciemat. ISBN84-7834-479-9, 505 pp.

Freikowski, D., Winter, J., & Gallert, C. (2010). Hydrogen formation by an arsenate-reducing Pseudomonas putida, isolated from arsenic-contaminated groundwater in West Bengal, India. Appl. Microbiol. Biotechnol., 88, 1363-1371. https://doi.org/10.1007/s1201000988520

García-Romero, E., María Manchado, E., Suárez, M., and García-Rivas, J. 2019. Spanish bentonites: a review and new data on their geology, mineralogy, and crystal chemistry. Fortschr. Mineral. 9:696. https://doi.org/10.3390/min9110696

Guo, G., & Fall, M. 2021. Advances in modelling of hydro-mechanical processes in gas migration within saturated bentonite: A state-of-art review. Eng. Geol., 287, 106123. https://doi.org/10.1016/j.enggeo.2021.106123

Hall, D.S., Behazin, M., Binns, W.J., and Keech, P.G. 2021. An evaluation of corrosion processes affecting copper-coated nuclear waste containers in a deep geological repository. Prog. Mater. Sci. 118, 100766. https://doi.org/10.1016/j.pmatsci.2020.100766

Hammer, O. 2001. PAST: paleontological statistics software package for education and data analysis. Palaeontol. Electron. *http://palaeo-electronicaorg*

He, R., Xia, F. F., Wang, J., Pan, C. L., & Fang, C. R. 2011. Characterization of adsorption removal of hydrogen sulfide by waste biocover soil, an alternative landfill cover. J. Hazard. Mater., 186(1), 773-778. https://doi.org/10.1016/j.jhazmat.2010.11.062

Hippe, H., & Stackebrandt, E. 2015. *Desulfosporosinus*. Bergey's Manual of Systematics of Archaea and Bacteria, 1-10. https://doi.org/10.1002/9781118960608.gbm00660

Hong, H., Kim, S. J., Min, U. G., Lee, Y. J., Kim, S. G., Roh, S. W., ... & Rhee, S. K. 2015. *Anaerosolibacter carboniphilus* gen. nov., sp. nov., a strictly anaerobic iron-reducing

bacterium isolated from coal-contaminated soil. Int. J. Syst. Evol. Microbiol., 65(Pt_5), 1480-1485. https://doi.org/10.1099/ijs.0.000124

Huertas, F., Fariña, P., Farias, J., García-Siñeriz, J.L., Villar, M.V., Fernández, A.M., Martin, P.L., Elorza, F.J., Gens, A., Sánchez, M., Lloret, A., Samper, J., Martínez, M. Á. 2021. Full-scale Engineered Barriers Experiment. Updated Final Report 1994-2004.

Huttunen-Saarivirta, E., Rajala, P., & Carpén, L. 2016. Corrosion behaviour of copper under biotic and abiotic conditions in anoxic ground water: Electrochemical study. Electrochim. Acta, 203, 350-365. https://doi.org/10.1016/j.electacta.2016.01.098

Ishii, S., Ashida, N., Ohno, H., Segawa, T., Yabe, S., Otsuka, S., ... & Senoo, K. 2017. *Noviherbaspirillum denitrificans* sp. nov., a denitrifying bacterium isolated from rice paddy soil and *Noviherbaspirillum autotrophicum* sp. nov., a denitrifying, facultatively autotrophic bacterium isolated from rice paddy soil and proposal to reclassify *Herbaspirillum massiliense* as *Noviherbaspirillum massiliense* comb. nov. Int. J. Syst. Evol. Microbiol., 67(6), 1841-1848. https://doi.org/10.1099/ijsem.0.001875

Johansson, A.J., Lilja, C., Sjögren, L., Gordon, A., Hallbeck, L., Johansson, L. 2017. Insights from post-test examination of three packages from the MiniCan test series of coppercast iron canisters for geological disposal of spent nuclear fuel: impact of the presence and density of bentonite clay. Corros. Eng. Sci. Technol. 52, 54-60. https://doi.org/10.1080/1478422X.2017.1296224

Keech, P. G., Vo, P., Ramamurthy, S., Chen, J., Jacklin, R., Shoesmith, D. W. 2014. Design and development of copper coatings for long term storage of used nuclear fuel. Corros. Eng. Sci. Technol., 49(6), 425-430. https://doi.org/10.1179/1743278214Y.0000000206

Krylova, V., Andrulevičius, M. 2009. Optical, XPS and XRD studies of semiconducting copper sulfide layers on a polyamide film. Int. J. Photoenergy. https://doi.org/10.1155/2009/304308

Kurmakova, I., Kupchyk, O., Bondar, O., Demchenko, N., & Vorobyova, V. 2019. Corrosion of copper in a medium of bacteria sulfate reduction proceeding. J. Chem. Technol. Metall., 54, 2, 2019, 416-422.

Kutty, T. R. N. 1991. A controlled copper-coating method for the preparation of ZnS: Mn DC electroluminescent powder phosphors. Mater. Res. Bull., 26(5), 399-406. https://doi.org/10.1016/0025-5408(91)90054-P

Liesack, W., & Finster, K. 1994. Phylogenetic analysis of five strains of gram-negative, obligately anaerobic, sulfur-reducing bacteria and description of *Desulfuromusa* gen. nov., including

Desulfuromusa kysingii sp. nov., *Desulfuromusa bakii* sp. nov., and *Desulfuromusa succinoxidans* sp. nov. Int. J. Syst. Evol. Microbiol., 44(4), 753-758. https://doi.org/10.1099/00207713-44-4-753

Liu, D., Dong, H., Bishop, M.E., Zhang, J., Wang, H., Xie, S., Wang, S., Huang, L., Eberl, D.D. 2012. Microbial reduction of structural iron in interstratified illite-smectite minerals by a sulfate-reducing bacterium. Geobiology, 10, 150-162. https://doi.org/10.1111/j.1472-4669.2011.00307.x

Lopez-Fernandez, M., Vilchez-Vargas, R., Jroundi, F., Boon, N., Pieper, D., & Merroun, M. L. 2018. Microbial community changes induced by uranyl nitrate in bentonite clay microcosms. Appl. Clay Sci., 160, 206-216. https://doi.org/10.1016/j.clay.2017.12.034

Lopez-Fernandez, M., Fernández-Sanfrancisco, O., Moreno-García, A., Martín-Sánchez, I., Sánchez-Castro, I., Merroun, M.L. 2014. Microbial communities in bentonite formations and their interactions with uranium. Appl. Geochem. 49, 77-86. https://doi.org/10.1016/j.apgeochem.2014.06.022

Martinez-Moreno, M.F., Povedano-Priego, C., Morales-Hidalgo, M., Mumford, A.D., Ojeda, J.J., Jroundi, F., Merroun, M. L. 2023. Impact of compacted bentonite microbial community on the clay mineralogy and copper canister corrosion: a multidiskiplinary approach in view of a safe Deep Geological Repository of nuclear wastes. J. Hazard. Mater. 131940. https://doi.org/10.1016/j.jhazmat.2023.131940

Masurat, P., Eriksson, S., Pedersen, K. 2010. Microbial sulphide production in compacted Wyoming bentonite MX-80 under in situ conditions relevant to a repository for high-level radioactive waste. Appl. Clay Sci. 47, 58-64. https://doi.org/10.1016/j.clay.2009.01.004

Matschiavelli, N., Kluge, S., Podlech, C., Standhaft, D., Grathoff, G., Ikeda-Ohno, A., ... & Cherkouk, A. 2019. The year-long development of microorganisms in uncompacted bavarian bentonite slurries at 30 and 60 ºC. Environ. Sci. Technol. 2019, 53, 10514−10524. https://doi.org/10.1021/acs.est.9b02670

Meleshyn, A. 2011. Microbial processes relevant for long-term performance of radioactive waste repositories in clays. GRS-291. ISBN 978-3-939355-67-0. Available from: https://www.grs.de/sites/default/files/pdf/GRS-291.pdf

Miettinen, H., Bomberg, M., Bes, R., Tiljander, M., & Vikman, M. 2022. Transformation of inherent microorganisms in Wyoming-type bentonite and their effects on structural iron. Appl. Clay Sci., 221, 106465. https://doi.org/10.1016/j.clay.2022.106465

Ojovan, M.I.; Steinmetz, H.J. 2022. Approaches to Disposal of Nuclear Waste. Energies, 15, 7804. https://doi.org/10.3390/en15207804

Pankhania, I. P., Spormann, A. M., Hamilton, W. A., & Thauer, R. K. 1988. Lactate conversion to acetate, CO_2 and H_2 in cell suspensions of *Desulfovibrio vulgaris* (Marburg): indications for the involvement of an energy driven reaction. Arch. Microbiol. 150, 26–31 (1988). https://doi.org/10.1007/BF00409713

Payer, J. H., Finsterle, S., Apps, J.A., Muller, R.A. 2019. Corrosion performance of engineered barrier system in deep horizontal drillholes. Energies. 12, 1491. https://doi.org/10.3390/en12081491

Pentráková, L., Su, K., Pentrák, M., Stucki, J.W. 2013. A review of microbial redox interactions with structural Fe in clay minerals. Clay Miner. 48, 543-560. https://doi.org/10.1180/claymin.2013.048.3.10

Povedano-Priego, C., Jroundi, F., Solari, P. L., Guerra-Tschuschke, I., del Mar Abad-Ortega, M., Link, A., ... & Merroun, M. L. 2023. Unlocking the bentonite microbial diversity and its implications in selenium bioreduction and biotransformation: Advances in deep geological repositories. J. Hazard. Mater., 445, 130557. https://doi.org/10.1016/j.jhazmat.2022.130557

Povedano-Priego, C., Jroundi, F., Lopez-Fernandez, M., Shrestha, R., Spanek, R., Martín-Sánchez, I., Villar, M.V., ˇSevců, A., Dopson, M. Merroun, M.L. 2021. Deciphering indigenous bacteria in compacted bentonite through a novel and efficient DNA extraction method: Insights into biogeochemical processes within the Deep Geological Disposal of nuclear waste concept. J. Hazard. Mater. 408, 124600. https://doi.org/10.1016/j.jhazmat.2020.124600

Povedano-Priego, C., Jroundi, F., Lopez-Fernandez, M., Sánchez-Castro, I., Martin-Sánchez, I., Huertas, F.J., Merroun, M.L. 2019. Shifts in bentonite bacterial community and mineralogy in response to uranium and glycerol-2-phosphate exposure. Sci. Total Environ. 692, 219-232. https://doi.org/10.1016/j.scitotenv.2019.07.228

Qin, Q. L., Li, Y., Zhang, Y. J., Zhou, Z. M., Zhang, W. X., Chen, X. L., ... & Zhang, Y. Z. 2011. Comparative genomics reveals a deep-sea sediment-adapted life style of *Pseudoalteromonas* sp. SM9913. ISME J 5, 274–284. https://doi.org/10.1038/ismej.2010.103

R Core Team. 2022. R: A language and environment for statistical computing. R Foundation for Statistical Computing, Vienna, Austria. URL https://www.Rproject.org/

Robertson, C.E., Harris, J.K., Wagner, B.D., Granger, D., Browne, K., Tatem, B., Feazel, L.M., Park, K., Pace, N.R., Frank, D.N. 2013. Explicet: graphical user interface software for metadata-driven management, analysis and visualization of microbiome data. Bioinformatics, 29, 3100-3101. https://doi.org/10.1093/bioinformatics/btt526

Rozalén, M., Brady, P. V., & Huertas, F. J. 2009. Surface chemistry of K-montmorillonite: Ionic strength, temperature dependence and dissolution kinetics. J. Colloid Interface Sci., 333(2), 474-484. https://doi.org/10.1016/j.jcis.2009.01.059

Ruiz-Fresneda, M. A., Martinez-Moreno, M. F., Povedano-Priego, C., Morales-Hidalgo, M., Jroundi, F., & Merroun, M. L. 2023. Impact of microbial processes on the safety of deep geological repositories for radioactive waste. Front. Microbiol., 14, 1134078. https://doi.org/10.3389/fmicb.2023.1134078

Ruiz-Fresneda, M. A., Gomez-Bolivar, J., Delgado-Martin, J., Abad-Ortega, M. D. M., Guerra-Tschuschke, I., & Merroun, M. L. 2019. The bioreduction of selenite under anaerobic and alkaline conditions analogous to those expected for a deep geological repository system. Molecules, 24(21), 3868. https://doi.org/10.3390/molecules24213868

Salehi Alaei, E., Guo, M., Chen, J., Behazin, M., Bergendal, E., Lilja, C., ... & Noël, J. J. 2023. The transition from used fuel container corrosion under oxic conditions to corrosion in an anoxic environment. Mater. Corros., 74(11-12), 1690-1706. https://doi.org/10.1002/maco.202313757

Sanchez-Castro, I., Ruiz-Fresneda, M. A., Bakkali, M., Kämpfer, P., Glaeser, S. P., Busse, H. J., ... & Merroun, M. L. 2017. Stenotrophomonas bentonitica sp. nov., isolated from bentonite formations. Int. J. Syst. Evol. Microbiol., 67(8), 2779. https://doi.org/10.1099%2Fijsem.0.002016

Sanford, R. A., Cole, J. R., & Tiedje, J. M. 2002. Characterization and description of *Anaeromyxobacter dehalogenans* gen. nov., sp. nov., an aryl-halorespiring facultative anaerobic myxobacterium. Appl. Environ. Microbiol., 68(2), 893-900. https://doi.org/10.1128/AEM.68.2.893-900.2002

Schütz, M. K., Schlegel, M. L., Libert, M., & Bildstein, O. 2015. Impact of iron-reducing bacteria on the corrosion rate of carbon steel under simulated geological disposal conditions. Environ. Sci. Technol., 49(12), 7483-7490. https://doi.org/10.1021/acs.est.5b00693

Shelobolina, E.S., VanPraagh, C.G., Lovley, D.R. 2003. Use of ferric and ferrous iron containing minerals for respiration by Desulfitobacterium frappieri. Geomicrobiol. J. 20, 143-156. https://doi.org/10.1080/01490450303884

Shiratori-Takano, H., Akita, K., Yamada, K., Itoh, T., Sugihara, T., Beppu, T., & Ueda, K. 2014. Description of *Symbiobacterium ostreiconchae* sp. nov., *Symbiobacterium turbinis* sp. nov. and *Symbiobacterium terraclitae* sp. nov., isolated from shellfish, emended description of the genus *Symbiobacterium* and proposal of *Symbiobacteriaceae* fam. nov. Int. J. Syst. Evol. Microbiol., 64(Pt_10), 3375-3383. https://doi.org/10.1099/ijs.0.063750-0

Shrestha, R., Cerna, K., Spanek, R., Bartak, D., Cernousek, T., & Sevcu, A. 2022. The effect of low-pH concrete on microbial community development in bentonite suspensions as a model for microbial activity prediction in future nuclear waste repository. Sci. Total Environ., 808, 151861. https://doi.org/10.1016/j.scitotenv.2021.151861

Spring, S., Sorokin, D. Y., Verbarg, S., Rohde, M., Woyke, T., & Kyrpides, N. C. 2019. Sulfate-reducing bacteria that produce exopolymers thrive in the calcifying zone of a hypersaline cyanobacterial mat. Front. Microbiol., 10, 862. https://doi.org/10.3389/fmicb.2019.00862

Spring, S. & Rosenzweig, F. 2006. The genera *Desulfitobacterium* and *Desulfosporosinus*: taxonomy. The prokaryotes, 4, 771-786. DOI: 10.1007/0-387-30744-3_24.

Stackebrandt, E., Sproer, C., Rainey, F. A., Burghardt, J., Päuker, O., & Hippe, H. 1997. Phylogenetic analysis of the genus *Desulfotomaculum*: evidence for the misclassification of *Desulfotomaculum guttoideum* and description of *Desulfotomaculum orientis* as *Desulfosporosinus orientis* gen. nov., comb. nov. Int. J. Syst. Evol. Microbiol., 47(4), 1134-1139. https://doi.org/10.1099/00207713-47-4-1134

Villar, M.V., Fernández-Soler, J.M., Delgado Huertas, A., Reyes, E., Linares, J., Jiménez de Cisneros, C., Linares, J., Reyes, E., Delgado, A., Fernandez-Soler, J.M., Astudillo, J. 2006. The study of Spanish clays for their use as sealing materials in nuclear waste repositories: 20 years of progress. J. Iber. Geol. 32, 15-36.

Wagner, C.D., Riggs, W.M., Davis, L.E., Moulder, J.F., Muilenberg, G.E. 1979. Handbook of x-ray photoelectron spectroscopy: a reference book of standard data for use in x-ray photoelectron spectroscopy. Perkin-Elmer Corporation: Eden Prairie, MN.

WNA. World Nuclear Association. 2023. Storage and disposal of radioactive waste. https://www.world-nuclear.org/

Yu, X. R., Liu, F., Wang, Z. Y., & Chen, Y. 1990. Auger parameters for sulfur-containing compounds using a mixed aluminum-silver excitation source. J. Electron Spectrosc. Relat. Phenom., 50(2), 159-166. https://doi.org/10.1016/0368-2048(90)87059-W

Supplementary material for:

Microbial influence in hyper-saturated Spanish bentonite microcosms: Unveiling a-year long geochemical evolution and early-stage copper corrosion related to nuclear waste repositories

Marcos F. Martinez-Moreno[1,*], Cristina Povedano-Priego[1], Mar Morales-Hidalgo[1], Adam D. Mumford[2], Elisabet Aranda[3], Jesus J. Ojeda[2], and Mohamed L. Merroun[1]

[1]Faculty of Sciences, Department of Microbiology, University of Granada, Granada, Spain.

[2]Department of Chemical Engineering, Faculty of Science and Engineering, Swansea University, Swansea, United Kingdom

[3]Institute of Water Research, Department of Microbiology, University of Granada, Granada, Spain

Supplementary Table S1.

ICP-MS analysis of the major elements composition of the equilibrium water (EW).

Element	PPB
Be	1.19
Sc	6.05
V	5.24
Cr	0.00
Mn	38.21
Co	0.49
Ni	1.97
Cu	1.24
Zn	0.36
As	2.73
Y	1.07
Mo	0.30
Cd	0.04
In	0.01
Sn	4.00
Sb	1.16
Ba	7.01
Tl	0.01
Pb	1.46
Bi	0.36
Th	0.32
U	0.51

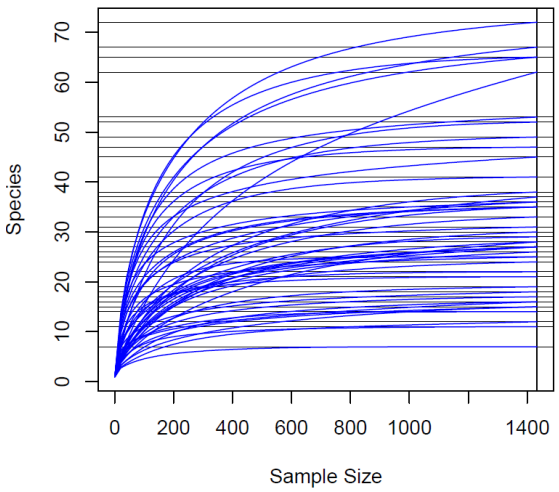

Supplementary Fig. S1. Rarefaction curves of the sequenced samples.

Supplementary Table S2.

Phyla relative abundance (%) of the bacterial phyla of the bentonite samples in triplicates (duplicates in StB.eD) Glossary: Bentonite (B), Sterile bentonite (StB), amended with acetate, lactate and sulfate (eD); and with BPAS consortium (BC).

	Total	B.eD.BC	B.eD	B.BC	B	StB.eD.BC	StB.eD	StB.BC	StB
Bacteria	100	100	100	100	100	100	100	100	100
>Acidobacteria	0.06	0.00	0.00	0.00	0.00	0.46	0.00	0.00	0.00
>Actinobacteria	2.67	2.45	1.38	0.12	1.74	3.42	9.50	0.00	7.26
>Bacteroidetes	0.74	0.19	0.36	0.00	4.50	0.96	0.14	0.00	0.00
>Candidatus_Saccharibacteria	0.03	0.00	0.00	0.00	0.12	0.07	0.09	0.00	0.00
>Chlamydiae	0.01	0.00	0.00	0.00	0.06	0.00	0.00	0.00	0.00
>Chloroflexi	0.00	0.00	0.00	0.00	0.00	0.00	0.00	0.00	0.00
>Cyanobacteria	0.06	0.00	0.00	0.00	0.41	0.00	0.14	0.00	0.00
>Firmicutes	19.74	12.20	23.94	4.53	21.90	5.80	64.14	7.23	49.64
>Gemmatimonadetes	0.02	0.00	0.00	0.00	0.15	0.00	0.00	0.00	0.00
>Ignavibacteriae	0.02	0.00	0.00	0.00	0.18	0.00	0.00	0.00	0.00
>Planctomycetes	0.02	0.00	0.00	0.00	0.18	0.00	0.00	0.00	0.00
>Proteobacteria	74.63	82.79	74.07	92.06	69.15	87.02	25.30	90.55	40.45
>Verrucomicrobia	0.03	0.00	0.00	0.07	0.15	0.00	0.00	0.00	0.00
> unclassified	1.97	2.36	0.26	3.22	1.47	2.26	0.69	2.22	2.65

Supplementary Table S3. OTU relative abundance (%) of the bacterial and archaeal communities of the bentonite samples in triplicates (duplicates in StB.eD). Some of the 0.00 values mean that the relative abundance of that OTU is <0.004 since are rounded to two decimal places. Glossary: Bentonite (B), Sterile bentonite (StB), amended with acetate, lactate and sulfate (eD); and with BPAS consortium (BC).

	Total	B.eD.BC	B.BC	B.eD	B	StB.eD.BC	StB.BC	StB.eD	StB
Pseudomonas	43.35	69.53	78.88	9.80	19.11	57.73	54.59	16.48	9.91
Stenotrophomonas	13.41	8.10	11.84	0.00	0.09	27.29	34.96	2.66	13.98
unclassified_Clostridiales	4.75	3.63	1.90	0.79	18.25	0.43	1.37	3.12	12.39
Pseudoalteromonas	4.64	0.71	0.00	24.17	0.00	0.00	0.00	0.96	12.36
Symbiobacterium	4.24	0.00	0.00	1.15	0.00	0.72	0.14	34.11	14.39
Desulfocurvibacter	3.08	0.31	0.00	22.72	0.00	0.00	0.00	0.00	0.00
unclassified_Firmicutes	2.98	0.85	0.92	0.74	1.97	0.12	1.44	16.94	9.12
Desulfuromonas	2.89	0.47	0.00	6.76	16.37	0.00	0.00	0.00	0.14
unclassified_Bacteria	1.97	2.36	3.22	0.26	1.47	2.26	2.22	0.69	2.65
Noviherbaspirillum	1.42	1.42	0.00	2.37	7.77	0.00	0.00	0.00	0.00
Clostridium_sensu_stricto	1.40	1.44	0.23	7.58	0.00	0.00	0.05	0.00	1.41
Anaerosolibacter	1.34	0.31	0.63	4.54	0.21	1.83	2.08	0.14	0.00
Amycolatopsis	1.28	2.31	0.12	0.00	0.00	2.05	0.00	0.00	6.44
Anaeromyxobacter	1.22	0.50	0.00	0.13	9.57	0.00	0.00	0.00	0.21
unclassified_Rhodospirillales	1.14	1.16	0.02	6.79	0.35	0.00	0.00	0.23	0.00
Desulfosporosinus	1.06	2.62	0.14	4.54	0.18	0.00	0.12	0.14	0.03
Alkalihalobacillus	1.05	1.79	0.07	0.00	0.00	0.00	0.00	0.00	7.81

unclassified_Bacillales	0.74	0.00	0.00	3.70	0.00	0.00	0.00	0.00	2.44
unclassified_Alphaproteobacteria	0.71	0.00	0.00	0.00	5.92	0.00	0.00	0.00	0.24
Nocardioides	0.49	0.02	0.00	0.69	0.32	0.43	0.00	3.95	0.00
unclassified_Gammaproteobacteria	0.42	0.21	0.99	0.08	0.18	0.51	0.85	0.00	0.17
Paenibacillus	0.41	0.00	0.00	0.00	0.00	0.00	0.00	5.46	0.00
Devosia	0.38	0.24	0.00	0.20	0.06	0.00	0.00	0.00	3.10
Alkaliphilus	0.38	0.05	0.02	0.00	0.77	0.72	0.26	0.32	1.20
unclassified_Burkholderiales	0.34	0.00	0.00	0.00	2.77	0.00	0.00	0.00	0.21
Arthrobacter	0.28	0.12	0.00	0.28	0.38	0.00	0.00	1.47	0.69
Sporacetigenium	0.25	0.00	0.12	0.00	0.00	0.05	1.56	0.00	0.00
unclassified_Cytophagales	0.24	0.14	0.00	0.05	1.83	0.00	0.00	0.00	0.00
unclassified_Clostridia	0.22	0.00	0.00	0.00	0.00	0.00	0.00	2.94	0.00
Sedimentibacter	0.22	0.38	0.33	0.89	0.00	0.00	0.00	0.00	0.00
unclassified_Bacilli	0.20	1.11	0.00	0.00	0.00	0.05	0.12	0.00	0.17
Pseudarthrobacter	0.19	0.00	0.00	0.31	0.41	0.00	0.00	1.42	0.00
unclassified_Betaproteobacteria	0.19	0.00	0.00	0.00	1.47	0.07	0.00	0.09	0.00
Pontibacter	0.19	0.00	0.00	0.31	1.32	0.00	0.00	0.00	0.00
Acidovorax	0.18	0.05	0.00	0.00	1.50	0.00	0.00	0.00	0.00
Chryseolinea	0.12	0.00	0.00	0.00	0.77	0.14	0.00	0.14	0.00
Gracilibacter	0.12	0.02	0.00	0.00	0.00	0.39	0.07	0.00	0.48
unclassified_Xanthomonadales	0.12	0.00	0.19	0.00	0.00	0.55	0.12	0.00	0.00
Phenylobacterium	0.10	0.00	0.00	0.00	0.44	0.07	0.00	0.51	0.00

Brevundimonas	0.10	0.12	0.00	0.36	0.32	0.00	0.00	0.00	0.00
Desulfotomaculum	0.10	0.00	0.00	0.00	0.53	0.24	0.02	0.00	0.00
Enterococcus	0.10	0.00	0.00	0.00	0.00	0.67	0.00	0.00	0.00
Paracoccus	0.09	0.00	0.00	0.00	0.00	0.07	0.00	1.06	0.00
Methyloversatilis	0.08	0.00	0.00	0.00	0.65	0.00	0.00	0.00	0.00
unclassified_Bacteroidetes	0.07	0.05	0.00	0.00	0.56	0.00	0.00	0.00	0.00
Cytobacillus	0.06	0.00	0.00	0.00	0.00	0.00	0.00	0.83	0.00
Promicromonospora	0.06	0.00	0.00	0.00	0.15	0.00	0.00	0.60	0.00
Chloroplast	0.06	0.00	0.00	0.00	0.41	0.00	0.00	0.14	0.00
Lysobacter	0.06	0.00	0.00	0.00	0.50	0.00	0.00	0.00	0.00
unclassified_Proteobacteria	0.06	0.00	0.09	0.15	0.00	0.17	0.00	0.05	0.00
unclassified_Acidobacteria	0.06	0.00	0.00	0.00	0.00	0.46	0.00	0.00	0.00
Ramlibacter	0.05	0.00	0.00	0.00	0.00	0.00	0.00	0.73	0.00
unclassified_Myxococcales	0.05	0.00	0.05	0.00	0.03	0.00	0.00	0.60	0.00
unclassified_Actinobacteria	0.05	0.00	0.00	0.00	0.12	0.07	0.00	0.23	0.14
Microvirga	0.05	0.00	0.00	0.00	0.00	0.19	0.00	0.32	0.00
Ferrovibrio	0.05	0.00	0.00	0.00	0.44	0.00	0.00	0.00	0.00
Sutterella	0.05	0.00	0.00	0.00	0.00	0.29	0.00	0.00	0.07
Pseudonocardia	0.04	0.00	0.00	0.00	0.00	0.00	0.00	0.55	0.00
unclassified	0.04	0.00	0.00	0.00	0.00	0.00	0.00	0.51	0.00
Sphingobium	0.04	0.00	0.00	0.33	0.00	0.00	0.00	0.00	0.00
unclassified	0.04	0.00	0.00	0.00	0.00	0.26	0.00	0.00	0.00

Mesorhizobium	0.03	0.00	0.00	0.00	0.00	0.00	0.00	0.41	0.00
Dongia	0.03	0.00	0.00	0.00	0.00	0.00	0.00	0.41	0.00
unclassified	0.03	0.00	0.00	0.00	0.00	0.10	0.00	0.28	0.00
Porphyrobacter	0.03	0.00	0.00	0.00	0.29	0.00	0.00	0.00	0.00
Streptococcus	0.03	0.00	0.00	0.00	0.00	0.14	0.00	0.14	0.00
Saccharibacteria_genera_incertae_sedis	0.03	0.00	0.00	0.00	0.12	0.07	0.00	0.09	0.00
Aromatoleum	0.03	0.00	0.00	0.00	0.26	0.00	0.00	0.00	0.00
Rubrobacter	0.03	0.00	0.00	0.00	0.00	0.24	0.00	0.00	0.00
Peredibacter	0.03	0.00	0.00	0.00	0.24	0.00	0.00	0.00	0.00
Subdivision3_genera_incertae_sedis	0.03	0.00	0.07	0.00	0.15	0.00	0.00	0.00	0.00
Desertimonas	0.03	0.00	0.00	0.00	0.00	0.22	0.00	0.00	0.00
Parabacteroides	0.03	0.00	0.00	0.00	0.00	0.22	0.00	0.00	0.00
Anaerostipes	0.03	0.00	0.00	0.00	0.00	0.22	0.00	0.00	0.00
Cutibacterium	0.02	0.00	0.00	0.00	0.00	0.00	0.00	0.28	0.00
Roseibium	0.02	0.00	0.00	0.00	0.00	0.00	0.00	0.28	0.00
Microcella	0.02	0.00	0.00	0.00	0.03	0.00	0.00	0.23	0.00
Skermanella	0.02	0.00	0.00	0.00	0.00	0.00	0.00	0.23	0.00
Streptomyces	0.02	0.00	0.00	0.00	0.21	0.00	0.00	0.00	0.00
Aquabacterium	0.02	0.00	0.00	0.00	0.21	0.00	0.00	0.00	0.00
Ignavibacterium	0.02	0.00	0.00	0.00	0.18	0.00	0.00	0.00	0.00
unclassified	0.02	0.00	0.00	0.00	0.18	0.00	0.00	0.00	0.00
unclassified	0.02	0.00	0.00	0.00	0.18	0.00	0.00	0.00	0.00

Mesobacillus	0.02	0.00	0.00	0.00	0.00	0.00	0.00	0.00	0.17
unclassified	0.02	0.00	0.00	0.00	0.00	0.17	0.00	0.00	0.00
Bacteroides	0.02	0.00	0.00	0.00	0.00	0.17	0.00	0.00	0.00
Barnesiella	0.02	0.00	0.00	0.00	0.00	0.17	0.00	0.00	0.00
Aminipila	0.02	0.00	0.16	0.00	0.00	0.00	0.00	0.00	0.00
Bosea	0.02	0.00	0.00	0.00	0.09	0.00	0.00	0.00	0.07
Gemmatimonas	0.02	0.00	0.00	0.00	0.15	0.00	0.00	0.00	0.00
Collinsella	0.02	0.00	0.00	0.00	0.00	0.14	0.00	0.00	0.00
Pseudoxanthomonas	0.02	0.00	0.00	0.13	0.00	0.00	0.00	0.00	0.00
Faecalibacillus	0.02	0.00	0.00	0.00	0.00	0.12	0.00	0.00	0.00
Saccharospirillum	0.01	0.00	0.00	0.00	0.03	0.00	0.00	0.14	0.00
Snodgrassella	0.01	0.00	0.00	0.00	0.00	0.00	0.00	0.14	0.00
Propionivibrio	0.01	0.00	0.00	0.00	0.12	0.00	0.00	0.00	0.00
Actinotalea	0.01	0.00	0.00	0.08	0.03	0.00	0.00	0.00	0.00
Parviterribacter	0.01	0.00	0.00	0.00	0.09	0.00	0.00	0.00	0.00
Novosphingobium	0.01	0.00	0.00	0.00	0.09	0.00	0.00	0.00	0.00
Nitrobacter	0.01	0.00	0.00	0.00	0.00	0.07	0.00	0.00	0.00
unclassified	0.01	0.00	0.00	0.00	0.06	0.00	0.00	0.00	0.00
Phreatobacter	0.01	0.00	0.00	0.00	0.06	0.00	0.00	0.00	0.00
Labilithrix	0.01	0.00	0.00	0.00	0.06	0.00	0.00	0.00	0.00
unclassified	0.01	0.00	0.00	0.05	0.00	0.00	0.00	0.00	0.00
Clostridium_IV	0.01	0.00	0.00	0.00	0.00	0.05	0.00	0.00	0.00

Fulvivirga	0.00	0.00	0.00	0.00	0.03	0.00	0.00	0.00	0.00
Georgenia	0.00	0.00	0.00	0.03	0.00	0.00	0.00	0.00	0.00
Blastomonas	0.00	0.00	0.00	0.03	0.00	0.00	0.00	0.00	0.00
Dorea	0.00	0.00	0.00	0.00	0.00	0.02	0.00	0.00	0.00
Dialister	0.00	0.00	0.00	0.00	0.00	0.02	0.00	0.00	0.00

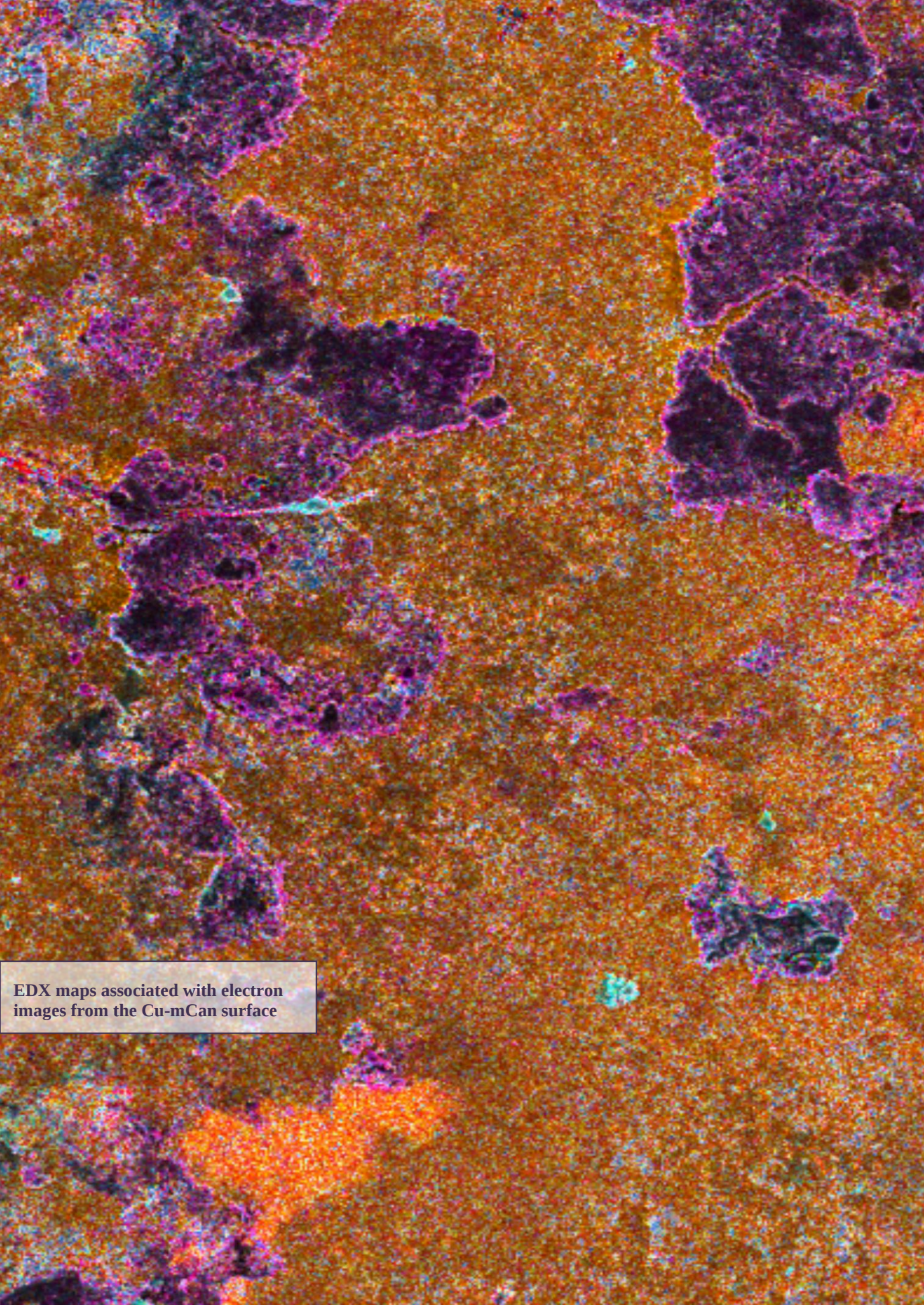

EDX maps associated with electron images from the Cu-mCan surface

Chapter IV:

Reveling the impact of selenium on the activity of microbial communities from hyper-saturated Spanish bentonite microcosms and copper corrosion in the context of radioactive waste disposal

Authors

Marcos F. Martinez-Moreno[1,*], Cristina Povedano-Priego[1], Mar Morales-Hidalgo[1], Guillermo Lazuén-López[1], Elisabet Aranda[3], Jesus J. Ojeda[2], and Mohamed L. Merroun[1]

[1]Faculty of Sciences, Department of Microbiology, University of Granada, Granada, Spain.

[2]Department of Chemical Engineering, Faculty of Science and Engineering, Swansea University, Swansea, United Kingdom

[3]Institute of Water Research, Department of Microbiology, University of Granada, Granada, Spain

Abstract

Deep Geological Repository (DGR) is the internationally agreed option for the final storage of high-level radioactive waste (HLW). The DGR design includes corrosion-resistant metal canisters surrounded by bentonite clay, and placed into a host rock. Despite DGRs are considered to be a hostile environment for microorganisms, scenarios where microbial-activity favorable conditions have to be taken in account for the safety performance assessment of this disposal system. This study investigates the impact of selenite [Se(IV)], as inactive analogue of ^{79}Se present in the HLW, in anoxic microcosms of hyper-saturated bentonite spiked with bacterial consortium and amended with lactate, acetate and sulfate. The addition of the bacterial consortium accelerated the rate of Se(IV) reduction to Se(0), while the pre-tyndallization of bentonite retards this process. Furthermore, whilst Se(IV) reduce the relative abundance of some Sulfate-Reducing Bacteria (SRB) genera, lactate, acetate, and sulfate stimulates the growth of Se-tolerant bacteria including SRB genera (e.g. *Desulfosporosinus*) among others, which may participate in the Se(IV) reduction. Regarding the addition of electron donors/acceptor, lactate was the primary energy source to be consumed linked to the production, and subsequent consumption, of acetate. The study revealed that Se(IV) reduction leads to the formation of amorphous Se(0) nanospheres, which undergo a biotransformation to more stable crystalline forms, contributing to the immobilization of Se in case of HLW release. Additionally, the biogenic sulfide generated by SRB activity react with Cu forming corrosion products (Cu_2S) on the copper canister surface.

Keywords: *DGR, selenium speciation, hypersaturated bentonite, microbial communities, copper corrosion*

1_ Introduction

One of the challenges associated with the nuclear power industry is the final management of high-level radioactive waste (HLW). Deep geological Repositories is widely agreed to be the best solution for final disposal of these wastes (WNA, 2023). The main objective is to ensure DGR integrity for hundreds to millions of years, preventing the release of HLW into the environment until their radiotoxicity decay to natural levels (Betandiieva et al., 2009). The multi-barrier system design of the DGR consists in the storage of HLW in corrosion-resistant metal canisters that will be surrounded by a backfilling and sealing material, and will be placed few hundred meters into a stable geological formation (host rock).

The nature of the DGR barriers will depend on the approach adopted by each country. Copper-coated metal canisters have been suggested or implemented by countries such as Canada, Korea, Sweden of Finland (Hall et al., 2021). Furthermore, bentonite clay has been chosen as the most appropriate material for buffering and sealing the DGR providing mechanical support for canisters, sealing canisters in case of cracks, preventing water infiltration from reaching the canisters, and retarding radionuclides diffusion (Garcia-Romero et al., 2019). The Spanish bentonite from El Cortijo de Archidona (Almeria), FEBEX, has been proposed as the buffer and sealing material for the DGR in Spain (Huertas et al., 2021; Villar et al., 2006). Since bentonites will not be sterile, it is vital to examine the structure and composition of their microbial community to ensure the repository's long-term stability (Meleshyn et al., 2011). While the conditions within the DGR may not be optimal for microbial growth (Martinez-Moreno et al., 2024), the infiltration of nutrient containing porewater from the host rock could support the development and activity of microorganisms. In this situation, microorganisms may cause direct or indirect corrosion of metal canisters know as microbially induced corrosion (MIC); contribute to the build-up of a gaseous phase by producing hydrogen, methane or carbon dioxide; influence inherent properties

of the bentonite by causing geochemical transformations; and influence the mobilization or immobilization of radionuclides (Ruiz-Fresneda et al., 2023).

Moreover, the microbial activity and canister corrosion will lead to the establishment of an anoxic environment after the sealing of the repository (Payer et al., 2019; Keech et al., 2014). Once this environment prevails, anaerobic bacteria such as sulfate-reducing bacteria (SRB) and iron-reducing bacteria (IRB) could remain active affecting negatively DGR barriers, through processes like MIC promotion, Fe(III) reduction to Fe(II) in smectite (major mineral in bentonites), and the reduction of sulfate to sulfide (metal canister corrosion agent) (Martinez-Moreno et al., 2024, 2023; Ruiz-Fresneda et al., 2023; Pentráková et al., 2013; Liu et al., 2012; Shelobolina et al., 2003). Sulfide generated by SRB, will be favored in areas farther from the canisters where lower temperatures and higher water activity will prevail (Bengtsson and Pedersen, 2017). This biogenic sulfide could compromise the stability of the canisters diffusing through the biologically inactive portion of the bentonite until reaching the canister's surface. In the worst case, canister's corrosion could result in the release of the HLW including Se.

One of the products generated by the nuclear fission of uranium fuel for the nuclear power generation is selenium (Se) (Hassan et al., 2021). Specifically, the isotope ^{79}Se is a component of spent nuclear fuel that can be found in HLW resulting for the reprocessing plants (Abdalla et al., 2020). The health risks associated with ^{79}Se stem from the emission of beta particles during its radioactive decay with a long half-life, being one of the few nuclides determining the long-term radiological impact of a repository (Jörg et al., 2010). Moreover, the chemical toxicity of Se is closely related to its oxidation state (Ruiz-Fresneda et al., 2020; Avedaño et al., 2016). Selenate [Se(VI)] and selenite [Se(IV)] are considered the most toxic forms due to their high solubility and mobility, being biologically available. In contrast, elemental selenium [Se(0)] and selenide [Se(-II)] forms are less soluble and less mobile, and therefore less biologically available, exhibiting low environmental

impact. Hence, it is crucial to investigate both biotic and abiotic processes that may affect the mobility of this metalloid within the DGR environment in addition to its impact on the different components of the multi-barrier system.

Several studies have reported the ability of microorganisms to tolerate and immobilize selenium. For instance, bacteria of the genus *Bacillus*, *Stenotrophomonas*, *Pseudomonas*, and SRB such as *Desulfosporosinus* and *Desulfurispirillum* (Baggio et al., 2021; Kora, 2018; Ruiz-Fresneda et al., 2023, 2019; Staicu et al., 2015; Aoyagi et al., 2021; Staicu and Barton, 2021). Furthermore, Povedano-Priego et al. (2023) demonstrated the microbial-mediated reduction and transformation of Se(IV) to Se(0) in a complex system of water-saturated Spanish bentonite amended with selenite and a bacterial consortium.

The present work simulated a 'worst-case' scenario where a release of selenium took place and the bentonite was in a state of water hyper-saturation and enriched with nutrients. To assess the impact of indigenous microorganisms' activity from the Spanish bentonite, optimal growth conditions were established by setting up of hyper-saturated microcosms amended with electron donors (acetate and lactate) and electron acceptor (sulfate). Furthermore, the addition of 2 mM of Se(IV) acted as an inactive analogue of ^{79}Se present in the HLW. Additionally, this metalloid has a similar chemistry to sulfur and can disrupt sulfur biogeochemical cycles, potentially leading to interference with copper corrosion. Therefore, this study aims to examine, by means of a multidisciplinary approach, the impact of selenium addition on the microbial communities of Spanish bentonite and the subsequent effect of the microorganisms on the geochemical evolution of the microcosms for one year of anaerobic incubation. Additionally, an early-stage characterization of microbial-mediated selenium reduction and copper corrosion were conducted. Our findings underscore the significance of bentonite microorganisms, potentially thriving under nutrient influx from water filtration in the clay and the potential release of HLW within the long-term stability of DGR.

2_ Materials and methods

2.1_ Bentonite clay sampling

The bentonite was aseptically collected in February 2020 from a maximum depth of 80 cm from El Cortijo de Archidona site in Almeria, Spain. Afterwards, the bentonite underwent manual disaggregation in the laboratory and was dried, to eliminate excess moisture, for a minimum of five days at room temperature within a laminar flow cabinet. To achieve a homogeneous powder, the bentonite was ground using a stainless-steel roller and mortar. Finally, it was stored at 4 ºC until microcosms were prepared.

2.2_ Copper mini-canisters (Cu-mCan) crafting and specifications

The elaboration of the Cu-mCan was previously described in Chapter 3. Briefly, the Cu-mCan manufacturing process was developed at the mechanical workshop of the Centro de Instrumentación Científica (University of Granada, Spain). For this purpose, two different 99.99%-purity copper rods (20.6 ± 0.05 mm and 16.0 ± 0.5 mm, UNS number C10100) were obtained from Goodfellow (goodfellow.com).

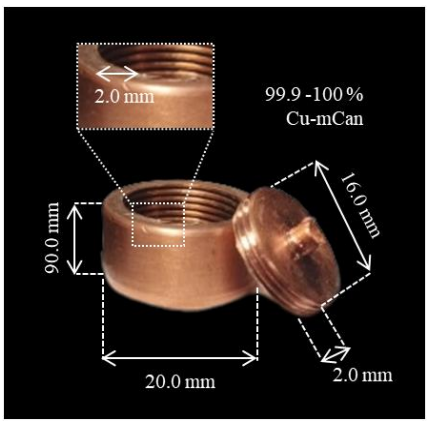

Fig. 1. Dimension of the high-purity copper mini-canisters (Cu-mCan) (Chapter 3).

The sterilization of the Cu-mCan was carried out by autoclaving 15 min at 121 ºC. The overall dimensions of the Cu-mCan are detailed in **Fig. 1**.

2.3_ Description and culture conditions of the BPAS bacterial consortium

A bacterial consortium of four bacterial strains (BPAS) was inoculated into the BC treatments. These strains were identified within the microbial community of Spanish bentonite and were employed in previous studies (Povedano-Priego et al., 2023; Lopez-Fernandez et al., 2018). *Stenotrophomonas bentonitica* BII-R7 and *Bacillus* sp. BII-C3 were isolated from the Spanish bentonite (Sanchez-Castro et al., 2017; Lopez-Fernandez et al., 2014). Additionally, *Pseudomonas putida* ATCC33015, and *Amycolatopsis ruanii* NCIMB14711 were purchase from the American Type Culture Collection (lgcstandards-atcc.org/), and National Collection of Industrial Food and Marine Bacteria (ncimb.com/), respectively.

S. bentonitica, *Bacillus* BII-C3, and *P. putida* were grown aerobically in Luria-Bertani (LB) medium (Miller, 1972), while *A. ruanii* was grown in YMG medium composed of yeast extract (4 g L^{-1}), malt extract (10 g L^{-1}), and D(+)-glucose monohydrate (4 g L^{-1}).

2.4_ Anaerobic microcosms assembly: specifications, content and sampling

Microcosms were set up as detailed in the previous chapter (Chapter 3) with some modifications. Overall, 24 microcosms were elaborated (8 treatments in triplicate). The sample ID and characteristic experimental conditions are summarized in **Table 1.**

For the interaction studies with selenium, all microcosms were supplemented with sodium selenite [Se(IV)] at a final concentration of 2 mM. For this purpose, 1 M of Se(IV) stock solution (Na_2SeO_3 • Sigma-Aldrich) was prepared and sterilized by 0.22 µm pore-sized filters. Several controls were considered to examine four different parameters (sample code between brackets): i) bentonite or sterilized

bentonite (B – StB); ii) acetate, lactate, and sulfate addition (eD); and iii) inoculated BPAS consortium (BC).

Table 1.
Sample ID and content of the different microcosms' treatments. All the anaerobic microcosms contained three Cu mini-canisters (Cu-mCan). The microcosms were set up in triplicate. ALS: acetate, lactate and sulfate concentrations; BPAS: bacterial consortium; +: presence; -: absence.

Sample ID	Bentonite	ALS (mM)	BPAS	Se(IV)
B.eD.Se.BC	Unsterilized	30:10:20	+	2 mM
B.Se.BC	Unsterilized	-	+	2 mM
B.eD.Se	Unsterilized	30:10:20	-	2 mM
B.Se	Unsterilized	-	-	2 mM
StB.eD.Se.BC	Pre-sterilized	30:10:20	+	2 mM
StB.Se.BC	Pre-sterilized	-	+	2 mM
StB.eD.Se	Pre-sterilized	30:10:20	-	2 mM
StB.Se	Pre-sterilized	-	-	2 mM

Glossary: B: bentonite; StB: sterilized bentonite; eD: addition of electron donors/acceptor; Se: selenium 2 mM; BC: bacterial consortium.

Briefly, 50 g of ground bentonite was added to autoclaved 250-mL borosilicate glass bottles. For the sterilized bentonite microcosms (StB), the bottles were heat-shocked by tyndallization (110 ºC for 45 min, 3 consecutive days) after introducing the bentonite into the bottles. The eD-microcosms were supplemented with electron donors/acceptor at the final concentration of 30 mM sodium acetate, 10 mM sodium lactate, and 20 mM sodium sulfate. Furthermore, BPAS consortium was spiked into the BC-treatments microcosms with an initial optical density (OD_{600}) of 0.4 for each bacterial strain. To achieve this, after separately growing the four strains, the cells were collected by centrifugation (10,000 rpm for 5 min) and washed twice with 0.9 % NaCl to eliminate the culture media. The final pellet was resuspended in autoclaved bentonite Equilibrium Water (EW: shaking

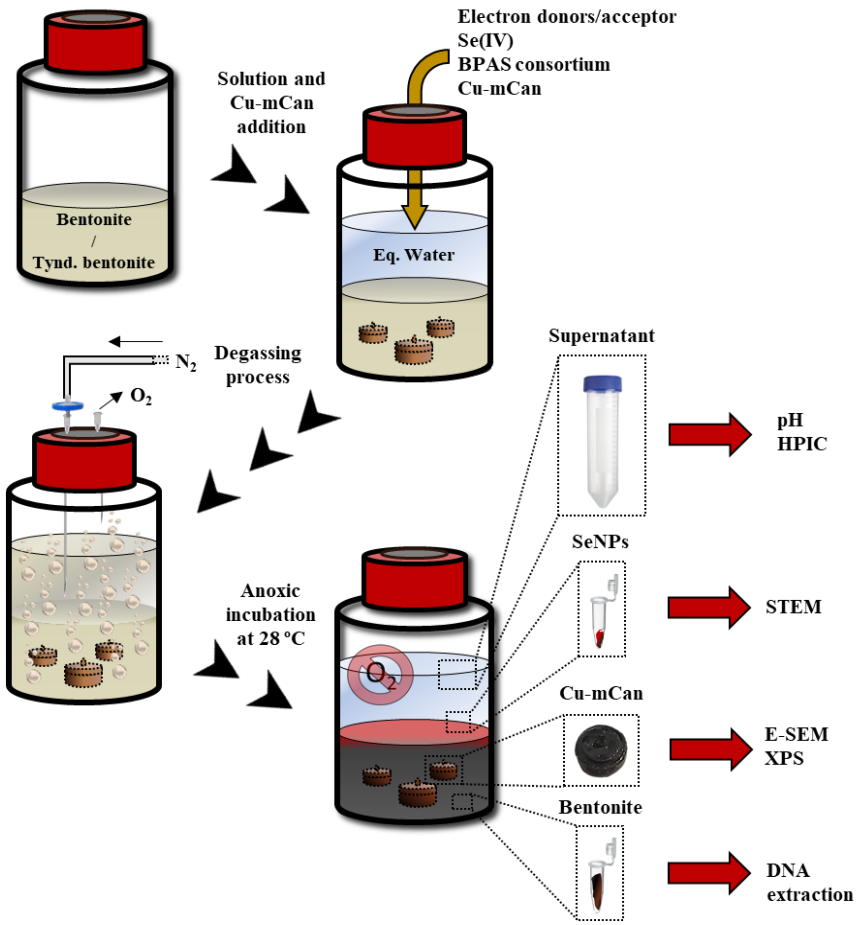

Fig. 2. Step-by-step of the anaerobic microcosm's assembly, specifications, content, and sampling.

bentonite powder in sterile distilled water in a 1:100 w:v ratio at 180 rpm for 24 h at 28 ºC, and recovering the supernatant by centrifugation). Subsequently, the initial OD_{600} was adjusted at 0.4 for each strain by a Genesys 10 S UV-Vis - Thermo scientific. The final volume in each bottle was calculated considering the addition of the different solutions (volume of Se, acetate, lactate, sulfate, and each bacterial strain) and filled up to 230 mL with the EW. Finally, three sterilized-by-autoclaving Cu-mCan were deposited into each microcosm. After the microcosms were assembled, the borosilicate bottles were sealed using butyl-rubber stoppers

and purged with nitrogen (N_2) to eliminate oxygen, establishing anaerobic conditions.

Subsequently, the microcosms were incubated at 28 ºC. The sampling procedure from the different constituent for the further analyses was carried out under anaerobic conditions within a glovebox. The step-by-step process of setting up the microcosms and sampling is showed in **Fig. 2**.

2.5_ Supernatant analyses: pH and electron donors/acceptor depletion

To determine the evolution of physicochemical parameters, 5 mL of supernatant (liquid phase) was collected from each microcosm within a nitrogen-atmosphere anaerobic chamber. Samples were measured at 45, 90, 135, and 365 days of incubation, previous filtration through a 0.22 µm filter. pH measurements were performed by Advanced Digital Handheld Portable Meter HQ40D from Hach, previously calibrated with commercially available reference solutions (pH 4.00 and 7.00).

The percentage of acetate, lactate and sulfate depletion were measured by High Pressure Ion Chromatography (HPIC). The analysis was conducted using a 925 Eco ICE instrument from Methrom Hispania (Herisau, Switzerland) equipped with an IC conductivity detector, a Metrohm Suppressor Module (MSM), a 250 µL injection loop with a peristaltic pump, a Metrohm high-pressure pump with a purge valve, and a 919 UF autosampler. Prior to injection, samples were filtered by 0.22 µm filter-sterilized and were diluted in ultrapure water. The analyses of target anions took place at room temperature in suppressor mode, utilizing a Metrosep A 5-250/4.0 column (250 x 4.0 mm) with a pre-column Metrosep A Supp 5 Guard/4.0 (Methrom Hispania - Herisau, Switzerland) at a flow rate of 0.7 mL min^{-1}. The mobile phase consisted of 3.2 mM Na_2CO_3 / $NaHCO_3$ 1 mM (Sigma-Aldrich). The MSM-Metrohm Suppressor Module for chemical suppression was employed with an aqueous solution of 250 mM H_2SO_4 (VWR. Madrid, Spain), 10 mM oxalic acid

(Sigma-Aldrich) and 10 % acetone (VWR. Madrid, Spain). Instrument calibration was performed by injecting standard solutions of the target compounds, and data analysis was conducted using MagIC Net 3.1 basic software for ion chromatography. Standard solutions of acetate ($C_2H_3O_2^-$), sulfate (SO_4^{2-}), and lactate ($C_3H_5O_3^-$) with a concentration of 1,000 mg L^{-1} were supplied by Sigma-Aldrich.

2.6_ Microbial DNA from bentonite: extraction procedure, sequencing and bioinformatic analyses

Total DNA from the bentonite microcosms was extracted (total samples: 24) according to the protocol detailed in Povedano-Priego et al. (2021). the concentration of the obtained DNA was assessed using the Qubit 3.0 Fluorometer (Life Technology, Invitrogen™).

For the library preparation, the steps were followed in detail as described in the previous chapter (Chapter 3). Briefly, two consecutive PCR reactions were conducted for each sample using a combination of regular and barcoded fusion primers. The amplification of the V5-V6 variable regions of the 16S rRNA gene employed the following primers: 807F (5′-GGATTAGATACCCBRGTAGTC-3′) and 1050R (5′-AGYTGDCGACRRCCRTGCA-3′) (Bohorquez et al., 2012). The initial PCR reaction comprised one cycle at 95 ºC for 15 min, followed by 35 cycles of 98 °C for 10 s, 55 °C for 10 s, and 72 °C for 45 s. The process concluded with a final extension step at 72 °C for 2 min. The same conditions were applied to the second PCR reaction (barcoding step), with only 10 PCR cycles. Library product quality was evaluated through electrophoresis. For FastaQ file generation, the libraries underwent sequencing using the MiSeq Illumina platform (2 × 250 bp, Hayward, California, USA).

FastaQ files were processing and normalized using the "dada2" and "phyloseq" packages within the R 4.2.1 software (R Core Team, 2022). Bayesian classification

was applied to assign phylotypes to taxonomic affiliations, using an 80 % pseudo-bootstrap threshold. Relative abundances and alpha diversity indices were calculated by Explicet 2.10.5 (Robertson et al., 2013). To evaluate the similarity between samples at the genus level, a matrix based on the Bray-Curtis algorithm was constructed. Subsequent analysis of sample similarity was conducted through Principal Coordinate Analysis (PCoA) using Past4 software (Hammer and Harper, 2001). Additionally, a heatmap was generated to visualize the OTUs causing dissimilarity between samples.

2.7_ Interphase: microscopic and spectroscopic characterization of selenium reduction products (SeRPs)

Samples from the interphase Bentonite:EW were recovered from the Se-amended microcosms and were analyzed by Ultra-High Resolution Transmission Electron Microscope and High-Angle Annular Dark-Field (HRTEM HAADF) FEI TITAN G2. For this propose, 1 mL of each homogenized interphase was centrifugated at 10,000 rpm during 5 min for microscopy sample preparation by thin sections. Samples were contrasted with osmium for the visualization of bacterial cells. Afterwards, selenium reduction products (SeRPs) were characterized by Selected-Area Electron Diffraction (SAED) and High-Resolution Transmission Electron Microscopy (HRTEM) combined with Fast Furier Transform (FFT).

2.8_ Cu-mCan: surface of copper and corrosion compound characterization

After 45 days of anoxic incubation, the Cu-mCan were recovered from the microcosms, unscrewed and dried under anaerobic conditions. Once dried, the base of the Cu-mCan were metallized with a carbon coating by evaporation using an EMITECH K975X Carbon Evaporator for high-resolution scanning electron microscopy (HRSEM) analysis by an AURIGA Carl Zeiss SMT microscope, coupled with qualitative and quantitative energy dispersive X-ray (EDX) microanalysis.

3_ Results and discussion

3.1_ Visual transformations in microcosms over one-year incubation

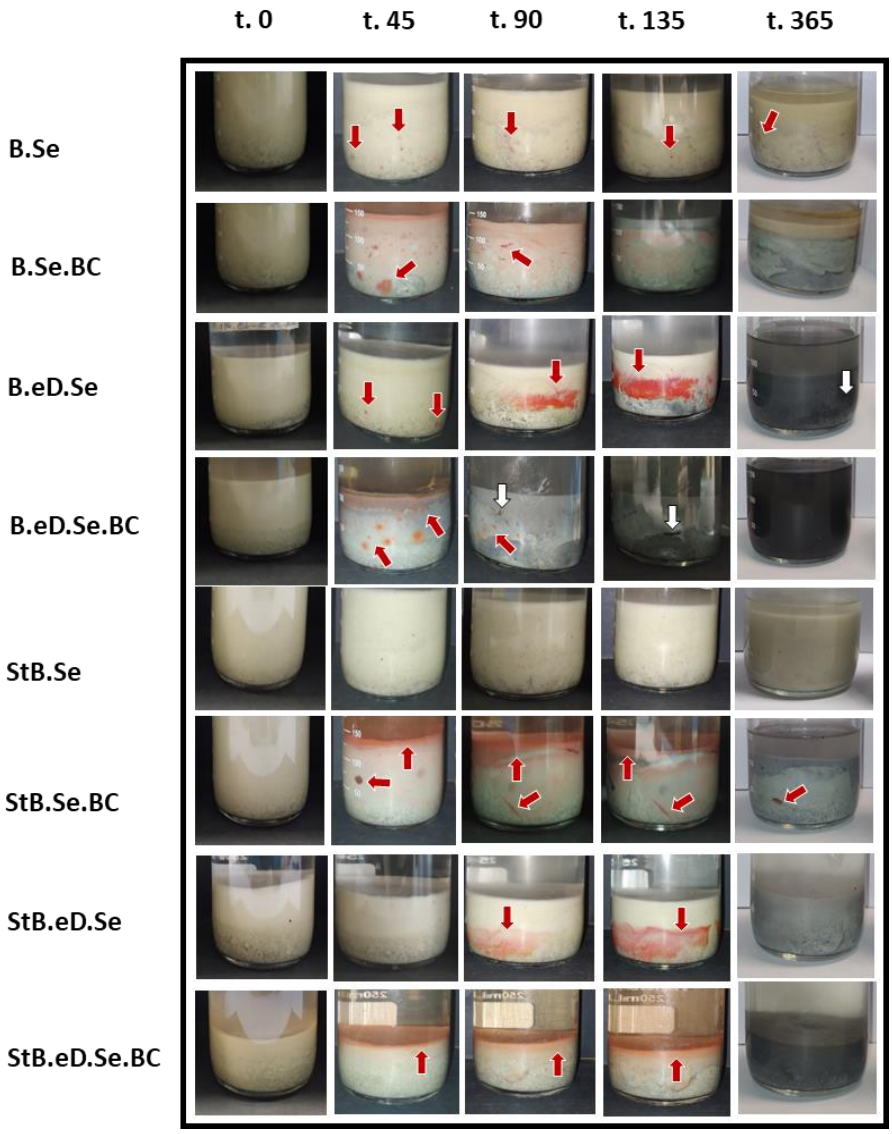

Fig. 3. Evolution of hyper-saturated Spanish bentonite microcosms with Se(IV) 2mM before and after 45, 90, 135, and 365 days of anaerobic incubation at 30 ºC. Red arrows show red precipitates attributed to Se(IV) reduction to Se(0). White arrows indicate the development of fissures and cavities attributed to gas formation. Glossary: Bentonite (B), Sterilized bentonite (StB), amended with acetate, lactate and sulfate (eD); Selenium(IV) 2mM (Se), and with BPAS consortium (BC).

The visual color evolution of the microcosms through incubation time is showed in **Fig. 3**. After 45 days , microcosms containing bacterial consortium (BC) showed a thin layer of reddish coloration at the bentonite:supernatant interface as well as accumulations in some of the samples in the bentonite phase (red arrows, **Fig. 3**) indicating the reduction of selenite [Se(IV)] to elemental selenium [Se(0)] (Povedano-Priego et al., 2023; Ruiz-Fresneda et al., 2018). These red Se(0) reduction products (SeRPs) shifted, or were masked, by metallic gray-black hues over the incubation period. The shift towards darker hues could be attributed to factors such as a transition in the allotropy of SeRPs to more stable forms, or related to the generation of H_2S, a byproduct of bacterial activity, which can react with iron and lead to the formation of black precipitates of reduced iron species (Ruiz-Fresneda et al., 2023b; Miettinen et al., 2022; Matschiavelli et al., 2019). The formation of small fissures in the bentonite phase of the microcosms (white arrows, **Fig. 3**) and the characteristic smell of rotten eggs after sampling could be related to the gas generation (e.g., hydrogen sulfide) mediated by bacterial activity (He et al., 2011) justifying the color transitions as showed in the previous chapter (**Fig. 5,** Chapter 3).

It should be noted that the addition of the bacterial consortium (BC) in the microcosms accelerated the selenium reduction processes, with reddish coloration typically observed in the early stages (before 45 days) of incubation in the samples. Moreover, the addition of electron donors/acceptor (eD) also enhanced the mentioned processes, while bentonite sterilization retarded the progression. Regarding the sample of sterilized bentonite with Se (StB.Se), no visual color change was observed throughout the year of incubation indicating no Se(IV) reduction either alteration to darker hues in the bentonite. Since tyndallization is not the most effective process for bentonite sterilization (Martinez-Moreno et al., 2024), it was observed that, under the studied conditions (e.g., hyper saturation of the bentonite), this process can impact bacterial activity.

3.2_ Dynamics in geochemistry over one-year of incubation

The pH values in the microcosms exhibited alkaline to neutral values ranging between 9.06 (StB.Se, t. 0) to 7.32 (StB.eD.Se, t. 365) (**Fig. 4**). In the microcosms exclusively supplemented with Se(IV) (samples B.Se and StB.Se), the initial pH

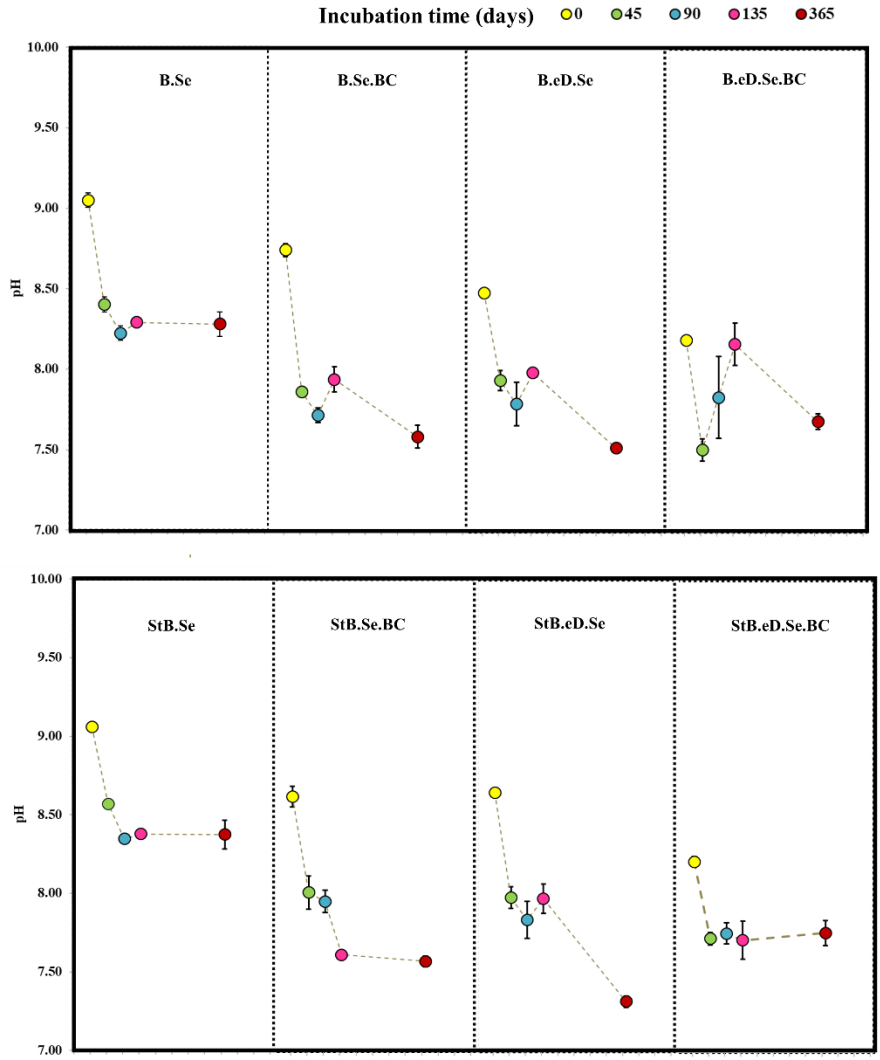

Fig. 4. pH evolution in hyper-saturated bentonite microcosms. Data were measured at time 0 (yellow), 45 (green), 90 (blue), 135 (pink) and 365 (red) days of incubation under anaerobic conditions. Data showed the mean values with standard derivations measured from three independent replicates. Glossary: Bentonite (B), Sterilized bentonite (StB), amended with acetate, lactate and sulfate (eD); Selenium(IV) 2mM (Se), and with BPAS consortium (BC).

(t. 0) presented a value around 9.00, gradually decreasing and stabilizing at ≈ 8.3 after one year of incubation (t. 365). This trend in the pH evolution was related to that observed in the analogous samples lacking Se(IV) (samples B and StB, Chapter 3). Hence, the addition of Se(IV) did not impact the pH of the microcosms. Moreover, the addition of the additional components in the microcosms (electron donors/acceptor -eD- and the bacterial consortium -BC-) slightly decrease the initial pH of the samples.

A different dynamic was observed comparing the microcosms with non-sterilized bentonite (B) and those in which the bentonite was previously sterilized (StB). In the StB samples, the pH values decreased progressively until reaching values around 7.50 after one year of incubation. In microcosms containing non-sterilized bentonite (B), the progression of pH to less alkaline values were truncated by a slight increase after 135 days of incubation.

Regardless of the treatment, over the course of incubation, the pH of bentonite exhibited a tendency to become less alkaline, stabilizing within the range of 7.32 to 8.37 after one-year incubation. This decrease in the pH could be attributed to leaching processes (Povedano-Priego et al., 2019). Specifically, this phenomenon could be related to the dissolution of calcite or to the ionic exchange occurring between bentonite and the different solvents (e.g., acetate, lactate, sulfate, and the EW) within the microcosms (Fernández-Díaz, 2004). Additionally, the microorganisms present in the microcosms could induce the production of gases such as hydrogen, methane, and carbon dioxide, through their metabolisms, contributing to the observed decrease in pH values (Bagnoud et al., 2016).

The content (depletion percentage) of lactate, acetate, and sulfate of the amended samples (eD) is shown in **Fig. 5**. The trend in the evolution of acetate, lactate, and sulfate percentages was similar to that found in the Se-untreated samples showed in the previous chapter (Chapter 3). Lactate was the initial electron donor to be

consumed (**Fig. 5A**). The depletion of this electron donor was particularly evident in the microcosms spiked with the bacterial consortium (B.eD.Se.BC), where total

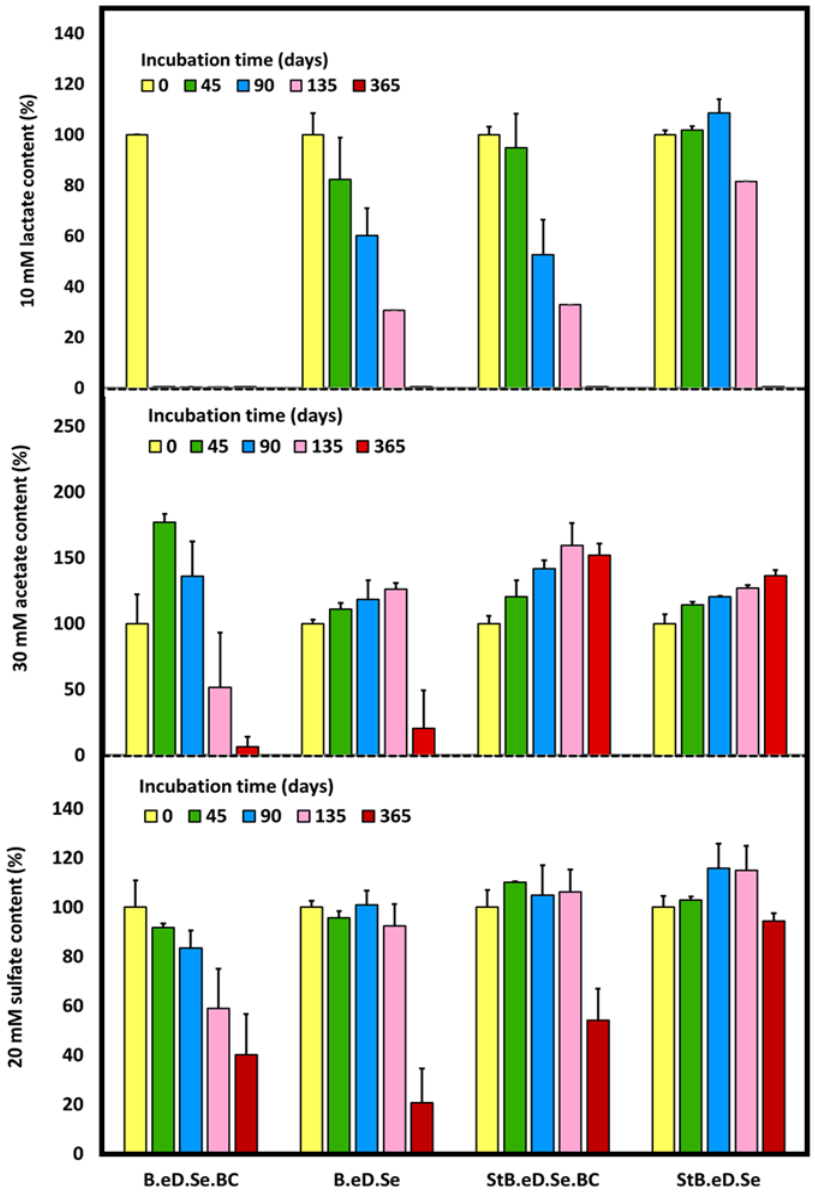

Fig. 5. Evolution of the initial concentration of 10 mM lactate (A), 30 mM acetate (B), and 20 mM sulfate (C) content recorded in Spanish bentonite selenium microcosms incubated anaerobically at 30 ºC for 1 year. Data showed the mean values with standard derivations measured from three independent replicates. Glossary: Bentonite (B), Sterilized bentonite (StB), amended with acetate, lactate and sulfate (eD); Selenium(IV) 2mM (Se), and with BPAS consortium (BC).

lactate consumption occurred within the first 45 days of incubation. This process exhibited a gradual slowdown in the absence of the bacterial consortium (B.eD.Se), followed by the sterilized-bentonite microcosms with bacterial consortium (StB.eD.Se.BC), and lastly, the samples with sterilized bentonite (StB.eD.Se). In these last samples, complete lactate consumption was achieved after 135 days of incubation and before the one-year incubation. However, the addition of Se(IV) in the samples appears to impact the lactate oxidation, showing a slowdown in the percentage of consumption compared to their selenium-free counterparts (Chapter 3). The lactate consumption exhibited a close correlation with acetate production in the microcosms (**Fig. 5B**). The rise in acetate content, along with subsequent depletion, was closely linked to lactate evolution, with the faster processes observed in the B.eD.Se.BC sample, followed by B.eD.Se, StB.eD.Se.BC, and StB.eD.Se.BC. It is noteworthy that, even after a year of incubation, acetate was not completely consumed in any of the treatments. Only the B.eD.Se.BC treatment approached complete acetate consumption before the end of the incubation year. This finding demonstrated the negative impact of the addition of Se(IV) on the treatments slowing down the consumption/production of lactate, acetate, and sulfate compared to Se(IV) untreated microcosms (Chapter 3) where the full consumption of acetate was reached before the year-incubation in the samples B.eD.BC and B.eD. Moreover, the evolution in sulfate content followed a similar trend to that found in the microcosms without Se(IV) (Chapter 3), with a decelerated consumption rate in the presence of this metalloid, albeit without reaching full depletion after the one-year incubation period (**Fig. 5C**).

In summary, the progression of lactate consumption was intricately associated with acetate production and, to a lesser extent, to sulfate consumption. Furthermore, the addition of the bacterial consortium in the microcosms stimulated the mentioned processes, whereas pre-sterilization of the bentonite hindered them. Matschiavelli et al. (2019) observed a simultaneous decrease in lactate and sulfate concentrations along with acetate formation in B25 Bavarian bentonite microcosms. Their study

proposed that lactate underwent metabolism through the reductive pathway of acetyl-CoA, leading to the incomplete oxidation of lactate and the concurrent reduction of sulfate, resulting in the formation of acetate and hydrogen sulfide. This last component formation could be related to the fissures showed in the microcosms (**Fig. 3**) and the rotten egg odor after sampling (He et al., 2011). Moreover, SRB can lead with the conversion of lactate to acetate, CO_2, and H_2 in the absence of sulfate, confirming the production of acetate in some of treatments (Pankhania et al., 1988).

Additionally, 2 mM of Se(IV) can be toxic to some bacteria (Povedano-Priego et al., 2023) and could reduce the bacterial activity within the microcosmos. Moreover, this metalloid could act as a competitor with sulfur as a final electron acceptor under anaerobic condition (Staicu and Barton, 2021) linking with the slow consumption in the microcosms (**Fig. 5C**). This phenomenon could lead to a deceleration of biogeochemical processes, attributed to a reduction in bacterial diversity and/or an extended adaptation period for selenium-tolerant microorganisms.

3.3_ Determination of microbial communities: implication on Se(IV) reduction and copper corrosion in an early-incubation stage

The impact of the biological and physicochemical parameters (bentonite pre-sterilization, electron donors/acceptor, bacterial consortium, and selenium) on the evolution of the microcosms at short incubation period (45 days) was characterized. During this time frame, the microcosms exhibited greater visual heterogeneity between treatments, facilitating a clearer distinction of the effects attributed to each parameter.

3.3.1_ Identification of microbial communities

The total DNA from the microcosms after 45 days of incubation was extracted and sequenced in triplicate. This section is dedicated to identifying bacterial

communities in the treatments: tyndallized (StB), presence of electron donors/acceptors (eD), and addition of the bacterial consortium (BC) during the early stage of incubation (45 days) to study their influence on the corrosion of copper material and selenium speciation at this initial phase. Some replicates were not included in this study due to their failure during the DNA extraction step (B.Se.BC_R1 and StB.eD.Se_R1). 353 phylotypes were detected and annotated in 12 phyla (98.34 %) being Proteobacteria (68.00 %) and Firmicutes (26.58 %) the most abundant (**Supplementary Table S1**). At genus level, the phylotypes were annotated in 135 OTUs (**Supplementary Table S2**) with *Pseudomonas* (40.30 %), *Stenotrophomonas* (12.52 %), *Symbiobacterium* (12.43 %), unclassified Clostridia (6.93 %), unclassified Rhodospirillales (6.00 %), and *Pseudoalteromonas* (2.79 %) presenting the higher relative abundance in the pool of samples.

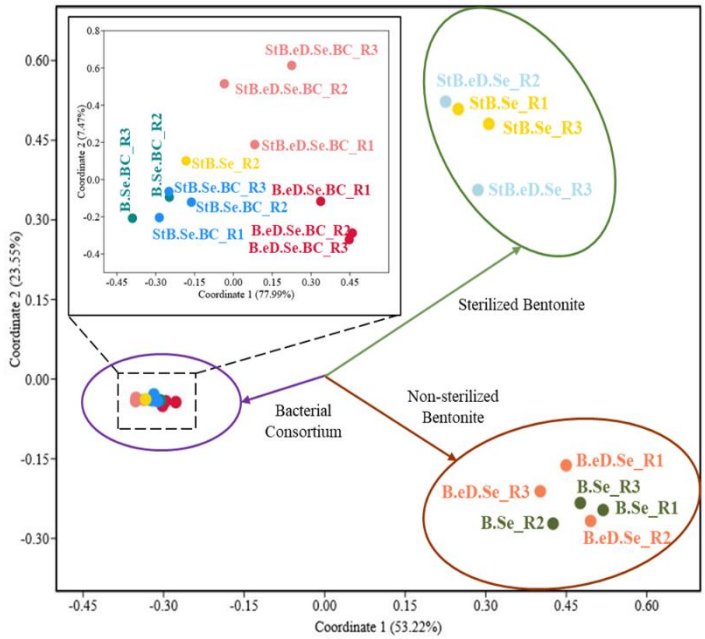

Fig. 6. Principal Coordinate Analysis (PCoA) plot showing the dissimilarity of bacterial communities at genus level from Se(IV)-containing bentonite-slurry microcosms after 45 days of anaerobic incubation. Glossary: Bentonite (B), Sterilized bentonite (StB), amended with acetate, lactate and sulfate (eD); Selenium(IV) 2mM (Se), and with BPAS consortium (BC).

To evaluate the distribution of dissimilarity among the microcosms, considering the relative abundance at the genus level, a Principal Coordinate Analysis (PCoA) was conducted using Bray-Curtis distance (**Fig. 6**). The dissimilarity between sterilized bentonite samples (StB.eD.Se and StB.Se), non-sterilized bentonite samples (B.eD.Se and B.Se), and the addition of the bacterial consortium (BC samples) was evidenced. Among the samples spiked with the bacterial consortium (BC samples), the dissimilarity between treatments was less evident corresponding with more homogeneity between those microcosms.

In order to identify the OTUs involved in the dissimilarity between samples, a heatmap was constructed (**Fig. 7**). In the absence of bacterial consortium in the sterilized bentonite samples (StB cluster, green line **Fig. 7**), bacterial diversity significantly diminished compared to that of the other treatments. The marked differentiation in these treatments was due to the abundance of *Pseudomonas*, *Symbiobacterium*, *Stenotrophomonas*, and unclassified Clostridia. Concerning the samples spiked with the bacterial consortium (BC cluster, purple line **Fig. 7**), the observed group was in line with expectations, as it was attributed to the bacterial genera inherent to the consortium, such as *Pseudomonas*, *Stenotrophomonas*, and to a lesser extent, *Amycolatopsis*. In the cluster of unsterilized-bentonite microcosms (B cluster, brown line **Fig. 7**), the abundance of unclassified Clostridia, unclassified Rhodospirillales, *Pseudoalteromonas*, *Noviherbaspirillum*, and, to a lesser extent, *Pseudomonas*, marked the dissimilarity from the other treatments.

The alpha-diversity indices of the treatments (duplicates in B.Se.BC and StB.eD.Se) at genus level are shown in **Table 2**. The richness indices (Sobs) of the unsterilized samples (B samples) showed higher values in the treatments without bacterial consortium (BC), particularly higher values in the absence of electron donors/acceptor (B.Se > B.eD.Se > B.eD.Se.BC > B.Se.BC) following the same trend as Se(IV) unamended samples (**Table 2,** Chapter 3). In contrast, the samples

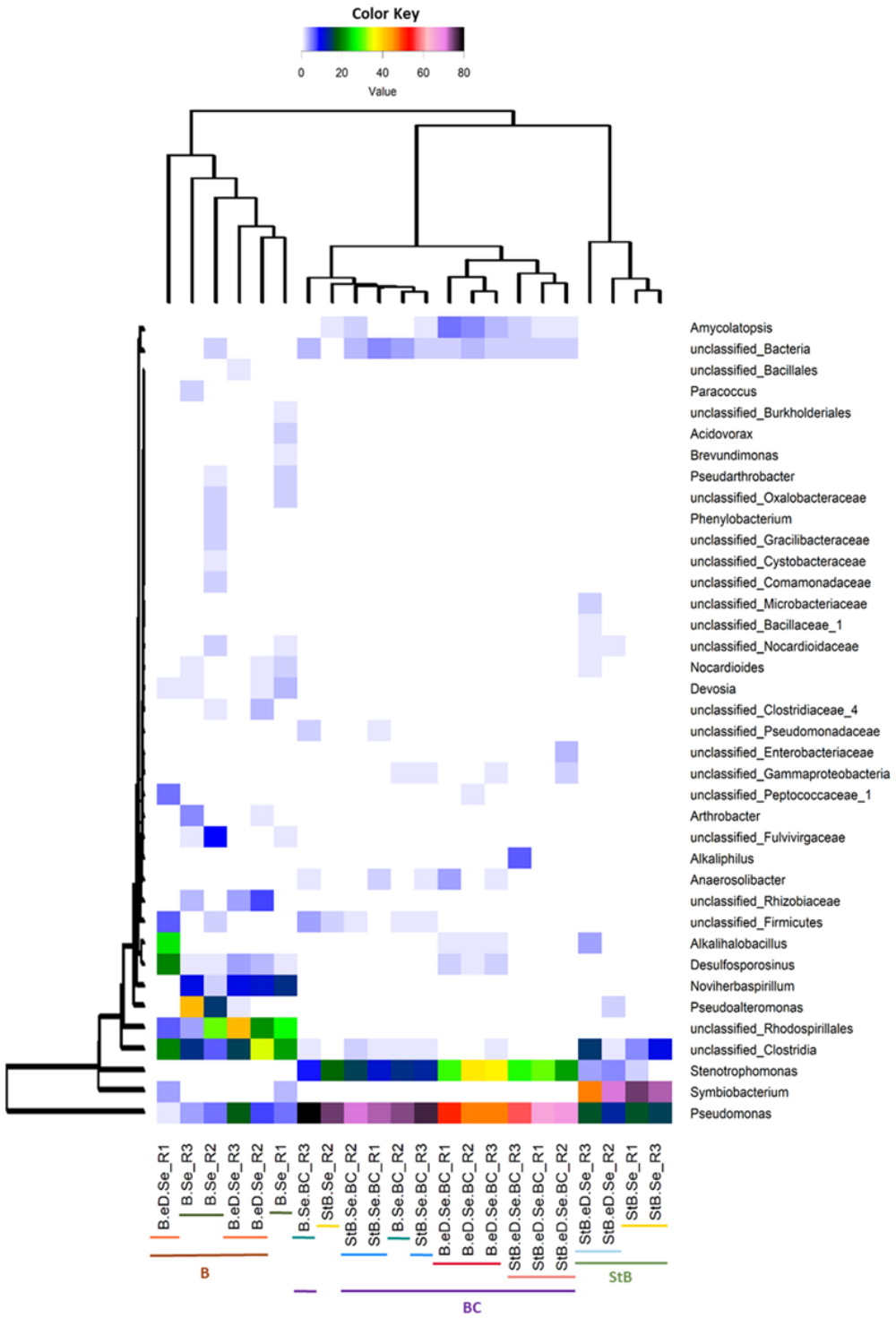
Color Key
0
20
40
60
80
Value
Amycolatopsis
unclassified_Bacteria
unclassified_Bacillales
Paracoccus
unclassified_Burkholderiales
Acidovorax
Brevundimonas
Pseudarthrobacter
unclassified_Oxalobacteraceae
Phenylobacterium
unclassified_Gracilibacteraceae
unclassified_Cystobacteraceae
unclassified_Comamonadaceae
unclassified_Microbacteriaceae
unclassified_Bacillaceae_1
unclassified_Nocardioidaceae
Nocardioides
Devosia
unclassified_Clostridiaceae_4
unclassified_Pseudomonadaceae
unclassified_Enterobacteriaceae
unclassified_Gammaproteobacteria
unclassified_Peptococcaceae_1
Arthrobacter
unclassified_Fulvivirgaceae
Alkaliphilus
Anaerosolibacter
unclassified_Rhizobiaceae
unclassified_Firmicutes
Alkalihalobacillus
Desulfosporosinus
Noviherbaspirillum
Pseudoalteromonas
unclassified_Rhodospirillales
unclassified_Clostridia
Stenotrophomonas
Symbiobacterium
Pseudomonas
B.eD.Se_R1
B.Se_R3
B.Se_R2
B.eD.Se_R3
B.eD.Se_R2
B.Se_R1
B.Se.BC_R3
StB.Se_R2
StB.Se.BC_R2
StB.Se.BC_R1
B.Se.BC_R2
StB.Se.BC_R3
B.eD.Se.BC_R1
B.eD.Se.BC_R2
B.eD.Se.BC_R3
StB.eD.Se.BC_R3
StB.eD.Se.BC_R1
StB.eD.Se.BC_R2
StB.eD.Se_R3
StB.eD.Se_R2
StB.Se_R1
StB.Se_R3
B
StB
BC

Fig. 7. Heatmap representing genus-level relative abundance and clustering based on Manhattan distance of the slurry-bentonite microcosms with Se(IV) after 45 days of incubation. The 1.33% cut-off, based on the maximums, represents the 38 most abundant OTUs. The relative abundance of each genus is shows with different colors (the warmer the color, the greater relative abundance). The colored lines in X axis represent the clustering observed in PCoA. Glossary: Bentonite (B), Sterilized bentonite (StB), amended with acetate, lactate and sulfate (eD); Selenium(IV) 2mM (Se), and with BPAS consortium (BC).

with sterilized bentonite (StB samples) exhibited a different trend. The richness indices were higher in the treatment with electron donors/acceptor (StB.eD.Se), followed by samples spiked with the bacterial consortium (StB.Se.BC), the treatment with selenium only (StB.Se), and finally, the samples amended with electron donors/acceptor and the bacterial consortium (StB.eD.Se.BC).

Table 2.
Richness (Sobs), diversity (ShannonH. and SimpsonD), and evenness (ShannonE) indices. Glossary: Bentonite (B), Sterilized bentonite (StB), amended with acetate, lactate and sulfate (eD); Selenium(IV) 2mM (Se), and with BPAS consortium (BC).

Treatment	Sobs	ShannonH	SimpsonD	ShannonE
B.eD.Se.BC	27.39	2.08	0.64	0.44
B.Se.BC	20.00	1.37	0.39	0.32
B.eD.Se	46.36	3.50	0.86	0.63
B.Se	68.06	4.05	0.89	0.67
StB.eD.Se.BC	16.22	1.59	0.53	0.40
StB.Se.BC	38.09	1.61	0.44	0.31
StB.eD.Se	46.00	2.36	0.62	0.43
StB.Se	19.60	1.79	0.62	0.42

Regarding the diversity values, the treatments with non-sterilized bentonite (B.Se) had the highest values, followed by the samples amended with electron donors/acceptor (B.eD.Se), whose ShannonH and SimpsonD values were greater than 3 and close to 1, respectively. The remaining treatments exhibited lower values, with ShannonH lower than 3 and SimpsonD further from 1. These values suggest reduced diversity in the samples and the potential taxa dominance in the microcosms. Comparing the results with those found in the equivalent samples without selenium in Chapter 3 (**Table 2**, Chapter 3), the addition of 2 mM Se(IV)

in the microcosms seems to affect, in general terms, the values of bacterial diversity in the microcosms.

The relative abundance of OTUs in each treatment in triplicate (duplicates in B.Se.BC and StB.eD.Se) are shown in **Fig. 8** and **Supplementary Table S2**. Overall, *Pseudomonas* emerged as the predominant OTU in this study across the entire sample pool (40.30% of the total relative abundance). Its dominance was particularly pronounced in samples spiked with the bacterial consortium (BC samples), where it constituted the taxa dominance in the community, ranging from 77.20 % of relative abundance in sample B.Se.BC to 48.18% in sample B.eD.Se.BC. Within this subset of samples, *Stenotrophomonas* (member of the bacterial consortium) emerged as the second most represented genus, with relative abundance ranging from 34.47 % in sample B.eD.Se.BC to 10.79 % in sample B.Se.BC. The relative abundance of *Amycolatopsis* in the BC treatments was

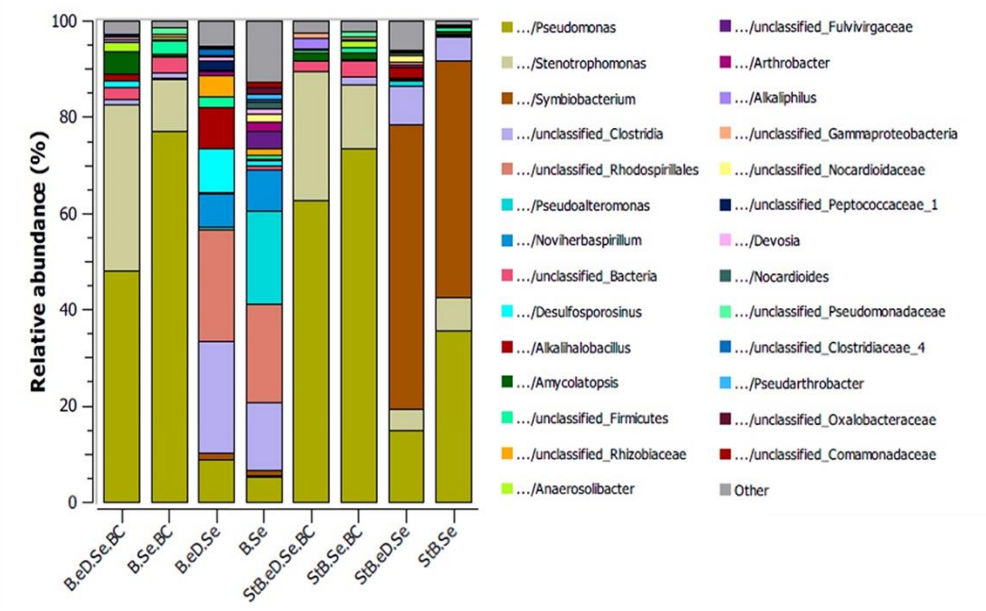

Fig. 8. OUT relative abundance of bacterial communities from the slurry-bentonite microcosms. Cutoff: 0.20% of relative abundance. Stacked bars show averages of biological replicates. Glossary: Bentonite (B), Sterilized bentonite (StB), amended with acetate, lactate and sulfate (eD); Selenium(IV) 2mM (Se), and with BPAS consortium (BC).

comparatively lower than the others members of the consortium, ranging between 4.63 % in sample B.eD.Se.BC and 0.38 % in sample B.Se.BC. Conversely, *Bacillus* was absent possibly due to being below the detection limits of the sequencing process.

Comparing the relative abundances of the bacterial strains belonging to the consortium in the spiked samples of this study with its counterparts without Se(IV) (**Supplementary Table S3,** Chapter 3), some differences were found. In the presence of Se(IV), *Pseudomonas* exhibits a decrease in relative abundance in the B.eD.Se.BC sample, approximately 21 % compared to its counterpart B.eD.BC. In contrast, in B.BC - B.Se.BC, this decrease was only by 0.91 %. Conversely, in the treatments with sterilized bentonite (StB), the opposite occurred, *Pseudomonas* increased by 10.47 % of relative abundance in sample StB.eD.Se.BC (compared to StB.eD.BC), and 18.85 % in sample StB.Se.BC (compared to StB.BC). In the case of *Stenotrophomonas*, the addition of Se(IV) in the microcosms had a pronounced effect on sample B.eD.Se.BC, where its relative abundance increased by 26.37 % compared to its counterpart B.eD.BC, while it decreased by 21.72 % in StB.Se.BC compared to StB.BC (**Supplementary Table S3**, Chapter 3). In the rest of the bacterial consortium treatments, this percentage remained relatively stable, with a decrease of approximately 1 %. Regarding *Amycolatopsis*, its relative abundance was 2.32 % higher in sample B.eD.Se.BC, and it was detected in the StB.Se.BC sample with a relative abundance of 1.21 % compared to its Se(IV)-free counterpart, where the presence of this bacterium was not detected. The effect of selenium addition in the microcosms appears to have a potentially negative or positive impact on the BPAS bacterial consortium members, depending on the treatment. This effect is compensated by a balanced increase-decrease in *Pseudomonas* and *Stenotrophomonas*, which were the dominant genera in the microcosms spiked with the bacterial consortium. *Pseudomonas* and *Stenotrophomonas* have demonstrated tolerance and the ability to interact with Se(IV) by reducing it to Se(0) under anaerobic conditions, resulting in the

formation of orange-reddish precipitates in form of selenium nanoparticles (SeNPs) (Staicu et al., 2015; Ruiz-Fresneda et al., 2019). This process is linked to the presence of red precipitates observed in microcosms spiked with bacterial consortium at 45 days-incubation (BC samples, **Fig. 3**), deposited in both the bentonite phase and the bentonite:supernatant interface. The presence of the bacterial consortium stimulates and accelerates the Se(IV) reduction processes. The addition of the bacterial consortium in the microcosms accelerate the reduction process. In treatments without the consortium, the reddish precipitates were less evidenced after 45 days of incubation (**Fig. 3**). Moreover, these bacteria have demonstrated the capacity to metabolize acetate and/or lactate as a carbon source under anoxic conditions (Freikowski et al., 2010; Sanchez-Castro et al., 2017) and may play an important role in the lactate consumption and acetate production observed at 45-days incubation in the bacterial consortium treatments (**Fig. 5**).

Regarding samples lacking bacterial consortium (B.eD.Se and B.Se), the OTU with the highest relative abundance was unclassified Rhodospirillales (23.18 % and 20.65 %, respectively), followed by unclassified Clostridia (23.14 %), *Desulfosporosinus* (9.05 %), and *Pseudomonas* (8.89 %) in sample B.eD.Se. In the case of B.Se, the following most abundant OTUs were *Pseudoalteromonas* (19.11 %), unclassified Clostridia (13.94 %), and *Noviherbaspirillum* (8.55 %). Interestingly, the composition of bacterial communities in the presence of Se(IV) within the microcosms exhibited some shifts compared to microcosms without Se(IV) (Chapter 3). In the absence of Se(IV) (Chapter 3), the most representative OTUs in sample B.eD were *Pseudoalteromonas* (24.17 %), *Desulfocurvibacter* (22.72 %), and *Pseudomonas* (9.80 %). Meanwhile, in sample B, the predominant OTUs were *Pseudomonas* (19.11 %), unclassified Clostridiales (18.25 %), and *Desulfuromonas* (16.37 %). Comparing the relative abundance of *Desulfocurvibacter* in sample B.eD with its counterpart with Se(IV) from this study (B.eD.Se), the addition of this element reduces to 100 % the presence of this SRB as occurred with *Desulfuromonas* in both samples (B.eD.Se and B.Se). The

bacterial diversity present in the microcosms was not greatly affected by the addition of electron donors/acceptor. However, there were some differences observed. Sample B.eD.Se had a higher presence of *Desulfosporosinus* and *Alkalihalobacillus* (9.05 % and 8.52 %, respectively) compared to sample B.Se (1.07 % and 0.21 %). On the other hand, *Pseudoalteromonas* was more prominent in sample B.Se (19.11 %) than in B.eD.Se (0.21 %). *Desulfosporosinus* is a SRB capable of reducing sulfate through incomplete oxidation of lactate resulting in lactate and CO_2 (Stackebrandt et al., 1997), and may be one of bacteria involved in the slight increase in acetate content observed after 45 days of incubation in the B.eD.Se sample (**Fig. 5**). In addition, their tolerance to selenium has also been demonstrated in previous studies (Povedano-Priego et al., 2023; Aoyagi et al., 2021). In addition, *Alkahalibacillus* is a recently described genus with some of its members being facultatively anaerobic, as well as tolerant to heavy metals and metalloids such as chromium or arsenic, which may be associated to the tolerance to Se(IV) (Patel and Gupta, 2020; Gautam et al., 2021; Haghi et al., 2023). Regarding the sterile bentonite treatments without bacterial consortium (StB.eD.Se and StB.Se), it is important to note the high relative abundance of *Symbiobacterium* (58.97 % and 49.21 %, respectively). This bacterial genus is anaerobic but can tolerate low levels of oxygen and can grow in temperatures ranging from 40 to 70 ºC (Shiratori-Takano et al, 2014). Previous studies have identified this genus with an important relative abundance in soils containing Se(IV) (Povedano-Priego et al., 2023; Aoyagi et al., 2021).

Overall, the presence of Se(IV) influences the bacterial communities within the microcosms. Therefore, it is important to the explore these communities' role on interaction with this metalloid and its impact on Se speciation.

3.3.2_ Characterization of microbial-mediated Se(IV) reduction

As showed in **Fig. 3**, selenium reduction was more pronounced in the samples containing the bacterial consortium (BC samples) after 45 days of incubation. In

contrast, the process was slower and less evident in the absence of the bacterial consortium. As previously mentioned, this section is focused on an early-stage (45 days incubation) characterization of the selenium reduction products (SeRPs) in order to achieve the first step of Se(IV) reduction.

The characterization of SeRPs' structure, morphology and elemental composition was determined by HAADF-TEM coupled by EDX maps, while their crystalline structure was achieved by SAED and lattice spacing measured using HRTEM. The microcosms lacking bacterial consortium did not show the red layer in the interface bentonite:supernatant at 45-days incubation (**Fig. 3**). No SeRPs were observed in the micrographs of these microcosms (**Supplementary Fig. S1**). Only bentonite was observed, as shown by the Si, Al, Fe, Mg signals in the microanalyses and the elemental distribution in the EDX maps (**Supplementary Fig. S1**).

In the consortium-containing samples (BC samples), micrographs of thin sections of the interface layer showed the presence of electron-dense precipitates of different sizes, shapes and location (**Fig. 9.1** and **9.2**). As indicated by the phosphorous (P) signal in the EDX maps (**Fig. 9.1C** and **9.2C**), all samples showed intracellular selenium nanostructures or were found near cellular biomass with a rounded shape. SAED analysis (**Fig. 9.1B** and **9.2B**) confirmed that these structures were amorphous (*a*-Se). In addition, extracellular SeRPs with different morphology and size were found in all samples (**Fig. 9.1** and **9.2**). The elemental mapping of these precipitates (**Fig. 9.1C** and **9.2C**) in each sample showed that contained Se and S. The SAED patterns (**Fig. 9.1B** and **9.2B**) indicated the crystallinity of the precipitates, while the lattice spacing observed at high resolution (**Fig. 9.1D** and **9.2D**) showed values of 0.30 nm and 0.37 nm, corresponding to the (101) and (100) plane of trigonal selenium (*t*-Se), respectively; and 0.38 nm corresponding to (211) plane of monoclinic selenium (*m*-Se).

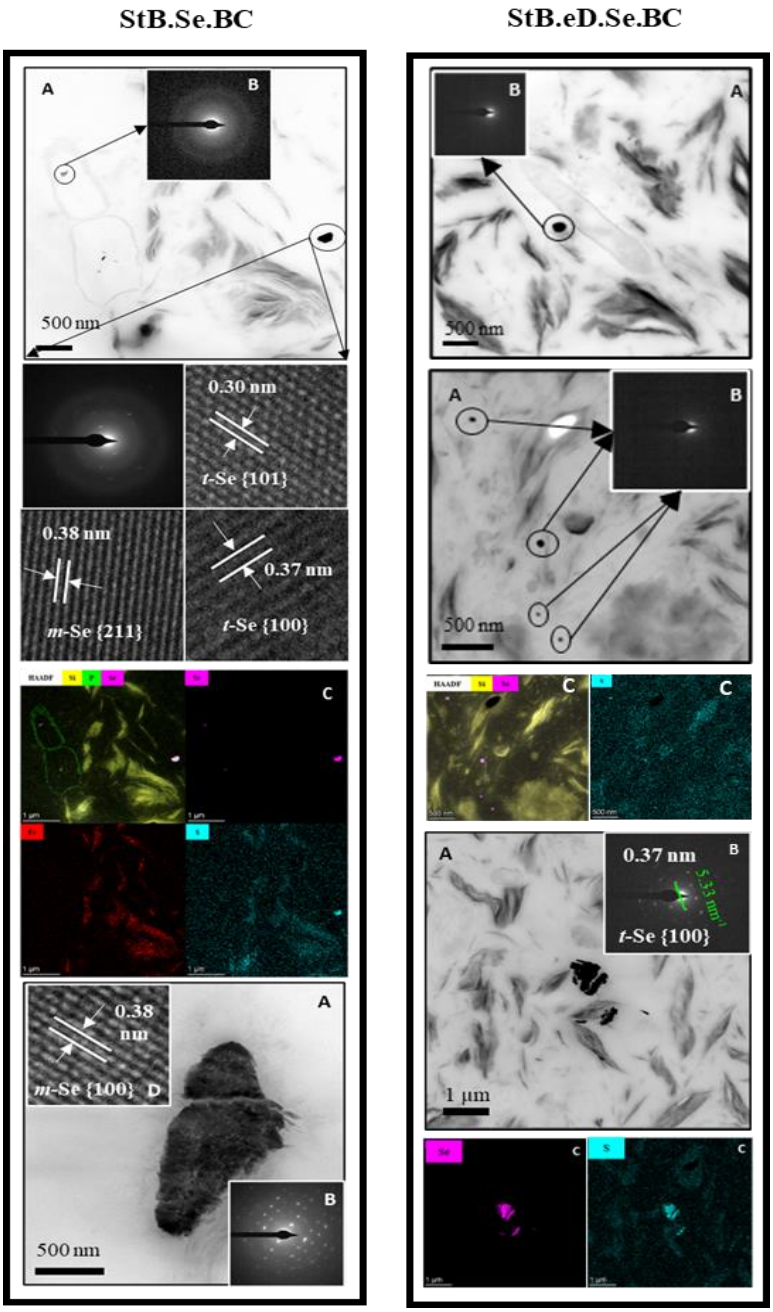

Fig. 9.1. HRTEM micrographs of the SeRPs in the bacterial consortium-containing microcosms (BC treatments) at 45 days of anaerobic incubation. A) HAADF images, B) associated SAED patterns, C) EDX maps showing the elemental distribution of Si, P, Se, Fe, and S; D) High resolution images and d-spacing. Glossary: Bentonite (B), Sterilized bentonite (StB), amended with acetate, lactate and sulfate (eD); Selenium(IV) 2mM (Se), and with BPAS consortium (BC).

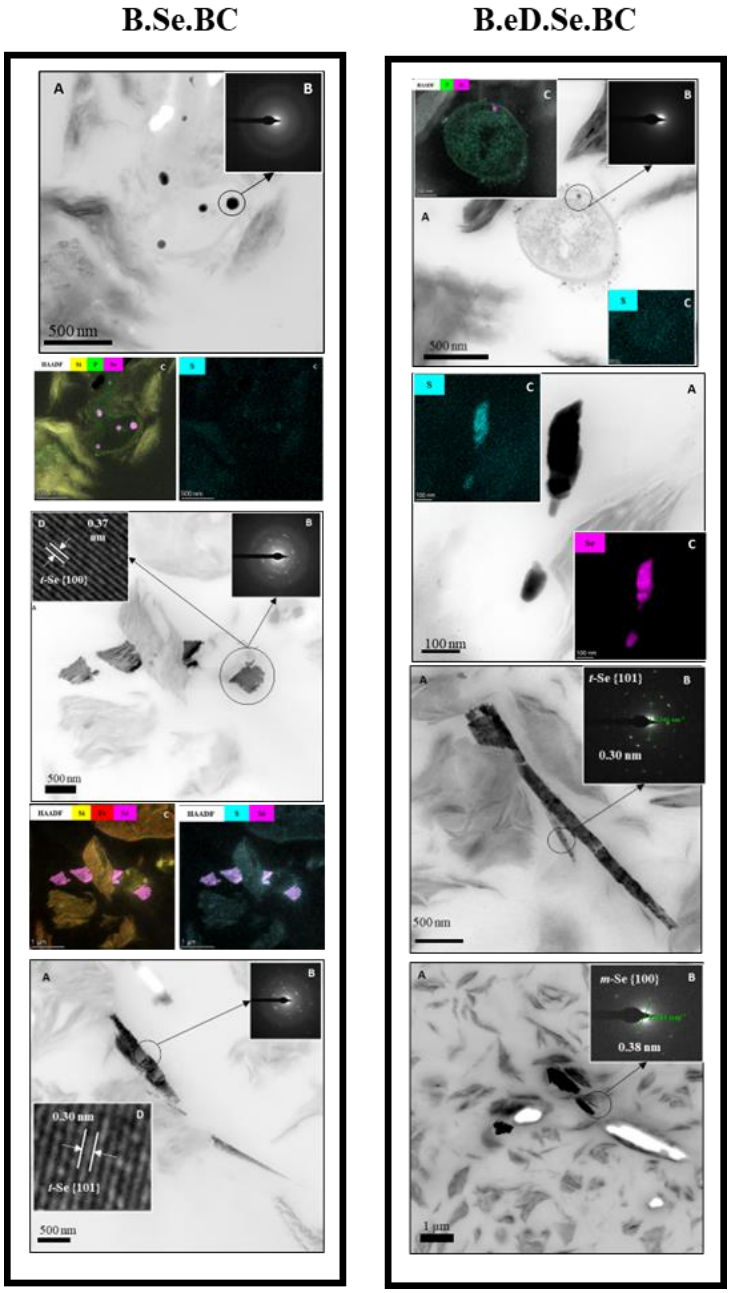

Fig. 9.2. HRTEM micrographs of the SeRPs in the bacterial consortium-containing microcosms (BC treatments) at 45 days of anaerobic incubation. A) HAADF images, B) associated SAED patterns, C) EDX maps showing the elemental distribution of Si, P, Se, Fe, and S; D) High resolution images and d-spacing. Glossary: Bentonite (B), Sterilized bentonite (StB), amended with acetate, lactate and sulfate (eD); Selenium(IV) 2mM (Se), and with BPAS consortium (BC).

The ability of the bacterial strains of the consortium to reduce Se(IV) to Se(0) has been previously demonstrated by Povedano-Priego et al. (2023), where these bacteria accelerated the reduction of 2 mM Se(IV) to Se(0) nanoparticles in anaerobic microcosms containing saturated bentonite. Furthermore, the predominant bacteria in the BC-containing microcosms of this study, *Pseudomonas* and *Stenotrophomonas*, were the most abundant genera (**Fig. 8**), which show the ability to tolerate selenium through its reduction to Se(0) nanoparticles (Staicu et al., 2015; Ruiz-Fresneda et al., 2019). In bentonites, selenite immobilization can be mediated by abiotic and biotic processes (Wang et al., 2022). Within the abiotic processes highlight the adsorption of Se to the surface of clay minerals, reduction to Se(0) mediated by pyrite (FeS_2) or via structural Fe(II) present in smectites (major mineral in bentonites) (Breynaert et al., 2010; Hoving et al., 2019; Kang et al., 2011). In contrast, no abiotic reduction of selenite was detected in our study (sample StB.Se, **Fig. 3**, **Supplementary Fig. S1**).

Selenium can manifest in three different allotropes: amorphous (*a*-Se), monoclinic (*m*-Se), and trigonal (*t*-Se), with *a*-Se considered thermodynamically unstable, while *t*-Se represents the most stable allotrope. The structural analysis of the SeRPs in this study, conducted through SAED and HRTEM, unveiled that intracellular selenium precipitates, appearing as SeNPs, exhibited an amorphous allotropy. In contrast, extracellular electron-dense aggregates were identified as SeRPs with monoclinic and trigonal allotropy, occasionally combined (sample StB.Se.BC, **Fig. 9**). Notably, the extracellular crystalline SeRPs demonstrated a close association with sulfur (S), as evidenced in the EDX maps (**Fig. 9C**). This could suggest that the reduction of Se(IV) to Se(0) might occur within the bacterial cells, resulting in the formation of amorphous SeNPs (*a*-Se). Subsequently, these particles could be released into the extracellular environment through mechanisms such as cellular detoxification or lysis. Once in the extracellular space, the transformation process to *m*-Se and, subsequently, to *t*-Se would take place. This finding aligns with conclusions drawn in previous research involving complex

saturated-bentonite microcosms under anaerobic conditions (Povedano-Priego et al., 2023) and supports the mechanism proposed by Ruiz-Fresneda et al. (2018). The suggested mechanism outlines a biotransformation process influenced by Se incubation time in *S. bentonitica* BII-R7 (strain belonging to our bacterial consortium). The mechanism initiated with the generation of intracellular amorphous Se nanospheres, expelled externally through cell lysis, leading to the formation of extracellular crystalline structures, specifically trigonal selenium. Moreover, the presence of sulfate in the microcosms could mediated the interaction of the SeNPs with S to form the observed selenium-sulfur precipitates in the extracellular environment (Vogel et al., 2018). The Se-S interaction manifested as precipitates may impede sulfate availability that could impact the corrosion of copper material. It is crucial to explore not only its influence on bacterial communities (section 3.3.1) but also how the presence of Se(IV) in the microcosms might affect the corrosion of Cu-mCan.

3.3.3_ Surface characterization of the Cu-mCan

To evaluate the impact of microbial communities and the presence of selenium on the copper surface after 45-day incubation, the Cu-mCan were recovered from the microcosms. The surfaces underwent microscopic and spectroscopic analysis by HRSEM, EDX, and XPS. The characterizations were focused on Cu-mCan derived from microcosms with non-sterilized bentonite.

Fig. 10 shows Cu-mCan and HRSEM images before (t. 0) and after a 45-day anaerobic incubation under the different treatments. Visual differences in coloration were observed compared to the initial state of Cu-mCan (t. 0). It is worthy to note that the bentonite adhered to the copper surface was intentionally retained to prevent the potential displacement of copper alteration-related compounds. The sample B.eD.Se.BC showed a significant shift towards dark gray-black coloration (**Fig. 10_B**). These hues was also observed in some regions of B.Se.BC and B.eD.Se (**Fig. 10_C,D**). At microscopic level, the post-incubation

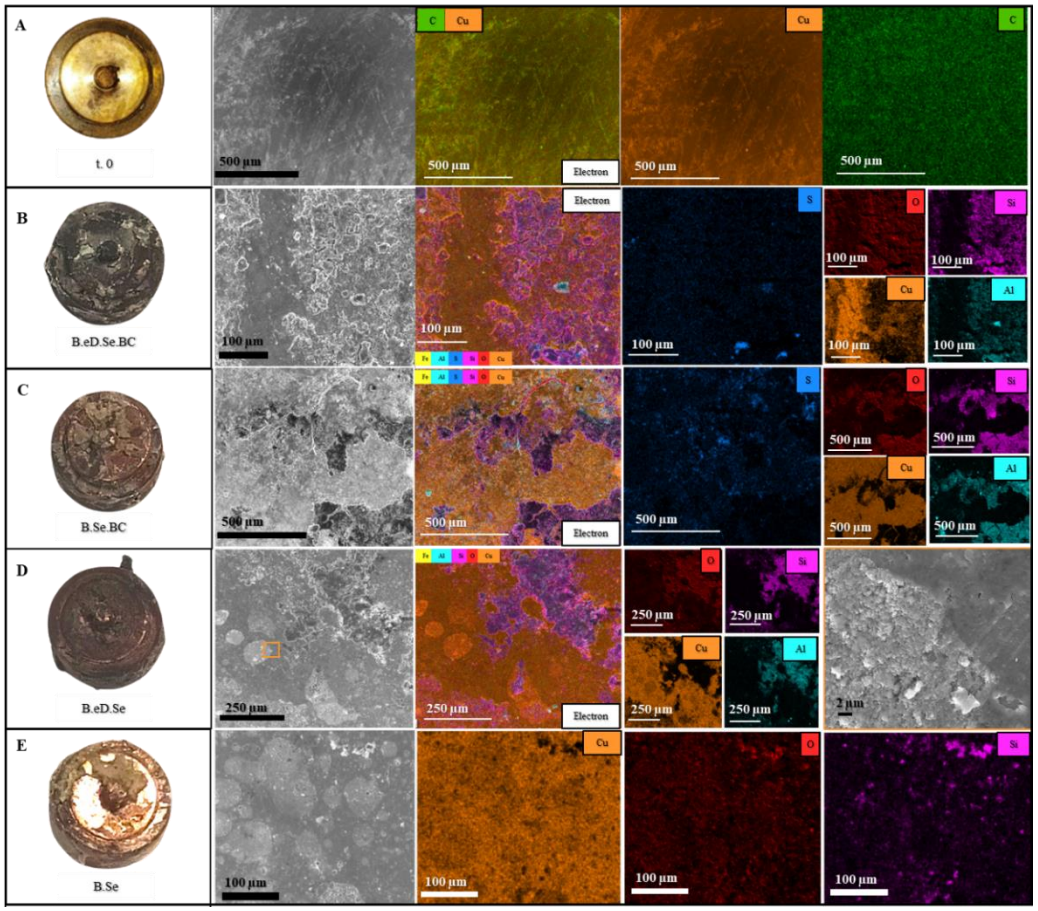

Fig. 10. Visual (first column), electron images (second column), and EDX maps of the Cu-mCan surface before experimental set-up (A) and after 45-days anoxic incubation from microcosms B.eD.Se.BC (B), B.Se.BC (C), B.eD.Se (D), and B.Se (E). EDX show the distribution of Cu (orange), Fe (yellow), S (dark blue), Si (pink), Al (cyan), O (red), and C (green) in the studied area. Glossary: Bentonite (B), Sterilized bentonite (StB), amended with acetate, lactate and sulfate (eD); Selenium(IV) 2mM (Se), and with BPAS consortium (BC).

samples exhibited heterogeneous topography (second column, **Fig. 10**), in contrast to the uniform topography observed in the t. 0 sample. Cu-mCan at t. 0 was already explained in the previous chapter (Chapter 3) only showing the presence of Cu and C, attributable to the metallization process during sample preparation for HRSEM, in the EDX maps. In addition, the subsequent columns of **Fig. 9** present elemental EDX maps that illustrate the distribution of Iron (Fe), Carbon (C), Aluminum (Al), Sulfur (S), Silicon (Si), Oxygen (O), and Copper (Cu) in selected areas. The Si (pink), Fe (yellow), and Al (cyan) signals were attributed to the presence of

bentonite adhered to the Cu surface. The detection of O (red) was mainly associated with Si (Si-O bonds), indicating its association with bentonite. Additionally, O was detected, to a lesser extent, on the copper surface. Sample B.eD.SeBC showed sulfur accumulates which may be related to copper corrosion compounds (Cu_xS) (**Fig. 10**) linking with the consumption of ≈ 8% in the content of sulfate (**Fig. 5**). The sample B.Se.BC also showed S-accumulates (**Fig. 10**). No sulfate was added as a final electron acceptor to stimulate bacterial activity in B.Se.BC microcosms, but it is worth noting that sulfur is present as a trace element in accessory minerals such as gypsum (as sulfate) or pyrite (as sulfide) in FEBEX bentonite (wt. 0.14% and 0.02%, respectively) (Fernández et al., 2004b). This sulfur could, potentially, participate in MIC processes. In samples B.eD.Se and B.Se, no sulfur was detected and detection of O was associated with the presence of Si (silicates signals from the bentonite) (**Fig. 10_E,D**). Moreover, on the surface of these Cu-mCan surfaces, some "patches" were observed. Upon closer examination at higher magnification, these patches appeared to indicate a flaking process on the copper surface, potentially exposing it to oxidation processes. During the characterization of the SeRPs, Se-S interaction was observed. However, no Se signal was detected on the copper surface by EDX.

As showed in the previous chapter (Chapter 3), the presence of S-accumulates in samples B.eD.Se.BC and B.Se.BC could be related to the presence of Cu_2S resulted from microbial activity. Under anoxic environments, SRB can use lactate as electron donor to reduce sulfate to sulfide via dissimilatory sulfate reduction (**Eq. 1,** Dou et al., 2020). This sulfide production was evidenced by the rotten egg odor detected in the microcosms (He et al., 2011). Moreover, Salehi Alaei et al. (2023) reported that the transformation of copper oxide (Cu_2O) into copper sulfide (Cu_2S) through a chemical exchange with sulfide (**Eq. 2**) can be thermodynamically possible. In addition, Dou et al. (2020) suggested that HS^-, from the SRB metabolite H_2S, could migrate to the copper surface and react to form Cu_2S (**Eq. 3**). SRB could bond to copper surfaces creating a primary

corrosion film of Cu_2S (Chen et al., 2014). The creation of this Cu_2S film and the production extracellular polymeric substances (EPS) by SRB can reduce the toxicity of copper (from the canister surface) to this group of bacteria. Moreover, the presence of SRB has been proven to cause high-purity copper corrosion in groundwater boreholes or MX-80 clay, leading to Cu_2S precipitate formation (Johansson et al., 2017; Masurat et al., 2010). The addition of acetate, lactate, and sulfate to Spanish bentonite has been demonstrated to stimulate bacterial activity leading to the formation of corrosion compounds on copper discs in compacted dry bentonite blocks (Martínez-Moreno et al., 2023). The water hyper-saturation of the bentonite in these experiments accelerated the corrosion process, with compound formation observed as early as 45 days into incubation. Although Se-S interaction has been observed by HRTEM, no Se signal was detected on the Cu-mCan surface. Therefore, further analysis are required to investigate the how the presence of Se(IV) could affect the corrosion of copper.

Eq. 1. $SO_4^{2-} + 9H^+ + 8e^- \rightarrow HS^- + 4H_2O$

Eq. 2. $Cu_2O\ (s) + SH^-\ (aq) \rightarrow Cu_2S\ (s) + OH^-\ (aq)$

Eq. 3. $2Cu + HS^- + H^+ \rightarrow Cu_2S\ (s) + H_2\ (g)$

4_ Overview and conclusions

The fission of uranium fuel for nuclear power generation produces High-Level Radioactive Waste (HLW). Among the generated products, selenium stands out, being the isotope ^{79}Se one of the few radionuclides that will determine the decay time of HLW during their final storage in Deep Geological Repositories (DGRs) due to its long half-live. Although the DGR environment is designed to be a hostile environment to the survival and activity of microorganisms (e.g., high temperature due to decay processes, high compaction density of bentonite, low water activity, etc.), it is important to consider all possible scenarios, including those where

wastes are released, in order to create a safe DGR, and protect the environment and future generations for period of time spanning millions of years. For this purpose, anaerobic microcosms were elaborated with favorable conditions for bacterial activity (uncompacted bentonite, high water activity, and the addition of nutrients in the form of electron donors and acceptor). The DGR is designed to prevent water infiltration, albeit nutrient flow within groundwater may be possible. Furthermore, in case of fissures or canister corrosion, they would be sealed by the bentonite, preventing the escape and diffusion of waste through the following barriers. Nevertheless, studying all the different scenarios through laboratory-scale models will help us understand and prevent different scenarios.

Visually, the addition of the BPAS consortium in the microcosms accelerates the processes of Se(IV) reduction to Se(0), followed by the addition of electron donors/acceptors. In contrast, the pre-sterilization of bentonite delays these processes, with no selenium reduction (red color) detected in the StB.Se sample during the year of incubation. Moreover, the addition of Se(IV) in the microcosms does not impact the initial pH significantly, and, except for some variations in specific samples, tends towards slightly less alkaline values (7.3 – 8.3), possibly due to gas production as a result of bacterial activity (manifested by a change in color and fissure formation in the bentonite, and the characteristic rotten egg odor, in most of the treatments) or the inherent buffering capacity of bentonite. Moreover, Se(IV) retard geochemical process due to its toxicity for some bacteria within the bentonite community. The presence of nutrients such as lactate, acetate and sulfate stimulate microbial activity.

The presence of Se(IV) in the microcosms reduce the presence of some SRB, while the bentonite amendment with electron donors/acceptor stimulate the growth of the Se-tolerant SRB *Desulfosporosinus*. Additionally, Se-tolerance bacteria such as *Pseudomonas, Stenotrophomonas,* and *Alkahalibacillus* can influence the visual changes observed in the microcosms indicated evidence of Se(IV) reduction to

Se(0) over the year-long anaerobic incubation period. In samples with electron donors/acceptors, lactate was the main energy source to be consumed, associated with acetate production and subsequent consumption, and to a lesser extent, sulfate reduction. The kinetic rate of these processes in the samples increased upon the nature of the biological of physicochemical parameter in the flowing order: spiked bacterial consortium / amended electron donors/acceptor / bentonite pre-sterilization.

The presence of the BPAS consortium revealed the reduction of selenium. The suggested process started with the intracellular uptake and reduction of Se(IV) to Se(0) in form of nanospheres with amorphous allotropy (*a*-Se), which in the extracellular space, led to the formation of extracellular crystalline structures, progressing from monoclinic selenium (*m*-Se) and concluding with the most stable form of trigonal selenium (*t*-Se). Moreover, the presence of sulfate could mediate the interaction of the Se(0) precipitates with sulfur, forming observed selenium-sulfur precipitates in the extracellular environment. This microbial-influence process can help with the immobilization of Se in case of a release of HLW.

SRB oxidize lactate by using sulfate as final electron acceptor via dissimilatory pathway. The resulting biogenic sulfide could mediate the transformation of copper oxides (potentially arising from trapped oxygen on the bentonite or by the reduction of H_2O molecules from the EW) to copper sulfide (Cu_2S) by a chemical substitution reaction. Moreover, HS^- can diffuse to copper surface and deal with the formation of Cu_2S. Additionally, further analysis are required to investigate the influence of Se(IV) on copper corrosion.

Overall, the presence of selenium impacts the bacterial communities inherent of the Spanish bentonite by affecting their activity. Furthermore, the enrichment of selenium-tolerant bacteria capable of reduce Se(IV) to Se(0) could benefit the

DGR safety due to the immobilization of this metalloid, enhancing the repository's environmental security.

Funding

The present work was supported by the grant RTI2018–101548-B-I00 “ERDF A way of making Europe” to MLM from the “Ministerio de Ciencia, Innovación y Universidades” (Spanish Government). The project leading to this application has received funding from the European Union’s Horizon 2020 research and innovation programme under grant agreement No 847593 to MLM. ADM acknowledges funding from the UK Engineering and Physical Sciences Research Council (EPSRC) DTP scholarship (project reference: 2748843).

Acknowledgements

The authors acknowledge the assistance of Dr. F. Javier Huertas (IACT, Spain) for his guidance and help in collecting the bentonite from the El Cortijo de Archidona site (Almería). Rahul (Instituto del Agua, University of Granada) for HPIC measurements. Moreover, Daniel García Muñoz Bautista Cerro and Alicia González Segura (Centro de Instrumentación Cientifica, University of Granada, Spain) for the sample preparation and microscopy assistance, respectively.

References

Abdalla, Z. A. Y., Ismail, M. Y. A., Njoroge, E. G., Hlatshwayo, T. T., Wendler, E., & Malherbe, J. B. 2020. Migration behaviour of selenium implanted into polycrystalline 3C–SiC. Vacuum, 175, 109235. https://doi.org/10.1016/j.vacuum.2020.109235

Aoyagi, T., Mori, Y., Nanao, M., Matsuyama, Y., Sato, Y., Inaba, T., ... & Hori, T. 2021. Effective Se reduction by lactate-stimulated indigenous microbial communities in excavated waste rocks. J. Hazard. Mater., 403, 123908. https://doi.org/10.1016/j.jhazmat.2020.123908

Avendaño, R., Chaves, N., Fuentes, P., Sánchez, E., Jiménez, J. I., & Chavarría, M. 2016. Production of selenium nanoparticles in *Pseudomonas putida* KT2440. Sci. Rep., 6(1), 37155. https://doi.org/10.1038/srep37155

Baggio, G., Groves, R. A., Chignola, R., Piacenza, E., Presentato, A., Lewis, I. A., ... & Turner, R. J. 2021. Untargeted metabolomics investigation on selenite reduction to elemental selenium by *Bacillus mycoides* SeITE01. Front. Microbiol., 12, 711000. https://doi.org/10.3389/fmicb.2021.711000

Bagnoud, A., De Bruijn, I., Andersson, A. F., Diomidis, N., Leupin, O. X., Schwyn, B., & Bernier-Latmani, R. 2016. A minimalistic microbial food web in an excavated deep subsurface clay rock. FEMS Microb. Ecol., 92(1), fiv138. https://doi.org/10.1093/femsec/fiv138

Batandjieva, B., Delcheva, T., Duhovnik, B. 2009. Classification of radioactive waste: safety guide: IAEA General Safety Guide GSG-1. Vienna. International Atomic Energy Agency.

Bengtsson, A., Pedersen, K. 2017. Microbial sulphide-producing activity in water saturated Wyoming MX-80, Asha and Calcigel bentonites at wet densities from 1500 to 2000 kg m^{-3}. Appl. Clay Sci. 137, 203-212. https://doi.org/10.1016/j.clay.2016.12.024

Bohorquez, L.C., Delgado-Serrano, L., López, G., Osorio-Forero, C., Klepac-Ceraj, V., Kolter, R., Junca, H., Baena, S., Zambrano, M.M., 2012. In-depth Characterization via Complementing Culture-Independent Approaches of the Microbial Community in an Acidic Hot Spring of the Colombian Andes. Micro Ecol. 63, 103–115. https://doi.org/10.1007/s00248-011-9943-3

Breynaert, E., Scheinost, A.C., Dom, D., Rossberg, A., Vancluysen, J., Gobechiya, E., Kirschhock, C.E.A., Maes, A. 2010. Reduction of Se(IV) in boom clay: XAS solid phase speciation. Environ. Sci. Technol. 44, 6649–6655. https://doi.org/10.1021/es100569e

Chen, S., Wang, P., Zhang, D. 2014. Corrosion behavior of copper under biofilm of sulfate-reducing bacteria. Corros. Sci. 87, 407 – 415. http://dx.doi.org/10.1016/j.corsci.2014.07.001

Dou, W., Pu, Y., Han, X., Song, Y., Chen, S., Gu, T. 2020. Corrosion of Cu by a sulfate reducing bacterium in anaerobic vials with different headspace volumes. Bioelectrochemistry, 133, 107478. https://doi.org/10.1016/j.bioelechem.2020.107478

Fernández-Díaz, A.M., 2004. Caracterización y modelización del agua intersticial de materiales arcillosos: estudio de la bentonita de Cortijo de Archidona. PhD Thesis. Universidad Autónoma de Madrid Editorial CIEMAT, p. 505.

Fernández, A. M., Baeyens, B., Bradbury, M., & Rivas, P. 2004b. Analysis of the porewater chemical composition of a Spanish compacted bentonite used in an engineered barrier. Phys. Chem. Earth., Parts A/B/C, 29(1), 105-118. https://doi.org/10.1016/j.pce.2003.12.001

Freikowski, D., Winter, J., & Gallert, C. 2010. Hydrogen formation by an arsenate-reducing Pseudomonas putida, isolated from arsenic-contaminated groundwater in West Bengal, India. Appl. Microbiol. Biotechnol., 88, 1363-1371. https://doi.org/10.1007/s1201000988520

García-Romero, E., María Manchado, E., Suárez, M., and García-Rivas, J. 2019. Spanish bentonites: a review and new data on their geology, mineralogy, and crystal chemistry. Fortschr. Mineral. 9:696. https://doi.org/10.3390/min9110696

Gautam, A., Kushwaha, A., & Rani, R. 2022. Reduction of Hexavalent Chromium [Cr (VI)] by heavy metal tolerant Bacterium *Alkalihalobacillus clausii* CRA1 and its toxicity assessment through flow cytometry. Curr. Microbiol., 79(1), 33. https://doi.org/10.1007/s00284-021-02734-z

Haghi, M., Diznabi, S. H., Karaboz, I., & Omeroglu, E. E. 2023. Arsenic pollution and arsenic-resistant bacteria of drying Urmia Salt Lake. Front. Environ. Sci. 11, 1195643. https://doi.org/10.3389/fenvs.2023.1195643

Hall, D.S., Behazin, M., Binns, W.J., and Keech, P.G. 2021. An evaluation of corrosion processes affecting copper-coated nuclear waste containers in a deep geological repository. Prog. Mater. Sci. 118, 100766. https://doi.org/10.1016/j.pmatsci.2020.100766

Hammer, O., & Harper, D. A. 2001. PAST: paleontological statistics software package for education and data analysis. Palaeontol. Electron. *http://palaeo-electronicaorg*

Hassan, R. S., Abass, M. R., Eid, M. A., & Abdel-Galil, E. A. 2021. Sorption of some radionuclides from liquid waste solutions using anionic clay hydrotalcite sorbent. Appl. Radiat. Isot., 178, 109985. https://doi.org/10.1016/j.apradiso.2021.109985

He, R., Xia, F. F., Wang, J., Pan, C. L., & Fang, C. R. 2011. Characterization of adsorption removal of hydrogen sulfide by waste biocover soil, an alternative landfill cover. J. Hazard. Mater., 186(1), 773-778. https://doi.org/10.1016/j.jhazmat.2010.11.062

Hoving, A.L., Münch, M.A., Bruggeman, C., Banerjee, D., Behrends, T., 2019. Kinetics of selenite interactions with Boom Clay: adsorption–reduction interplay. Geol. Soc., Lond., Spec. Publ. 482, 225–239. https://doi.org/10.1144/SP482-2018-60.

Huertas, F., Fariña, P., Farias, J., García-Siñeriz, J.L., Villar, M.V., Fernández, A.M., Martin, P.L., Elorza, F.J., Gens, A., Sánchez, M., Lloret, A., Samper, J., Martínez, M. Á. 2021. Full-scale Engineered Barriers Experiment. Updated Final Report 1994-2004.

Johansson, A.J., Lilja, C., Sjögren, L., Gordon, A., Hallbeck, L., Johansson, L. 2017. Insights from post-test examination of three packages from the MiniCan test series of coppercast iron canisters for geological disposal of spent nuclear fuel: impact of the presence and density of bentonite clay. Corros. Eng. Sci. Technol. 52, 54-60. https://doi.org/10.1080/1478422X.2017.1296224

Jörg, G., Bühnemann, R., Hollas, S., Kivel, N., Kossert, K., Van Winckel, S., & Gostomski, C. L. V. 2010. Preparation of radiochemically pure ^{79}Se and highly precise determination of its half-life. Appl. Radiat. Isot., 68(12), 2339-2351. https://doi.org/10.1016/j.apradiso.2010.05.006

Kang, M., Chen, F., Wu, S., Yang, Y., Bruggeman, C., Charlet, L. 2011. Effect of pH on Aqueous Se(IV) Reduction by Pyrite. Environ. Sci. Technol. 45, 2704–2710. https://doi.org/10.1021/es1033553.

Keech, P. G., Vo, P., Ramamurthy, S., Chen, J., Jacklin, R., Shoesmith, D. W. 2014. Design and development of copper coatings for long term storage of used nuclear fuel. Corros. Eng. Sci. Technol., 49(6), 425-430. https://doi.org/10.1179/1743278214Y.0000000206

Kora, A. J. 2018. *Bacillus cereus*, selenite-reducing bacterium from contaminated lake of an industrial area: A renewable nanofactory for the synthesis of selenium nanoparticles. Bioresour. Bioprocess., 5(1), 1-12. https://doi.org/10.1186/s40643-018-0217-5

Liu, D., Dong, H., Bishop, M.E., Zhang, J., Wang, H., Xie, S., Wang, S., Huang, L., Eberl, D.D. 2012. Microbial reduction of structural iron in interstratified illite-smectite minerals by a sulfate-reducing bacterium. Geobiology, 10, 150-162. https://doi.org/10.1111/j.1472-4669.2011.00307.x

Lopez-Fernandez, M., Vilchez-Vargas, R., Jroundi, F., Boon, N., Pieper, D., & Merroun, M. L. 2018. Microbial community changes induced by uranyl nitrate in bentonite clay microcosms. Appl. Clay Sci., 160, 206-216. https://doi.org/10.1016/j.clay.2017.12.034

Lopez-Fernandez, M., Fernández-Sanfrancisco, O., Moreno-García, A., Martín-Sánchez, I., Sánchez-Castro, I., Merroun, M.L. 2014. Microbial communities in bentonite formations and their interactions with uranium. Appl. Geochem. 49, 77-86. https://doi.org/10.1016/j.apgeochem.2014.06.022

Martinez-Moreno, M. F., Povedano-Priego, C., Mumford, A. D., Morales-Hidalgo, M., Mijnendonckx, K., Jroundi, F., Ojeda, J. J., & Merroun, M. L. 2024. Microbial responses to elevated temperature: Evaluating bentonite mineralogy and copper canister corrosion within

the long-term stability of deep geological repositories of nuclear waste. Sci. Total Environ., 170149. https://doi.org/10.1016/j.scitotenv.2024.170149

Martinez-Moreno, M.F., Povedano-Priego, C., Morales-Hidalgo, M., Mumford, A.D., Ojeda, J.J., Jroundi, F., Merroun, M. L. 2023. Impact of compacted bentonite microbial community on the clay mineralogy and copper canister corrosion: a multidiskiplinary approach in view of a safe Deep Geological Repository of nuclear wastes. J. Hazard. Mater. 131940. https://doi.org/10.1016/j.jhazmat.2023.131940

Masurat, P., Eriksson, S., Pedersen, K. 2010. Microbial sulphide production in compacted Wyoming bentonite MX-80 under in situ conditions relevant to a repository for high-level radioactive waste. Appl. Clay Sci. 47, 58-64. https://doi.org/10.1016/j.clay.2009.01.004

Matschiavelli, N., Kluge, S., Podlech, C., Standhaft, D., Grathoff, G., Ikeda-Ohno, A., ... & Cherkouk, A. 2019. The year-long development of microorganisms in uncompacted bavarian bentonite slurries at 30 and 60 ºC. Environ. Sci. Technol. 2019, 53, 10514−10524. https://doi.org/10.1021/acs.est.9b02670

Meleshyn, A. 2011. Microbial processes relevant for long-term performance of radioactive waste repositories in clays. GRS-291. ISBN 978-3-939355-67-0. Available from: https://www.grs.de/sites/default/files/pdf/GRS-291.pdf

Miettinen, H., Bomberg, M., Bes, R., Tiljander, M., & Vikman, M. 2022. Transformation of inherent microorganisms in Wyoming-type bentonite and their effects on structural iron. Appl. Clay Sci., 221, 106465. https://doi.org/10.1016/j.clay.2022.106465

Miller, J.H., 1972. Experiments in Molecular Genetics. Cold Spring Harbor Laboratory, Cold Spring Harbor, New York, pp. 352–355.

Pankhania, I. P., Spormann, A. M., Hamilton, W. A., & Thauer, R. K. 1988. Lactate conversion to acetate, CO_2 and H_2 in cell suspensions of *Desulfovibrio vulgaris* (Marburg): indications for the involvement of an energy driven reaction. Arch. Microbiol. 150, 26–31 (1988). https://doi.org/10.1007/BF00409713

Patel, S., & Gupta, R. S. 2020. A phylogenomic and comparative genomic framework for resolving the polyphyly of the genus *Bacillus*: Proposal for six new genera of *Bacillus* species, *Peribacillus* gen. nov., *Cytobacillus* gen. nov., *Mesobacillus* gen. nov., *Neobacillus* gen. nov., *Metabacillus* gen. nov. and *Alkalihalobacillus* gen. nov. Int. J. Syst. Evol. Microbiol., 70(1), 406-438. https://doi.org/10.1099/ijsem.0.003775

Payer, J. H., Finsterle, S., Apps, J.A., Muller, R.A. 2019. Corrosion performance of engineered barrier system in deep horizontal drillholes. Energies. 12, 1491. https://doi.org/10.3390/en12081491

Pentráková, L., Su, K., Pentrák, M., Stucki, J.W. 2013. A review of microbial redox interactions with structural Fe in clay minerals. Clay Miner. 48, 543-560. https://doi.org/10.1180/claymin.2013.048.3.10

Povedano-Priego, C., Jroundi, F., Solari, P. L., Guerra-Tschuschke, I., del Mar Abad-Ortega, M., Link, A., ... & Merroun, M. L. 2023. Unlocking the bentonite microbial diversity and its implications in selenium bioreduction and biotransformation: Advances in deep geological repositories. J. Hazard. Mater., 445, 130557. https://doi.org/10.1016/j.jhazmat.2022.130557

Povedano-Priego, C., Jroundi, F., Lopez-Fernandez, M., Shrestha, R., Spanek, R., Martín-Sánchez, I., Villar, M.V., ˇSevců, A., Dopson, M. Merroun, M.L. 2021. Deciphering indigenous bacteria in compacted bentonite through a novel and efficient DNA extraction method: Insights into biogeochemical processes within the Deep Geological Disposal of nuclear waste concept. J. Hazard. Mater. 408, 124600. https://doi.org/10.1016/j.jhazmat.2020.124600

Povedano-Priego, C., Jroundi, F., Lopez-Fernandez, M., Sánchez-Castro, I., Martin-Sánchez, I., Huertas, F.J., Merroun, M.L. 2019. Shifts in bentonite bacterial community and mineralogy in response to uranium and glycerol-2-phosphate exposure. Sci. Total Environ. 692, 219-232. https://doi.org/10.1016/j.scitotenv.2019.07.228

R Core Team. 2022. R: A language and environment for statistical computing. R Foundation for Statistical Computing, Vienna, Austria. URL https://www.Rproject.org/

Robertson, C.E., Harris, J.K., Wagner, B.D., Granger, D., Browne, K., Tatem, B., Feazel, L.M., Park, K., Pace, N.R., Frank, D.N. 2013. Explicet: graphical user interface software for metadata-driven management, analysis and visualization of microbiome data. Bioinformatics, 29, 3100-3101. https://doi.org/10.1093/bioinformatics/btt526

Ruiz-Fresneda, M. A., Martinez-Moreno, M. F., Povedano-Priego, C., Morales-Hidalgo, M., Jroundi, F., & Merroun, M. L. 2023. Impact of microbial processes on the safety of deep geological repositories for radioactive waste. Front. Microbiol., 14, 1134078. https://doi.org/10.3389/fmicb.2023.1134078

Ruiz-Fresneda, M. A., Staicu, L. C., Lazuén-López, G., & Merroun, M. L. 2023(b). Allotropy of selenium nanoparticles: Colourful transition, synthesis, and biotechnological applications. Microb. Biotechnol., 16(5), 877-892. https://doi.org/10.1111/1751-7915.14209

Ruiz-Fresneda, M. A., Eswayah, A. S., Romero-González, M., Gardiner, P. H., Solari, P. L., & Merroun, M. L. 2020. Chemical and structural characterization of Se^{IV} biotransformations by *Stenotrophomonas bentonitica* into Se^{0} nanostructures and volatiles Se species. Environ. Sci. Nano, 7(7), 2140-2155. https://doi.org/10.1039/D0EN00507J

Ruiz-Fresneda, M. A., Gomez-Bolivar, J., Delgado-Martin, J., Abad-Ortega, M. D. M., Guerra-Tschuschke, I., & Merroun, M. L. 2019. The bioreduction of selenite under anaerobic and alkaline conditions analogous to those expected for a deep geological repository system. Molecules, 24(21), 3868. https://doi.org/10.3390/molecules24213868

Ruiz-Fresneda, M. A., Delgado-Martín, J., Gomez-Bolívar, J., Fernandez-Cantos, M. V., Bosch-Estévez, G., Martinez-Moreno, M. F., & Merroun, M. L. 2018. Green synthesis and biotransformation of amorphous Se nanospheres to trigonal 1D Se nanostructures: impact on Se mobility within the concept of radioactive waste disposal. Environ. Sci. Nano, 5(9), 2103-2116. https://doi.org/10.1039/C8EN00221E

Salehi Alaei, E., Guo, M., Chen, J., Behazin, M., Bergendal, E., Lilja, C., ... & Noël, J. J. 2023. The transition from used fuel container corrosion under oxic conditions to corrosion in an anoxic environment. Mater. Corros., 74(11-12), 1690-1706. https://doi.org/10.1002/maco.202313757

Sanchez-Castro, I., Ruiz-Fresneda, M. A., Bakkali, M., Kämpfer, P., Glaeser, S. P., Busse, H. J., ... & Merroun, M. L. 2017. *Stenotrophomonas bentonitica* sp. nov., isolated from bentonite formations. Int. J. Syst. Evol. Microbiol., 67(8), 2779. https://doi.org/10.1099%2Fijsem.0.002016

Shelobolina, E.S., VanPraagh, C.G., Lovley, D.R. 2003. Use of ferric and ferrous iron containing minerals for respiration by Desulfitobacterium frappieri. Geomicrobiol. J. 20, 143-156. https://doi.org/10.1080/01490450303884

Shiratori-Takano, H., Akita, K., Yamada, K., Itoh, T., Sugihara, T., Beppu, T., & Ueda, K. 2014. Description of *Symbiobacterium ostreiconchae* sp. nov., *Symbiobacterium turbinis* sp. nov. and *Symbiobacterium terraclitae* sp. nov., isolated from shellfish, emended description of the genus *Symbiobacterium* and proposal of *Symbiobacteriaceae* fam. nov. Int. J. Syst. Evol. Microbiol., 64(Pt_10), 3375-3383. https://doi.org/10.1099/ijs.0.063750-0

Stackebrandt, E., Sproer, C., Rainey, F. A., Burghardt, J., Päuker, O., & Hippe, H. 1997. Phylogenetic analysis of the genus *Desulfotomaculum*: evidence for the misclassification of *Desulfotomaculum guttoideum* and description of *Desulfotomaculum orientis* as *Desulfosporosinus orientis* gen. nov., comb. nov. Int. J. Syst. Evol. Microbiol., 47(4), 1134-1139. https://doi.org/10.1099/00207713-47-4-1134

Staicu, L. C., & Barton, L. L. 2021. Selenium respiration in anaerobic bacteria: Does energy generation pay off?. J. Inorg. Biochem., 222, 111509. https://doi.org/10.1016/j.jinorgbio.2021.111509

Staicu, L. C., Ackerson, C. J., Cornelis, P., Ye, L., Berendsen, R. L., Hunter, W. J., ... & Pilon-Smits, E. A. 2015. *Pseudomonas moraviensis* subsp. stanleyae, a bacterial endophyte of hyperaccumulator *Stanleya pinnata*, is capable of efficient selenite reduction to elemental selenium under aerobic conditions. J. Appl. Microbiol., 119(2), 400-410. https://doi.org/10.1111/jam.12842

Villar, M.V., Fernández-Soler, J.M., Delgado Huertas, A., Reyes, E., Linares, J., Jiménez de Cisneros, C., Linares, J., Reyes, E., Delgado, A., Fernandez-Soler, J.M., Astudillo, J. 2006. The study of Spanish clays for their use as sealing materials in nuclear waste repositories: 20 years of progress. J. Iber. Geol. 32, 15-36.

Vogel, M., Fischer, S., Maffert, A., Hübner, R., Scheinost, A. C., Franzen, C., & Steudtner, R. 2018. Biotransformation and detoxification of selenite by microbial biogenesis of selenium-sulfur nanoparticles. J. Hazard. Mater., 344, 749-757. https://doi.org/10.1016/j.jhazmat.2017.10.034

Wang, D., Rensing, C., & Zheng, S. 2022. Microbial reduction and resistance to selenium: Mechanisms, applications and prospects. J. Hazard. Mater., 421, 126684. https://doi.org/10.1016/j.jhazmat.2021.126684

WNA. World Nuclear Association. 2023. Storage and disposal of radioactive waste. https://www.world-nuclear.org/

Supplementary material for:

Reveling the impact of selenium on the activity of microbial communities from hyper-saturated Spanish bentonite microcosms and copper corrosion in the context of radioactive waste disposal

Marcos F. Martinez-Moreno[1,*], Cristina Povedano-Priego[1], Mar Morales-Hidalgo[1], Guillermo Lazuén-López[1], Elisabet Aranda[3], Jesus J. Ojeda[2], and Mohamed L. Merroun[1]

[1]Faculty of Sciences, Department of Microbiology, University of Granada, Granada, Spain.

[2]Department of Chemical Engineering, Faculty of Science and Engineering, Swansea University, Swansea, United Kingdom

[3]Institute of Water Research, Department of Microbiology, University of Granada, Granada, Spain

Supplementary Table S1.

Phyla relative abundance (%) of the bacterial phyla from hyper-saturated bentonite microcosms in triplicates (duplicates in B.Se.BC and StB.eD.Se) Bentonite (B), Sterilized bentonite (StB), amended with acetate, lactate and sulfate (eD); Selenium(IV) 2mM (Se), and with BPAS consortium (BC).

	Total	B.eD.Se.BC	B.Se.BC	B.eD.Se	B.Se	StB.eD.Se.BC	StB.Se.BC	StB.eD.Se	StB.Se
Bacteria	100.00	100.00	100.00	100.00	100.00	100.00	100.00	100.00	100.00
>Acidobacteria	0.02	0.00	0.00	0.00	0.09	0.00	0.02	0.00	0.00
>Actinobacteria	3.04	4.75	0.38	2.49	7.24	1.77	1.51	4.96	0.98
>Bacteroidetes	0.63	0.00	0.00	0.02	4.12	0.00	0.26	0.10	0.16
>Candidatus_Saccharibacteria	0.03	0.00	0.00	0.00	0.07	0.00	0.05	0.10	0.00
>Chloroflexi	0.01	0.00	0.00	0.05	0.00	0.00	0.00	0.00	0.00
>Cyanobacteria	< 0.01	0.00	0.00	0.00	0.00	0.00	0.00	0.03	0.00
>Firmicutes	26.58	8.66	6.11	49.35	19.37	3.54	6.26	71.75	55.84
>Fusobacteria	< 0.01	0.00	0.00	0.00	0.00	0.00	0.02	0.00	0.00
>Parcubacteria	0.02	0.00	0.00	0.16	0.00	0.00	0.00	0.00	0.00
>Planctomycetes	< 0.01	0.00	0.00	0.00	0.02	0.00	0.00	0.00	0.00
>Proteobacteria	68.00	84.01	90.05	47.74	68.06	92.53	88.43	22.59	42.78
>Verrucomicrobia	0.01	0.00	0.00	0.00	0.05	0.00	0.00	0.00	0.00
>unclassified	1.66	2.58	3.46	0.19	0.98	2.16	3.45	0.45	0.23

Supplementary material S2.

OTU relative abundance of the bacterial and archaeal communities of the bentonite samples in triplicates (duplicates in B.Se.BC and StB.eD.Se). Bentonite (B), Sterilized bentonite (StB), amended with acetate, lactate and sulfate (eD); Selenium(IV) 2mM (Se), and with BPAS consortium (BC).

	Total	B.eD.Se.BC	B.Se.BC	B.eD.Se	B.Se	StB.eD.Se.BC	StB.Se.BC	StB.eD.Se	StB.Se
Pseudomonas	40.30	48.18	77.20	8.89	5.26	62.80	73.44	14.77	35.61
Stenotrophomonas	12.52	34.47	10.79	0.00	0.30	26.75	13.24	4.61	6.80
Symbiobacterium	12.43	0.00	0.07	1.37	1.09	0.00	0.14	58.97	49.21
unclassified_Clostridia	6.93	0.95	1.08	23.14	13.94	0.00	1.56	8.07	5.14
unclassified_Rhodospirillales	6.00	0.00	0.00	23.18	20.65	0.00	0.00	0.03	0.16
Pseudoalteromonas	2.79	0.00	0.00	0.47	19.11	0.00	0.02	1.26	0.05
Noviherbaspirillum	2.16	0.00	0.00	7.17	8.59	0.00	0.00	0.07	0.00
unclassified_Bacteria	1.66	2.58	3.46	0.19	0.98	2.16	3.45	0.45	0.23
Desulfosporosinus	1.60	1.51	0.00	9.05	1.07	0.02	0.09	0.00	0.00
Alkalihalobacillus	1.58	1.21	0.00	8.52	0.21	0.00	0.14	2.03	0.14
Amycolatopsis	1.14	4.63	0.38	0.00	0.00	1.77	1.21	0.00	0.51
unclassified_Firmicutes	1.07	0.14	2.97	2.26	0.98	0.54	1.09	0.10	0.81
unclassified_Rhizobiaceae	0.77	0.02	0.07	4.38	1.23	0.00	0.00	0.00	0.00
Anaerosolibacter	0.60	1.98	0.70	0.16	0.02	0.09	1.37	0.07	0.28
unclassified_Fulvivirgaceae	0.50	0.00	0.00	0.00	3.68	0.00	0.00	0.00	0.00
Arthrobacter	0.43	0.00	0.00	0.63	1.91	0.00	0.05	0.45	0.28
Alkaliphilus	0.41	0.49	0.00	0.00	0.00	2.16	0.35	0.00	0.00

unclassified_Gammaproteobacteria	0.41	0.54	0.56	0.09	0.00	1.09	0.58	0.45	0.00
unclassified_Nocardioidaceae	0.37	0.00	0.00	0.23	1.54	0.00	0.00	1.40	0.00
unclassified_Peptococcaceae_1	0.33	0.51	0.07	1.86	0.00	0.00	0.00	0.00	0.00
Devosia	0.32	0.00	0.00	0.98	1.35	0.00	0.00	0.03	0.00
Nocardioides	0.28	0.00	0.00	0.33	1.30	0.00	0.02	0.56	0.00
unclassified_Pseudomonadaceae	0.27	0.00	1.40	0.00	0.00	0.12	0.91	0.03	0.00
unclassified_Clostridiaceae_4	0.24	0.00	0.00	1.26	0.47	0.00	0.07	0.00	0.00
Pseudarthrobacter	0.22	0.00	0.00	0.37	1.02	0.00	0.00	0.28	0.00
unclassified_Oxalobacteraceae	0.22	0.00	0.00	0.00	1.63	0.00	0.00	0.00	0.00
unclassified_Comamonadaceae	0.20	0.00	0.00	0.26	0.98	0.00	0.12	0.17	0.00
unclassified_Bacillaceae_1	0.17	0.16	0.21	0.12	0.12	0.14	0.16	0.66	0.00
unclassified_Gracilibacteraceae	0.17	0.09	0.03	0.09	0.88	0.00	0.16	0.00	0.00
Phenylobacterium	0.17	0.00	0.00	0.09	1.16	0.00	0.00	0.00	0.00
Sedimentibacter	0.16	0.74	0.00	0.40	0.00	0.00	0.00	0.00	0.00
unclassified_Enterobacteriaceae	0.16	0.00	0.00	0.00	0.00	1.14	0.00	0.00	0.00
Clostridium_sensu_stricto	0.14	0.44	0.17	0.23	0.21	0.00	0.00	0.00	0.00
Brevundimonas	0.13	0.00	0.00	0.49	0.49	0.00	0.00	0.00	0.00
Desulfocurvibacter	0.13	0.37	0.00	0.00	0.21	0.00	0.00	0.35	0.12
unclassified_Xanthomonadaceae	0.13	0.05	0.00	0.16	0.56	0.16	0.00	0.00	0.00
unclassified_Microbacteriaceae	0.12	0.00	0.00	0.00	0.00	0.00	0.00	1.29	0.00
Paracoccus	0.12	0.00	0.00	0.00	0.86	0.00	0.00	0.07	0.00
Acidovorax	0.12	0.00	0.00	0.00	0.88	0.00	0.00	0.00	0.00

unclassified_Bacillales	0.09	0.00	0.00	0.65	0.00	0.00	0.00	0.00	0.00
Bosea	0.09	0.00	0.00	0.00	0.68	0.00	0.00	0.00	0.00
unclassified_Actinobacteria	0.08	0.12	0.00	0.16	0.12	0.00	0.12	0.14	0.00
unclassified_Burkholderiales	0.08	0.00	0.00	0.00	0.58	0.00	0.00	0.00	0.00
unclassified_Proteobacteria	0.08	0.26	0.03	0.12	0.19	0.00	0.00	0.00	0.00
Actinotalea	0.07	0.00	0.00	0.28	0.21	0.00	0.00	0.00	0.00
Paenibacillus	0.07	0.00	0.00	0.00	0.00	0.00	0.00	0.49	0.16
unclassified_Zoogloeaceae	0.07	0.00	0.00	0.42	0.12	0.00	0.00	0.00	0.00
Microcella	0.06	0.00	0.00	0.42	0.00	0.00	0.00	0.00	0.00
Bacteroides	0.06	0.00	0.00	0.00	0.00	0.00	0.26	0.07	0.14
Sporacetigenium	0.06	0.07	0.00	0.00	0.00	0.40	0.00	0.00	0.00
unclassified_Cystobacteraceae	0.06	0.00	0.00	0.00	0.44	0.00	0.00	0.00	0.00
unclassified	0.06	0.00	0.00	0.00	0.00	0.44	0.00	0.00	0.00
Brachybacterium	0.05	0.00	0.00	0.00	0.12	0.00	0.00	0.38	0.00
unclassified	0.05	0.00	0.00	0.00	0.35	0.00	0.00	0.00	0.00
Mesobacillus	0.05	0.00	0.00	0.00	0.00	0.00	0.00	0.56	0.00
unclassified	0.05	0.00	0.00	0.00	0.35	0.00	0.00	0.00	0.00
Caulobacter	0.05	0.00	0.00	0.00	0.40	0.00	0.00	0.00	0.00
Ramlibacter	0.05	0.00	0.00	0.09	0.28	0.00	0.00	0.00	0.00
Marinobacter	0.05	0.00	0.00	0.00	0.40	0.00	0.00	0.00	0.00
Promicromonospora	0.04	0.00	0.00	0.05	0.28	0.00	0.00	0.00	0.00
unclassified	0.04	0.00	0.00	0.00	0.00	0.19	0.09	0.00	0.00

unclassified	0.04	0.00	0.28	0.00	0.00	0.00	0.14	0.00	0.00
Ferrovibrio	0.04	0.00	0.00	0.00	0.28	0.00	0.00	0.00	0.00
Anaeromyxobacter	0.04	0.00	0.00	0.00	0.30	0.00	0.00	0.00	0.00
Lysobacter	0.04	0.00	0.00	0.19	0.09	0.00	0.00	0.00	0.00
Pseudonocardia	0.03	0.00	0.00	0.00	0.19	0.00	0.00	0.07	0.00
unclassified	0.03	0.00	0.00	0.00	0.19	0.00	0.00	0.00	0.00
Pontibacter	0.03	0.00	0.00	0.00	0.23	0.00	0.00	0.00	0.00
Saccharibacteria_genera_incertae_sedis	0.03	0.00	0.00	0.00	0.07	0.00	0.05	0.10	0.00
Exiguobacterium	0.03	0.05	0.31	0.00	0.00	0.00	0.00	0.00	0.00
Streptococcus	0.03	0.00	0.00	0.00	0.00	0.00	0.21	0.00	0.00
unclassified	0.03	0.02	0.00	0.00	0.00	0.00	0.07	0.14	0.00
Desulfotomaculum	0.03	0.00	0.00	0.23	0.00	0.00	0.00	0.03	0.00
unclassified	0.03	0.09	0.10	0.00	0.00	0.00	0.00	0.07	0.00
unclassified	0.03	0.00	0.00	0.00	0.00	0.00	0.12	0.17	0.00
Microvirga	0.03	0.00	0.00	0.00	0.00	0.00	0.00	0.28	0.00
unclassified	0.03	0.00	0.00	0.12	0.14	0.00	0.00	0.00	0.00
Porphyrobacter	0.03	0.00	0.00	0.23	0.00	0.00	0.00	0.00	0.00
unclassified	0.03	0.00	0.00	0.23	0.00	0.00	0.00	0.00	0.00
Parasutterella	0.03	0.00	0.00	0.00	0.00	0.00	0.00	0.35	0.00
unclassified	0.03	0.00	0.00	0.00	0.19	0.00	0.00	0.00	0.00
Acinetobacter	0.03	0.00	0.00	0.00	0.21	0.00	0.00	0.00	0.00
unclassified	0.02	0.00	0.00	0.00	0.00	0.00	0.00	0.21	0.00

unclassified	0.02	0.00	0.00	0.00	0.00	0.00	0.07	0.10	0.00
Enterococcus	0.02	0.00	0.00	0.00	0.00	0.00	0.00	0.24	0.00
Lactococcus	0.02	0.00	0.00	0.00	0.00	0.00	0.12	0.00	0.00
Parcubacteria_genera_incertae_sedis	0.02	0.00	0.00	0.16	0.00	0.00	0.00	0.00	0.00
unclassified	0.02	0.00	0.00	0.00	0.05	0.00	0.09	0.00	0.00
Sphingomonas	0.02	0.00	0.00	0.00	0.16	0.00	0.00	0.00	0.00
unclassified	0.02	0.12	0.00	0.00	0.00	0.02	0.00	0.00	0.00
unclassified	0.01	0.00	0.00	0.00	0.09	0.00	0.00	0.00	0.00
Desertimonas	0.01	0.00	0.00	0.00	0.00	0.00	0.05	0.00	0.00
unclassified	0.01	0.00	0.00	0.00	0.09	0.00	0.00	0.00	0.00
Nocardia	0.01	0.00	0.00	0.00	0.00	0.00	0.00	0.00	0.09
Cutibacterium	0.01	0.00	0.00	0.00	0.00	0.00	0.00	0.00	0.07
unclassified	0.01	0.00	0.00	0.00	0.00	0.00	0.00	0.07	0.00
Streptomyces	0.01	0.00	0.00	0.00	0.05	0.00	0.00	0.00	0.00
unclassified	0.01	0.00	0.00	0.00	0.07	0.00	0.00	0.00	0.02
Chryseolinea	0.01	0.00	0.00	0.00	0.00	0.00	0.00	0.03	0.02
unclassified	0.01	0.00	0.00	0.05	0.00	0.00	0.00	0.00	0.00
Cytobacillus	0.01	0.00	0.00	0.00	0.00	0.00	0.00	0.00	0.09
Brassicibacter	0.01	0.07	0.00	0.00	0.00	0.00	0.00	0.00	0.00
unclassified	0.01	0.09	0.00	0.00	0.00	0.00	0.00	0.00	0.00
Agathobacter	0.01	0.00	0.00	0.00	0.00	0.00	0.07	0.00	0.00
Anaerostipes	0.01	0.00	0.00	0.00	0.00	0.00	0.07	0.00	0.00

Romboutsia	0.01	0.00	0.00	0.00	0.00	0.00	0.09	0.00	0.00
Tissierella	0.01	0.02	0.10	0.00	0.00	0.00	0.00	0.00	0.00
Erysipelothrix	0.01	0.00	0.00	0.00	0.00	0.00	0.00	0.10	0.00
Veillonella	0.01	0.00	0.00	0.00	0.00	0.00	0.07	0.00	0.00
Roseomonas	0.01	0.00	0.00	0.00	0.07	0.00	0.00	0.00	0.00
Azospirillum	0.01	0.00	0.00	0.00	0.00	0.00	0.00	0.07	0.00
unclassified	0.01	0.00	0.00	0.00	0.05	0.00	0.00	0.00	0.00
Thalassobaculum	0.01	0.00	0.00	0.00	0.05	0.00	0.00	0.00	0.00
Sphingobium	0.01	0.00	0.00	0.05	0.02	0.00	0.00	0.00	0.00
unclassified	0.01	0.00	0.00	0.05	0.00	0.00	0.00	0.00	0.00
unclassified	0.01	0.00	0.00	0.09	0.00	0.00	0.00	0.00	0.00
Desulfuromonas	0.01	0.00	0.00	0.00	0.00	0.00	0.00	0.00	0.05
Alcanivorax	0.01	0.00	0.00	0.00	0.07	0.00	0.00	0.00	0.00
Subdivision3_genera_incertae_sedis	0.01	0.00	0.00	0.00	0.05	0.00	0.00	0.00	0.00
Gp4	0.00	0.00	0.00	0.00	0.00	0.00	0.02	0.00	0.00
unclassified	0.00	0.00	0.00	0.02	0.00	0.00	0.00	0.00	0.00
Imperialibacter	0.00	0.00	0.00	0.00	0.02	0.00	0.00	0.00	0.00
Ohtaekwangia	0.00	0.00	0.00	0.02	0.00	0.00	0.00	0.00	0.00
unclassified	0.00	0.00	0.00	0.00	0.00	0.00	0.00	0.03	0.00
Cellulosilyticum	0.00	0.00	0.00	0.00	0.02	0.00	0.00	0.00	0.00
Fusicatenibacter	0.00	0.00	0.00	0.00	0.00	0.00	0.02	0.00	0.00
Dysosmobacter	0.00	0.00	0.00	0.00	0.00	0.00	0.00	0.03	0.00

Turicibacter	0.00	0.00	0.00	0.00	0.00	0.00	0.02	0.00	0.00
unclassified	0.00	0.00	0.00	0.00	0.00	0.00	0.02	0.00	0.00
Fusobacterium	0.00	0.00	0.00	0.00	0.00	0.00	0.02	0.00	0.00
unclassified	0.00	0.00	0.00	0.00	0.02	0.00	0.00	0.00	0.00
unclassified	0.00	0.00	0.00	0.00	0.02	0.00	0.00	0.00	0.00
Mesorhizobium	0.00	0.00	0.00	0.00	0.00	0.00	0.00	0.03	0.00
Blastomonas	0.00	0.00	0.00	0.00	0.02	0.00	0.00	0.00	0.00
Methylotenera	0.00	0.00	0.00	0.00	0.00	0.00	0.02	0.00	0.00

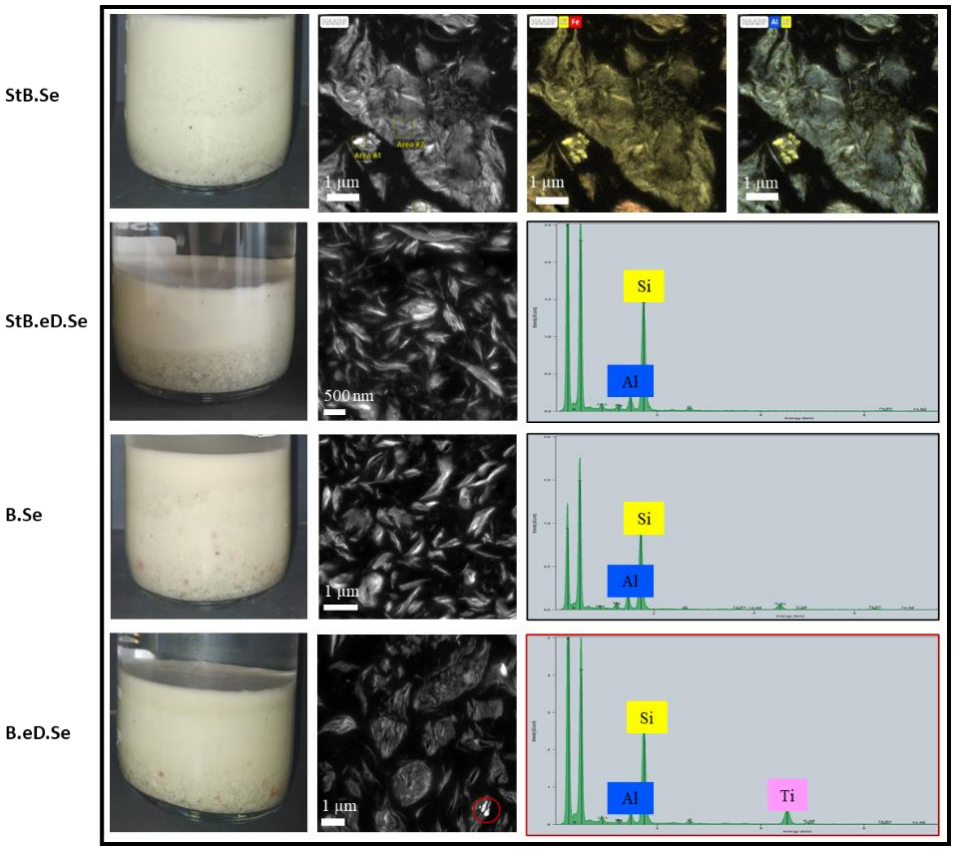

Supplementary Fig. S1. TEM micrographs and microanalysis of the microcosms lacking bacterial consortium at 45 days of anaerobic incubation showing the elemental composition and distribution of Si, Al, Fe, Mg, and Ti. Glossary: Bentonite (B), Sterilized bentonite (StB), amended with acetate, lactate and sulfate (eD); Selenium(IV) 2mM (Se), and with BPAS consortium (BC).

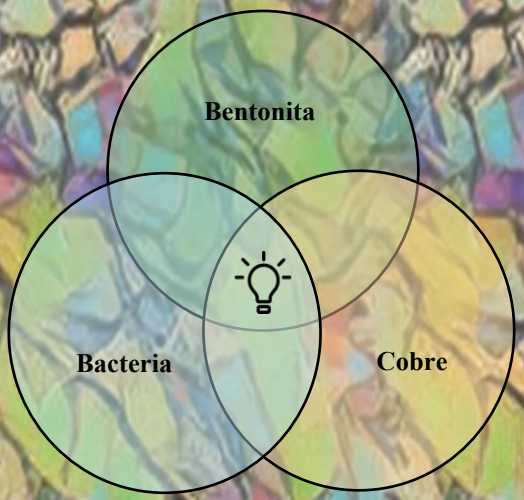
Bentonita
Bacteria
Cobre

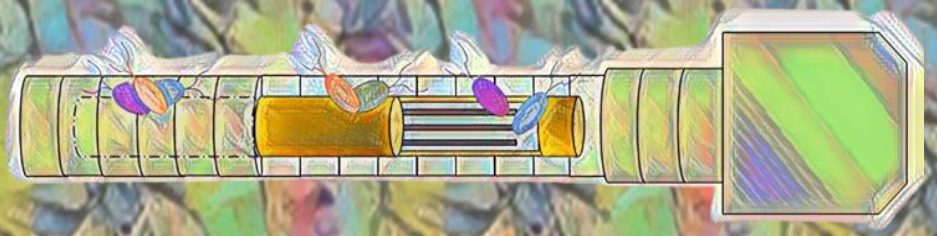

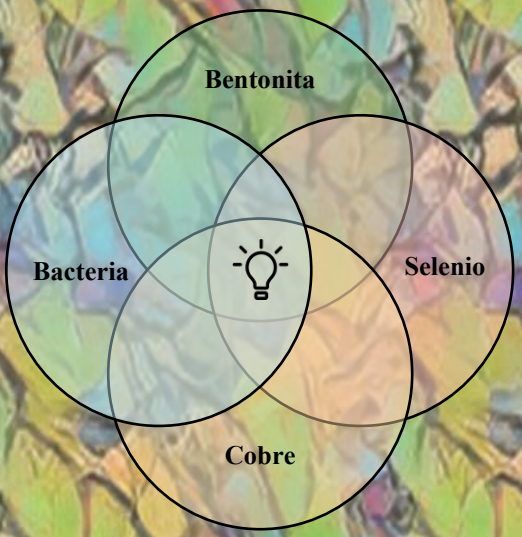
Bentonita
Bacteria
Selenio
Cobre

Discusión General

DISCUSIÓN GENERAL

Para asegurar el aislamiento de los residuos radiactivos a largo plazo en el marco del Almacenamiento Geológico Profundo (AGP) es necesario estudiar los factores que podrían comprometer la estabilidad de las barreras (e.j. bentonita y contendor metálico) que lo constituye. La bentonita ha sido seleccionada como el material para la barrera de relleno y sellado en los AGP. En el caso de España la bentonita, procedente del yacimiento arqueológico del Cortijo de Archidona en Almería (comercializada como FEBEX), ha sido ampliamente caracterizada a nivel geoquímico, mineralógico y microbiológico, proponiéndola para su uso en futuros AGP (Povedano-Priego et al., 2021; Huertas et al., 2021; Lopez-Fernandez et al., 2014; Villar et al., 2006). Además, esta bentonita confiere apoyo mecánico, presenta baja permeabilidad, capacidad de intercambios iónicos fuertes, buena conductividad térmica, muy buenas propiedades de compactación, y capacidad sellante (García-Romero et al., 2019).

Debido a que la bentonita no es ni estará estéril, entender y estudiar la estructura y composición de las comunidades microbianas presentes en ella es crucial para comprender y prever los procesos biogeoquímicos que puedan comprometer la estabilidad del AGP a largo plazo. En este aspecto, los microorganismos podrían alterar la mineralogía y propiedades de la bentonita, afectar a la integridad de los contenedores metálicos mediante mecanismos activos y/o pasivos de corrosión, contribuir a la producción de gases incrementando la presión dentro del AGP e, incluso, interactuar con los residuos radiactivos (Ruiz-Fresneda et al., 2023). Una vez que el AGP se selle se producirá un consumo gradual del oxígeno, debido a la actividad microbiana y a la corrosión de

los contenedores metálicos, generando un ambiente anaerobio (Payer et al., 2019; Keech et al., 2014). Una vez establecido este ambiente ciertos grupos de bacterias anaerobias, como las bacterias hierrorreductoras y sulfatorreductoras (IRB y SRB, por sus siglas en inglés, respectivamente), podrían permanecer metabólicamente activas. La actividad de estos grupos de bacterias podría tener consecuencias adversas en cuanto a la seguridad del AGP, entre las que se incluyen la corrosión de los contenedores metálicos basados en hierro y/o cobre, mediar en la reducción de Fe(III) a Fe(II) de la esmectita (mineral mayoritario en la bentonita) y producir la reducción de sulfato a sulfuro (principal agente corrosivo de los contenedores de cobre en anaerobiosis) (Pentráková et al., 2013; Liu et al., 2012; Shelobolina et al., 2003). En el diseño del AGP la bentonita se encontrará en forma de bloques altamente compactados (WNA, 2023). Además, el cobre de alta pureza ha sido seleccionado por países como Canadá, Suecia o Finlandia como material de revestimiento exterior para los contenedores (Hall et al., 2021). El microambiente en la bentonita compactada que rodea al contenedor metálico será predominantemente cálido, seco y oxidante debido, principalmente, a la disposición del AGP y al calor emitido por la desintegración de los radionucleidos; mientras que, más alejado del contenedor, el microambiente será más frio, húmedo y anóxico (King et al., 2017). Debido a estas circunstancias, el microambiente cercano al contenedor dificultará la actividad bacteriana, por lo que la producción de sulfuro, atribuido a la actividad de las SRB, se espera que ocurra más alejado de los contenedores metálicos dónde la temperatura será menor y el contenido de agua será mayor (Bengtsson and Pedersen, 2017). El sulfuro producido podría difundir a través de la bentonita e influir en la tasa de corrosión del contenedor de cobre. En el peor de los escenarios,

la corrosión de cobre podría producir grietas o fisuras en los contenedores, por lo que la estanqueidad de los residuos podría verse comprometida. En esta hipotética situación, los residuos entrarían en contacto con los microorganismos, lo que podría conllevar su interacción con los mismos, de forma positiva o negativa, mediante diversos mecanismos (Ruiz-Fresneda et al., 2023).

Por todo ello, esta Tesis Doctoral trata de explorar el efecto de distintos parámetros fisicoquímicos, relevantes para las condiciones en el AGP, sobre las comunidades microbianas (ej. alta densidad de compactación de la bentonita, alta temperatura, adición de nutrientes en forma de donadores y/o aceptores de electrones, presencia de selenio, etc.) y, como consecuencia, el impacto de los microorganismos sobre la mineralogía de la bentonita, la corrosión del cobre y la interacción con el selenio. Todo ello ha sido estudiando en conjunto, en sistemas complejos ternarios (bacteria/bentonita/cobre) y cuaternarios (bacteria/bentonita/cobre/selenio) (**Fig. 1**), mediante un enfoque multidisciplinar combinando técnicas de microbiología clásica, biología molecular, química analítica, microscopía y espectroscopía.

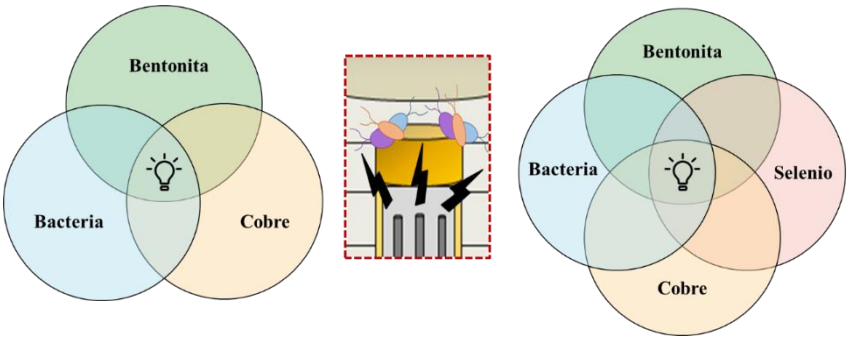

Fig. 1. Sistema ternario y cuaternario en los que se basa esta Tesis Doctoral.

En primer lugar, se estudiaron los procesos biogeoquímicos y fisicoquímicos en la interfaz cobre/bentonita compactada, así como la caracterización de compuestos de corrosión en la superficie del material de cobre. Para ello, se elaboraron bloques de bentonita compactadas a una densidad seca de 1,7 g/cm^3 cuyo interior contenían un disco de cobre de alta pureza. Para estimular la actividad de las bacterias anaerobias autóctonas (ej. SRB), se añadió acetato y lactato, como donadores de electrones, y sulfato, como aceptor final de electrones (Povedano-Priego et al., 2021; Matschiavelli et al., 2019; Grigoryan et al., 2018). Tras un año de incubación en condiciones anaerobias a 30 ºC, los bloques fueron retirados y cada uno de sus componentes fueron analizados.

Los análisis realizados mediante difracción de rayos X (DRX) a los agregados orientados de la bentonita, tratados bajo nuestras condiciones experimentales, no evidenciaron illitización en ninguno de los tratamientos (adición de donadores y aceptor de electrones, proceso de tindalización, condiciones anaerobias, etc.). Estos resultados son interesantes ya que una de las principales preocupaciones en cuanto al AGP es la transformación irreversible de esmectita a illita, lo que afectaría a la capacidad de hinchamiento de la bentonita (Kaufhold and Dohrmann, 2010).

El proceso de illitización puede deberse a la unión de iones K^+, posiblemente procedentes de los K-feldespatos de la bentonita, presentes en la capa intermedia de la esmectita, creando enlaces covalentes con el oxígeno. Este proceso de transformación depende de factores como la temperatura (100 – 200 ºC) y el tiempo, pero la actividad microbiana podría promover esta transformación. Además, algunas bacterias metanogénicas y sulfatorreductoras podrían utilizar el Fe(III) estructural,

presente en la esmectita, como aceptor de electrones unido a la oxidación de H_2 y/o materia orgánica, dando lugar a la formación de illita (Kim et al., 2019). A pesar de que esta Tesis Doctoral no está enfocada a una caracterización en profundidad de la estabilidad físico-química de la bentonita, es importante tener en cuenta el impacto de los microorganismos en sus propiedades. En este sentido, los análisis de la diversidad microbiana, basados en *16S rRNA Next Generation Sequencing*, mostraron ligeros cambios entre las muestras tindalizadas y no tindalizadas. Además, las muestras no tindalizadas se dividieron en dos grupos bien diferenciados: las tratadas con donadores/aceptor de electrones y las no tratadas. Esto indicaría que la estimulación de ciertas bacterias aerobias podría estar relacionada con la capacidad de la bentonita para "atrapar" moléculas de oxígeno, llegando a estar disponible para dichas bacterias (Burzan et al., 2022). Además, tras el proceso de tindalización, algunas bacterias mesófilas no podrían recuperarse de la exposición a altas temperaturas, produciendo así un efecto negativo en la diversidad bacteriana (Gilmour et al., 2022). En cuanto a la adición de acetato, sulfato y lactato, esta adición produjo un aumento de ciertos tipos de bacterias, tales como *Gaiella*, *Iamia* y *Sphingomonas,* capaces de asimilar alguno/s de estos compuestos (Albuquerque et al., 2011; Vaïtilingom et al., 2010; Cui et al., 2016, White et al., 1996). En cuanto al grupo de SRB, fueron detectadas en muy baja abundancia relativa (< 0,2 %). Algunas especies pertenecientes a este grupo de bacterias son capaces de tolerar duras condiciones ambientales (como las de este estudio) mediante el proceso de esporulación, o formando células latentes desecadas, en bentonita seca (Grigoryan et al., 2018; Masurat et al., 2010). Por ello, aunque su abundancia relativa fue baja, se cuantificó la viabilidad mediante el

método de número más probable (MPN, por sus siglas en inglés) en medio Postgate modificado. Todos los tratamientos mostraron presencia y viabilidad de una población de SRB de entre 20 MPN y 2.50 x 10^3 MPN por gramo de bentonita, indicando que su actividad metabólica puede ser restaurada cuando las condiciones se vuelven favorables. Este método nos da una aproximación de las células SRB potencialmente viables presentes por gramo de bentonita y los resultados podrían depender de diversas variables, por ejemplo, el tiempo de almacenamiento de las muestras a 4 ºC, que podría disminuir el número de células anaerobias viables (Maanoja et al., 2020). Por lo tanto, este tipo de estudios deberían complementarse en el futuro mediante la cuantificación de genes específicos implicados en la reducción de sulfato (por ejemplo, *dsrA* y *aspA*) por qPCR del ADN o ARN extraído de la bentonita. Por otra parte, debido a que el sulfuro producido por la actividad de las SRB es la principal fuente de corrosión del cobre en las condiciones relevantes del AGP (Bengtsson and Pedersen, 2017), se llevaron a cabo los análisis pertinentes, mediante microscopía VP-FESEM, micro-FTIR y XPS para caracterizar la superficie de los discos de cobre. La superficie de cobre de los bloques de bentonita, en presencia de los donadores/aceptor de electrones, mostró la presencia de compuestos orgánicos (posiblemente de origen celular) próximos a precipitados de Cu_xS. La detección de pequeños precipitados de este compuesto sugirió la presencia de un estadio temprano de corrosión de la superficie de cobre (Dou et al., 2020).

Puesto que cabe esperar que, con el tiempo, los AGP sufrirán cambios en la temperatura, en segundo lugar, se llevó a cabo un estudio basado en la metodología anterior, en el que los bloques se incubaron a 60 ºC. Este estudio es interesante ya que la evolución de la temperatura en los

contenedores metálicos dependerá del diseño del AGP, localización y materiales usados como barreras de ingeniería. Por ejemplo, el diseño canadiense (basado en contenedores revestidos de cobre), predice una evolución de la temperatura que aumentará hasta un pico máximo de unos 100 ºC en las primeras décadas, seguido de un descenso gradual hasta alcanzar la temperatura ambiental (King et al., 2017). Por lo tanto, en este estudio se exploró el impacto de la alta temperatura (60 ºC) y la densidad de compactación (1,7 g/cm^3) de la bentonita sobre la evolución de las comunidades microbianas, la corrosión de la superficie del cobre y la estabilidad de la mineralogía de la bentonita en la interfaz cobre/bentonita compactada en condiciones anóxicas. Al igual que en el caso anterior, no hubo indicios de illitización en la bentonita tras un año bajo las condiciones de incubación. En cuanto a la viabilidad y supervivencia bacteriana, el recuento de SRB de entre 9,5 x 10^1 y 2,5 x 10^3 MPN por gramo de bentonita, demostró la viabilidad de este grupo tras ser enriquecidas en medio Postgate modificado e incubadas a 30 ºC, pero no a 60 ºC (dónde no se detectó crecimiento). Estos resultados apoyan la capacidad de las SRB de hacer frente a ambientes hostiles mediante la formación de esporas, o entrando en un estado latente (células desecadas) en bentonita seca (Grigoryan et al., 2018; Masurat et al., 2010b). El aislamiento de bacterias, a partir de estas muestras, en medio Postgate modificado apoya esta teoría. De hecho, se consiguieron cultivos puros de cepas anaerobias como *Pseudomonas* sp. (IRB con cepas presentando tolerancia a metales, incluyendo cobre), *Anaerosolibacter* sp. (IRB y SRB anaerobia estricta), o *Pelosinus* sp. (IRB formadora de esporas), entre otras (Kumar et al., 2021; Jia et al., 2017; Hong et al., 2015; Shelobolina et al., 2007). En cuanto a la viabilidad de bacterias aerobias a 60 ºC destacaron *Aeribacillus* sp.

(bacteria con representantes formadores de esporas y termófilos moderados) y *Staphylococcus* sp. (bacteria con representantes anaerobios facultativos y termófilos moderados) (Finore et al., 2017; Pandey et al., 2015). La presencia y supervivencia de estas bacterias aerobias apoya la teoría de la presencia de moléculas de oxígeno atrapadas en la bentonita durante el proceso de compactación (Burzan et al., 2022; Stroes-Gayscone et al., 2010). A nivel de las comunidades bacterianas, el estudio reveló que la temperatura de incubación a 60 ºC parece ser un claro factor limitante. Esta temperatura redujo la diversidad microbiana de la bentonita, siendo *Pseudomonas* el género dominante en la comunidad, en términos de abundancia relativa, tras un año de incubación. *Pseudomonas* es una bacteria anaerobia facultativa que, en condiciones anaerobias, puede utilizar acetato y lactato como donador de electrones (Chen et al., 2020; Essén et al., 2007; Eschbach et al., 2004). Además, estudios previos han demostrado que especies de este género, como *P. syringae*, disminuyen su tamaño celular en condiciones adversas (Monier y Lindow, 2003). *Pseudomonas* podría intervenir en la corrosión de materiales de acero al carbono y de cobre en el contexto del AGP, mediante la reducción de hierro y nitratos, respectivamente (Shrestha et al., 2022; Jia et al., 2017; Dou et al., 2022). La presencia de SRB tras el periodo de incubación fue menor que en el estudio anterior a 30 ºC. La abundancia relativa de este grupo de bacterias fue ≤ 0,03 % en el conjunto de muestras (ej. *Desulfosporosinus*, *Desulfotomaculum*, *Pelosinus*, y *Sporacetigenium*), aunque destacó la presencia de *Anaerosolibacter* (1,06 % – 1,50 % de abundancia relativa). En cuanto al efecto de este grupo de bacterias sobre la superficie del cobre, la detección de azufre en la superficie de los discos podría estar relacionada con la actividad bacteriana (Pedersen, 2010). En este estudio no se

observaron precipitados por microscopía tras un año de incubación a 60 ºC. Sin embargo, el azufre se detectó en forma de sulfato y sulfuro. La identificación de sulfuro sugiere la posibilidad de actividad de SRB (Dou et al., 2020), que podría influir potencialmente en la corrosión del cobre. Sin embargo, es esencial llevar a cabo investigaciones adicionales para corroborar esta hipótesis, ya que no se observaron por microscopía precipitados relacionados con la formación de Cu_xS.

En tercer lugar, se quiso profundizar más en cómo los microorganismos afectan a las condiciones geoquímicas a corto plazo, simulando condiciones óptimas para el crecimiento y actividad de las bacterias, los cuales representarían uno de los peores escenarios para el AGP. Para ello, se elaboraron microcosmos de bentonita hipersaturada en agua de equilibrio (EW, por sus siglas en inglés), se enriquecieron con acetato, lactato y sulfato (simulando un aporte de nutrientes debido a la infiltración de agua en la bentonita); y se gasearon con nitrógeno para eliminar el oxígeno. Este estudio tuvo como objetivo examinar exhaustivamente el impacto de los microorganismos en la evolución geoquímica de un sistema complejo de bentonita hipersaturada durante un año de incubación anaeróbica. Además, se centró en investigar las comunidades microbianas y su influencia en la corrosión del cobre en un estado temprano de incubación (45 días). Tras un año de incubación, los valores de pH tendieron a ser menos alcalinos y a estabilizarse entre 7,51 y 8,37 en todos los tratamientos, pudiendo deberse a procesos de lixiviación de la bentonita, a la generación de gases como H_2, CH_4 o CO_2, como resultado del metabolismo microbiano, o la capacidad innata de la bentonita como material amortiguador (buffer) (Fernández-Díaz 2004; Povedano-Priego et al., 2019; Bagnoud et al., 2016). En cuanto a la evolución de los donadores de electrones/aceptor, se observó un rápido

consumo de lactato asociado a la producción, y posterior consumo, de acetato y, en menor medida, consumo de sulfato. Estos resultados concuerdan con los obtenidos por Matschiavelli et al. (2019), quienes observaron una disminución en la concentración de lactato, relacionada con la producción de acetato, en microcosmos de bentonita bávara B25. En este estudio dedujeron que el lactato se metabolizaba a través de la vía reductora del acetil-CoA. Esta oxidación incompleta del lactato, junto con la reducción simultánea del sulfato, daba lugar a la formación de acetato y sulfuro de hidrógeno. Esta formación de gases se observó en nuestro estudio mediante la presencia de fisuras en la bentonita y el característico olor a huevo podrido durante el muestreo de los microcosmos, olor que está relacionado con la formación de H_2S (He et al., 2011). Además, la alteración del color de la bentonita a tonos más oscuros pudo estar relacionado con la generación de H_2S, como subproducto de la actividad bacteriana, pudiendo reaccionar con el hierro y dar lugar a la formación de precipitados negros de especies reducidas de hierro (Miettinen et al., 2022; Matschiavelli et al., 2019). Cabe destacar que estos procesos se vieron incrementados en presencia del consorcio bacteriano BPAS, formado por *Bacillus* sp. BII-C3, *Pseudomonas putida*, *Amycolatopsis ruanii* y *Stenotrophomonas bentonitica*, todas ellas presentes en la bentonita procedente del Cortijo de Archidona (Povedano-Priego et al., 2021; Lopez-Fernandez et al., 2018, 2014). Por otra parte se observó que, en los microcosmos inoculados con el consorcio BPAS, la diversidad bacteriana se veía reducida, en la fase temprana de incubación de 45 días, con *Pseudomonas* y *Stenotrophomonas* como bacterias predominantes. Por el contrario, los microcosmos carentes del consorcio BPAS, y enriquecidos con donadores/aceptor de electrones, o con bentonita

esterilizada, mostraron una mayor diversidad y heterogeneidad microbiana. Además, la adición de donadores/aceptor de electrones contribuyó a la estimulación de determinadas bacterias como *Desulfocurvibacter* (SRB anaerobia obligada que oxida de forma incompleta sustratos orgánicos a acetato), *Pseudoalteromonas* (IRB cuando el contenido en oxígeno es bajo), *Anaerosolibacter* (IRB y SRB), y *Desulfosporosinus* (bacteria anaerobia que reduce el sulfato mediante la oxidación incompleta del lactato a acetato) (Spring et al., 2019; Cheng et al., 2019; Stackebrandt et al., 1997). A pesar de la presencia de SRB en este tratamiento no se detectaron cambios en la concentración de sulfato. Esta ausencia de consumo podría atribuirse al tiempo limitado disponible para este proceso (45 días), ya que las IRB como *Pseudomonas*, *Anaerosolibacter* y *Pseudoalteromonas* podrían estar participando activamente en la reducción de Fe(III) a Fe(II) hasta que las condiciones redox dentro de los microcosmos se volvieran favorables para la reducción del sulfato. En general, la adición de donadores de electrones y sulfato pareció estimular la presencia de IRB y SRB, las cuales están implicadas en la corrosión de los contenedores metálicos (Schütz et al., 2015; Bengtsson y Pedersen, 2017). Por ello, se investigó su potencial impacto en la corrosión de los mini contenedores de cobre (Cu-mCan). La formación de las especies de CuO en la superficie de los Cu-mCan podría estar relacionada con moléculas de oxígeno atrapadas en la bentonita o estar impulsada por la reducción de H_2O procedente del agua de equilibrio (EW) usada para la elaboración de los microcosmos (Burzan et al., 2022; Huttunen-Saarivirta et al., 2016). Por el contrario, la identificación de Cu_2S en las muestras resultó de la influencia microbiana, siendo uno de los principales compuestos de corrosión del cobre en condiciones anaerobias (Hall et al., 2021; Bengtsson and

Pedersen, 2017). En condiciones anaeróbicas las SRB pueden oxidar lactato (donador de electrones) acoplado a la reducción de sulfato (aceptor final de electrones) a través de la reducción disimilatoria de sulfato (Dou et al., 2020). La producción del sulfuro en los microcosmos se relacionó con el característico olor a huevo podrido tras el muestreo (He et al., 2011). Otro posible mecanismo sería la conversión de óxidos de cobre (Cu_2O) en Cu_2S mediante la sustitución entre el sulfuro y el óxido (Salehi Alaei et al., 2023). Además, el metabolito HS^-, procedente del H_2S secretado por las SRB, podría difundir hasta la superficie del cobre y reaccionar con él para formar Cu_2S (Dou et al., 2020).

Por último, en el cuarto capítulo se quiso simular un escenario en el cual se producía una liberación de selenio (Se). Este elemento es uno de los productos generados por la fisión nuclear del combustible de uranio para la generación de energía nuclear (Hassan et al., 2021). Concretamente, el isótopo ^{79}Se es un componente del combustible nuclear gastado que puede encontrarse en los residuos de alta actividad procedente de las plantas de reprocesamiento (Abdalla et al., 2020). Para nuestro ensayo, se montaron un conjunto de microcosmos basándonos en el experimento anterior, a los cuales se les adicionó selenito sódico [Se(IV)] a una concentración de 2 mM como análogo inactivo del ^{79}Se presente en los residuos. Este estudio se centró en investigar el impacto de la adición de Se(IV) sobre la actividad de las comunidades microbianas de la bentonita y en la evolución geoquímica de los microcosmos durante un año de incubación anaerobia. Además, se llevó a cabo una caracterización temprana de la reducción del selenio mediada por microorganismos y de la corrosión de cobre en los Cu-mCan. Tras 45 días de incubación, los microcosmos inoculados con el consorcio BPAS mostraron una fina capa de coloración rojiza en la interfaz bentonita:sobrenadante, así como

acumulaciones rojizas en algunas de las muestras en la fase de bentonita, indicando la reducción de selenito [Se(IV)] a selenio elemental [Se(0)] (Povedano-Priego et al., 2023; Ruiz-Fresneda et al., 2018, 2019). Estos productos de reducción rojos de Se(0) (SeRPs) viraron, o quedaron enmascarados, por tonalidades grises-negras metálicas a lo largo del periodo de incubación, lo que puede atribuirse a una transición en la alotropía de los SeRPs hacia formas más estables, o a la reducción de especies de hierro en la bentonita que podrían reaccionar con el sulfuro de hidrógeno producido por la actividad bacteriana (Ruiz-Fresneda et al., 2023b; Miettinen et al., 2022; Matschiavelli et al., 2019). Además, la presencia de donadores/aceptor de electrones también potenció los procesos mencionados, mientras que la esterilización de la bentonita los retardó. No se observó ningún cambio de color a lo largo del año de incubación en el control abiótico (microcosmos de bentonita estéril con Se), lo que indica que no hubo reducción de Se(IV) ni alteración en la tonalidad de la bentonita. A pesar de que la tindalización no es el proceso más eficaz para la esterilización de la bentonita (Martinez-Moreno et al., 2024), se observó que, en las condiciones estudiadas, este proceso puede afectar a la actividad bacteriana. La adición de Se(IV) no influyó en la evolución del pH, mostrando una tendencia a volverse menos alcalino, estabilizándose dentro del rango de 7,32 a 8,37 tras un año de incubación, al igual que ocurría en el caso anterior. Esta disminución del pH podría atribuirse a procesos de lixiviación, disolución de la calcita, intercambio iónico entre la bentonita y los diferentes solventes (e.g., acetato, lactato, sulfato y el EW), o a la generación de gases procedentes del metabolismo microbiano dentro de los microcosmos (Povedano-Priego et al., 2019; Fernández-Díaz, 2004; Bagnoud et al., 2016). Como en el caso anterior, el consumo de lactato estuvo asociado a la producción, y posterior

consumo, de acetato y, en menor medida, al consumo de sulfato. La presencia de 2 mM de Se(IV) puede ser tóxico para algunas bacterias (Povedano-Priego et al., 2023), pudiendo reducir la actividad bacteriana dentro del microcosmos. Además, este metaloide podría actuar como competidor con el azufre como aceptor final de electrones en condiciones anaerobias (Staicu y Barton, 2021), relacionándose con el lento consumo en los microcosmos. Este fenómeno podría conducir a una desaceleración de los procesos biogeoquímicos, atribuida a una reducción de la diversidad bacteriana y/o a un periodo de adaptación de los microorganismos tolerantes al selenio. Para comprender el impacto de cada parámetro (esterilización de la bentonita, adición de donadores/aceptore de electrones, consorcio bacteriano e interacción con el selenio) en la evolución de los microcosmos, la opción de estudio óptima implica un periodo de incubación corto (45 días), en el que los microcosmos mostraron una mayor heterogeneidad visual. La presencia de Se(IV) redujo la presencia de algunas SRB, mientras que la presencia de donadores/aceptor de electrones estimuló la presencia de la SRB *Desulfosporosinus* la cual, además de oxidar de forma incompleta el lactato a acetato y CO_2, es tolerante al Se (Stackebrandt et al., 1997; Povedano-Priego et al., 2023; Aoyagi et al., 2021). La alta abundancia relativa de bacterias selenotolerantes, como *Pseudomonas*, *Stenotrophomonas* y *Alkahalibacillus*, pudieron influir en la reducción del Se(IV) a Se(0) observada en los microcosmos durante el período de incubación anaeróbica (Staicu et al., 2015; Ruiz-Fresneda et al., 2019; Povedano-Priego et al., 2023; Patel and Gupta, 2020; Gautam et al., 2022). Además, La presencia del consorcio BPAS ayudó a desvelar el proceso de interacción e inmovilización del selenito (soluble, móvil y tóxico) a selenio elemental (menos soluble, menos móvil y menos

tóxico). El mecanismo propuesto se basó en la reducción intracelular de Se(IV) a Se(0) en forma de nanoesferas con alotropía amorfa (*a*-Se) que, una vez liberadas al espacio extracelular mediante lisis celular, podían sufrir procesos de transformación a estructuras cristalinas de selenio monoclínico (*m*-Se) y, posteriormente, a la forma más termodinámicamente estable y menos tóxica: selenio trigonal (*t*-Se) (Povedano-Priego et al., 2023; Ruiz-Fresneda et al., 2018). La presencia de sulfato podría mediar en la interacción de los precipitados de Se(0) con el azufre, formando los precipitados de selenio-azufre observados en el medio extracelular (Vogel et al., 2018).

En definitiva, los microorganismos naturales de la bentonita desempeñarán un papel importante (positivo, negativo o neutral) en la evolución de las condiciones geoquímicas de los AGP, pudiendo comprometer la estabilidad de las diferentes barreras. Los resultados obtenidos en esta Tesis Doctoral proporcionan nuevas perspectivas para comprender cómo los microorganismos, y los procesos biogeoquímicos asociados, podrían afectar la interfaz contenedor de cobre/bentonita española/selenio. No obstante, las investigaciones realizadas subrayan la importancia de continuar profundizando en el estudio de las comunidades bacterianas presentes en las bentonitas como material de relleno y sellado. Sobre todo, en el comportamiento de estas bajo condiciones fisicoquímicas relevantes al AGP como, por ejemplo, estudiar el efecto de la radiación, además del estudio de nuevos materiales (ej. contenedores metálicos basados en titanio o aleaciones de níquel), o la interacción con elementos radiactivos como el ^{79}Se, ^{99}Tc, ^{36}Cl, o ^{129}I, entre otros, resultantes de la fisión nuclear del uranio, marcando así un punto de partida para futuras investigaciones en esta área. Todo ello con la finalidad y perspectivas de crear un

Almacenamiento Geológico Profundo de residuos radiactivos seguro y estable durante más de 100.000 años.

Bibliografía

Abdalla, Z. A. Y., Ismail, M. Y. A., Njoroge, E. G., Hlatshwayo, T. T., Wendler, E., & Malherbe, J. B. 2020. Migration behaviour of selenium implanted into polycrystalline 3C–SiC. Vacuum, 175, 109235. https://doi.org/10.1016/j.vacuum.2020.109235

Albuquerque, L., França, L., Rainey, F. A., Schumann, P., Nobre, M. F., da Costa, M. S. 2011. *Gaiella occulta* gen. nov., sp. nov., a novel representative of a deep branching phylogenetic lineage within the class Actinobacteria and proposal of Gaiellaceae fam. nov. and Gaiellales ord. nov. Syst. Appl. Microbiol. 34, 595-599. https://doi.org/10.1016/j.syapm.2011.07.001

Aoyagi, T., Mori, Y., Nanao, M., Matsuyama, Y., Sato, Y., Inaba, T., ... & Hori, T. 2021. Effective Se reduction by lactate-stimulated indigenous microbial communities in excavated waste rocks. J. Hazard. Mater., 403, 123908. https://doi.org/10.1016/j.jhazmat.2020.123908

Bagnoud, A., De Bruijn, I., Andersson, A. F., Diomidis, N., Leupin, O. X., Schwyn, B., & Bernier-Latmani, R. 2016. A minimalistic microbial food web in an excavated deep subsurface clay rock. FEMS Microb. Ecol., 92(1), fiv138. https://doi.org/10.1093/femsec/fiv138

Bengtsson, A., Pedersen, K. 2017. Microbial sulphide-producing activity in water saturated Wyoming MX-80, Asha and Calcigel bentonites at wet densities from 1500 to 2000 kg m^{-3}. Appl. Clay Sci. 137, 203-212. https://doi.org/10.1016/j.clay.2016.12.024

Burzan, N., Lima, R. M., Frutschi, M., Janowczyk, A., Reddy, B., Rance, A., Diomidis, N., Bernier-Latmani, R. 2022. Growth and Persistence of an Aerobic Microbial Community in Wyoming Bentonite MX-80 Despite Anoxic in situ Conditions. Front. Microbiol. 13: 858324 https://doi.org/10.3389%2Ffmicb.2022.858324

Chen, Z., Jiang, Y., Chang, Z., Wang, J., Song, X., Huang, Z., Chen, S., Li, J. 2020. Denitrification characteristics and pathways of a facultative anaerobic denitrifying strain, *Pseudomonas denitrificans* G1. J. Biosci. Bioeng., 129(6), 715-722. https://doi.org/10.1016/j.jbiosc.2019.12.011

Cui, X., Zhao, S., Wang, B. 2016. Microbial desulfurization for ground tire rubber by mixed consortium-*Sphingomonas* sp. and *Gordonia* sp. Polym. Degrad. Stab. 128, 165-171. https://doi.org/10.1016/j.polymdegradstab.2016.03.011

Dou, W., Pu, Y., Gu, T., Chen, S., Chen, Z., Xu, Z., 2022. Biocorrosion of copper by nitrate reducing Pseudomonas aeruginosa with varied headspace volume. Int. Biodeterior. Biodegradation 171, 105405. https://doi.org/10.1016/j.ibiod.2022.105405.

Dou, W., Pu, Y., Han, X., Song, Y., Chen, S., Gu, T. 2020. Corrosion of Cu by a sulfate reducing bacterium in anaerobic vials with different headspace volumes. Bioelectrochemistry, 133, 107478. https://doi.org/10.1016/j.bioelechem.2020.107478

Eschbach, M., Schreiber, K., Trunk, K., Buer, J., Jahn, D., Schobert, M. 2004. Long-term anaerobic survival of the opportunistic pathogen *Pseudomonas aeruginosa* via pyruvate fermentation. J. Bacteriol., 186(14), 4596-4604. https://doi.org/10.1128/jb.186.14.4596-4604.2004

Essén, S. A., Johnsson, A., Bylund, D., Pedersen, K., Lundström, U. S. 2007. Siderophore production by *Pseudomonas stutzeri* under aerobic and anaerobic conditions. Appl. Environ. Microbiol., 73(18), 5857-5864. https://doi.org/10.1128/AEM.00072-07

Fernández-Díaz, A.M., 2004. Caracterización y modelización del agua intersticial de materiales arcillosos: estudio de la bentonita de Cortijo de Archidona. PhD Thesis. Universidad Autónoma de Madrid Editorial CIEMAT, p. 505.

Finore, I., Gioiello, A., Leone, L., Orlando, P., Romano, I., Nicolaus, B., Poli, A. 2017. *Aeribacillus composti* sp. nov., a thermophilic bacillus isolated from olive mill pomace compost. Int. J. Syst. Evol. Microbiol., 67(11), 4830-4835. https://doi.org/10.1099/ijsem.0.002391

García-Romero, E., María Manchado, E., Suárez, M., and García-Rivas, J. 2019. Spanish bentonites: a review and new data on their geology, mineralogy, and crystal chemistry. Fortschr. Mineral. 9:696. https://doi.org/10.3390/min9110696

Gautam, A., Kushwaha, A., & Rani, R. 2022. Reduction of Hexavalent Chromium [Cr (VI)] by heavy metal tolerant Bacterium *Alkalihalobacillus clausii* CRA1 and its toxicity assessment through flow cytometry. Curr. Microbiol., 79(1), 33. https://doi.org/10.1007/s00284-021-02734-z

Gilmour, K.A., Davie, C.T., Gray, N. 2022. Survival and activity of an indigenous iron-reducing microbial community from MX80 bentonite in high temperature/low water environments with relevance to a proposed method of nuclear waste

disposal. Sci. Total Environ. 814, 152660. https://doi.org/10.1016/j.scitotenv.2021.152660

Grigoryan, A.A., Jalique, D.R., Medihala, P., Stroes-Gascoyne, S., Wolfaardt, G.M., McKelvie, J., Korber, D.R. 2018. Bacterial diversity and production of sulfide in microcosms containing uncompacted bentonites. Heliyon. 4, e00722. https://doi.org/10.1016/j.heliyon.2018.e00722

Hall, D.S., Behazin, M., Binns, W.J., and Keech, P.G. 2021. An evaluation of corrosion processes affecting copper-coated nuclear waste containers in a deep geological repository. Prog. Mater. Sci. 118, 100766. https://doi.org/10.1016/j.pmatsci.2020.100766

Hassan, R. S., Abass, M. R., Eid, M. A., & Abdel-Galil, E. A. 2021. Sorption of some radionuclides from liquid waste solutions using anionic clay hydrotalcite sorbent. Appl. Radiat. Isot., 178, 109985. https://doi.org/10.1016/j.apradiso.2021.109985

He, R., Xia, F. F., Wang, J., Pan, C. L., & Fang, C. R. 2011. Characterization of adsorption removal of hydrogen sulfide by waste biocover soil, an alternative landfill cover. J. Hazard. Mater., 186(1), 773-778. https://doi.org/10.1016/j.jhazmat.2010.11.062

Hong, H., Kim, S. J., Min, U. G., Lee, Y. J., Kim, S. G., Roh, S. W., Kim, J. G., Na J. G., Rhee, S. K. 2015. *Anaerosolibacter carboniphilus* gen. nov., sp. nov., a strictly anaerobic iron-reducing bacterium isolated from coal-contaminated soil. Int. J. Syst. Evol. Microbiol., 65(Pt_5), 1480-1485. https://doi.org/10.1099/ijs.0.000124

Huertas, F., Fariña, P., Farias, J., García-Siñeriz, J.L., Villar, M.V., Fernández, A.M., Martin, P.L., Elorza, F.J., Gens, A., Sánchez, M., Lloret, A., Samper, J., Martínez, M. Á. 2021. Full-scale Engineered Barriers Experiment. Updated Final Report 1994-2004.

Huttunen-Saarivirta, E., Rajala, P., & Carpén, L. 2016. Corrosion behaviour of copper under biotic and abiotic conditions in anoxic ground water: Electrochemical study. Electrochim. Acta, 203, 350-365. https://doi.org/10.1016/j.electacta.2016.01.098

Jia, R., Yang, D., Xu, D., Gu, T. 2017. Anaerobic corrosion of 304 stainless steel caused by the *Pseudomonas aeruginosa* biofilm Front. Microbiol., 8, 2335. https://doi.org/10.3389/fmicb.2017.02335

Kaufhold, S., Dohrmann, R. 2010. Stability of bentonites in salt solutions: II. Potassium chloride solution — Initial step of illitization? Appl. Clay Sci. 49, 98-107. https://doi.org/10.1016/j.clay.2010.04.009

Keech, P. G., Vo, P., Ramamurthy, S., Chen, J., Jacklin, R., Shoesmith, D. W. 2014. Design and development of copper coatings for long term storage of used nuclear fuel. Corros. Eng. Sci. Technol., 49(6), 425-430. https://doi.org/10.1179/1743278214Y.0000000206

Kim, J., Dong, H., Yang, K., Park, H., Elliott, W. C., Spivack, A., ... and Heuer, V. B. 2019. Naturally occurring, microbially induced smectite-to-illite reaction. Geol. Soc. Am. Bull. 47, 535-539.

King, F., Hall, D. S., Keech, P. G. 2017. Nature of the near-field environment in a deep geological repository and the implications for the corrosion behaviour of the container. Corros. Eng. Sci. Technol., 52(sup1), 25-30. https://doi.org/10.1080/1478422X.2017.1330736

Kumar, A., Voropaeva, O., Maleva, M., Panikovskaya, K., Borisova, G., Rajkumar, M., Bruno, L. B. 2021. Bioaugmentation with copper tolerant endophyte *Pseudomonas lurida* strain EOO26 for improved plant growth and copper phytoremediation by *Helianthus annuus*. Chemosphere, 266, 128983. https://doi.org/10.1016/j.chemosphere.2020.128983

Liu, D., Dong, H., Bishop, M.E., Zhang, J., Wang, H., Xie, S., Wang, S., Huang, L., Eberl, D.D. 2012. Microbial reduction of structural iron in interstratified illite-smectite minerals by a sulfate-reducing bacterium. Geobiology, 10, 150-162. https://doi.org/10.1111/j.1472-4669.2011.00307.x

Lopez-Fernandez, M., Vilchez-Vargas, R., Jroundi, F., Boon, N., Pieper, D., & Merroun, M. L. 2018. Microbial community changes induced by uranyl nitrate in bentonite clay microcosms. Appl. Clay Sci., 160, 206-216. https://doi.org/10.1016/j.clay.2017.12.034

Lopez-Fernandez, M., Fernández-Sanfrancisco, O., Moreno-García, A., Martín-Sánchez, I., Sánchez-Castro, I., Merroun, M.L. 2014. Microbial communities in bentonite formations and their interactions with uranium. Appl. Geochem. 49, 77-86. https://doi.org/10.1016/j.apgeochem.2014.06.022

Martinez-Moreno, M. F., Povedano-Priego, C., Mumford, A. D., Morales-Hidalgo, M., Mijnendonckx, K., Jroundi, F., Ojeda, J. J., & Merroun, M. L. 2024. Microbial responses to elevated temperature: Evaluating bentonite mineralogy and copper canister corrosion within the long-term stability of deep geological repositories of nuclear waste. Sci. Total Environ., 170149. https://doi.org/10.1016/j.scitotenv.2024.170149

Masurat, P., Eriksson, S., Pedersen, K. 2010. Microbial sulphide production in compacted Wyoming bentonite MX-80 under in situ conditions relevant to a repository for high-level radioactive waste. Appl. Clay Sci. 47, 58-64. https://doi.org/10.1016/j.clay.2009.01.004

Masurat, P., Eriksson, S., Pedersen, K. 2010b. Evidence of indigenous sulphate-reducing bacteria in commercial Wyoming bentonite MX-80. Appl. Clay Sci. 47, 51-57. https://doi.org/10.1016/j.clay.2008.07.002

Matschiavelli, N., Kluge, S., Podlech, C., Standhaft, D., Grathoff, G., Ikeda-Ohno, A., ... & Cherkouk, A. 2019. The year-long development of microorganisms in uncompacted bavarian bentonite slurries at 30 and 60 ºC. Environ. Sci. Technol. 2019, 53, 10514−10524. https://doi.org/10.1021/acs.est.9b02670

Miettinen, H., Bomberg, M., Bes, R., Tiljander, M., & Vikman, M. 2022. Transformation of inherent microorganisms in Wyoming-type bentonite and their effects on structural iron. Appl. Clay Sci., 221, 106465. https://doi.org/10.1016/j.clay.2022.106465

Monier, J. M., Lindow, S. E. 2003. *Pseudomonas syringae* responds to the environment on leaves by cell size reduction. Phytopathology, 93(10), 1209-1216. https://doi.org/10.1094/PHYTO.2003.93.10.1209

Pandey, A., Dhakar, K., Sharma, A., Priti, P., Sati, P., Kumar, B. 2015. Thermophilic bacteria that tolerate a wide temperature and pH range colonize the Soldhar (95 C) and Ringigad (80 C) hot springs of Uttarakhand, India. Ann. Microbiol, 65(2), 809-816. https://doi.org/10.1007/s13213-014-0921-0

Patel, S., & Gupta, R. S. 2020. A phylogenomic and comparative genomic framework for resolving the polyphyly of the genus *Bacillus*: Proposal for six new genera of *Bacillus* species, *Peribacillus* gen. nov., *Cytobacillus* gen. nov., *Mesobacillus* gen. nov., *Neobacillus* gen. nov., *Metabacillus* gen. nov. and *Alkalihalobacillus* gen. nov. Int. J. Syst. Evol. Microbiol., 70(1), 406-438. https://doi.org/10.1099/ijsem.0.003775

Payer, J. H., Finsterle, S., Apps, J.A., Muller, R.A. 2019. Corrosion performance of engineered barrier system in deep horizontal drillholes. Energies. 12, 1491. https://doi.org/10.3390/en12081491

Pedersen, K. 2010. Analysis of copper corrosion in compacted bentonite clay as a function of clay density and growth conditions for sulfate-reducing bacteria. J. Appl. Microbiol., 108, 1094-1104. https://doi.org/10.1111/j.1365-2672.2009.04629.x

Pentráková, L., Su, K., Pentrák, M., Stucki, J.W. 2013. A review of microbial redox interactions with structural Fe in clay minerals. Clay Miner. 48, 543-560. https://doi.org/10.1180/claymin.2013.048.3.10

Povedano-Priego, C., Jroundi, F., Solari, P. L., Guerra-Tschuschke, I., del Mar Abad-Ortega, M., Link, A., ... & Merroun, M. L. 2023. Unlocking the bentonite microbial diversity and its implications in selenium bioreduction and biotransformation: Advances in deep geological repositories. J. Hazard. Mater., 445, 130557. https://doi.org/10.1016/j.jhazmat.2022.130557

Povedano-Priego, C., Jroundi, F., Lopez-Fernandez, M., Shrestha, R., Spanek, R., Martín-Sánchez, I., Villar, M.V., ˇSevců, A., Dopson, M. Merroun, M.L. 2021. Deciphering indigenous bacteria in compacted bentonite through a novel and efficient DNA extraction method: Insights into biogeochemical processes within the Deep Geological Disposal of nuclear waste concept. J. Hazard. Mater. 408, 124600. https://doi.org/10.1016/j.jhazmat.2020.124600

Povedano-Priego, C., Jroundi, F., Lopez-Fernandez, M., Sánchez-Castro, I., Martin-Sánchez, I., Huertas, F.J., Merroun, M.L. 2019. Shifts in bentonite bacterial community and mineralogy in response to uranium and glycerol-2-phosphate exposure. Sci. Total Environ. 692, 219-232. https://doi.org/10.1016/j.scitotenv.2019.07.228

Ruiz-Fresneda, M. A., Martinez-Moreno, M. F., Povedano-Priego, C., Morales-Hidalgo, M., Jroundi, F., & Merroun, M. L. 2023. Impact of microbial processes on the safety of deep geological repositories for radioactive waste. Front. Microbiol., 14, 1134078. https://doi.org/10.3389/fmicb.2023.1134078

Ruiz-Fresneda, M. A., Staicu, L. C., Lazuén-López, G., & Merroun, M. L. 2023(b). Allotropy of selenium nanoparticles: Colourful transition, synthesis, and biotechnological applications. Microb. Biotechnol., 16(5), 877-892. https://doi.org/10.1111/1751-7915.14209

Ruiz-Fresneda, M. A., Gomez-Bolivar, J., Delgado-Martin, J., Abad-Ortega, M. D. M., Guerra-Tschuschke, I., & Merroun, M. L. 2019. The bioreduction of selenite under anaerobic and alkaline conditions analogous to those expected for a deep geological repository system. Molecules, 24(21), 3868. https://doi.org/10.3390/molecules24213868

Ruiz-Fresneda, M. A., Delgado-Martín, J., Gomez-Bolívar, J., Fernandez-Cantos, M. V., Bosch-Estévez, G., Martinez-Moreno, M. F., & Merroun, M. L. 2018. Green synthesis and biotransformation of amorphous Se nanospheres to trigonal 1D Se nanostructures: impact on Se mobility within the concept of radioactive waste disposal. Environ. Sci. Nano, 5(9), 2103-2116. https://doi.org/10.1039/C8EN00221E

Salehi Alaei, E., Guo, M., Chen, J., Behazin, M., Bergendal, E., Lilja, C., ... & Noël, J. J. 2023. The transition from used fuel container corrosion under oxic conditions to corrosion in an anoxic environment. Mater. Corros., 74(11-12), 1690-1706. https://doi.org/10.1002/maco.202313757

Schütz, M. K., Schlegel, M. L., Libert, M., & Bildstein, O. 2015. Impact of iron-reducing bacteria on the corrosion rate of carbon steel under simulated geological disposal conditions. Environ. Sci. Technol., 49(12), 7483-7490. https://doi.org/10.1021/acs.est.5b00693

Shelobolina, E. S., Nevin, K. P., Blakeney-Hayward, J. D., Johnsen, C. V., Plaia, T. W., Krader, P., Woodard, T., Holmes, D. E., VanPraagh, C. G., Lovley, D. R. 2007. *Geobacter pickeringii* sp. nov., *Geobacter argillaceus* sp. nov. and *Pelosinus fermentans* gen. nov., sp. nov., isolated from subsurface kaolin lenses. Int. J. Syst. Evol. Microbiol., 57(1), 126-135. https://doi.org/10.1099/ijs.0.64221-0

Shelobolina, E.S., VanPraagh, C.G., Lovley, D.R. 2003. Use of ferric and ferrous iron containing minerals for respiration by Desulfitobacterium frappieri. Geomicrobiol. J. 20, 143-156. https://doi.org/10.1080/01490450303884

Shrestha, R., Cerna, K., Spanek, R., Bartak, D., Cernousek, T., & Sevcu, A. 2022. The effect of low-pH concrete on microbial community development in bentonite suspensions as a model for microbial activity prediction in future nuclear waste repository. Sci. Total Environ., 808, 151861. https://doi.org/10.1016/j.scitotenv.2021.151861

Spring, S., Sorokin, D. Y., Verbarg, S., Rohde, M., Woyke, T., & Kyrpides, N. C. 2019. Sulfate-reducing bacteria that produce exopolymers thrive in the calcifying zone of a hypersaline cyanobacterial mat. Front. Microbiol., 10, 862. https://doi.org/10.3389/fmicb.2019.00862

Stackebrandt, E., Sproer, C., Rainey, F. A., Burghardt, J., Päuker, O., & Hippe, H. 1997. Phylogenetic analysis of the genus *Desulfotomaculum*: evidence for the misclassification of *Desulfotomaculum guttoideum* and description of *Desulfotomaculum orientis* as *Desulfosporosinus orientis* gen. nov., comb. nov. Int. J. Syst. Evol. Microbiol., 47(4), 1134-1139. https://doi.org/10.1099/00207713-47-4-1134

Staicu, L. C., & Barton, L. L. 2021. Selenium respiration in anaerobic bacteria: Does energy generation pay off? J. Inorg. Biochem., 222, 111509. https://doi.org/10.1016/j.jinorgbio.2021.111509

Stroes-Gascoyne, S., Hamon, C. J., Maak, P., & Russell, S. 2010. The effects of the physical properties of highly compacted smectitic clay (bentonite) on the

culturability of indigenous microorganisms. Appl. Clay Sci., 47(1-2), 155-162. https://doi.org/10.1016/j.clay.2008.06.010

Vaïtilingom, M., Amato, P., Sancelme, M., Laj, P., Leriche, M., Delort, A.M. 2010. Contribution of microbial activity to carbon chemistry in clouds. Appl. Environ. Microbiol. 76, 23-29. https://doi.org/10.1128/AEM.01127-09

Villar, M.V., Fernández-Soler, J.M., Delgado Huertas, A., Reyes, E., Linares, J., Jiménez de Cisneros, C., Linares, J., Reyes, E., Delgado, A., Fernandez-Soler, J.M., Astudillo, J. 2006. The study of Spanish clays for their use as sealing materials in nuclear waste repositories: 20 years of progress. J. Iber. Geol. 32, 15-36.

Vogel, M., Fischer, S., Maffert, A., Hübner, R., Scheinost, A. C., Franzen, C., & Steudtner, R. 2018. Biotransformation and detoxification of selenite by microbial biogenesis of selenium-sulfur nanoparticles. J. Hazard. Mater., 344, 749-757. https://doi.org/10.1016/j.jhazmat.2017.10.034

White, D.C., Sutton, S.D., Ringelberg, D. B. (1996). The genus *Sphingomonas*: physiology and ecology. Curr. Opin. Biotechnol. 7, 301-306. https://doi.org/10.1016/S0958-1669(96)80034-6

WNA. World Nuclear Association. 2023. Storage and disposal of radioactive waste. https://www.world-nuclear.org/

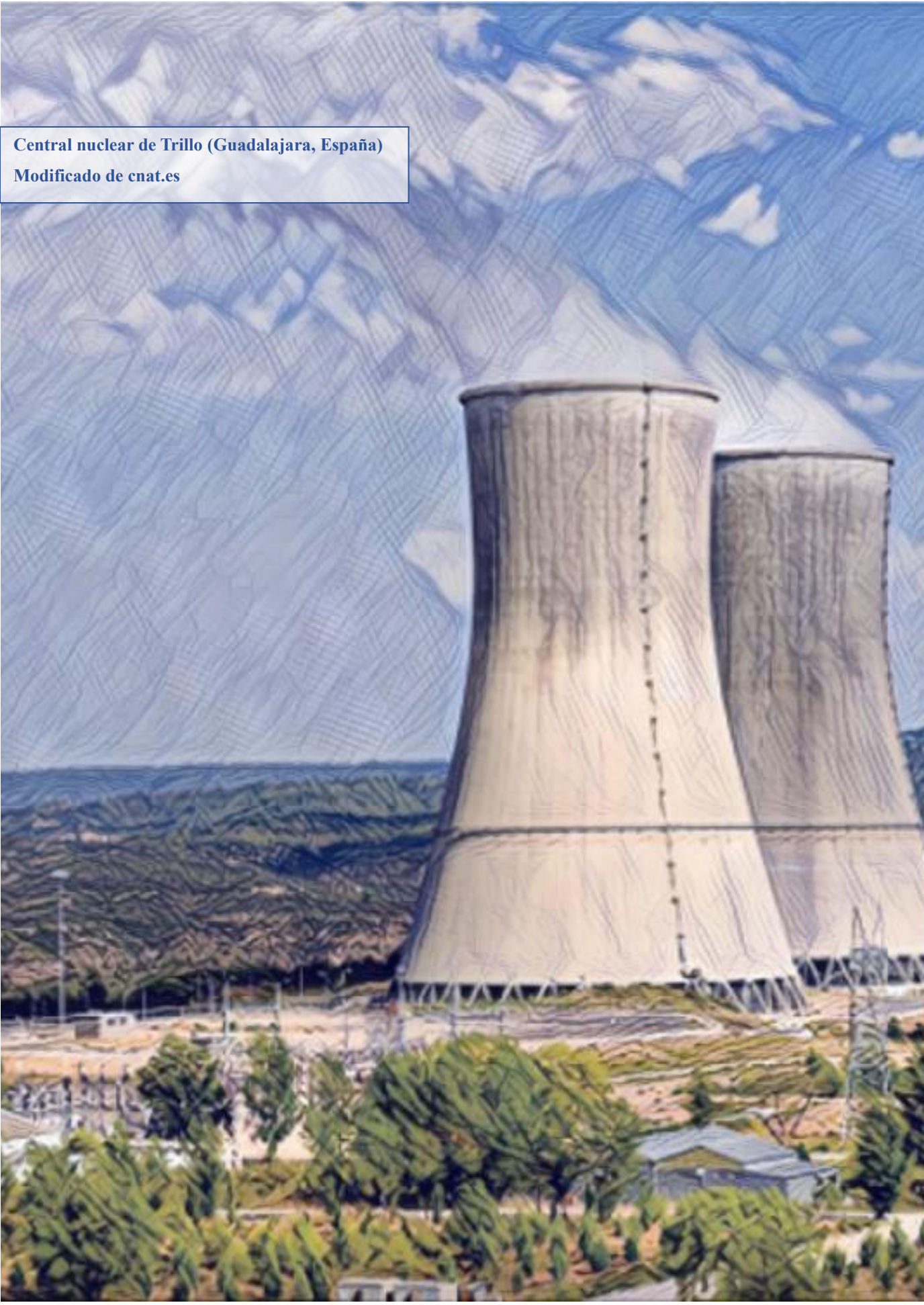

Central nuclear de Trillo (Guadalajara, España)
Modificado de cnat.es

CONCLUSIONES

CONCLUSIONES

1) La mineralogía de la bentonita compactada no se ve afectada por factores bióticos (microorganismos) ni abióticos (adición de donadores y aceptor de electrones, o proceso de tindalización) durante un año de incubación anóxica a 30 ºC y 60 ºC, lo que indica la estabilidad de este material.
2) Las bentonitas compactadas e incubadas a 30 ºC y 60 ºC presentaron un bajo número de bacterias sulfatorreductoras (SRB) (ej. *Anaerosolibacter*), las cuales demostraron capacidad de sobrevivir y volverse metabólicamente activas bajo condiciones favorables.
3) La alta temperatura de incubación (60 ºC) reduce la diversidad microbiana en bentonitas compactadas, con *Pseudomonas* como el género dominante, además de disminuir el número de SRB. A esta temperatura, bacterias aerobias como *Aeribacillus* presentan capacidad de crecimiento; mientras que, ciertas bacterias anaerobias, no.
4) La presencia de acetato, lactato y sulfato incrementa la actividad de los microorganismos, los cuales influyen y aceleran los procesos biogeoquímicos como la reducción de la alcalinidad de la bentonita, la corrosión del cobre, la formación de gases o la reducción de Se(IV) a Se(0), entre otros.
5) Se ha demostrado que el proceso de tindalización no es el método más eficaz para la esterilización de la bentonita, aunque presenta un efecto negativo sobre la diversidad y la actividad bacteriana.
6) La detección de azufre en forma de sulfato y sulfuro en la superficie de los discos de cobres en bentonita compactada sugiere

una etapa temprana de corrosión mediada por la actividad de bacterias sulfatorreductoras.

7) Las condiciones de alta actividad de agua y adición de nutrientes favorecen el crecimiento de las bacterias sulfatorreductoras (ej. *Desulfosporosinus*, *Desulfocurvibacter* y *Anaerosolibacter*), que oxidan lactato reduciendo sulfatos a sulfuros, interviniendo en la formación de productos de corrosión en la superficie del cobre.
8) Los sulfuros pueden reaccionar con el cobre metálico o mediar en la conversión de óxidos de cobre dando como resultado sulfuro de cobre (Cu_2S), principal producto de corrosión de este material en condiciones anaerobias.
9) La presencia de Se(IV) influye en las comunidades bacterianas, reduciendo la abundancia relativa de algunas bacterias sulfatorreductoras (SRB). Sin embargo, cuando los microcosmos están enriquecidos con donadores/aceptor de electrones se estimulan ciertas SRB tolerantes al selenio, como *Desulfosporosinus*, en términos de abundancia relativa.
10) La presencia de bacterias tolerantes al selenio influye en los procesos de reducción intracelular de Se(IV) a Se(0). Una vez liberado al medio, este Se(0) sufre una transformación alotrópica desde nanoesferas amorfas a estructuras cristalinas de selenio monoclínico a trigonal (forma más estable y menos tóxica).

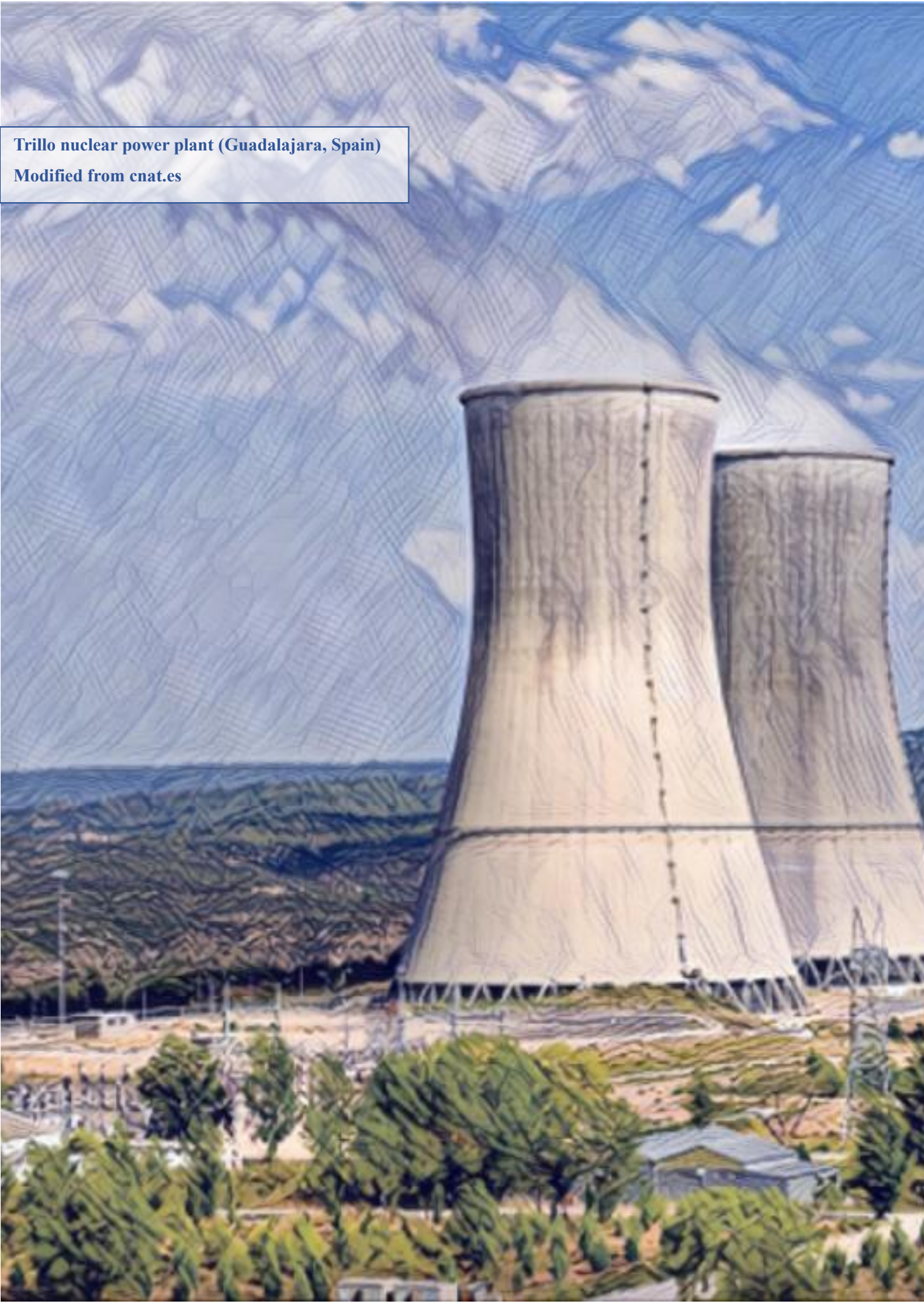

Trillo nuclear power plant (Guadalajara, Spain)
Modified from cnat.es

CONCLUSIONS

CONCLUSIONS

1) The mineralogical stability of compacted bentonite was not affected by either biotic (microorganisms) or abiotic (addition of electron donors/acceptor, tyndallization process) factors after one year of anoxic incubation at both 30 ºC and 60 ºC.
2) Compacted bentonites incubated at 30 ºC and 60 ºC presented a low number of sulfate-reducing bacteria (SRB) (e.g., *Anaerosolibacter*), which exhibited the capacity to survive and become metabolically active under favorable nutritional conditions.
3) High incubation temperature (60 ºC) reduced the microbial diversity in compacted bentonites, with *Pseudomonas* remaining as the dominant genus. Moreover, the number of SRB species was decreased. At this temperature, whilst aerobic bacteria such as *Aeribacillus* showed growth capacity, certain anaerobic bacteria did not survive.
4) The presence of acetate, lactate, and sulfate increased the activity of microorganisms, which in turn influenced and accelerated biogeochemical processes such as the decrease of the alkalinity of bentonite, corrosion of copper, formation of gases, or the reduction of Se(IV) to Se(0), among others.
5) It has been proven that the tyndallization process is not the most effective method for the sterilization of bentonite, although it negatively affects its bacterial diversity and activity.
6) The detection of sulfur as sulfate and sulfide on the surface of the copper disks in compacted bentonite suggests an early stage of corrosion, mediated by the activity of sulfate-reducing bacteria.

7) High water activity and addition of nutrients promote the growth of sulfate-reducing bacteria (e.g., *Desulfosporosinus*, *Desulfocurvibacter* and *Anaerosolibacter*), which oxidize lactate, hence reducing sulfates to sulfides, and leading to the formation of corrosion products on the copper surface.
8) Sulfides can react with the copper metal or mediate the conversion of copper oxides to copper sulfides (Cu_2S), which is the main corrosion product of copper under anaerobic conditions.
9) The presence of Se(IV) influences bacterial communities, dropping the relative abundance of some SRB. However, when microcosms are enriched with electron donors/acceptor, an increase of selenium-tolerant SRB, such as *Desulfosporosinus*, was observed in terms of relative abundance.
10) The enrichment of selenium-tolerant bacteria trigger the intracellular reduction processes of Se(IV) to Se(0). Once released into the extracellular medium, this Se(0) undergoes an allotropic transformation, from amorphous nanospheres to crystalline structures of monoclinic to trigonal selenium (more stable and less toxic form) over time.

UNIVERSIDAD DE GRANADA